# Biosynthesis of Xylitol from Sugarcane Bagasse: Process Optimization, Modelling and Intensification

**A**

**Thesis**

**Submitted in**

**Partial Fulfilment of the**

**Requirements for the Degree of**

## DOCTOR OF PHILOSOPHY

**By**

**Belachew Zegale Tizazu**


**DEPARTMENT OF CHEMICAL ENGINEERING**

**Indian Institute of Technology Guwahati**

**Guwahati – 781 039, Assam, India**

**August, 2018**

*Dedicated*

*to*

*Those Who Lost Their Life for Freedom and Justice of the People of Ethiopia at Bahir Dar on August 7, 2016*

*and*

*My beloved wife and parents for their continuous support and encouragement throughout my life*

**INDIAN INSTITUTE OF TECHNOLOGY GUWAHATI**

**DEPARTMENT OF CHEMICAL ENGINEERING**

# STATEMENT

I do hereby declare that the content embodied in this thesis entitled **"Biosynthesis of Xylitol from Sugarcane Bagasse: Process Optimization, Modelling and Intensification"** is the result of investigations carried out by me at Department of Chemical Engineering, Indian Institute of Technology Guwahati, Guwahati, India, under the guidance of Professor Vijayanand S. Moholkar.

In keeping with the general practice of reporting scientific observations, due acknowledgements have been made wherever the work described is based on the findings of other investigators.

Date: August 27, 2018

Belachew Zegale Tizazu

(Roll No. 156107037)

# CERTIFICATE

It is certified that the work contained in thesis entitled **"Biosynthesis of Xylitol from Sugarcane Bagasse: Process Optimization, Modelling and Intensification"**, by **Belachew Zegale Tizazu** (Roll No. 156107037), has been carried out under my supervision and that this work has not been submitted elsewhere for degree.

Date: August 27, 2018

Professor Vijayanand S. Moholkar
Department of Chemical Engineering
Indian Institute of Technology Guwahati
Guwahati – 781 039, Assam, India

## ACKNOWLEDGEMENTS

First of all I would like to thank the almighty of God.

A special and foremost gratefulness goes to my thesis supervisor **Prof. V.S. Moholkar** for his valuable guidance and encouragement throughout the research work. I would also like to acknowledge my gratitude to my doctoral committees, **Prof. K. Mohanty**, **Dr. V.V. Goud** and **Dr. S. Senthilkumar**, for their advice, suggestions and encouragement throughout the research work.

My acknowledgement goes to the course instructors, *Dr. Mahuya De, Prof. Mihir K. Purkait, Dr. Dipankar Bandyopadhyay, Prof. Kaustubha Mohanty, Prof. Aiyagari Ramesh and Prof. Kannan Pakshirajan*, who enabled me to a better understanding of the subjects related to the present research work.

My sincere acknowledgments go to faculty members of Department of Chemical Engineering, IIT Guwahati for their suggestion and encouragement. I also like to thank technical and office staff members of Department of Chemical Engineering, IIT Guwahati for their valuable help. Central Instrument Facility, Centre for Energy and Department of Biosciences and Bioengineering, IIT Guwahati are also acknowledged.

My sincere acknowledgement goes to Ministry of Education and Addis Ababa Science and Technology University, Ethiopia for providing phD scholarship and financial support during the entire research work.

I would like to thank my research group members, Shyamli, Kuldeep, Amit, Neharica, Neha, Philip, Arup, Retish, Maneesh, Pritam, Dr. Binota, Debarsh, Bahskar, of Chemical and Biofuels Lab for their support and suggestion.

Finally, I express my appreciation to my beloved wife, **Selam Asmare**, my daughter, **Bezawit Belachew** and my beloved parents: **Zegale Tizazu**, my father, **Tiruayehu Nega**, my mother and **Belete Zegale**, my brother for their valuable support, motivation and encouragement throughout my life.

# TABLE OF CONTENTS

# *THESIS ABSTRACT*

In the first part of this thesis, statistical optimization of process parameters for dilute acid hydrolysis of sugarcane bagasse for maximum xylose yield was reported. Prior to statistical optimization, the chemical composition of sugarcane bagasse and the effect of solid to liquid ratio on xylose yield were analysed. The process parameters considered for optimization were hydrolysis temperature, acid concentration (or acid load) and hydrolysis time. Optimum levels of these parameters were determined by Box Behnken design (BBD) method of optimization. The optimum values of the process parameters for dilute acid hydrolysis of sugarcane bagasse were investigated. The composition of monomeric sugars (xylose, glucose, and arabinose) and inhibitory products (acetic acid, furfural, and 5–HMF) in the hydrolysate has also been analyzed under optimal conditions of dilute sulfuric acid hydrolysis of sugarcane bagasse. In subsequent investigations, we addressed the kinetic and thermodynamic features of dilute acid (2% v/v $H_2SO_4$, 1:30 w/v) hydrolysis of sugarcane bagasse. Time profiles of xylose formation in range of 100°–130°C and treatment period of 0–120 min were analysed with modified biphasic Saeman model. Generation of glucose, arabinose and inhibitory products (furfural, 5–HMF and acetic acid) were also analysed. Easy–to–hydrolyse fraction of hemicellulose increased with temperature. Activation energies for hydrolysis and xylose degradation were investigated. Thermodynamic analysis ($\Delta H$, $\Delta S$, and $\Delta G$) revealed that xylose formation is thermodynamically more favoured than degradation.

In the second part of the thesis, optimization of medium components and process parameters for xylitol production from sugarcane bagasse using *C. tropicalis* MTCC 184 immobilized on PU foam were investigated. Plackett–Burman design revealed that out of seven medium components, 4 medium components, viz. yeast extract, $MgSO_4 \cdot 7H_2O$, $KH_2PO_4$ and $(NH_4)_2SO_4$; as significant components. These medium components were further optimized using central composite design (CCD) method to find their optimum values. Optimization of process parameters, viz. temperature, initial pH, shaking speed and substrate (xylose) concentration, was done at the optimized values of medium components. Optimum values of these parameters for maximum xylitol yield = 0.65 g/g of xylose are: yeast extract = 5.78 g/L, $(NH_4)_2SO_4$ = 3.22 g/L, $KH_2PO_4$ = 0.58 g/L, $MgSO_4 \cdot 7H_2O$ = 0.57 g/L and temperature = 29.3$^oC$, initial pH = 6.2, shaking speed = 151 rpm and initial xylose concentration = 20.9 g/L. Medium components provide essential growth factors and utilizable potassium, phosphate,

nitrogen, sulphur sources. Activity of xylose reductase in metabolic pathway is stabilized and augmented by $Mg^{2+}$.

In the third part, we addressed ultrasound–assisted xylitol production through fermentation of dilute acid (pentose–rich) hydrolysate of sugarcane bagasse using free and immobilized cells of *Candida tropicalis*. Sonication of fermentation mixture at optimum conditions (optimized in the second part) was carried out in ultrasound bath (37 kHz and 10% duty cycle). Time profiles of substrate and product in control (mechanical shaking) and test (mechanical shaking + sonication) fermentations were fitted to kinetic model using Genetic Algorithm (GA) optimization. Maximum xylitol yield of 0.56 g/g and 0.61 g/g of xylose was achieved in control and test fermentations, respectively, in free cells of *C. tropicalis*. Moreover, the xylitol yield of 0.65 g/g and 0.66 g/g of xylose was obtained in control and test experiments, respectively in immobilized cells of *C. tropicalis*, which essentially corresponded to 71% and 73% of the theoretical yield.

Although sonication of fermentation mixture resulted in marginal (17–20%) rise in final xylitol and biomass yields, the kinetics of the fermentation showed drastic enhacement. 2.5× enhancement in xylitol productivity and 2× rise in specific uptake rate of xylose was achieved under ultrasound assisted fermentation. Comparative assessment of the parameters of kinetic model for fermentation under test and control condition revealed that sonication promoted the uptake and utilization of substrates for cell growth and increased enzyme–substrate affinity. The inhibition effect of substrate was also reduced with sonication. 10–20× enhancement in permeability of cell membrane caused faster diffusion of substrates, nutrients and metabolite products across the cell membrane, which resulted in faster xylose metabolism and enhanced kinetics of fermentation. Flow cytometry analysis of in control (mechanical shaking) and test (ultrasound–treated) fermentations was carried out. The results of flow cytometry essentially confirmed that SSC and FSC of the *C. tropicalis* cells remain practically unaltered after sonication. Thus, the internal complexity and morphology of the cells remain unchanged after exposure to ultrasound, or in other words, no noticeable adverse impact of sonication is seen on the yeast cells.

# LIST OF TABLES

# LIST OF FIGURES

**APPENDIX**

# NOMENCLATURE AND ABBREVIATIONS

| | |
|---|---|
| $A$ | pre–exponential factor ($min^{-1}$) |
| $a_{cell}$ | Specific surface area of yeast cells ($m^2/g$) |
| AKR | Aldo–keto reductase |
| $A_r$ | arabinose concentration (g/L) |
| $A_{rno}$ | potential arabinan concentration (g/L) |
| $A_{ro}$ | initial arabinose concentration (g/L) |
| BBD | Box Behnken design |
| $C_A$ | acetic acid concentration (g/L) |
| $C_{Ao}$ | potential acetic acid concentration (g/L) |
| CCD | Central Composite Design |
| $C_F$ | furfural concentration (g/L) |
| $C_g$ | Glucose concentration (g/L) |
| $C_H$ | xylan concentration (g/L) |
| $C_{Hf}$ | fast reacting xylan concentration (g/L) |
| $C_{Hs}$ | slow reacting xylan concentration (g/L) |
| $C_X$ | xylose concentration (g/L) |
| $C_{xy}$ | Xylose concentration (g/L) |
| $C_{xit}^{ex}$ | Extracellular xylitol concentration (g/L) |
| $C_{xit}^{in}$ | Intracellular xylitol concentration (g/L) |
| $D$ | decomposition products (g/g) |
| DoEs | Design of Experiments |

| | |
|---|---|
| $E$ | activation energy (kJ/mol) |
| $F$ | furfural (g/g) |
| $G$ | glucose concentration (g/L) |
| $G_{no}$ | Glucan concentration (g/L) |
| $\Delta G$ | Gibbs free energy (kJ/mol) |
| $h$ | Planck's constant (6.626 x $10^{-34}$ J.s) |
| HMF | hydroxymethyl furfural (g/g) |
| $\Delta H$ | enthalpy change (kJ/mol) |
| $K_{i,g}$ | Inhibition constant of xylose uptake by glucose (g/L) |
| $K_{i,xy}$ | Inhibition constant of glucose uptake by xylose (g/L) |
| $K_r$ | Repression constant by glucose (g/L) |
| $K_{s,g}$ | Monod saturation constants for glucose (g/L) |
| $K_{s,xit}$ | Monod saturation constants for xylitol (g/L) |
| $k$ | reaction rate constant ($min^{-1}$) |
| $k_B$ | Boltzmann constant (1.381 x 10–23 J/ K) |
| $k_f$ | reaction rate constant for easy–to–hydrolyse fraction ($min^{-1}$) |
| $k_s$ | reaction rate constant for hard–to–hydrolyse fraction ($min^{-1}$) |
| $k_2$ | reaction rate constant for xylose degradation ($min^{-1}$) |
| $M$ | monomer (g/g) |
| MTCC | Microbial Type Culture Collection |
| $M_{w,xit}$ | Molecular weight of xylitol (g/mol) |
| $M_{w,xy}$ | Molecular weight of xylose (g/mol) |
| NAD(P)H | Nicotinamide adenine dinucleotide phosphate (reduced form) |
| $O$ | oligomer (g/g) |

| | |
|---|---|
| $P$ | polymer (g/g) |
| PBD | Plackett–Burman Design |
| PU | Polyurethane |
| $P_{xit}$ | Permeability coefficient of membrane (m/s) |
| $q_g^{max}$ | Maximum specific uptake rates of glucose ($h^{-1}$) |
| $q_{xy}^{max}$ | Maximum specific uptake rates of xylose ($h^{-1}$) |
| $R$ | universal gas constant (8.3143 x $10^{-3}$kJ/mol/ K) |
| $\Delta S$ | entropy change |
| $T$ | hydrolysis temperature (K) |
| $X$ | xylose (g/g) |
| $X$ | Biomass concentration (g/L) |
| $X_i$ & $X_j$ | Independent variables of i and j |
| XR | Xylose reductase |
| $Y$ | Response variable (xylitol concentration) (g/L) |
| YPD | Yeast Peptone Dextrose |
| $Y_{X/xit}$ | Biomass yield on xylitol (g/g) |
| $\alpha$ | easy–to–hydrolyse fraction of xylan |
| $\beta$ | g of susceptible glucan/g of total glucan |
| $\gamma$ | g of susceptible arabinan/g of total arabinan |
| $\mu$ | Specific growth rate ($h^{-1}$) |
| $\mu_g^{max}$ | Maximum specific growth rates of glucose ($h^{-1}$) |
| $\mu_{xit}^{max}$ | Maximum specific growth rates of xylitol ($h^{-1}$) |
| $\rho_X$ | Mass density of yeast cells (g/L) |

| | |
|---|---|
| $\beta_o$ | Intercept term |
| $\beta_i$ | Linear coefficients |
| $\beta_{ii}$ | Quadratic coefficients |
| $\beta_{ij}$ | Interaction coefficients |
| $\mu$ | Specific growth rate ($h^{-1}$) |
| $\mu_g^{max}$ | Maximum specific growth rates of glucose ($h^{-1}$) |
| $\mu_{xit}^{max}$ | Maximum specific growth rates of xylitol ($h^{-1}$) |
| $\rho_X$ | Mass density of yeast cells (g/L) |

# CHAPTER 1

## GENERAL INTRODUCTION AND MOTIVATION FOR THE THESIS

# CHAPTER 1

# GENERAL INTRODUCTION AND MOTIVATION FOR THE THESIS

## 1.1 Introduction

At present, our society is extremely dependent on finite fossil fuels (petroleum, coal and natural gas) to meet basic needs of energy, fuels, organic chemicals and polymers. Thus, more than 80% of energy and ~90% of organic chemicals in the world are derived from fossil fuels alone. Moreover, the energy and organic chemicals consumptions are growing (~7% per annum) continuously due to rapid increase of world's population with improved standards of living (BP Statistical Reviews, 2017). The increasing energy demands, gradual depletion of fossil fuels and hence rise of crude oils price are main reasons for investigation of renewable resources for sustainable production of energy, biofuels and value–added chemicals (Fernando et al., 2006). The deterioration of environmental hygiene due to emissions of harmful and greenhouse gases such as $CH_4$, $CO_2$, $N_2O$ by huge usage of fossil fuels is another reason for shifting dependency away from limited fossil fuels to carbon–neutral renewable resources.

The global energy consumption data from the years 2006 to 2016 are given in Table 1.1. The global energy consumption increased from 11266.7 million tons of oil equivalent in 2006 to 13276.3 million tons of oil equivalent by the end of 2016 (BP Statistical Reviews, 2017). Global energy consumption increased by just 1% in 2016, following growth of 0.9% in 2015 and 1% in 2014. In this period the energy consumption of India also increased from 414.0 million tons of oil

equivalent in 2006 to 723.9 million tons of oil equivalent by the end of 2016. Energy consumption in India grew by just 5.4% in 2016.

The global energy consumption by fuels type data in 2015 for only renewable and by the end of 2016 for all fuel types are given in Table 1.2. The global renewable (excluding nuclear and hydro) energy consumption increased from 366.7 million tons of oil equivalent in 2015 to 419.6 million tons of oil equivalent by the end of 2016 which grew just by 14%. The global energy consumption share of renewables (excluding nuclear and hydro) was 3% by the end of 2016. In this period in India the renewable (excluding nuclear and hydro) energy consumption increased from 12.7 million tons of oil equivalent in 2015 to 16.5 million tons of oil equivalent by the end of 2016 which grew just by 30%. The renewable energy consumption share of India in the World was 4% by the end of 2016.

The global oil (which include crude oil, shell oil, oil sands and natural gas liquids) and biofuels production data for 10 years, starting from 2006 to 2016 is shown in Table 1.3 and 1.4, respectively (BP Statistical Reviews, 2017). The global biofuels production increased from 27848 thousand tons of oil equivalent in 2006 to 82306 thousand tons of oil equivalent by the end of 2016. In 2016, global oil and biofuels production increased by 0.3% and 2.6%, respectively. The global oil production was changing very marginally while the global biofuels production showed marked growth as compared to oil production. In this period the biofuels production in India also increased from 146,000 tons of oil equivalent in 2006 to 505,000 tons of oil equivalent by the end of 2016. The biofuels production in India grew by 23% at the end of 2016. Thus, nations have undertaken emphasize that biochemicals production along with biofuels from renewable sources such as biomass is supplementaryto increase the economy.

**Table 1.1.** Global energy consumption data (million tons of oil equivalent) from 2006 to 2016 (BP Statistical Review of World Energy June 2017)

| | 2006 | 2007 | 2008 | 2009 | 2010 | 2011 | 2012 | 2013 | 2014 | 2015 | 2016 |
|---|---|---|---|---|---|---|---|---|---|---|---|
| Total North America | 2824.1 | 2866.5 | 2819.2 | 2689.7 | 2777.8 | 2778.6 | 2724.3 | 2795.9 | 2821.2 | 2792.4 | 2788.9 |
| Total South & Central America | 567.8 | 593.9 | 613.2 | 606.0 | 641.7 | 665.4 | 680.9 | 696.7 | 704.1 | 710.4 | 705.3 |
| Total Europe & Eurasia | 3023.5 | 3017.7 | 3022.2 | 2839.8 | 2952.6 | 2937.9 | 2936.3 | 2900.6 | 2838.3 | 2846.6 | 2867.1 |
| Total Middle East | 592.2 | 625.6 | 667.6 | 690.3 | 734.2 | 750.3 | 780.8 | 812.4 | 840.0 | 874.6 | 895.1 |
| Total Africa | 334.8 | 347.9 | 369.5 | 373.4 | 388.9 | 388.0 | 402.9 | 415.4 | 427.9 | 433.5 | 440.1 |
| Total Asia Pacific | 3924.3 | 4175.0 | 4292.1 | 4402.2 | 4674.7 | 4935.1 | 5095.5 | 5245.0 | 5357.2 | 5447.4 | 5579.7 |
| **Total World** | **11266.7** | **11626.6** | **11783.8** | **11601.5** | **12170.0** | **12455.3** | **12620.7** | **12866.0** | **12988.8** | **13105.0** | **13276.3** |

**Table 1.2.** Global energy consumption by fuel type data (million tons) for 2015 (renewables) and 2016 (BP Stat. Review of World Energy Jun 2017)

| | 2015 | 2016 | | | | | | |
|---|---|---|---|---|---|---|---|---|
| | Renewables | Oil | Natural gas | Coal | Nuclear energy | Hydro electricity | Renewables | Total |
| Total North America | 83.6 | 1046.9 | 886.8 | 386.9 | 217.4 | 153.9 | 97.1 | 2788.9 |
| Total South & Central America | 24.0 | 326.2 | 154.7 | 34.7 | 5.5 | 156.0 | 28.2 | 705.3 |
| Total Europe & Eurasia | 141.6 | 884.6 | 926.9 | 451.6 | 258.2 | 201.8 | 144.0 | 2867.1 |
| Total Middle East | 0.5 | 417.8 | 461.1 | 9.3 | 1.4 | 4.7 | 0.7 | 895.1 |
| Total Africa | 4.2 | 185.4 | 124.3 | 95.9 | 3.6 | 25.8 | 5.0 | 440.1 |
| Total Asia Pacific | 112.7 | 1557.3 | 650.3 | 2753.6 | 105.9 | 368.1 | 144.5 | 5579.7 |
| **Total World** | **366.7** | **4418.2** | **3204.1** | **3732.0** | **592.1** | **910.3** | **419.6** | **13276.3** |

**Table 1.3.** Global oil production (in million tons) data from 2006 to 2016 (BP Statistical Review of World Energy June 2017)

| | 2006 | 2007 | 2008 | 2009 | 2010 | 2011 | 2012 | 2013 | 2014 | 2015 | 2016 |
|---|---|---|---|---|---|---|---|---|---|---|---|
| Total North America | 637.6 | 632.6 | 612.0 | 621.9 | 638.6 | 659.2 | 719.6 | 783.8 | 869.2 | 908.3 | 882.6 |
| Total South & Central America | 382.2 | 374.3 | 380.5 | 377.3 | 378.4 | 381.1 | 378.9 | 379.2 | 392.9 | 398.6 | 384.5 |
| Total Europe & Eurasia | 852.9 | 864.2 | 855.4 | 861.6 | 859.5 | 844.5 | 833.6 | 833.3 | 834.7 | 847.3 | 860.6 |
| Total Middle East | 1236.0 | 1214.1 | 1267.8 | 1176.6 | 1219.2 | 1325.6 | 1344.0 | 1326.1 | 1338.7 | 1411.6 | 1496.9 |
| Total Africa | 475.1 | 486.1 | 485.3 | 466.1 | 478.2 | 402.3 | 440.1 | 408.9 | 394.2 | 393.7 | 374.8 |
| Total Asia Pacific | 381.0 | 381.8 | 388.4 | 384.3 | 402.7 | 395.2 | 400.2 | 393.9 | 396.5 | 400.0 | 383.0 |
| **Total World** | **3964.8** | **3953.2** | **3989.6** | **3887.8** | **3976.5** | **4007.9** | **4116.4** | **4125.3** | **4226.2** | **4359.5** | **4382.4** |

**Table 1.4.** Global biofuels production (in thousand tons of oil equivalent) from 2006 to 2016 (BP Statistical Review of World Energy June 2017)

| | 2006 | 2007 | 2008 | 2009 | 2010 | 2011 | 2012 | 2013 | 2014 | 2015 | 2016 |
|---|---|---|---|---|---|---|---|---|---|---|---|
| Total North America | 10844 | 15216 | 21485 | 24552 | 28866 | 32147 | 30840 | 32171 | 34137 | 35049 | 36997 |
| Total South & Central America | 10278 | 13351 | 17085 | 17285 | 19220 | 17519 | 17961 | 20131 | 21703 | 22442 | 22378 |
| Total Europe & Eurasia | 5269 | 7021 | 8482 | 10646 | 11604 | 10876 | 11734 | 12503 | 14445 | 14012 | 13777 |
| Total Middle East | – | – | – | – | 5 | 5 | 5 | 5 | 5 | 5 | 5 |
| Total Africa | 9 | 6 | 11 | 18 | 8 | 8 | 23 | 32 | 40 | 40 | 40 |
| Total Asia Pacific | 1446 | 1876 | 3074 | 3435 | 4306 | 5280 | 6300 | 7450 | 9374 | 8476 | 9110 |
| **Total World** | **27848** | **37471** | **50138** | **55936** | **64008** | **65834** | **66863** | **72293** | **79703** | **80024** | **82306** |

Annually, about 220 billion tons (oven–dried) biomass availability is being considered as the world's largest sustainable energy resource (World Energy Council, 2004). Thus, the biomass has remarkable potentials to provide societal needs of all useable forms of energies (electricity, heat and transportation fuels), organic chemicals and polymers. Thus, new engineering concepts are incessantly advancing to produce a range of biofuels and variety of bio–products from biomass. The complex biomass processing technologies are analogous to today's integrated petroleum refinery and petrochemical industries commonly known as biorefinery (Kamm and Kamm, 2007).

The global annual production of sugarcane is 171 million metric tons in 2016/17. Sugarcane bagasse, residue left after the extraction of juice from sugar cane, availability as a source of lignocellulosic biomass for the production of biofuels and biochemicals in the world is in–line with the production capacity of sugar cane. With annual production of 330 million tons of sugarcane in 2016/17, India stands second in the world (after Brazil) in sugarcane production. Most of the sugarcane is utilized for sugar production. The sugarcane bagasse left over after crushing of sugarcane is a potential low cost feedstock for fermentation–based biofuels and biochemicals production due to its high cellulose and hemicellulose content. Production of biofuels and biochemicals from lignocellulosic biomass essentially involves two steps: hydrolysis of hemicellulosic and cellulosic fractions of biomass followed by fermentation of the reducible sugars in the hydrolysate.

Werpy and Petersen (2004) reported that top 12 building block chemicals (platform chemicals) have been produced from biomass. The top 12 building block chemicals have been produced from sugars via biological or chemical conversions. These can subsequently be converted to various derivative chemicals. Xylitol is among the top 12 platform chemical produced from biomass either in chemical or biological routes. The annual xylitol market size and revenue forcast from 2013 to 2024 is given in Fig. 1.1. The global xylitol market size and the revenue obtained from it were 160 million metric tons and 700 million US dollar, respectively in 2013. By

2024, xylitol market size and the revenue obtained from it will have expected to be 310 million metric tons and 1100 million US dollars, respectively. This indicates that xylitol market volume grows 6.5% annually.


**Figure 1.1.** Xylitol market volume size and revenue forcast (Source: *http://www.grandviewresearch.com/industry-analysis/xylitol-market*)

The main actors in the international trade of chemicals (top 10 countries and EU–28) in 2016 are given in Table 1.5 (Eurostat, 2017). The trade balance in all countries except EU–28, South Korea and Singapore was negative value (Table 1.5) indicating that import of chemicals is greater than export of chemicals. Thus, countries are expected to produce more bio–based chemicals from low cost lignocellulosic biomass to satisfy their societal needs and also to balance the import/export trade.

**Table 1.5.** Trade of chemicals in top 10 countries and EU–28 in 2016 (Eurostat: August, 2017)

| Countries | Exports | Imports | Trade balance | Total trade |
|---|---|---|---|---|
| EU–28 | 313.6 | 185.1 | 128.4 | 498.7 |
| United States | 189.0 | 200.2 | –11.2 | 389.1 |
| China | 110.1 | 148.3 | –38.1 | 258.4 |
| Japan | 58.1 | 58.8 | –0.7 | 117.0 |
| South Korea | 53.7 | 38.8 | 15.0 | 92.5 |
| India | 33.3 | 39.1 | –5.8 | 72.3 |
| Canada | 32.9 | 39.3 | –6.4 | 72.3 |
| Singapore | 41.7 | 20.9 | 20.8 | 62.6 |
| Mexico | 12.3 | 37.1 | –24.8 | 49.3 |
| Brazil | 10.0 | 30.8 | –20.8 | 40.7 |
| Russia | 14.2 | 24.7 | –10.4 | 38.9 |

## 1.2 Biorefinery concept

A major global energy and value–added products produced from crude oil in petroleum refinery. However, the on–going price increase of crude oil, their uncertain availability, and their environmental concerns, alternative solutions able to alleviate climate change and reduce the consumption of fossil fuels should be promoted in the near future. Therefore, the replacement of crude oil with biomass as raw material for enery and chemical production is an interesting option and is the driving force for the development of today's biorefinery concept. US Department of Energy (DOE) defined biorefinery as a "processing plant where biomass feedstocks are transformed and extracted into a spectrum of valuable products". American National Renewable Energy Laboratory (NREL) defined "a biorefinery is a facility that integrates biomass conversion processes and equipment to produce fuels, power and chemicals from biomass". These definitions of biorefinery (shown in Fig. 1.2) are analogous to today's integrated petroleum refinery and petrochemical industry that produce various fuels and chemicals from crude oil. As depicted in Fig. 1.2 in biorefinery, almost all types of biomass feedstocks can be converted to different

classes of biofuels and biochemicals through jointly applied conversion technologies. The conversion technologies may be either catalytic chemical conversion or biological route. Figure 1.3 shows the integration of conventional sugarcane processing mills in modern biorefinery for the production of energy, biofuels and value–added chemicals such as xylitol.

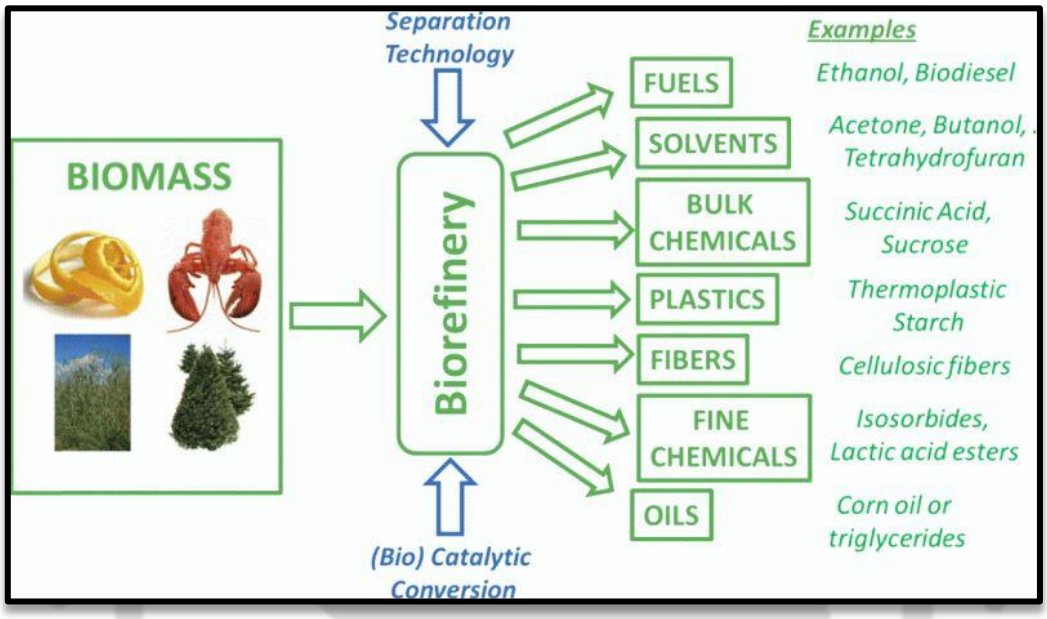


**Figure 1.2.** Schematic diagram of biorefinery (*Source:* https://labiotech.eu/features/biorefinery-review-europe-biobased/)

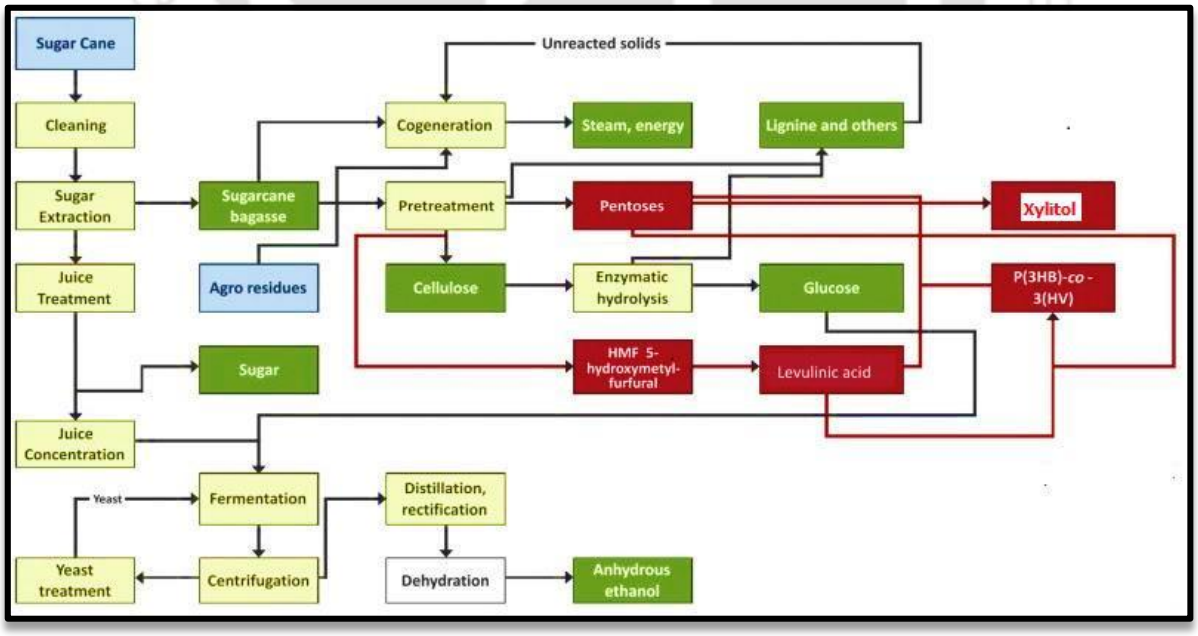


**Figure 1.3.** Integration of conventional sugarcane processing mills in modern biorefinery (*Adopted from Silva et al., 2014*)

## 1.3 Types of modern biorefinery

The classification of biorefinery includes all biomass ranges and is based on known conversion technologies. Thus, biorefinery is classified in to 3 broad categories based on the chemical nature of biomass. These are: (1) Triglyceride biorefinery, in which biodiesel as a main product and glycerol as by–product is produced with successful technologies of alkali, acid or enzyme catalyzed transesterification process. Glycerol can be further converted into various biofuels and biochemicals. (2) Sugar and starchy biorifinery, the fermentative conversion of the carbohydrate (starch) to bioethanol for the application of gasoline additives. The bioethanol can be also transformed to various petrochemical building blocks and organic chemicals. (3) Lignocellulosic biorefinery, the conversion of lignocellulosic biomass in to various fuels and chemicals through chemical routes such as combustion, gasification and pyrolysis or microbial and enzymatic fermentative route.

A set of building block chemicals (platform chemicals) are derived from petrochemical industry. Similarly, as mentioned earlier, building block chemicals can also be produced from biomass in biorefinery. 12 top value–added chemicals were screened as building block chemicals (platform chemicals) based on their potential markets and technical complexity of production route (NREL, 2004). List of platform chemicals with chemical structure and derivatives obtained from them is shown in Table 1.6. The platform chemicals can be converted to other derivatives through chemical or biological routes.

**Table 1.6.** List of platform chemicals with chemical structure and their derivatives

| List of platform chemicals | Chemical structure | Derivatives |
|---|---|---|
| 1,4–Diacids | 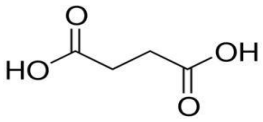 | 1,4– Butadanol, Butyrolacetone, 1,4–Diaminobutane, Succinonitrile etc. |

| | | |
|---|---|---|
| 3–Hydroxypropanoic acid | 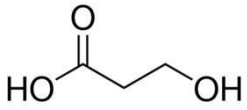 | 1,3–Propanediol, Acrylonitrile, Propiolactone etc. |
| Aspartic acid | 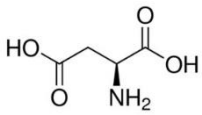 | Amino–2–pyrrolidone, –Amino–1,4–butanediol, Aspartic anhydride etc. |
| Glucaric acid | 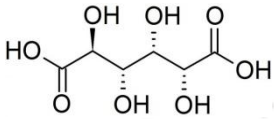 | Glucarodilactone, Glucaro–γ–lactone, Polyhydroxypolyamides etc. |
| Glutamic acid | 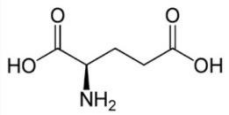 | Polyglutamic acid, Glutaminol, Proline etc. |
| Itaconic acid | 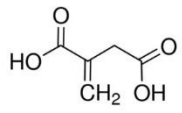 | Itaconic diamide, 2–Methyl–1,4–butanediamine, 3–Methylpyrrolidine etc. |
| Levulinic acid | 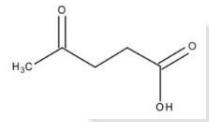 | Levulinate esters, Diphenolic acid, 1,4–Pentanediol etc. |
| 3–Hydroxybutyrolactone | 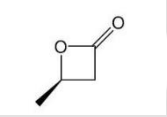 | 3–Hydroxytetrahydrofuran, Epoxy–lactone, Acrylate–lactone etc. |
| Glycerol | 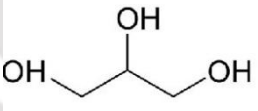 | Propylene glycol, Propanol, Glycerol carbonate etc. |
| Sorbitol (Alcohol Sugar of Glucose) | 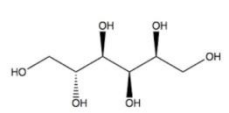 | Ethylene glycol, 1,4–Sorbitan, Propylene glycol etc. |
| Xylitol/arabinitol (Sugar alcohols from xylose/ arabinose) | 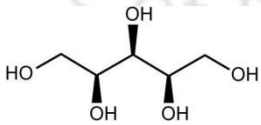 | Xylaric Acid, Mixture of Hydroxy furans, Lactic acid etc. |

## 1.4 Challenges of biorefinery

Lignocellulosic biomass is the most abundant and inexpensive source of sugars. Thus, lignocellulosic biomass has enormous potentials to meet societal needs of energy, fuels and chemicals. However, the following factors which affect the integration of lignocellulosic biomass

(biorefinery) for the production of biofuels and biochemicals – mostly through biochemical (or more specifically fermentative) route. These are: (1) feedstock diversity, (2) biomass collection and transportation logistics, (3) compatibility with refinery infrastructure, (4) market and economic viability, (5) sustainability, (6) seasonal variation and land usage, and (7) consistent research and development investment. To solve the aforementioned challenges of biorefinery, government, academia and industry has made significant contributions in developing feed stock and technologies to foster growth of biorefinery. However, most of these technologies are in early stages of development. Thus, continuous and consistent supports are crucial for scientific understanding and technological development of cost–effective biorefinery processes (Taylor et al., 2008).

## 1.5 Aim, Approach and Scope of the Present Thesis

The present research work was aimed at: (1) dilute acid hydrolysis of sugarcane bagasse to obtained fermentable pentose rich (xylose) hemicellulosic hydrolysate, (2) fermentation of pentose rich hydrolysate for the production of xylitol, and (3) intensification of the fermentation process for xylitol production. The microorganism used for fermentation is a natural isolate of *Candida tropicalis*, which is a widely used strain for xylitol production. In addition to fermentation with free cells of *C. tropicalis*, the present study also involved use of immobilized cells of *C. tropicalis*, as immobilized microbial cultures are highly suited for large scale operations. Commercial polyurethane foam (PU foam) was selected as immobilization support due its highly porous structure with large surface area. This thesis essentially describes a step–by–step approach for optimization and modelling of dilute acid hydrolysis of sugarcane bagasse to obtained fermentable pentose rich (xylose) hydrolysate as a substrate for subsequent fermentation followed by optimization, modelling, and intensification of the fermentation of pentose rich (xylose) hydrolysate for xylitol production. The thesis comprises of 7 chapters (including the present one) that describes various results of dilute acid hydrolysis of sugarcane

bagasse and the fermentation of pentose rich hydrolysate for xylitol production. The content of each chapter is briefly outlined below:

- Chapter 1 presents general introduction to the subject matter of the thesis. We have given comprehensive data for the global energy consumption, biofuel production, biomass production capacity for the production of biofuels and biochemicals, import/export trade balance. We have also highlighted the concept of biorefinery and its present challenges.
- Chapter 2 presents a brief literature review of pretreatment and hydrolysis of lignocellulosic biomass; fermentation aspects of xylitol production using free and immobilized cells, and the techniques of intensification of the bioconversion process.
- Chapter 3 describes optimization of process parameters (temperature, acid concentration, solid to liquid ratio and hydrolysis time) for dilute acid hydrolysis of sugarcane bagasse to obtain pentose rich (maximum xylose yield) hydrolysate for subsequent xylitol production.
- Chapter 4 deals with kinetic and thermodynamic analysis of dilute acid hydrolysis of sugarcane bagasse. In this chapter experimental time profiles of various pentose and hexose sugars from dilute acid hydrolysis were fitted to the biphasic model to obtain the kinetic parameters. Different thermodynamic parameters were also determined using thermodynamic equations.
- Chapter 5 presents statistical optimization of medium components and process parameters for xylitol production using immobilized *C. tropicalis* on PU foam. We have devised a two–step procedure for statistical optimization of medium components viz. Plackett–Burman design followed by central composite design. The four process parameters (viz. temperature, pH, substrate concentration and shaking speed) were optimized using central composite design.
- Chapter 6 addresses the mathematical modelling of the fermentation of pentose rich hydrolyste for production of xylitol using *C. tropicalis* cells at optimum condition. This chapter also describes the important facets of intensification of the fermentation process for

xylitol production with free and immobilized *C. tropicalis* cells using sonication or ultrasound irradiation. Sonication of fermentation mixture at optimum conditions was carried out in ultrasound bath at 37 kHz and 10% duty cycle. Time profiles of glucose, xylose, biomass and xylitol were fitted to the adopted model equations to determine the model kinetic parameters using Genetic Algorithm (GA) optimization. Analysis of the kinetic parameters of the model gives mechanistic investigations of the fermentation of the hydrolysate.

- Chapter 7 summarizes the results and overall conclusion of the thesis. Some suggestions have been made to carry the present work forward to an advance level.

**References**

Balat, M. and Ayar, G., 2005. Biomass energy in the world, use of biomass and potential trends. Energy sources, 27(10), 931–940.

BP statistical Review of World Energy June 2017. bp.com/statisticalreview

Fernando, S., Adhikari, S., Chandrapal, C. and Murali, N., 2006. Biorefineries: current status, challenges, and future direction. Energy Fuels, 20(4), 1727–1737.

Kamm, B. and Kamm, M., 2007. Biorefineries multi–product processes. White Biotechnol. 175–204, Springer Berlin Heidelberg.

Taylor, G., 2008. Biofuels and the biorefinery concept. Energy policy, 36(12), 4406–4409.

Werpy, T. and Petersen, G., 2004. US Department of Energy, Top Value Added Chemicals from Biomass. Volume I-Results of Screening for Potential Candidates from Sugars and Synthesis Gas.

World Energy Council, Survey of Energy Resources, Elsevier, Oxford, UK, 20th edition, 2004.

# CHAPTER 2

# XYLITOL BIOPRODUCTION FROM LIGNOCELLULOSIC BIOMASS: LITERATURE REVIEW AND ANALYSIS

# CHAPTER 2

# XYLITOL BIOPRODUCTION FROM LIGNOCELLULOSIC BIOMASS: LITERATURE REVIEW AND ANALYSIS

## 2.1 Introduction

Lignocellulosic biomass (LCB) represents an abundant and inexpensive source of sugars, which can be biotransformed into various value–added products. Among these products, xylitol has received much attention worldwide. Xylitol, a pentahydroxy sugar alcohol, is a value–added chemical and is naturally found in small amounts in various fruits and vegetables. The most important application of xylitol is its use as an ideal sweetener for people suffering from diabetes and obesity because of its insulin–independent metabolism and low calories (Rafiqul and Sakinah, 2013). Morover, xylitol is identified as one of the top 12 high–value products that can be manufactured from LCBs. It can also serve as a valuable building block for the synthesis of various industrially important chemicals such as lactic acid, glycols, xylaric acid etc. (Li et al., 2013). Industrially, xylitol is produced by chemical hydrogenation of pure xylose in the presence of a nickel catalyst at elevated temperature and pressure. The chemical process has some disadvantages such as a high energy requirement, extensive separation and purification steps, being laborious, and an expensive product (Rafiqul and Sakinah, 2013). Biotechnological approaches for xylitol production are based on the utilization of microorganisms or isolated enzymes.

In the following sections and subsections we have reviewed the three major parts of the thesis: (1) conversion of lignocellulosic biomass (sugarcane bagasse) to pentose rich hydrolysate (xylose) or preparation of substrate for xylitol production, which includes the characteristics and composition of biomass, pretreatment of biomass, fermentation inhibitors and their detoxification strategies to reduce their effect on fermentation; (2) fermentation of pentose rich hydrolysate (xylose) for xylitol production, which describes xylitol fermentation routes (viz. chemical or biological route), microorganisms for xylitol production and metabolic pathway of xylose fermentation, parameters which affect the fermentation process, xylitol production using free and immobilized cells ; and (3) intensification of the fermentation process using ultrasound irradiation.

## 2.2 Characteristics of lignocellulosic biomass

### 2.2.1 Composition

Cellulose, hemicellulose and lignin are the major components of lignocellulosic biomass. Moreover, it also consists of extractives, ash and others (Harmsen et al., 2010). The composition of lignocellulosic biomass largely depends on its sources. It also depends on the following conditions: (1) plant genetics, (2) growth conditions, (3) age, and (4) processing conditions (Rafiqul and Sakinah, 2013). The average composition of different lignocellulosic biomass as reported by Sun and Cheng, (2002) is summarized in Table 2.1. The composition of sugarcane bagasse reported by various authors is summarized in Table 2.2.

**Table 2.1.** Composition of various lignocellulosic biomass on dry basis (Sun and Cheng, 2002)

| Lignocellulosic materials | Cellulose (%) | Hemicellulose (%) | Lignin (%) |
|---|---|---|---|
| Hardwoods stems | 40−55 | 24−40 | 18−25 |
| Softwoods stems | 45–50 | 25−35 | 25−35 |
| Corn cobs | 45 | 35 | 15 |
| Wheat straw | 30 | 50 | 15 |
| Switchgrass | 45 | 31.4 | 12 |
| Nut shells | 25−30 | 25−30 | 30−40 |
| Grasses | 25–40 | 35−50 | 10−30 |

| | | | |
|---|---|---|---|
| Pine | 40−45 | 25−30 | 26−34 |
| Maple | 45−50 | 21−36 | 22−30 |
| Moso bamboo | 42−50 | 24−28 | 24−26 |
| Rice straw | 41−57 | 33 | 8−19 |
| Rice husk | 35−45 | 19−25 | 20 |
| Bagasse | 40−46 | 25−29 | 12.5−20 |
| Cotton stalk | 43−44 | 27 | 27 |

**Table 2.2.** Average composition of sugarcane bagasse on dry basis

| Cellulose (%) | Hemicellulose %) | Lignin (%) | Extractives (%) | Ash (%) | References |
|---|---|---|---|---|---|
| 36.38 ± 1.3 | 34 ± 0.9 | 27.16 ± 0.6 | 2.46 ± 0.2 | - | Present study |
| 35.28 | 33.28 | 25.20 | 2.14 | 4.1 | Adeeyo et al. 2015 |
| 40.15 | 22.78 | 20.81 | 15.1 | - | Timung et al. 2016 |
| 39 | 26.2 | 24 | - | - | Aguilar et al. 2002 |
| 32–44 | 27–32 | 19–24 | – | 4.5–9 | Soccol et al. 2010 |
| 45.5 | 27 | 21.1 | 4.6 | 2.2 | de Moraes Rocha et al. 2011 |
| 47−51 | 27−29 | 20−21 | 0.8−3 | – | Bertoti et al. 2009 |

### 2.2.2 Structure

As stated earlier, lignocellulosic biomass has a complex internal structure. In the foregoing subsections, we have described the structure and physical properties of the major components of lignocellulosic biomass.

#### 2.2.2.1 Cellulose

Cellulose is the major component in lignocellulosic biomass, comprising ~30–50 wt% of it. Cellulose is a polymer of D–glucose units which condense through β (1–4)–glycosidic bonds (Fig. 2.1). The linkage in cellulose is different from that for α (1–4)–glycosidic bonds present in other polymers such as starch or glycogen. It is a linear, un–branched homo–polysaccharide

molecule comprising of 800–10000 degree of polymerization, i.e. the number of glucose units that make up one polymer molecule (Kirk–Othmer, 2001). Cellulose has the following properties: (1) the linear chains in cellulose are highly stable and resistant to chemical or enzyme attacks, (2) the polymer is more rigid because of hydrogen bonding between cellulose chains, (3) cellulose molecules have a strong tendency to form intramolecular and intermolecular hydrogen bonds which may result in several ordered crystalline arrangements (Nelson et al., 2008). Cellulose molecules are aggregated together and form micro–fibrils, in which highly ordered (crystalline) regions alternate with less ordered (amorphous) regions resulting in low accessibility to enzymes. The susceptibility of cellulose to hydrolysis is determined by its degree of crystallinity and degree of polymerization. It has been shown that the amorphous portion can easily be hydrolyzed while the crystalline portion is more resistant to hydrolysis (Zhang et al., 2007)

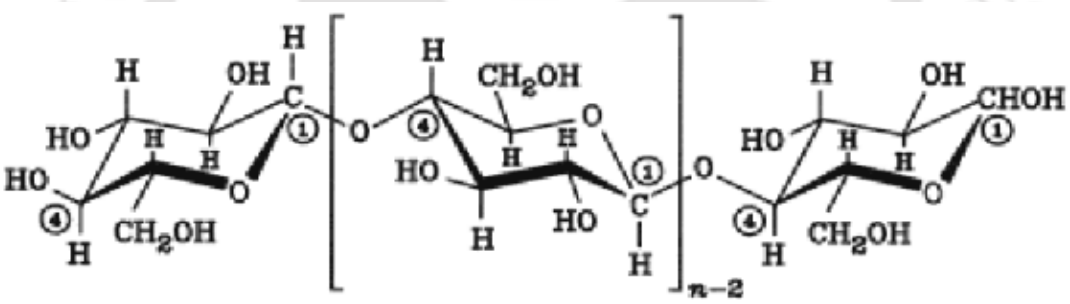

**Figure 2.1.** Schematic diagram of single cellulose molecule (*Adopted from Harmsen et al., 2010*)

### 2.2.2.2 Hemicellulose

Hemicellulose is the second most common polysaccharides, which represents 20–40 wt% of lignocellulosic biomass. Unlike cellulose, hemicelluloses are not chemically homogeneous; they are highly complex, branched polymers made up of pentoses (xylose, arabinose), hexoses (mannose, glucose, and galactose) and sugar acid. Lignocellulosic biomass such as corn stover and sugarcane bagasse, contain large amounts of xylan, some arabinan, and only very small amounts of mannan. Hardwood hemicellulose mostly contains xylans while softwood hemicellulose contains large amounts of glucomannan. Xylan is the most abundant hemicellulose, while in softwoods mannan tends to be the most abundant hemicellulose.

The structure of xylan is characterized by a long linear backbone chain of 1,4–β–D–xylopyranose units (Fig. 2.2). The frequency and composition of branches are dependent on the source of xylan (Aspinall, 1980). The side chains consist of O–acetyl, α–L–arabinofuranosyl, α–1,2–linked glucuronic or 4–O–methylglucuronic acid. The degree of polymerization of hemicellulose is about 500–3000 which is much lower than cellulose. Hemicellulose is the most thermal and chemical sensitive among the three main components of biomass due to its amorphous structure and low degree of polymerization. It is the first main component to be hydrolysed by acid pretreatment (Schell, 2003).

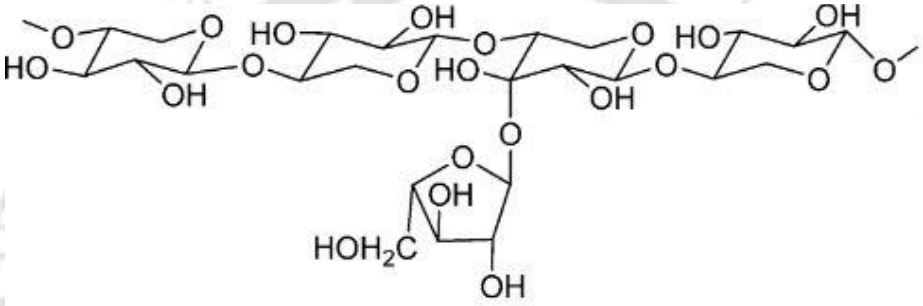


**Figure 2.2.** Schematic diagram of hemicellulose molecule (*Adopted from Dutta et al., 2012*)

### 2.2.2.3 Lignin

Lignin is the major non–carbohydrate component of lignocellulosic biomass comprising of 15–25 wt%. Lignin is a complex phenylpropanoid polymer that gives a vital role in providing structural rigidity to bind plant fibers together. Coniferyl alcohol, sinapyl alcohol and p–coumaryl alcohol are the main substituents of lignin (Fig. 2.3). These constituents are linked together via β–O–4, α–O–4, β–5, β–1, 5–5, 4–O–5 and β–β linkages (Buranov and Mazza, 2008). As compared to hardwood, lignin from softwood is made up of more than 90% of coniferyl alcohol with the remaining being mainly p–coumaryl alcohol units. However, lignin contained in hardwood is made up of varying ratios of coniferyl and sinapyl alcohol type of units (Kirk–Othmer, 2001).

Like hemicellulose polydispersity characterizes lignin as well. Different branching and bonding of similar molecules are encountered in lignin (Lin and Lin, 2002). Lignin in wood behaves as an insoluble three–dimensional network. It plays a vital function in the cell's strength and

development, as it influences the transport of water, nutrients and metabolites in the plant cell. Lignin acts as binder between cells creating a composite material that has a remarkable resistance to impact, compression and bending.

Lignin can be significantly dissolved in solvents such as low molecular alcohols, di–oxane, acetone dimethyl sulfoxide, and pyridine. Moreover, thermal softening of lignin takes place at elevated temperatures, which allows depolymeristation reactions of acidic or alkaline nature to accelerate (O'Connor et al., 2007). The lignin must be separated from carbohydrates during lignocellulosic biomass conversion to open the protective biomass structure.

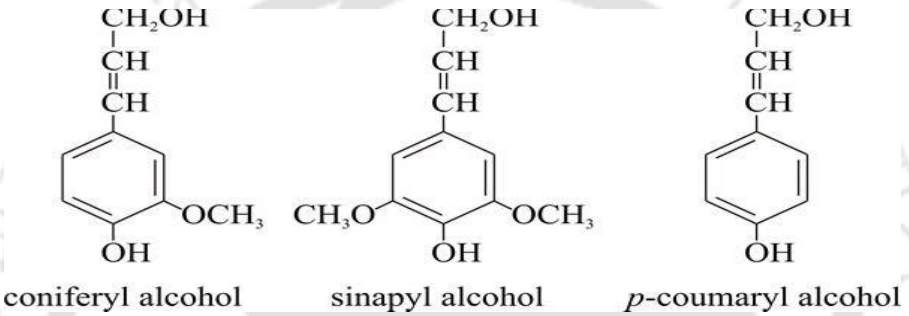


**Figure 2.3.** Schematic diagram of the three common constituents of lignin (*Adopted from Moore et al., 2011*)

## 2.3 Pretreatment of lignocellulosic biomass

### 2.3.1 Need for pretreatment

Pretreatment is a vital process step for the biochemical conversion of lignocellulosic biomass into biofuels and biochemicals. Thus, it is required to change the structure of cellulosic biomass to make cellulose more susceptible to the enzymes that convert the carbohydrate polymers into fermentable sugars (Mosier et al., 2005). Pretreatment has been recognised as one of the most expensive processing steps in cellulosic biomass–to–fermentable sugars conversion. As shown in Fig. 2.4, the overall purpose of pretreatment is to break down the shield formed by lignin and hemicellulose, disrupt the crystalline structure and reduce the degree of polymerization of cellulose (Mosier et al., 2005).

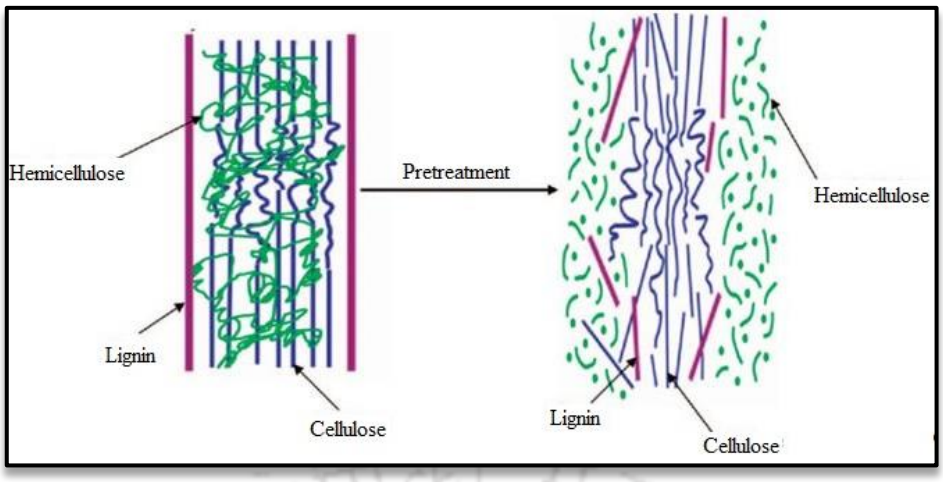


**Figure 2.4.** Effect of pretreatment on lignocellulosic biomass (*Adopted from Mosier et al., 2005*)

Pretreatment involves the change of biomass such that hydrolysis of cellulose and hemicellulose can be achieved more rapidly and with greater yields. The following are the possible goals of pretreatment of lignocellulosic biomass: (1) increase the surface area and porosity, (2) modification of lignin structure, (3) removal of lignin, (4) partial or total depolymerization of hemicellulose, (5) removal of hemicellulose, and (6) reduce the crystallinity of cellulose (Kumar et al., 2009). An effective pretreatment should avoid the need for reducing the size of biomass particle, preserves the pentose (hemicellulose) fractions, limit the formation of degradation products that inhibit the growth of fermentative microorganism, minimize energy demands and the pretreatment agent should have low cost and be capable of recycling inexpensively (Karp et al., 2013). In the foregoing subsections, the most common pretreatment techniques of lignocellulosic biomass are described.

### 2.3.2 Physical pretreatment

Physical pretreatment does not involve the use of chemicals. Physical pretreatment methods disrupt the structural integrity of lignocellulosic substrates and thereby increase their accessibility to acids or enzymes. Various types of physical pretreatment methods which can improve the efficiency of lignocellulosic saccharification include reducing size through chipping, grinding, or

milling and irradiation by gamma rays, electron beam or microwave (Taherzadeh and Karimi, 2008). The power required for physical pretreatment is usually very high. Thus, due to its high cost, physical pretreatment is not considered an attractive option in lignocellulosic biomass pretreatment.

#### 2.3.2.1 Mechanical pretreatment

Reduction of particle size is often needed to make material handling easier and to increase surface/volume ratio. This can be done by chipping, milling or grinding. The desired particle size to be obtained due to size reduction process is dependent on subsequent need of the processing steps. For mechanical pretreatment factors such as requirements of power, capital costs, operating costs, scale–up possibilities and depreciation of equipment are very crucial.

#### 2.3.2.2 Ultrasonic pretreatment

Ultrasonic pretreatment for lignocellulosic biomass is physical pretreatment and investigated at laboratory scale. It is a familiar technique for treatment of sludge from waste water treatment plants. Imai et al. (2004) reported that when a suspension of cellulose is provided with energy by ultrasound irradiation, the reaction rate of the subsequent enzymatic hydrolysis is increased by approximately 200%. The mode of action of ultrasound irradiation is not investigated so far. Probably, it is the hydrogen bonds of the cellulose crystalline structure that break if treated with enough energy of ultrasound.

### 2.3.3 Chemical pretreatment

Chemical pretreatment methods involve the use of acids, alkali, ammonia, organic solvents, oxidative agents and other chemicals. These methods are effective and give good conversion yields in less span of time. However, the chemical used in the treatment has to be recovered after the process which needs additional energy input.

#### 2.3.3.1 Acid pretreatment (acid hydrolysis)

Acid treatment is one of the most effective pretreatment methods for lignocellulosic biomass. Various acids such as sulfuric acid, hydrochloric acid, phosphoric acid, and nitric acid can be used in this process (Kim and Mazza, 2008). The concentrated acid process has relatively high sugar yield with very little sugar degradation. However, it is extremely difficult to recover most of the acid, thus making this process economically unfeasible. Dilute acid processes have been most favored for industrial application, since these processes achieve reasonable high sugar yields from hemicellulose. Lignin is not removed and the cellulose crystallinity is not affected at these pretreatment conditions (Sun and Cheng, 2002, 2005; Hsu et al., 2010). In addition to the hydrolysis of hemicellulose, dilute acid pretreatment decreases the degree polymerization of cellulose, thus, improves the remaining cellulose susceptibility to enzymes. Since the hemicellulose can be used for the production of biofuels and other value–added products, the liquid stream rich in hemicellulose is used as a substrate for fermentation. Certain levels of furfural and lignin degradation products will be produced during the dilute acid pretreatment process. These are inhibitory to fermentation organisms and/or enzymes. So, a detoxification step is usually needed to both neutralize and detoxify the pretreatment liquor. Another disadvantage of the dilute acid process is that it requires a significant investment in equipment and materials as a consequence of frequent replacement due to acid corrosion (Guo et al., 2008; Zhu et al., 2009).

#### 2.3.3.2 Alkaline pretreatment (Alkaline hydrolysis)

Unlike the acid process, alkaline pretreatment is more effective for delignification. Only minor amounts of cellulose and hemicellulose are solubilized (Carvalheiro et al., 2008). Alkaline hydrolysis induces swelling which leads to an increase in the internal surface area. Next, a decrease in the degree of polymerization and crystallinity occurs with a consequent cleavage of lignin–hemicellulose bonds. Then, degradation of lignin takes place. Reagents used in alkaline pretreatment can be categorized into two groups: (1) sodium hydroxide, potassium hydroxide, or

calcium hydroxide; and (2) ammonia. Sodium hydroxide and lime are stronger reagents as compared to ammonia. For lignocellulosic feedstocks with higher lignin content, NaOH is a better delignifying reagent since those feedstocks are more recalcitrant. Ammonia, on the other hand, shows higher efficiencies in the pretreatment of agricultural residues that have low lignin content. Recovery of the reagents is an important part of alkaline pretreatment. The recovery of sodium hydroxide has been well documented and the high volatility of ammonia makes it easy to recover and reuse. However, the main disadvantage of these alkaline reagents is that they are expensive.

#### 2.3.3.3 Organosolv pretreatment

Organosolv pretreatment uses organic solvents such as ethanol, acetone, carboxylic acid, etc. as reagents. This process is usually operated at a high temperature and pressure (Zhao et al., 2009; Hallac et al., 2010). Lignin and hemicellulose can be solubilized while cellulose is protected from solubilization. The advantage of organosolv pretreatment is that the organic solvents are recoverable through distillation and are recycled for pretreatment. However, organosolv pretreatment must be performed under extremely tight and efficient control due to the volatility of organic solvent. Therefore, organosolv pretreatment is not a feasible choice at present.

#### 2.3.3.4 Oxidative delignification

Delignification of lignocellulose can also be achieved by treatment with an oxidising agent such as hydrogen peroxide, ozone, oxygen or air (Zhang et al., 2007). The effectiveness in delignification can be attributed to the high reactivity of oxidising chemicals with the aromatic ring. Thus, the lignin polymer will be converted into carboxylic acids. Since these acids formed will act as inhibitors in the fermentation step, they have to be neutralized or removed. In addition to an effect on lignin, oxidative treatment also affects the hemicellulose fraction of the lignocellulose complex. A substantial part of the hemicellulose might be degraded and can no longer be used for sugar production (Sun and Cheng, 2002).

#### 2.3.3.5 Pretreatment with ionic liquids

Ionic liquids are salts that are in the liquid phase at temperature as low as room temperature. There is a vast variety of different ionic liquids at room temperature; however, they share a common characteristic, which is that they are usually comprised of an inorganic anion and an organic cation of very heterogeneous molecular structure. The difference in the molecular structure renders the bonding of the ions weak enough for the salt to appear as liquid at room temperature (Van Rantwijk, 2003). There is no industrial application employing ionic liquids at room temperature. Furthermore, very limited information exists in literature to describe their action with lignocellulose (Imai et al., 2004). However, there is indication that mainly due to their polarity and in general their unique properties, they can function as selective solvents of lignin or cellulose. That would result in separation of lignin and increase of cellulose accessibility under ambient conditions and with no use of acid or alkaline solution. The formation of inhibitor compounds could also be avoided. Despite the potential this method appears to have, there are several uncertainties due to lack of experience. Among the most important ones are the ability to recover the room temperature ionic liquids used, the toxicity of the compounds, and the combination of water with room temperature ionic liquids.

#### 2.3.3.6 Steam explosion

Steam explosion (uncatalysed or catalysed) is one of the most applied pretreatment processes owing to its low use of chemicals and limited energy consumption. With this method high pressure saturated steam is injected into a batch or continuous reactor filled with biomass. During the steam injection, the temperature rises to 160–260ºC. Subsequently, as a result of sudden pressure reducation, the biomass undergoes an explosive decompression with hemicellulose degradation and lignin matrix disruption.

Results of steam–explosion pretreatment depend on residence time, temperature, particle size and moisture content (Sun and Cheng, 2002). Various studies have been carried out to try to improve

the results of steam explosion by addition of chemicals such as acid or alkali (Cara et al., 2008, Zimbardi et al., 2007). Limitations of steam explosion include the formation of degradation products such as furfural and 5–HMF that may inhibit downstream processes (Garcia–Aparicio et al., 2006).

#### 2.3.3.7 Ammonia fibre explosion (AFEX)

In the AFEX process, biomass is treated with liquid ammonia at high temperature and pressure. After a few seconds, pressure is swiftly reduced. It reduces the lignin content and removes some hemicellulose while decrystallising cellulose (Teymouri et al., 2005). The cost of ammonia and especially of ammonia recovery drives the cost of the pretreatment although ammonia is easily recovered due to its volatility.

#### 2.3.3.8 $CO_2$ explosion

The method is similar to steam and ammonia fibre explosion; high pressure $CO_2$ is injected into the batch reactor and then liberated by an explosive decompression. It is believed that $CO_2$ reacts to form carbonic acid (carbon dioxide in water), thereby improving the hydrolysis rate. Yields of $CO_2$ explosion are lower than those obtained with steam or ammonia explosion, but they are higher than those reached with enzymatic hydrolysis without pretreatment (Sun and Cheng, 2002).

### 2.3.4 Biological pretreatment

Biological pretreatment uses lignin degrading microorganisms, such as white, brown and soft rot fungi and bacteria to modify the chemical composition and/or structure of the cellulosic biomass (Kirk and Farrell, 1987). The advantage of biological pretreatment is that the enzymes and microbes are very specific, and rarely produce inhibitors or toxins and effectively degrading lignin. Also, this process requires low energy input and mild environmental conditions. But reaction times tend to be long. This slow rate, as compared to chemical treatments, has prevented

the usage of biological pretreatment in commercial scale plants (Tengerdy and Szakacs, 2003; Cardona and Sanchez, 2007).

### 2.4 Fermentation inhibitors

Pretreatment of lignocellulosic biomass may produce degradation products with an inhibitory effect on the fermentation process. These inhibitors have toxic effects on the fermenting organisms, thus reducing the yield and productivity. The level of toxicity depends in part on fermentation variables including cell physiological conditions, dissolved oxygen concentration and pH of the medium. In addition, the fermenting organisms may, to some extent, be resistant to inhibitors or may become gradually adapted to their presence. However, the optimal approach is to prevent the formation of inhibitors as much as possible through the pretreatment process conditions or other measures. The inhibitory effect of these compounds is higher when they are present together due to a synergistic effect (Mussatto and Roberto, 2004). The major types of fermentation inhibitors are discussed as follows.

#### 2.4.1 Sugar degradation products

Subsequent to hemicellulose hydrolysis, pentose sugar monomers may dehydrate to the inhibitor furfural. Similarly, hexose sugars may degrade to the toxic hydroxymethyl–furfural (HMF). Furfural and HMF affect cell growth and respiration. HMF is considered less toxic than furfural and its concentration in (hemi)cellulose hydrolysates is usually low.

It is clear that extensive degradation of (hemi)cellulose is responsible for the formation of the latter inhibitor compounds. Kinetic studies have shown that the production of furfural strongly increases with temperature and reaction time. Temperatures higher than 160$^{o}$C and residence time of acid pretreatment longer than 4 hours have been reported to be sufficient for furfural or HMF to form, with their formation being more significant at higher temperature or longer residence times (McKillip and Collin, 2002).

### 2.4.2 Lignin degradation products

A variety of compounds (viz. aromatic, polyaromatic, phenolic and aldehydic) may be released from the lignin fraction. Phenolic compounds have a considerable inhibitory effect and are more toxic (even at low concentrations) than furfural and HMF. Low molecular weight phenolics are the most toxic. Phenolic compounds cause partition and loss of integrity of cell membranes of the fermenting organisms reducing cell growth and sugar assimilation. The main factors influencing formation are process temperature and residence time. At temperatures lower than 180°C lignin degradation is negligible, if no strong acid or alkaline conditions are present.

### 2.4.3 Acetic acid

Acetic acid is derived from the acetyl groups in hemicellulose. At low pH in the fermentation medium the acetic acid is in the undissociated form, is liposoluble and diffuses into the cells. In the cell the acid dissociates causing a lowering of cell pH that inhibits cell activity. The toxicity varies according to the fermentation conditions. Since the formation of acetic acid is inherent to hemicellulose hydrolysis, its formation cannot be prevented. However, a higher fermentation pH can reduce this effect or the acid can be neutralized before fermentation.

### 2.4.4 Inhibitory extractives and heavy metal ions

Extractives are derived from the lignocellulose structure and include acidic resins, tanninic and terpene acids. These extractives are less toxic than lignin breakdown products or acetic acid. Heavy metal ions such as Fe, Cr, Ni and Cu may originate from corrosion of process equipment. Their toxicity may inhibit enzymes in the fermenting organism metabolism.

## 2.5 Detoxification of hydrolysate (reduction of fermentation inhibitors)

With the aim to eliminate the microbial growth inhibitors and to enhance the fermentability of a hydrolysate, a number of detoxification strategies have been developed including physical, chemical, and biological techniques. However, the requirements for detoxification must be studied in each case, as it is dependent upon the strain employed and chemical composition of

hydrolysate. Moreover, the effectiveness of detoxification process is also dependent on raw material, type of hydrolysis process, and microorganism employed (Rao et al., 2006). There are different approaches to reduce the inhibitory effect of hydrolysate which include use of bioconversion friendly hydrolysis process; detoxification of hydrolysate before using for fermentation; use of microorganisms which are resistant to inhibitor; conversion of toxic compounds into nontoxic. However, the detoxification may increase the production cost, it is important to apply cost effective and efficient ways to overcome detoxification (Zhu et al., 2011). Combined detoxification methodologies, i.e. chemical and biological, are more effective as compared to single treatment process on xylitol production from sugarcane bagasse and corn cob hydrolysate. Various researchers reported that pH adjustment followed by activated charcoal and resin has tremendously helped up to certain level and adaptation of microbial strain would be the better option for effective and efficient use of sugary compounds (Siti et al., 2011; Arruda et al., 2011).

## 2.6 Dilute Acid Hydrolysis of Sugarcane Bagasse

Acid treatment is one of the most effective pretreatment methods for lignocellulosic biomass. Various acids such as sulfuric acid, hydrochloric acid, phosphoric acid, and nitric acid can be used in this process (Kim and Mazza, 2008). In addition to the hydrolysis of hemicellulose, dilute acid pretreatment decreases the degree polymerization of cellulose, thus, improves the remaining cellulose susceptibility to enzymes. Since the hemicellulose can be used for the production of biofuels and other value–added products, the liquid stream rich in xylose is used as a substrate for fermentation. Certain levels of furfural and lignin degradation products will be produced during the dilute acid pretreatment process. These are inhibitory to fermentation organisms and/or enzymes. So, a detoxification step is usually needed to both neutralize and detoxify the pretreatment liquor. The effects of acid concentration, reaction time, temperature, and solid to

liquid ratio on total reducing sugar (TRS) yield of lignocellulosic biomass were reported by various authors. Literature review summary on acid hydrolysis is shown in Table 2.3.

**Table 2.3.** Summary of literature review on TRS and xylose yield on acid hydrolysis

| Lignocellulosic biomass | Hydrolysis conditions | Maximum yield | Reference |
|---|---|---|---|
| Sugarcane bagasse | 0.1–0.9 M $H_2SO_4$, 80–120$^oC$, 30–120 min, S : L; 1 : 10 | 487.50 mg/g TRS | Timung et al. 2016 |
| Spent citronella | 0.1–0.9 M $H_2SO_4$, 80–120$^oC$, 30–120 min, S : L; 1 : 10 | 452.27 mg/g TRS | Timung et al. 2016 |
| Sugarcane bagasse | 2.9% $H_2SO_4$, 130$^oC$, 30 min, S : L; 1 : 4 | 58 g/L xylose | Moutta et al. 2014 |
| Sugarcane leaves straw | 0.5–3.5% $H_2SO_4$, 110–130$^oC$, 10–60 min, S : L; 1: 2–1 : 10 | 56.5 g/L xylose | Moutta et al. 2012 |
| Sugarcane bagasse | 0.5–3.5% HCl, 140$^oC$, 30 min, S : L; 1 : 10 | 30.3 g/L xylose | Chandel et al. 2007 |
| Sugarcane bagasse | 0.25–7% $H_2SO_4$, 121$^oC$, 15–240 min, S : L; 1 : 1.7 | 24.5 g/L xylose | Pattra et al. 2008 |
| Sugarcane bagasse | 0.5–1.75% $H_2SO_4$, 121$^oC$, 27–93 min, S : L; 1 : 1.7–1 : 3.3 | 52 g/L xylose | Vargas Betancur and Pereira Jr 2010 |
| Sugarcane bagasse | 2–6% $H_2SO_4$, 100–128$^oC$, 0–300 min, S : L; 1 : 10 | 21.6 g/L xylose | Aguilar et al. 2002 |
| Sugarcane bagasse | 0.25–1.0% $H_2SO_4$, 30–121$^oC$, 15–60 min, S : L; 1 : 10–1 : 20 | 52 g/L xylose | Jonglertjunya et al. 2014 |
| Sugarcane bagasse | 0.25–1.5% $H_2SO_4$, 140–160$^oC$, 15–60 min | 37.7% xylose | Jiang et al. 2013 |
| Sugarcane bagasse | 10% $H_2SO_4$, 100$^oC$, 0–60 min | 81.50 g/L xylose | RG et al. 2012 |
| Sugarcane tops | 3% $H_2SO_4$, 60 min, 25% w/w biomass | 685 mg/g TRS | Sindhu et al. 2011 |
| Rice hulls | 0.25–1% $H_2SO_4$, 140–180$^oC$, 15–60 min | 189 mg/g TRS | Saha et al. 2005 |

## 2.7 Kinetics of Acid Hydrolysis

The kinetics of acid hydrolysis of the lignocellulosics is affected by a number of factors: feedstock characteristics such as particle shape, size, structure, composition, chemical structure of various compounds, etc., and operating conditions like time of hydrolysis/digestion, temperature, pressure, mixing intensity, etc. Various researchers have listed the difficulties in the kinetic modelling of hydrolysis because of several factors such as protection against the chemical/biological attacks to the structure of the whole cells, difficulty in the access of protons to the raw material caused by lignin hydrophobicity, interaction with other components, presence of robust bonds between units of glucose, acetyl groups, uronic acid, other sugars, lignin etc., and varying exposure of hemicellulose surface to the chemical attack during the reaction (Jensen et al., 2008, Lu et al., 2008). Analysis of kinetics of acid hydrolysis of lignocellulosic biomass has been reported by various researchers. The literature review summary on the kinetic analysis of acid hydrolysis is given in Table 2.4.

**Table 2.4.** Summary of literature review on the kinetic analysis of acid hydrolysis of various lignocellulosic biomass

| Lignocellulosic biomass | Hydrolysis conditions | Kinetic parameters of hemicellulose hydrolysis | | Kinetic parameters of xylose degradation | | References |
|---|---|---|---|---|---|---|
| | | $A$ ($min^{-1}$) | $E$ (kJ/mol) | $A$ ($min^{-1}$) | $E$ (kJ/mol) | |
| Corn stover | 110–130°C, 0.15 M $H_2SO_4$, 2–60 min | $1.4 \times 10^7$ – $6.06 \times 10^8$ | 83.2 – 83.3 | $9.17 \times 10^{13}$ | 159.6 | Jonglertjunya et al. 2014 |
| *Parthenium hysterophorus* | 150–210°C, 1–5% (w/v) $H_2SO_4$, 4–30 min | – | 14.6 – 16.3 | – | – | Swati et al. 2013 |
| Sweet sorghum | 110–150°C, 3% (w/v) $H_2SO_4$, 20–120 min | $1.8 \times 10^5$ – $3.53 \times 10^6$ | 58.1 – 60.7 | 0.62 | 14.5 | Liu et al. 2012 |
| Hazelnut shell | 100–120°C, 0.3–0.5 M $H_2SO_4$, 30–190 min | $5.4 \times 10^6$ | 52.7 | $2.9 \times 10^4$ | 46.6 | Arslan et al. 2012 |
| Corn stover | 90–100°C, 30–180 min | $1.4 \times 10^{14}$ | 111.6 | $3.3 \times 10^{10}$ | 95.7 | Jin et al. 2011 |
| Timber varieties and swichgrass | 160–190°C, 0.25–1% (w/v) $H_2SO_4$ | $7.5 \times 10^4$ – $2.6 \times 10^{20}$ | 49 – 180 | $6.8 \times 10^{13}$ – $3.7 \times 10^{17}$ | 130 – 170 | Yat et al. 2008 |
| Sugarcane bagasse | 80–200°C, 0.25–8% (w/v) $H_2SO_4$ or HCl, 10–200 min | $1.5 \times 10^6$ – $9.8 \times 10^7$ | 73.5 – 88.1 | $2.9 \times 10^{11}$ | 111.2 | Lavarack et al. 2002 |

## 2.8 Xylitol production from lignocellulosic biomass/xylose

Xylitol production from lignocellulosic biomass or pure xylose has 2 routes: (1) conventional process (chemical route), (2) biological route using microbes, or using enzymes. We have described the details of each route in the forgoing subsections.

### 2.8.1 Conventional xylitol production process (chemical route)

Although xylitol occurs in many fruits and vegetables, it would be very uneconomical to extract it from such sources due to their high cost and relatively low xylitol content. On a large scale, xylitol is currently produced by chemical reduction of xylose derived mainly from lignocellulosic biomass hydrolysate using nickel or palladium catalyst (Melaja and Hamalainen, 1977, Hyvönen et al., 1982). The conventional process of xylitol production includes four main steps: (1) acid hydrolysis of lignocellulosic biomass, (2) purification of the hydrolysate to either a pure xylose solution or a pure crystalline xylose, (3) hydrogenation of the xylose to xylitol, and (4) crystallization of the xylitol (Aminoff et al., 1978). The critical step in this process is the purification of the xylose from the acid hydrolysate. Ion exchange chromatography is employed to remove salts and charged degradation products, and activated carbon is used to remove color (Nikolaev et al., 1983; Kind et al., 1987). Ion exchange chromatography, however, does not remove or separate the various hemicellulosic sugars. This is a problem because acid hydrolysis releases appreciable amounts of D–galactose, D–mannose and L–arabinose in addition to D–xylose. The exact proportions of the various sugars depend on the nature of the feedstock and the manner in which it is hydrolyzed. The existing drawbacks of conventional xylitol production methods motivated researchers to seek alternative ways for its production. One of the most attractive procedures, today, is microbial production.

### 2.8.2 Microbial xylitol production (biological route)

Biotechnological production of xylitol was extensively studied as an alternative to the conventional xylitol production using various microbes. However, limited literatures are available

on enzymatic production of xylitol. In the foregoing sections, we have reviewed the literature on xylitol production using microbial routes.

### 2.8.2.1 Microorganisms for xylitol production

Microorganisms more readily assimilate and ferment glucose than xylose. However, there are bacteria, yeast and fungi capable of assimilating and fermenting xylose to xylitol, ethanol and other compounds (Barnett et al., 1990). A few bacteria such as *Corynebacteriurn sp*. (Yoshitake et al., 1971), *Enterobacter liquefaciens* (Yoshitake et al., 1973; Yoshitake et al., 1976), and *Mycobacterium smegmatis* (Izumori and Tuzaki, 1988) have been reported to produce xylitol. However, due to the relatively small quantities of xylitol formed, xylitol producing bacteria do not presently attract researchers' interest. Regarding the fungi, there is only one significant report regarding *Petromyces albertensis* (Dahiya, 1991). This fungus accumulated 39.8 g/L of xylitol when cultured for 10 days on 100 g/L D–xylose. Nevertheless, after initial studies regarding the effects of environmental conditions on xylitol production by this fungus, no further reports were published. In general, among microorganisms, the yeasts are considered to be the best xylitol producers and therefore, the majority of publications deal with them. Some of the yeasts screened for xylitol production are given in Table 2.5.

**Table 2.5.** Summary of native strain of yeasts for xylitol production

| Native strain of yeast | Carbon substrate | Fermentation conditions | Xylitol yield (g/g) | References |
|---|---|---|---|---|
| *C. guilliermondii* | Sucrose supplementation of sugarcane straw | Batch, 30$^{o}$C | 0.75 | Hernández et al. 2016 |
| *C. alapagoensis* | Sugarcane bagasse | Batch, pH 5.5, 200 rpm, 30°C | 0.64 | Guamán–Burneo et al. 2015 |
| *K. sp.* | Sugarcane bagasse | Batch, pH 5.0, 50°C | 0.61 | Kumar et al. 2015 |
| *K. marxianus* | glucose and xylose | Batch, pH 5.5, 45$^{o}$C | 0.88 | Arora et al. 2015 |

| | | | | |
|---|---|---|---|---|
| *P. tannophilus* | Olive stones | Batch, 30°C, 150 rpm | 0.44 | Saleh et al. 2014 |
| *D. nepalensis* | Corn cob | Batch, 30°C, 180 rpm | 0.30 | Paidimuddala and Gummadi 2014 |
| *C. magnolia* | Corn cob | Micro–aerobic condition | 0.18 | Tada et al. 2012 |
| *C. athensensis* | Horticultural waste | Batch, 30°C, 250 rpm | 0.83 | Zhang et al. 2012 |
| *C. tropicalis* | Corn cob | Batch, 35°C, 200 rpm | 0.73 | Ling Het al. 2011 |
| *P. stiptis* | Sugarcane bagasse | Batch, 30°C, pH 5.5 | 0.29 | Buaban et al. 2010 |
| *D. hansenii* | D–xylose | Micro–aerobic condition | 0.54 | Sampaio et al. 2008 |
| *C. maltosa* | D–xylose | Micro–aerobic condition | 0.43 | Guo et al. 2006 |
| *C. guilliermondii* | D–xylose | Micro–aerobic condition | 0.63 | Guo et al. 2006 |
| *H. polymorpha* | D–xylose and glycerol | pH 8, 30°C | 0.52 | Suryadi et al. 2000 |
| *C. tropicalis* | D–xylose | Aerobic condition, 30°C | 0.96 | Gong et al. 1981 |

#### 2.8.2.2 Metabolic pathway for xylose in yeast

The first step in the metabolism of D–xylose is the transport of sugar across the cell membrane. Once inside the yeast cell, D–xylose is reduced to xylitol by either NADH or NADPH dependent xylose reductase. Xylitol is either secreted from the cell or oxidized to xylulose by NAD or NADP dependent xylitol dehydrogenase. The first two reactions are considered to be limiting in D–xylose fermentation. The phosphorylation of xylulose to xylulose–5–phosphate is catalyzed by xylulokinase. The conversion of pentoses to xylulose–5–phosphate is a prerequisite for its utilization by the central catabolic pathways (Slininger et al. 1986). Xylulose–5–phosphate can

subsequently enter the pentose phosphate pathway (Fig. 2.5). This pathway consists of an oxidative phase that converts hexose phosphates to pentose phosphates providing NADPH needed in biosynthetic pathways and a non–oxidative phase in which the pentose phosphates are converted into hexose and triose phosphates (Jeffries, 1983). The pentose phosphate pathway also yields ribose–5–phosphate used for the synthesis of nucleic acids and histidine and of erythrose–4–phosphate necessary for the synthesis of aromatic amino acids. Glyceraldehyde–3–phosphate and fructose–6–phosphate are products of the non–oxidative phase of the pentose phosphate pathway. Both of them can be converted to pyruvate in the Embden–Meyerhof–Parnas pathway. Pyruvate can either be decarboxylated and reduced to ethanol or can enter the tricarboxylic acid cycle (Jeffries, 2006). The conversion of xylulose–5–phosphate into glyceraldehyde–3–phosphate and acetyl phosphate by xylulose–5–phosphate phosphoketolase presents an alternative route for the utilization of xylulose–5–phosphate (Prior et al., 1989).

Xylose metabolism in yeasts yields a variety of carbon containing products which include carbon dioxide, ethanol, acetic acid and polysaccharides. Product yields are dependent upon the regulation of carbon flow through available metabolic routes (Slininger et al. 1986). D–Xylose conversion to xylitol in yeasts cannot be separated from the conversion of D–xylose to these products. The process of xylitol formation cannot be stopped after the first step, when D–xylose is converted to xylitol. Cell growth depends on some of the above metabolic products and it is also necessary that the cofactors be regenerated through different steps in the metabolic pathway. Therefore, for obtaining good yields of xylitol, the amount of xylose being converted to xylitol and the amount of xylitol which is available for further metabolism have to be well balanced.

***Coenzyme specificity***: The first two enzymes, D–xylose reductase and xylitol dehydrogenase are key enzymes in xylitol production by yeasts. They both require pyridine nucleotide cofactors exhibiting different cofactor specificity in different yeasts. Under anaerobic or oxygen–limited conditions, the difference in the cofactor requirements of these enzymes causes a redox imbalance which influences xylitol accumulation in yeasts (Bruinenberg et al., 1984). Xylitol

formation is favored under oxygen–limited conditions, because of the NADH accumulation and subsequent inhibition of NAD linked xylitol dehydrogenase. This phenomenon, known as the Custer effect, results from the incapability of the yeasts to compensate for excess NADH as they have no trans hydrogenase activity (van Dijken and Scheffers, 1986).

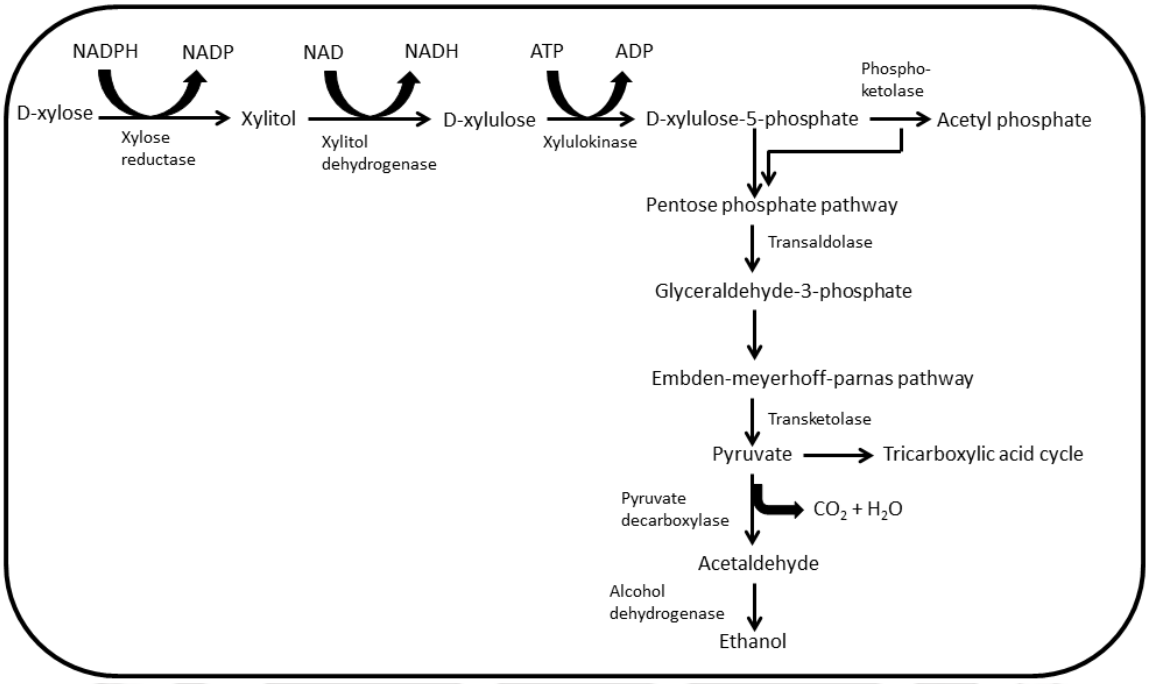


**Figure 2.5.** Schematic representation of D–xylose metabolism in yeasts (*Adopted from Jeffries, 2006*)

### 2.8.3 Factors affecting xylitol production

There are a few factors affecting xylitol production in yeasts. These are: (1) carbon source/xylose concentration, (2) co–substrate concentration, (3) aeration, (4) inoculum, (5) temperature, (6) pH, and (7) nitrogen source.

***Xylose concentration***: One of the crucial parameters that impact the yeast growth and the fermentation process is substrate concentration (D–xylose). The initial concentration of xylose can affect the xylitol production. In the case of microorganisms that can grow in high osmotic pressure conditions or in the presence of elevated glucose concentrations, a high initial xylose concentration could presumably lead to a higher quantity of xylitol. As the initial concentration of

xylose increases, oxygen level increases and thus avoiding the inhibition of the microbial growth (Ghindea et al., 2010).

***Effect of co–substrate***: When glucose is used as co–substrate in low concentration it leads to improved growth in yeast cells and the production efficiency of xylitol. This effect can be explained by the fact that the glucose is used in cell growth, D–xylose being consumed only afterwards for xylitol production (Gurpilhares et al., 2008).

***Effect of aeration***: Aeration is a key parameter for xylitol producing yeasts and determines whether D–xylose will be fermented or respired. It is found to be an effective process to determine the oxygen flux that will enable balanced utilization of carbon, both for growth and xylitol production. Prakasham et al. (2009) reported that xylitol production by yeasts is associated with micro–aerobic conditions. Several authors have reported effect of aeration and agitation rate on yeast growth and xylitol production (Branco et al., 2007, Sreenivas Rao et al., 2006, Sreenivas Rao et al., 2004).

***Effect of temperature***: The suitable temperature for xylitol production by *C. tropicalis* is 30$^{o}$C. The xylitol production may be a temperature freelance method, if the yeast is genteel at a temperature between 30$^{o}$ and 37$^{o}$C and it is found that the yield decreases dramatically higher than temperature (Ghindea et al., 2010). Sreenivas et al. (2006) reported that a variation of the 3$^{o}$C affects (27%) the assembly of xylitol. However, the conversion to xylitol by *C. sp*. B–22 has been reported constant over the temperature range of 35$^{o}$–40$^{o}$C whereas at ≥45$^{o}$C, the xylitol yield declined greatly. This could ensue to the reduction within the activities of NADPH and NADH dependent sugar enzyme.

***Effect of pH***: The ideal pH for *D. hansenii* is 5.5, though for *C. parapsilosis*, *C. guilliemondii* and *C. boidinii* the ranges are 4.5–5, 6.0, and 7.0, respectively. It has been observed that inhibition of microbial growth is due to undissociated form of acetate (Ghindea et al., 2010). However, when pH is increased, the undissociated form of acetic acid may be decreased. The optimum pH for xylitol production in *C. sp*. is 4.5–7 (Ghindea et al., 2010). According to the

observation of Cheng et al. (2009), as pH increases from 4.5 to 6.0, it leads to dramatic increase in xylitol productivity. However, the highest production of xylitol is found at pH 6.0. The finding of El–Batal and Khalaf (2004) shows that there is low xylitol production at pH 3.0 compared to pH 6.0.

***Effect of nitrogen sources***: Type and concentration of nitrogen source in the medium play a key role in influencing the xylitol production by microorganism. Palnitkar and Lachke (1992) found that xylose consumption enhanced when media were supplemented with an organic nitrogen source. These organic nitrogen sources were yeast extract and the urea by the yeasts for the production of xylitol (Tesfaw and Assefa, 2014). Lu et al., (1995) reported the effect of glycine, asparagine, urea, yeast extract, $(NH_4)_2SO_4$, $NH_4NO_3$, $NaNO_3$, $NH_4Cl$, and $NH_4H_2PO_4$ as nitrogen sources for the production of xylitol by utilizing mutant *C. sp*. L–102. The results of their study showed that maximum xylitol production was obtained with urea as the nitrogen source. A final xylitol concentration and productivity of 100 g/L and 0.46 g/g.h, respectively from 114 g/L D–xylose was obtained within 65 h of fermentation using 0.3% urea.

### 2.8.4 Xylitol production using free cells

Camargo et al. (2015) have studied biotechnological production of xylitol from hemicellulosic hydrolysate obtained from biomass of three sorghum varieties of A, B, and C using *C. guillier–mondii* in Erlenmeyer flasks containing 50 mL medium, at 200 rpm, at 30°C for 96 h. The results of the study revealed that there was no significant difference among the three varieties with respect to the contents of cellulose, hemicellulose, and lignin, although differences were found in the hydrolysate fermentability. Maximum xylitol yield and productivity of 0.35 g/g and 0.16 g/L h were obtained for variety A. Sapci et al. (2015) have studied the combined effects of different oxygen concentration, inoculum level and substrate concentration have been reported for the production of xylitol with *C. tropicalis* Kuen 1022 using cotton stalk hemicellulose hydrolysate. The results of their study revealed that under the optimum conditions (xylose concentration = 10.41 g/L, inoculum level = 0.99 g/L, airflow rate = 1.02 vvm) xylitol yield and productivity of

0.36 g/g and 0.06 g/L h were obtained from cotton stalk hydrolysate. Ping et al. (2013) have studied xylitol production using *C. tropicalis* CCTCC M2012462 from hemicellulose hydrolysate obtained from corncobs without detoxification. A maximal xylitol concentration of 38.8 g/L was obtained after 84 h of fermentation, corresponding xylitol yield and productivity of 0.7 g/g xylose and 0.46 g/L h, respectively. Huang et al. (2011) have reported xylitol production using *C. tropicalis* JH030 from a rice straw hydrolysate. The results of their study revealed that maximum xylitol concentration of 31.1 g/L, with a corresponding xylitol yield and volumetric productivity of 0.71 g/g and 0.44 g/L h, respectively were obtained. Cheng et al. (2009) have studied the effect of acetic acid in the fermentation medium on xylitol production using *C. tropicalis* W103 from corncob hydrolysate. When acetic acid concentration was lower than 2 g/L, xylose consumption by *C. tropicalis* W103 strain was not affected. The acetic acid in the medium was consumed completely if its concentration was lower than 2 g/L. The xylitol concentration, yield, and productivity of 68.4 g/L, 0.7 g/g, and 0.95 g/L h, respectively were obtained. Hernández et al. (2016) have reported bioproduction of xylitol from sugarcane straw hemicellulosic hydrolysate supplemented with maltose, sucrose, cellobiose or glycerol, and their effect as co–substrates on xylitol production by *C guilliermondii* FTI 20037. Supplementation of sucrose (10 g/L) and glycerol (0.7 g/L) led to an increase of 8.88% and 6.86% on xylose uptake rate, respectively. With only sucrose, an increment of 12.88% and 8.69% on final xylitol concentration and productivity, respectively were obtained. Based on these results, utilization of complex sources of sucrose, derived from agro industries, as nutritional supplementation for xylitol production can be proposed as a strategy for improving the yeast performance and reducing the cost of the bioprocess by replacing more expensive nutrients. Hima Bindu et al. (2012) have studied optimization of medium components on xylitol production using *D. nepalensis* NCYC 3413 and xylose as a sole carbon source. Plackett-Burman design was used to determine the specific medium components affecting xylitol production. Thus, xylose, $K_2HPO_4$, and $ZnSO_4$ were selected as a significant medium in augmenting xylitol production. These significant parameters

were further optimized using central composite design. Under these optimal conditions (xylose concentration = 100 g/L, $K_2HPO_4$, = 10.6 g/L, $ZnSO_4$ = 8.9 mg/L) the xylitol production increased from 27 g/L to 36 g/L with a yield of 0.44 g/g (57% increment in total yield). Moreover, formation of the by product (glycerol) was decreased under optimal conditions. A number of studies have focused on improvement of microbial xylitol fermentation by detoxification. After detoxification by ion exchange resins or activated charcoal adsorption, some inhibitors, such as furfural and 5-hydroxymethylfurfural, were removed totally or partly (Ding and Xia, 2006; Ko et al., 2008; Tada et al., 2004; Villarreal et al., 2006). Similar observations were reported during the detoxification of sugarcane bagasse and corncob acid catalyzed hemicellulose hydrolysate with overliming (Cheng et al., 2009; Rodrigues et al., 2003). However, detoxification resulted in the loss of sugar about 5–10% and increased unit operation. The maximum xylitol concentration and yield from these studies varied widely from 18.7 to 68.4 g/L and 0.6 to 0.76 g/g depending on the outcome of the detoxification process and the hydrolysate composition. Bioproduction of xylitol using free cells from various lignocellulosic biomass is summarized in Table 2.6.

**Table 2.6** Summary of literature on production of xylitol using free cells

| Microorganisms | Carbon Substrate Source | Xylitol | | References |
|---|---|---|---|---|
| | | Yield (g/g) | Productivity (g/L h) | |
| *C. guilliermondii* FTI 20037 | Sugarcane straw hemicellulosic hydrolysate | – | 0.75 | Hernández et al. 2016 |
| *C. guilliermondii* | Sorghum forage hemicellulosic hydrolysate | 0.35 | 0.16 | Camargo et al. 2015 |
| *C. tropicalis Kuen* 1022 | Cotton stalk hemicellulose hydrolysate | 0.36 | 0.06 | Sapci et al. 2015 |
| *C. tropicalis* CCTCC M2012462 | Corncobs hemicellulose hydrolysate | 0.70 | 0.46 | Ping et al. 2013 |

| | | | | |
|---|---|---|---|---|
| *D. nepalensis* NCYC 3413 | Xylose | 0.44 | – | Hima Bindu et al. 2012 |
| *C. tropicalis* JH030 | Rice straw hydrolysate | 0.71 | 0.44 | Huang et al. 2011 |
| *C. tropicalis* W103 | Corncob hydrolysate | 0.70 | 0.95 | Cheng et al. 2009 |
| *Candida sp*. ZU04 | Corncob hydrolysate | 0.60 | 0.32 | Ding and Xia 2006 |
| *C. tropicalis* BCRC 20520 | Hard wood hydrolysate | 0.73 | 0.54 | Ko et al. 2008 |
| *C. guilliermondii* FTI 20037 | Eucalyptus hemicellulose hydrolysate | 0.68 | 0.57 | Villarreal et al. 2006 |
| *C. magnoliae* FERMP–16522 | Corncob hydrolysate | 0.75 | 0.52 | Tada et al. 2004 |
| *C. guilliermondii* FTI 20037 | Sugarcane bagasse hydrolysate | 0.76 | 0.64 | Rodrigues et al. 2003 |

### 2.8.5 Xylitol production using immobilized cells

Due to lower yield and productivity of xylitol fermentation with free cells of microbial cells, various researchers tried to search methods of agumenting the xylitol production. Among them, use of immobilized cells using various immobilization supports was reviewed by various authors, as immobilized microbial cultures are tolerant to inhibitory by–products and drastic changes during fermentation, reuseability of the biocatalyst, and highly suited for large scale operations. In this section, we have reviewed some literature on xylitol production using immobilized cells.

Zhang et al. (2014) have studied optimization of process parameters (viz. reducing sugar concentration, initial pH value and inoculation ratio of yeast) for bioconversion of hemicellulose hydrolysate obtained from cotton stalk to xylitol by *C tropicalis* CICC 1779 immobilized on calcium alginate gel beads. The results of their study revealed that a maximum xylitol concentration of 13.02 g/L under the fermentative optimal condition of reducing sugar concentration of 94 g/L and initial pH value of 5.1 were obtained. Yewale et al. (2016) have reported different immobilization matrices/media (alginate, polyvinyl alcohol, agarose gel,

polyacrylamide, gelatin, and j-carrageenan) to immobilize *C. tropicalis* NCIM 3123 cells for xylitol production from non-detoxified corn cob hemicellulosic hydrolysate. Among this, calcium alginate immobilized cells produced maximum xylitol concentration of 11.1 g/L and yield of 0.34 g/g. Moreover, the process for immobilization using calcium alginate beads was optimized using a statistical method with sodium alginate (20, 30 and 40 g/L), calcium chloride (10, 20 and 30 g/L) and number of freezing-thawing cycles (2, 3 and 4) as the parameters. Using optimized conditions (calcium chloride 10 g/L, sodium alginate 20 g/L and 4 number of freezing-thawing cycles) for immobilization, xylitol production increased to 41.0 g/L (4 times the initial production) with a corresponding xylitol yield and productivity of 0.73 g/g and 0.43 g/L h, respectively with corn cob hydrolysate as sole carbon source and urea as minimal nutrient source. Wang et al. (2012) have also studied xylitol production from xylose containing corncob hemicellulose hydrolysate using polyurethane foam (PU foam) as a carrier for *C. tropicalis* immobilization in the multi-batches fermentation. Moreover, the effects fermentation parameters such as initial cell concentration, PU foam dosage, pH value and temperature on xylitol fermentation have been studied. In 21–day durability tests, the optimal xylitol yield and productivity reached 0.71 g/g and 2.10 g/L h, respectively. Moreover, the average xylitol yield and productivity were 0.66 g/g and 1.90 g/L h, respectively for ten batchwise operations. The research demonstrated that PU foam immobilization could serve as an efficient method for improving the cells vitality and enzyme reactivity in the continuous operation of fermentation. Wang et al. (2016) have reported the immobilization efficiency of nitric acid treated carbon fibre rich in hydrophilic groups of *C. tropicalis* and xylitol fermentation yield by investigating the surface properties of nitric acid treated carbon fibre, specifically, the acidic group content, and zero charge point, degree of moisture and contact angle. The morphology of the nitric acid treated carbon fibre was characterized using scanning electron microscopy. The results of their study revealed that adhesion is the major mechanism for cell immobilization and that it is greatly affected by the hydrophilic–hydrophilic surface properties. An optimal time of 3 h for treating

carbon fibre with nitric acid, resulted in an improved immobilized efficiency of *C. tropicalis* of 0.98 g/g and the highest xylitol yield and productivity of 0.70 g/g and 1.22 g/L h, respectively were obtained. Thus, the nitric acid treated carbon fibre represents a promising method for preparing biocompatible biocarriers for multi-batches fermentation. Pérez–Bibbins et al. (2013) have reported the influence of bead size, chitosan, bead charge, volume of liquid media, and the use of corncob hydrolysate and vinasses as culture medium on xylitol production by *D. hansenii* immobilized in alginate beads. The results of their study showed xylitol production was not affected by the size of particle; however chitosan had a negative effect. The xylitol concentration of 13.7 g/L with corresponding xylitol yield and productivity 0.56 g/g and 0.29 g/L h, respectively with the use of corn cob as a carbon source and 2–fold diluted vinasses were obtained. The results showed the feasibility of employing these cheap substrates, reflected the importance of the microaerobical conditions, and pointed to the favourable effect of cell immobilization on the metabolism of xylitol production. Pérez–Bibbins et al. (2014) have also studied the potential of the airlift bioreactor for xylitol production in fed-batch cultures by *D. hansenii* immobilized in alginate beads. The results showed that the airlift bioreactor is an adequate system for immobilization since the minimum air flow required for fluidization was even lower than that leading to the microaerobic conditions that trigger xylitol accumulation by the yeast. It is also used for maintaining the integrity of the alginate beads and the viability of the immobilized cells until 3 months of reuse. With initial xylose concentration of 60 g/L, maximum xylitol yield and productivity of 0.71 g/g and 0.43 g/L h were achieved. The xylose feeding rate, the air flow, and the biomass concentration at the beginning of the fed-batch operation have shown to be critical parameters for achieving high yields and productivities. Liaw et al. (2008) have studied xylitol production using *C. subtropicalis* WF79 cells immobilized in polyacrylic hydrogel thin films of 200 μm thickness from rice straw hemicellulose hydrolysate. The results of their study revealed that the maximum xylitol yield of 0.73 g/g of xylose was obtained from rice straw hydrolysate fermentation in an Erlenmeyer flask. De Carvalho et al. (2004) have reported

the performance of four different resins, in sequence, to detoxify sugarcane bagasse hemi–cellulosic hydrolysate and to improve xylitol production by calcium alginate-entrapped *C. guilliermondii* FTI20037 cells under conditions of low oxygen concentration. This treatment resulted in removal of 82.1% furfural, 66.5% HMF, 61.9% phenolic compounds derived from lignin degradation. On the other hand, the removal of acetic acid was not significant. Maximum xylitol yield and productivity of 0.62 g/g and 0.24 g/L h were attained in the fermentation process for xylitol production from detoxified hydrolysate. Fouad Sarrouh et al. (2007) have studied xylitol production from concentrated hemicellulose hydrolysate of sugarcane bagasse in a fluidized bed bioreactor using cells of *C. guilliermondii* entrapped in Ca alginate beads. The maximum xylitol concentration of 28.9 g/L with corresponding xylitol yield and productivity of 0.58 g/g and 0.4 g/L h, respectively was obtained at a high aeration rate of 600 mL/min after 70 h of fermentation, indicating that the use of high aeration rate in this system is favoured for better oxygen transfer into the immobilized cells. After 90 h of fermentation, xylitol yield and productivity decreased to 0.47 g/g and 0.25 g/L h, respectively indicating the beginning of xylitol consumption by the yeast. Carvalho et al. (2004) have also studied xylitol production from sugarcane bagasse hemicellulosic hydrolysate in a stirred tank reactor using *C. guilliermondii* FTI 20037 cells immobilized in Ca alginate beads. Using a five-fold concentrated hydrolysate, air flow rate of 1.30 L/min, agitation speed of 300 rpm, initial cell concentration of 1.4 g/L and initial pH value of 6.0 for the fermentation medium resulted in a maximum xylitol concentration of 47.5 g/L after 120 h of fermentation, with corresponding xylitol yield and productivity of 0.81 g/g and 0.40 g/L h, respectively. Silva et al. (2007) have studied xylitol production by *C. guilliermondii* yeast with sugarcane bagasse pretreated by three different procedures (with 2% v/v polyethyleneimine (PEI), with 2% w/v NaOH, or with a sequence of NaOH and PEI) used as cell immobilization support. Fermentations using the pretreated carriers were performed in semi defined medium and in a hydrolysate medium produced from sugarcane bagasse hemicellulose. Sugarcane bagasse pretreated with NaOH was the best carrier obtained with respect to

immobilization efficiency, because it was able to immobilize a major quantity of cells (0.30 g of cells/g of bagasse). Fermentation in semi–defined medium using the NaOH pretreated carrier attained a high efficiency of xylose to xylitol bioconversion (96% of the theoretical value). From hydrolysate medium, the bioconversion efficiency was lower (63%), probably owing to the presence of other substances in the medium that caused an inadequate mass transfer to the cells. In the fermentation medium, better results with relation to xylitol production were obtained by using PEI pretreated support (xylose to xylitol bioconversion of 81% of the theoretical and xylitol productivity of 0.43 g/L h). The results showed that sugarcane bagasse is a low cost material with great potential for use as cell immobilization support in the fermentative process for xylitol production. Soleimani and Tabil (2014) have reported the importance of aeration in free and immobilized cell systems in an aerated bioreactor for xylitol production from an oat hull hemicellulosic hydrolysate. The aeration rate (AR) or oxygen mass transfer coefficient ($k_{La}$) showed a significant role in controlling *C. guilliermondii* FTI 20037 regeneration and bioconversion performance in free and immobilized cell systems. In the free cell system, an aeration rate of 1.25 vvm corresponding to $k_{La}$ of 15.8 L/h resulted in maximum final xylitol concentration of 55 g/L with corresponding xylitol yield and productivity of 0.87 g/g and 0.57 g/L h, respectively from the hydrolysate. However, in the aerated immobilized cell system, almost similar results of xylitol concentration, yield and productivity of 54 g/L, 0.84 g/g, and 0.57 g/L h, respectively were obtained with aeration rates from 1.25 to 1.5 vvm using composites based on polypropylene (PP) and partially delignified fiber (PDF). Composites based on acid treated fiber (ATF) containing high amount of lignin showed some inhibitory impact on xylose uptake and xylitol formation (concentration 47 g/L and productivity < 0.49 g/L h) with the optimal aeration rate of 1.5 vvm in the initial cycle of the bioconversion; the inhibition impact could be resolved in the next consecutive cycles. The surface modifier polyethyleneimine (PEI) slightly enhanced cell retention in the immobilized form on the ATF-based cell support. Ding (2011) have studied batch xylitol production from corn cob hemicellulosic hydrolysate carried

out in a three phase fluidized bed bioreactor using immobilized *C. sp*. ZU04 cells. The results of their study revealed that two phase aeration process was more effective than single phase process in xylitol production. In the first 24 h of aerobic phase, glucose was soon consumed and biomass in the Ca alginate beads increased quickly at high aeration rate of 1.00 vvm. In the second fermentation phase, aeration rate was reduced to 0.30 vvm and the xylitol yield increased remarkably. The immobilized cells could be reused successfully for 6 batch cycles with average xylitol yield of 0.73 g/g and productivity of 0.84 g/L h in the bioreactor. Da Cunha et al. (2009) have studied immobilization of *C. guilliermondii* cells immobilized by inclusion into polyvinyl alcohol (PVA) hydrogel using the freezing thawing method in Erlenmeyer flasks as the pellet capability to catalyze the xylose to xylitol bioconversion of a medium based on sugarcane bagasse hemicellulosic hydrolysate. The cell pellets were then used to perform the same bioconversion in a stirred tank reactor operated at 400 rpm, 30$^{o}$C, and 1.04 vvm air flow rate. With this fermentation condition, a maximum xylitol concentration of 28.7 g/L, with corresponding xylitol yield and productivity of 0.49 g/g and 0.24 g/L h were obtained. Carvalho et al. (2000) have also reported xylitol production from concentrated sugarcane bagasse hemicellulosic hydrolysate in a repeated batch system using cells of *C. guilliermondii* FTI 20037 immobilized by entrapment in Ca–alginate beads (2.5 to 3 mm diameter). The results of their study showed that cell viability was substantially high (98%) in all fermentative cycles. The xylitol yield and productivity increased significantly with the reutilization of the immobilized biocatalysts. The maximum xylitol concentration of 11.05 g/L, with corresponding xylitol yield and productivity of 0.47 g/g and 0.22 g/L h, respectively, were obtained in 250 mL Erlenmeyer flasks containing 80 mL of medium and 20 mL of immobilized biocatalysts. Sarrouh and Da Silva (2013) have studied the biotechnological production of xylitol using sugarcane bagasse hydrolysate in a repeated batch fermentation system with immobilized cells of *C. guilliermondii* FTI20037. Seven repeated batches were performed in a fluidized bed bioreactor using immobilized cells in calcium alginate beads. The immobilized cells of *C. guilliermondii* were

reused for six successive batches maintaining an average xylitol yield of 0.7 g/g and productivity of 0.42 g/L h at the end of fermentation. In the seventh batch, a decrease of 44% in the final xylitol concentration was observed. The reduction could be explained by the possible diffusion and accumulation of insoluble substances, found in the hemicellulosic hydrolysate, in the interior of the immobilization support resulting in substrate mass transfer limitations. Prakash et al. (2011) have reported the production of xylitol from D-xylose and sugarcane bagasse hemicellulose by free and Ca alginate immobilized cells of thermotolerant yeast (*D. hansenii*) capable of fermenting xylose to xylitol at 40$^{o}$C. With free cells fermentation, the maximum xylitol concentration of 68.6 g/L, with a corresponding xylitol yield and productivity of 0.76 g/g and 0.44 g/L h, respectively from D–xylose, and the xylitol yield and productivity of 0.69 g/g and 0.28 g/L h, respectively from hemicellulosic hydrolysate of sugarcane bagasse after detoxification with activated charcoal and ion exchange resins were obtained. With Ca alginate immobilized *D. hansenii* cells fermentation, xylitol yield and productivity of 0.82 g/g and 0.46 g/L h were obtained. Summary of literature on bio–production of xylitol using immobilized cells from various lignocellulosic biomass is given in Table 2.7.

**Table 2.7.** Summary of literature on production of xylitol using immobilized cells

| Microorganisms | Carbon substrate source | Type of system | Immobilization support | Xylitol | | References |
|---|---|---|---|---|---|---|
| | | | | Yield (g/g) | Productivity (g/L h) | |
| *C. tropicalis* | Cotton stalk hydrolysate | Shake flask | Calcium alginate gel beads | – | – | Zhang et al. 2014 |
| *C. tropicalis* NCIM 3123 | Non-detoxified corn cob hemicellulosic hydrolysate | Shake flask | Calcium alginate gel beads | 0.73 | 0.43 | Yewale et al. 2016 |
| *C. tropicalis* As 2.1776 | Corncob hemicellulose hydrolysate | Multi-batches | PU foam | 0.66 | 1.9 | Wang et al. 2012 |
| *C. tropicalis* | D-xylose | Multi-batches | $HNO_3$-treated carbon fiber | 0.70 | 1.22 | Wang et al. 2016 |
| *D. hansenii* | Non-detoxified corn cob hemicellulosic hydrolysate | Shake flask | Calcium alginate gel beads | 0.56 | 0.29 | Pérez–Bibbins et al. 2013 |
| *D. hansenii* | D-xylose | ALBR | Calcium alginate | 0.71 | 0.43 | Pérez–Bibbins et al. 2014 |
| *C. subtropicalis* WF79 | Rice straw hemicellulose hydrolysate | Shake flask | Polyacrylic hydrogel thin films | 0.73 | – | Liaw et al. 2008 |
| *C. guilliermondii* FTI20037 | Sugarcane bagasse hemicellulosic hydrolysate | Shake flask | Calcium alginate | 0.62 | 0.24 | Carvalho et al. 2004 |
| *C. guillermondii* | Sugarcane bagasse hemicellulosic hydrolysate | FBR | Calcium alginate beads | 0.58 | 0.40 | Fouad Sarrouh et al. 2007 |
| *C. guilliermondii* FTI 20037 | Sugarcane bagasse hemicellulosic hydrolysate | STR | Calcium alginate beads | 0.81 | 0.40 | Carvalho et al. 2004 |

| | | | | | | |
|---|---|---|---|---|---|---|
| *C. guillermondii* | Sugarcane bagasse hemicellulosic hydrolysate | Shake flask | Sugarcane bagasse | – | 0.43 | Silva et al. 2007 |
| *C. guilliermondii* FTI 20037 | Oat hull hemicellulosic hydrolysate | Bio Reactor | Polypropylene (PP) and partially delignified fiber (PDF) | 0.84 | 0.57 | Soleimani and Tabil, (2014) |
| *C. sp.*ZU04 | Corn cob hemicellulosic hydrolysate | 3-phase FBR | Calcium alginate beads | 0.73 | 0.84 | Ding et al. 2011 |
| *C. guillermondii* | Sugarcane bagasse hemicellulosic hydrolysate | Shake flask | Polyvinyl alcohol (PVA) hydrogel | 0.49 | 0.24 | da Cunha et al. 2009 |
| *C.guillermondii* | Sugarcane bagasse hemicellulosic hydrolysate | Shake flask | Calcium alginate | 0.47 | 0.22 | Carvalho et al. 2000 |
| *C. guillermondii* | Sugarcane bagasse hemicellulosic hydrolysate | FBR | Calcium alginate | 0.70 | 0.42 | Sarrouh et al. 2013 |
| *D. hansenii* | D-xylose and sugarcane bagasse hemicellulose | 5X-batches | Calcium alginate | 0.82 | 0.46 | Prakash et al. 2011 |
| *C. tropicalis* | Corn cob hydrolysate | Erlenmeyer flasks | PVA and HEMA (7%:10% w/w) hydrogel copolymer | 0.44 | – | El–Batal and Khalaf 2004 |
| *C. tropicalis* *CCTCC M2012462* | Non–detoxified corncob hydrolysate | Bioreactor | Ca–alginate | 0.70 | 0.46 | Ping et al. 2013 |

## 2.9 Concept of ultrasound and its application in the fermentation process

The longitudinal acoustic waves beyond upper limit of human hearing range (16 kHz to 20 kHz) are referred as ultrasound. Typical frequency range of ultrasound extends from 20 kHz to 20 MHz. Due to its longitudinal nature, ultrasound passes through a compressible medium such as air and water, in the form of alternate compression and refraction cycles. Propagation of ultrasound waves in the medium generates periodic variation in bulk pressure as well as density of the medium. Passage of ultrasound wave in the medium sets fluid elemnets in the medium in oscillatory motion around the mean position (Shah et al., 1999). Ultrasound wave is characterized by physical properties of frequency, velocity and pressure amplitude. During propagation through medium, the pressure amplitude of the ultrasound wave is attenuated or dampened by various physical mechanisms. These mechanisms include thermal loss, frictional loss and scattering due to bubbles. Frictional loss is manifestation of finite viscosity of the medium. During oscillatory motion of fluid elements of the medium, some of the momentum of the fluid elements is dissociated in the medium, which results in their unidirectional (and not truly oscillatory) motion. Thermal loss is attributed to heat conduction between adjacent regions of compression and rarefaction that results in loss of compression work. For propagation of ultrasound wave through liquid, bubbles present in the medium scatter the ultrasound waves causing severe attenuation. Presence of gas bubbles in the liquid also alters the compressibility of the medium, as a result of which the speed of sound in the medium reduces. The properties of ultrasound wave in gaseous medium are strongly influenced by the static pressure in the medium. For sound wave propagation in liquids, the static pressure in the medium does not affect much, as the liquid properties are relatively insensitive to static pressure (at least for moderate levels of pressure).

### 2.9.1 Cavition bubble dynamics

Cavition is the phenomena of nucleation, growth, oscillation and transient collapse of gas/vapour bubbles driven by variation in bulk pressure in the medium. The cause leading to variation in bulk pressure could be propagation of an acoustic wave or variation in flow geometry, in case of

flow cavitation such as hydrodynamic cavitation, or in general, energy dissipation in the system. The efficiency of any physical/ chemical/ biological processes depends on the method of introducing energy into the system. Cavitation has proven to be an efficient tool of introducing energy into the system for intensification of large number of physical/ chemical/ biological processes. Ultrasound makes available energies on extremely small time and spatiall scales that are not available from any other sources.

Using the criterion of nature of energy dissipation in the system, cavitation can be categorized as: (1) Acoustic cavitation, which is generated due to pressure variation generated due to passage of aoucstic wave, and (2) Hydrodynamic cavitation, which results due to pressure variation in the liquid flow due to change in flow geometry. Hypothetically, the phemonema of cavitation refers to creation of voids in the liquid medium by pulling adjacent molecules apart by overcoming the Laplace pressure ( $2\sigma / R$). As R $\rightarrow$ 0, Laplace pressure $\rightarrow$ 0. Thus, theoretically, extremely high acoustic pressure amplitudes (exceeding ~100 MPa) would be required for generation of cavitation. However, in actual practice, cavitation occurs at very low pressure amplitudes (~1 bar). This result is attributed to phenomena of nucleation that drastically lowers the intermolecular forces. Nucleation in the liquid medium is induced by solid particles suspended or tiny free–floating bubbles present in the liquid. Another source of nuclei for occurrence of cavitation are gas pockets trapped in the crevices of the solid boundaries in the liquid medium. These gas pockets can grow in response to reduction in bulk pressure in the rarefaction cycle of acoustic wave.

### 2.9.2 Radial motion of cavitation bubbles

The periodic variation of bulk pressure in the medium induces volume oscillations of cavitation bubbles. The amplitude of these oscillations is directely proportional to pressure amplitude of acoustic wave. For relatively low acoustic pressure amplitudes (typically < 1 bar), the volume oscillations of the buble are small and in phase with acoustic wave. These oscillations are mainly driven by the pressure forces. As the acoustic pressure amplitude increases (and typically crosses

the static pressure in the medium), the radial motion of bubbles becomes increasingly non–linear with large volumetric oscillations, in which radius of the cavitation bubbles increases several times its initial value. This explosive growth is ensued by transient collapse and few after–bounces. In this case, the volume oscillation (or radial motion) of the bubble are dominated by inertial forces (Flynn, 1975).

### 2.9.3 Physical effects ultrasound and cavitation on reaction system

Ultrasound and its secondary effect cavitation render several physical effects on reaction systems. The main manifestion of all these results is generation of intense micro–convection and micro–mixing in the reaction system. A brief description of all physical effects of ultrasound and cavitation is given as follows:

**Micro–streaming**: This is essentially small amplitude oscillatory motion of fluid elements around a mean position, which is induced by propagation of ultrasound wave. For a typical ultrasound wave with pressure amplitude of 120 kPa in water ($\rho$ = 1000 kg/m$^3$, C = 1500 m/s), the micro–streaming velocity = 0.08 m/s.

**Acoustic streaming**: During propagation of ultrasound wave, the momentum of the wave is absorbed by the medium of finite viscosity. This results in setting up of low velocity unidirectional currents of the fluid known as acoustic streaming (Kolb and Nyborg, 1956; Nyborg, 1958).

**Microturbulence**: The oscillatory motion of fluid elements induced due to volume oscillations of cavitation bubble is called microturbulence. In the expansion phase of radial motion of cavitation bubble, the liquid is diplaced away from the bubble interface. During the collapse phase of the bubble, liquid is pulled towards the bubble as it fills the vacuum created in the liquid with size reduction of bubble. The mean velocity of microturbulence depends on the amplitude of bubble oscillation.

**Acoustic (shock) waves**: During the compression phase of radial motion, as the bubble contracts void space is created in the liquid and the fluid elements spherically converge in this void space

and work is done on the bubble. For a cavitation bubble containing non–condensable gas such as air, the adiabatic compression results in rapid rise of pressure inside the bubble. At the point of minimum radius (maximum compression), the bubble wall comes to a sudden halt. At this instance, the fluid elements converging towards the bubble are reflected back from the interface. This reflection creates a high pressure shock wave that propagates through the medium. The pressure exerted by the non–condensable gas inside the bubble causes re–bounce of the bubble.

**Microjets:** During radial motion driven by ultrasound wave, the cavitation bubble maintains spherical geometry as long as the motion of the liquid in its vicinity is symmetric and uniform, and thus, there are no pressure gradients. If the bubble is located close to the phase boundary, either solid–liquid, gas–liquid or liquid–liquid, the motion of the liquid in its vicinity is hindered, resulting in development of pressure around it. This non–uniformity of pressure results in the loss of spherical geometry of the bubble. During the asymmetric radial motion, the portion of bubble exposed to higher pressure collapses faster than rest of the bubble, which gives rise to the formation of high speed liquid jet directed towards the boundary. The velocity of these microjets has been estimated in the range of 120–150 m/s, and they can cause severe damage at the point of impact (leading to effects like particle size reduction, microbial cell disruption, degradation of polymer chains etc.). For the case of metal surfaces, these microjets can cause erosion of the surface.

### 2.9.4 Applications of ultrasound in fermentation systems

Application of sonication (or ultrasound irradiation) has been attempted for past few years for enhancement of kinetics and yield of biological/biochemical processes – especially the fermentation–based processes. A sizeable literature has been published in the area of ultrasound–assisted processes for production of biochemical and biofuels. Table 2.8 depicts the summary of literature reviewed in ultrasound–assisted intensification of fermentation based systems for the production of biofuels and biochemicals from various biomass sources.

**Table 2.8.** Summary of representative literature on ultrasound–assisted fermentations

| Microorganism | Substrate | Sonication conditions | Major resuts | References |
|---|---|---|---|---|
| *C. tropicalis* | Sugarcane bagasse | 37 kHz, 80 W, 30$^{o}$C, @ 10% duty cycle | 2.5× rise in xylitol productivity, 2× rise in specific uptake rate of xylose and fermentation time reduced from 36 h to 15 h | Present study |
| *G. oxydans* | Crude glycerol | 37 kHz, 130 W, 31$^{o}$C, @ 20% duty cycle | 60–84% enhancement in glycerol consumption, no significant change in cell morphology and conformational changes in protein structure (reduction in α–helix and β–sheet content) | Dikshit et al. 2018 |
| *C. pasteurianum* | Crude glycerol | 35 kHz, 35 W, 36$^{o}$C, @ 20% duty cycle | 50% increase in glycerol consumption and 40% rise in bio–hydrogen yield | Sarma et al. 2017 |
| *R. rhodochrous* | Dibenzothiophene | 35 kHz, 35 W, 31$^{o}$C, @ 20% duty cycle | Faster degradation of the organo–sulfur compound dibenzothiophene through 4–S metabolic pathway, and conformational changes in the secondary structure of the Dsz enzyme | Agarwal et al. 2016 |
| T. reesei | Sugarcane bagasse | 24 kHz, 400 W, 37$^{o}$C, 30 s sonication | 35.3% increment in bio–ethanol yield, and improved secretion of a multi–enzyme complex by *T. reesei* | Velmurugan and Incharoensakdi 2016 |
| *S. cerevisiae* and *P. stipites* | Sugar beet pulp | 24 kHz, 100% amplitude, 37$^{o}$C, 30 min sonication | 13.9% rise in bio–ethanol yield | Berlowska et al. 2016 |

| | | | | |
|---|---|---|---|---|
| *S. cerevisiae* | *P. hysterophorus* | 35 kHz, 35 W, 30oC, @10% duty cycle | 10% marginal rise in ethanol yield and time of fermentation decreased from 30 h to 15 h | Singh et al. 2015a |
| K. marxianus | Lactose | 20 kHz, 15 W, 30oC, @ 20% duty cycles | 3.5× enhancement in ethanol productivity | Sulaiman et al. 2011 |
| *S. cerevisiae var. ellipsoideus* | Corn starch | 40 kHz, 600 W, 60$^{o}$C, 5 min sonication | 11.2% increment in bio–ethanol concentration, and stimulated degradation of starch granules and release of glucose | Nikolić et al. 2010 |

## 2.10 Inference and Justification for Present Thesis Research

More than 80% of energy and ~90% of organic chemicals in the world are derived from fossil fuels alone. Moreover, the energy and organic chemicals consumptions are growing (~7% per annum) continuously due to rapid increase of world's population with improved standards of living. The increasing energy demands, gradual depletion of fossil fuels and deterioration of environmental hygiene due to emissions of harmful and greenhouse gases such as $CH_4$, $CO_2$, $N_2O$ by huge usage of fossil fuels are main reasons for investigation of renewable resources for sustainable production of energy, biofuels and value–added chemicals. An obvious option for the production of biofuels and value–added chemicals is utilization of lignocellulosic biomass as a source of sugars. Therefore, the conversion of lignocellulosic biomass to biofuels and value–added chemicals is a feasible solution, and also a matter of intensive research area in the past two decades. Xylitol is among the top value–added chemicals produced with chemical reduction of xylose using nickel/palladium catalyst from lignocellulosic biomass hemicellulosic hydrolysate. The bioconversion route is a potential alternative to the conventional chemical reduction route of xylitol production. The reasons for this are as follows: (1) high specificity, i.e. high selectivity and very few by–products, (2) ambient reaction conditions, (3) no requirement of expensive catalyst in the process. These features of biochemical process also make it economically viable and environmentally friendly. However, slower kinetics, and lower yield and productivity are the demerits of the bioconversion route. Nonetheless, even with these limitations, the bioconversion route is a viable process and has a potential of implementation on commericial scale. Laboratory as well as bench/pilot scale research on bioconversion of sugarcane bagasse to xylitol has shown good promise for commercial scale production. In this thesis work, we have adressed the important issues of optimization, modelling and intensification of the biochemical process for converting sugarcane bagasse to a value–added chemical, xylitol. The microorganism used in this work is a native strain of *Candida tropicalis*. We have adopted a hierarchical or step–by–step approach for the development of the bioconversion process. Optimization of process parameters

for dilute acid ahydrolysis of sugarcane bagasse and its kintetic and thermodynamic studies to obtained fermentable sugars hydrolysate rich in xylose followed by optimization of medium components and process parameters for the fermentation of the hydrolysate using immobilized *C. tropicalis* on PU foam support, as immobilized cells are highly suited for large scale operation. We have also attepted a possible solution for slow kinetics of the bioconversion process in terms of application of ultrasound in the fermentation mixture and have tried to get a mechanistic insight into the enhancement through analysis of the enzymatic kinetics and physical/chemical facets of cavitation. We believe that the results and analysis presented in this thesis work addressing important issues of sugarcane bagasse to xylitol bioconversion process will give important inputs for design, optimization and scale–up of the bioconversion process.

**References**

Adeeyo, O., Oresegun, O.M., Oladimeji, T.E., 2015. Compositional analysis of lignocellulosic materials: Evaluation of an economically viable method suitable for woody and non–woody biomass. Am. J. Eng. Res. 4(4), 14–19.

Agarwal, M., Dikshit, P.K., Bhasarkar, J.B., Borah, A.J. and Moholkar, V.S., 2016. Physical insight into ultrasound–assisted biodesulfurization using free and immobilized cells of Rhodococcus rhodochrous MTCC 3552. Chem. Eng. J. 295, 254–267.

Aguilar, R., Ramırez, J., Garrote, G., Vázquez, M., 2002. Kinetic study of the acid hydrolysis of sugar cane bagasse. J. Food Eng. 55(4), 309–318.

Aminoff, C., Vanninen, E., Doty, T. E., 1978. The occurrence, manufacture and properties of xylitol. Appl. Sci. Publishers, London, 1–9.

Arora, R., Behera, S., Sharma, N.K., Kumar, S., 2015. A new search for thermotolerant yeasts, its characterization and optimization using response surface methodology for ethanol production. Front. Microbiol. 6, 889.

Arruda, P.V., Rodrigues, R.D.C.L.B., Silva, D.D.V., Felipe, M.D.G.D.A., 2011. Evaluation of hexose and pentose in pre–cultivation of *Candida guilliermondii* on the key enzymes for xylitol production in sugarcane hemicellulosic hydrolysate. Biodeg. 22 (8), 15–22.

Arslan, Y., Takaç, S., Eken–Saraçoğlu, N., 2012. Kinetic study of hemicellulosic sugar production from hazelnut shells. Chem. Eng. J. 185, 23–28.

Aspinall, G. O., 1980. Chemistry of cell wall polysaccharides. The Biochemistry of plants: a comprehensive treatise, USA.

Barnett, J. A., Payne, R. W, Yarrow, D., 1990. Yeasts: characteristics and identification, 2nd edition. Cambridge University Press, New York.

Berłowska, J., Pielech–Przybylska, K., Balcerek, M., Dziekońska–Kubczak, U., Patelski, P., Dziugan, P. and Kręgiel, D., 2016. Simultaneous saccharification and fermentation of sugar beet pulp for efficient bioethanol production. BioMed. Res. Int.

Bertoti, A.R., Luporini, S., Esperidião, M.C.A., 2009. Effects of acetylation in vapor phase and mercerization on the properties of sugarcane fibers. Carbohydr. Polym. **77**(1), 20–24.

Branco, R.F., Santos, J.C., Murakami, L.Y., Mussatto, S.I., Dragone, G., Silva, S.S., 2007. Xylitol production in a bubble column bioreactor: Influence of the aeration rate and immobilized system concentration. Process Biochem. 42, 258–62.

Bruinenberg, P.M., de Bot, P. H. M., van Dijken, J. P., Scheffers, W. A., 1984. NADH–linked aldose reductase: the key to anaerobic alcoholic fermentation of xylose by yeasts. Appl. Microbial. Biotechnol. 19, 256–260.

Buaban, B., Inoue, H., Yano, S., Tanapongpipat, S., Ruanglek, V., Champreda, V., Pichyangkura, R., Rengpipat, S. Eurwilaichitr, L., 2010. Bioethanol production from ball milled bagasse using an on–site produced fungal enzyme cocktail and xylose–fermenting *Pichia stipitis*. J. Biosci. Bioeng. 110(1), 18–25.

Buranov, A. U., Mazza, G., 2008. Lignin in straw of herbaceous crops. Ind. Crop Prod. 28(3), 237–259.

Camargo, D., Sene, L., Variz, D.I.L.S., de Almeida Felipe, M.d.G., 2015. Xylitol bioproduction in hemicellulosic hydrolysate obtained from sorghum forage biomass. Appl. Biochem. Biotechnol. 175(8), 3628–3642.

Cara, C., Ruiz, E., Ballesteros, M., Manzanares, P., Negro, M.J., Castro, E., 2008. Production of fuel ethanol from steam–explosion pretreated olive tree pruning. Fuel 87(6), 692–700.

Cardona, C.A., Sanchez, O.J., 2007. Fuel ethanol production: Process design trends and integra–tion opportunities. Bioresour. Technol. 98(12), 2415–2457.

Carvalho, W.d., Silva, S.S.d., Vitolo, M., Mancilha, I.M.d., 2000. Use of immobilized *Candida* cells on xylitol production from sugarcane bagasse. Z. Naturforsch. C. 55(3–4), 213–217.

Carvalho, W., Santos, J.C., Canilha, L., e Silva, J.B.A., Felipe, M.G., Mancilha, I.M., Silva, S.S., 2004. A study on xylitol production from sugarcane bagasse hemicellulosic hydrolysate by Ca–alginate entrapped cells in a stirred tank reactor. Process Biochem. 39(12), 2135–2141.

Carvalheiro, F., Duarte, L.C., Gírio, F.M., 2008. Hemicellulose biorefineries: a review on biomass pretreatments. J. Sci. Ind. Res. 849–864.

Chandel, A.K., Kapoor, R.K., Singh, A., Kuhad, R.C., 2007. Detoxification of sugarcane bagasse hydrolysate improves ethanol production by *Candida shehatae* NCIM 3501. Bioresour. Technol. 98(10), 1947–1950.

Cheng, K.K., Zhang, J.A., Ling, H.Z., Ping, W.X., Huang, W., Ge, J.P. and Xu, J.M., 2009. Optimization of pH and acetic acid concentration for bioconversion of hemicellulose from corncobs to xylitol by *Candida tropicalis*. Biochem. Eng. J. 43, 203–07.

da Cunha, M.A., Converti, A., Santos, J.C., Ferreira, S.T., da Silva, S.S., 2009. PVA–hydrogel entrapped *Candida guilliermondii* for xylitol production from sugarcane hemicellulose hydrolysate. Appl. Biochem. Biotechnol. 157(3), 527–537.

Dahiya, J. S., 1991. Xylitol production by *Petromyces albertensis* grown on medium containing D–xylose. Can. J. Microb. 37, 14–18

de Moraes Rocha, G.J., Martin, C., Soares, I.B., Maior, A.M.S., Baudel, H.M., De Abreu, C.A.M., 2011. Dilute mixed–acid pretreatment of sugarcane bagasse for ethanol production. Biomass Bioenerg. 35(1), 663–670.

De Carvalho, W., Canilha, L., Mussatto, S.I., Dragone, G., Morales, M.L., Solenzal, A.I.N., 2004. Detoxification of sugarcane bagasse hemicellulosic hydrolysate with ion-exchange resins for xylitol production by calcium alginate-entrapped cells. J. Chem. Technol. Biotechnol. 79(8), 863–868.

Dikshit, P.K., Kharmawlong, G.J. Moholkar, V.S., 2018. Investigations in sonication–induced intensification of crude glycerol fermentation to dihydroxyacetone by free and immobilized *Gluconobacter oxydans*. Bioresour. Technol. 256, 302–311.

Ding, X., Xia, L., 2006. Effect of aeration rate on production of xylitol from corncob hemicellulose hydrolysate. Appl. Biochem. Biotechnol. 133(3), 263–270.

Ding, X., 2011. Fermentation of xylitol using immobilized *Candida sp*. ZU04 cells in three–phase fluidized–bed bioreactor. Remote Sensing, Environment and Transportation Engineering (RSETE), Int. Conference on IEEE 7591–7593.

Dutta, S., De, S., Saha, B., Alam, M.I., 2012. Advances in conversion of hemicellulosic biomass to furfural and upgrading to biofuels. Catal. Sci. Technol. 2(10), 2025-2036.

El–Batal, A., Khalaf, S., 2004. Xylitol Production from corn cobs hemicellulosic hydrolysate by *Candida tropicalis* immobilized cells in hydrogel copolymer carrier. Int. J. Agric. Biol. 6, 1066–73.

Fouad Sarrouh, B., Tresinari dos Santos, D., Silvério da Silva, S., 200. Biotechnological production of xylitol in a three-phase fluidized bed bioreactor with immobilized yeast cells in Ca-alginate beads. Biotechnol. J. 2(6), 759–763.

García–Aparicio, M.P., Ballesteros, I., González, A., Oliva, J.M., Ballesteros, M. and Negro, M.J., 2006. Effect of inhibitors released during steam–explosion pretreatment of barley straw on enzymatic hydrolysis. Appl. Biochem. Biotechnol. 129(1–3), 278–288.

Ghindea, R., Csutak, O., Stoica, I., Tanase, A.M., Vassu, T., 2010. Production of xylitol by yeasts. Roman. Biotechnol. Lett. 15(3), 5217–5222.

Gong, C.S., Chen, L.F., Tsao, G., 1981. Quantitative production of xylitol from D–xylose by a high–xylitol producing yeast mutant *Candida tropicalis* HXP2. Biotechnol. Lett. 3, 125–130.

Guamán–Burneo, M.C., Dussán, K.J., Cadete, R.M., Cheab, M.A., Portero, P., Carvajal–Barriga, E.J., da Silva, S.S. and Rosa, C.A., 2015. Xylitol production by yeasts isolated from rotting wood in the Galápagos Islands, Ecuador, and description of *Cyberlindnera galapagoensisf.a., sp. nov*. A Van Leeuw J. Microb. 108 (4), 919–31.

Guo, C., Zhao, C., He, P., Lu, D., Shen, A., Jiang, N., 2006. Screening and characterization of yeasts for xylitol production. J Appl. Microbiol. 101, 1096–104.

Guo, G. L., Chen, W. H., Chen, W. H., Men, L. C., Hwang, W. S., 2008. Characterization of dilute acid pretreatment of silvergrass for ethanol production. Bioresour. Technol. 99(14), 6046–6053.

Gurpilhares, D.B., Hasmann, F.A., Pessoa, A.J., Roberto, I.C., 2008. The behavior of key enzymes of xylose metabolism on the xylitol production by *Candida guilliermondii* grown in hemicellulosic hydrolysate. J. Ind. Microbiol. Biotechnol. 36(1), 87–93.

Hallac, B. B., Sannigrahi, P., Pu, Y., Ray, M., Murphy, R. J., Ragauskas, A. J., 2010. Effect of ethanol organosolv pretreatment on enzymatic hydrolysis of Buddleja davidii stem biomass. Ind. Eng. Chem. Res. 49(4), 1467–1472.

Harmsen, P., Huijgen, W., Bermudez, L., Bakker, R., 2010. Literature review of physical and chemical pretreatment processes for lignocellulosic biomass. Energ. Res. Centre Nether. 10–13.

Hernández–Pérez, A.F., Costa, I.A.L., Silva, D.D.V., Dussan, K.J., Villela, T.R., Canettieri, E.V., Carvalho Jr, J.A., Neto, T.S. Felipe, M.G.A., 2016. Biochemical conversion of sugarcane

straw hemicellulosic hydrolyzate supplemented with co–substrates for xylitol production. Bioresour. Technol. 200, 1085–1088.

Kumdam, H.B., Murthy, S.N., Gummadi, S.N., 2012. A statistical approach to optimize xylitol production by *Debaryomyces nepalensis* NCYC 3413 in vitro. Food Nutrition Sci. 3(08), 1027.

Hsu, T. C., Guo, G. L., Chen, W. H., Hwang, W. S., 2010. Effect of dilute acid pretreatment of rice straw on structural properties and enzymatic hydrolysis. Bioresour. Technol. 101(13), 4907–4913.

Huang, C.F., Jiang, Y.F., Guo, G.L., Hwang, W.S., 2011. Development of a yeast strain for xylitol production without hydrolysate detoxification as part of the integration of co–product generation within the lignocellulosic ethanol process. Bioresour. Technol. 102(3), 3322–3329.

Hyvönen, L., Koivistoinen, P., Voirol, F., 1982. Food technological evaluation of xylitol. Adv. Food Res. 28, 373–403.

Imai, M., Ikari, K., Suzuki, I., 2004. High–performance hydrolysis of cellulose using mixed cellulase species and ultrasonication pretreatment. Biochem. Eng. J. 17(2), 79–83.

Izumori, K., Tuzaki, K., 1988. Production of xylitol from D–xylulose by *Mycobacterium smegmatis*. J. Ferment. Technol. 66, 33–36.

Jeffries, T. W., 1983. Utilization of xylose by bacteria, yeasts and fungi. Adv. Biochem. Eng. Biotechnol. 27, l–32.

Jeffries, T.W., 2006. Engineering yeasts for xylose metabolism. Curr. Opin. Biotechnol. 17, 320–326.

Jensen, J., Morinelly, J., Aglan, A., Mix, A., Shonnard, D.R., 2008. Kinetic characterization of biomass dilute sulfuric acid hydrolysis: Mixtures of hardwoods, softwood, and switchgrass. AIChE J. 54(6), 1637–1645.

Jiang, L.Q., Fang, Z., Li, X.K., Luo, J., Fan, S.P., 2013. Combination of dilute acid and ionic liquid pretreatments of sugarcane bagasse for glucose by enzymatic hydrolysis. Process Biochem. 48(12), 1942–1946.

Jin, Q., Zhang, H., Yan, L., Qu, L., Huang, H., 2011. Kinetic characterization for hemicellulose hydrolysis of corn stover in a dilute acid cycle spray flow–through reactor at moderate conditions. Biomass Bioenerg. 35(10), 4158–4164.

Jonglertjunya, W., Makkhanon, W., Siwanta, T., Prayoonyong, P., 2014. Dilute Acid Hydrolysis of Sugarcane Bagasse for Butanol Fermentation. Chiang Mai J. Sci. 41(1), 60–70.

Karp, S.G., Woiciechowski, A.L., Soccol, V.T., Soccol, C.R., 2013. Pretreatment strategies for delignification of sugarcane bagasse: a review. Braz. Arch. Biol. Technol. 56(4), 679–689.

Kim, J.W., Mazza, G., 2008. Optimization of phosphoric acid catalyzed fractionation and enzymatic digestibility of flax shives. Ind. Crop Prod. 28(3), 346–355.

Kind, V. B., Vyglazov, V.V., Kholkin, Y. J., 1987. Use of cationic surfactants for clarification of pentose hydrolyzates in xylitol production. Gidroliz. Lesokhim. Prom–St. 3, 11–12.

Kirk, T. K., Farrell, R. L., 1987. Enzymatic combustion: the microbial degradation of lignin. Annu. Rev. Microbiol. 41(1), 465–501.

Ko, C.H., Chiang, P.N., Chiu, P.C., Liu, C.C., Yang, C.L., Shiau, I.L., 2008. Integrated xylitol production by fermentation of hardwood wastes. J. Chem. Technol. Biotechnol. 83(4), 534–540.

Kirk–Othmer 4$^{th}$ edition (2001), vol 5.

Kumar, P., Barrett, D.M., Delwiche, M.J., Stroeve, P., 2009. Methods for pretreatment of lignocellulosic biomass for efficient hydrolysis and biofuel production. Ind. Eng. Chem. Res. 48(8), 3713–3729.

Kumar, S., Dheeran, P., Singh, S.P., Mishra, I.M., Adhikari, D.K., 2015. Bioprocessing of bagasse hydrolysate for ethanol and xylitol production using thermotolerant yeast. Bioprocess Biosyst. Eng. 38(1), 39–47.

Lavarack, B., Griffin, G., Rodman, D., 2002. The acid hydrolysis of sugarcane bagasse hemicellulose to produce xylose, arabinose, glucose and other products. Biomass Bioenerg. 23(5), 367–380.

Liaw, W.C., Chen, C.S., Chang, W.S., Chen, K.P., 2008. Xylitol production from rice straw hemicellulose hydrolyzate by polyacrylic hydrogel thin films with immobilized *Candida subtropicalis* WF79. J. Biosci. Bioeng. 105(2), 97–105.

Li, Z., Qu, H., Li, C., Zhou, X., 2013. Direct and efficient xylitol production from xylan by *Saccharomyces cerevisiae* through transcriptional level and fermentation processing optimizations. Bioresour. Technol. 149, 413–419.

Lin, S.Y., Lin, I.S., 2002. Ullmann's Encyclopedia Ind. Chem. 6th edition. Wein–heim, Germany, Wiley–VCH.

Ling, H., Cheng, K., Ge, J., Ping, W., 2011. Statistical optimization of xylitol production from corncob hemicellulose hydrolysate by *Candida tropicalis* HDY–02. New Biotechnol. 28(6), 673–78.

Liu, X., Lu, M., Ai, N., Yu, F., Ji, J., 2012. Kinetic model analysis of dilute sulfuric acid–catalyzed hemicellulose hydrolysis in sweet sorghum bagasse for xylose production. Ind. Crop Prod. 38, 81–86.

Lu, J., Larry, B., Gong, C.S., Tsao, G.T., 1995. Effect of nitrogen sources on xylitol production from D–xylose by *Candida Sp*.L–102. Biotech. Lett. 17, 167–70.

Lu, X., Zhang, Y., Liang, Y., Yang, J., Zhang, S., Suzuki, E., 2008. Kinetic studies of hemicellulose hydrolysis of corn stover at atmospheric pressure. Korean J. Chem. Eng. 25(2), 302–307.

McKillip, W.J., Collin, G., 2002. Ullmann's Encyclopedia Ind. Chem. 6th edition. Weinheim, Germany, Wiley–VCH.

Melaja, A.J., Hamalainen, L., 1977. Process for making xylitol. Google Patents.

Mosier, N., Wyman, C., Dale, B., Elander, R., Lee, Y. Y., Holtzapple, M., Ladisch, M., 2005. Features of promising technologies for pretreatment of lignocellulosic biomass. Bioresour. Technol. 96(6), 673–686.

Moutta, R., Chandel, A.K., Rodrigues, R., Silva, M., Rocha, G., Silva, S., 2012. Statistical optimization of sugarcane leaves hydrolysis into simple sugars by dilute sulfuric acid catalyzed process. Sugar Technol. 14(1), 53–60.

Moutta, R.D.O., Ferreira–Leitão, V.S., Bon, E.P.D.S., 2014. Enzymatic hydrolysis of sugarcane bagasse and straw mixtures pretreated with diluted acid. Biocatal. Biotransform. 32(1), 93–100.

Mussatto, S.I., Roberto I.C., 2004. Alternatives for detoxification of diluted–acid lignocellulosic hydrolyzates for use in fermentative processes: A review. Bioresour. Technol. 93(1), 1–10.

Nelson, D.L., Lehninger, A.L., Cox, M.M., 2008. Lehninger principles of biochemistry. Macmillan.

Nikolaev, D.I., Chernikova, L.P., Glazman, B.A., Kostyuk, I.N., Rutskaya, M.S., Chivyaga, A.A., 1983. New ion– exchange resins in xylitol production. Gidroliz. Lesokhim. Prom–St. 2, 16–18.

Nikolić, S., Mojović, L., Rakin, M., Pejin, D., Pejin, J., 2010. Ultrasound–assisted production of bioethanol by simultaneous saccharification and fermentation of corn meal. Food Chem. 122(1), 216–222.

O'Connor, R.P., Woodley, R., Kolstad, J.J., Kean, R., Glassner, D.A., Mastel, B., Ritzenthaler, J.M., John, H. J., Warwick, J.R., Hettenhaus, R.K., 2007. Process for fractionating lignocellulosic biomass into liquid and solid products. Assignee U.S.A. Nature works LLC, patent number WO 120210. 36 ECN–E–10–013.

Paidimuddala, B., Gummadi, S.N., 2014. Bioconversion of non–detoxified hemicellulose hydrolysates to xylitol by halotolerant yeast *Debaryomyces nepalensis* NCYC 3413. J. Microb. Biochem. Technol. 6(6), 327–33.

Palnitkar, S., Lachke, A., 1992. Effect of nitrogen sources on oxidoreductive enzymes and ethanol production during D–xylose fermentation using *Candida shehatae*, Can. J. Microbiol. 38(3), 358–60.

Pattra, S., Sangyoka, S., Boonmee, M., Reungsang, A., 2008. Bio–hydrogen production from the fermentation of sugarcane bagasse hydrolysate by *Clostridium butyricum*. Int. J. Hydrogen Energ. 33(19), 5256–5265.

Pérez–Bibbins, B., Salgado, J.M., Torrado, A., Aguilar–Uscanga, M.G., Domínguez, J.M., 2013. Culture parameters affecting xylitol production by *Debaryomyces hansenii* immobilized in alginate beads. Process Biochem. 48(3), 387–397.

Pérez–Bibbins, B., de Souza Oliveira, R.P., Torrado, A., Aguilar–Uscanga, M.G., Domínguez, J.M., 2014. Study of the potential of the air lift bioreactor for xylitol production in fed–batch cultures by *Debaryomyces hansenii* immobilized in alginate beads. Appl. Microbiol. Biotechnol. 98(1), 151–161.

Ping, Y., Ling, H.–Z., Song, G., Ge, J.P., 2013. Xylitol production from non–detoxified corncob hemicellulose acid hydrolysate by *Candida tropicalis*. Biochem. Eng. J. 75, 86–91.

Prakash, G., Varma, A., Prabhune, A., Shouche, Y., Rao, M., 2011. Microbial production of xylitol from D–xylose and sugarcane bagasse hemicellulose using newly isolated thermotolerant yeast *Debaryomyces hansenii*. Bioresour. Technol. 102(3), 3304–3308.

Prakasham, R.S., Rao, R.S., Hobbs, P.J., 2009. Current trends in biotechnology production of xylitol and future prospects. Curr. Trends Biotechnol. Pharm. 3, 8–36.

Prior, B. A., Killian, S. G., du Preez, J. C., 1989. Fermentation of D–xylose by the yeasts *Candida shehatae* and *Pichia stipitis*. Process. Biochem. 24, 21–32.

Rafiqul, I., Sakinah, A.M., 2013. Processes for the production of xylitol: a review. Food Rev. Int. 29(2), 127–156.

Rao, R.S., Jyothi, P.C., Prakasham, R.S., Sarma, P.N., Rao, V.L., 2006. Xylitol production from corn fibre and sugarcane bagasse hydrolysates by *Candida tropicalis*. Bioresour. Technol. 97, 1974–1978.

RG, C., Godoy, G., Gonçalves, A., 2012. Study of sugarcane bagasse pretreatment with sulfuric acid as a step of cellulose obtaining. World Academy of Science, Engineering and Technology. Int. J. Biol. Biomol. Agric. Food Biotechnol. Eng. 6(1), 6–10.

Rodrigues, R., Felipe, M., Roberto, I., Vitolo, M., 2003. Batch xylitol production by *Candida guilliermondii* FTI 20037 from sugarcane bagasse hemicellulosic hydrolyzate at controlled pH values. Bioprocess Biosyst. Eng. 26(2), 103–107.

Saha, B.C., Iten, L.B., Cotta, M.A., Wu, Y.V., 2005. Dilute acid pretreatment, enzymatic saccharification, and fermentation of rice hulls to ethanol. Biotechnol. Prog. 21(3), 816–822.

Saleh, M., Cuevas, M., Juan, F., Sanchez, G.S., 2014. Valorization of olive stones for xylitol and ethanol production from dilute acid pretreatment via enzymatic hydrolysis and fermentation by *Pachysolen tannophilus*. Biochem. Eng. J. 15, 286–93.

Sampaio, F.C., Chaves–Alves, V.M., Converti, A., Lopes Passos, F.M., Cavalcante Coelho, J.L., 2008. Influence of cultivation conditions on xylose–to–xylitol bioconversion by a new isolate of *Debaryomyces hansenii*. Bioresour. Technol. 99,502–8.

Sapcı, B., Akpinar, O., Bolukbasi, U. and Yilmaz, L., 2016., Evaluation of cotton stalk hydrolysate for xylitol production. Prep. Biochem. Biotechnol. 46(5), 474–482.

Sarma, S., Anand, A., Dubey, V.K., Moholkar, V.S., 2017. Metabolic flux network analysis of hydrogen production from crude glycerol by *Clostridium pasteurianum*. Bioresour. Technol. 242, 169–177.

Sarrouh, B., Da Silva, S.S., 2013. Repeated batch cell–immobilized system for the biotechnological production of xylitol as a renewable green sweetener. Appl. Biochem. Biotechnol. 169(7), 2101–2110.

Schell, D.J., Farmer, J., Newman, M., McMILLAN, J.D., 2003. Dilute–sulfuric acid pretreatment of corn stover in pilot–scale reactor. Biotechnol. Fuels Chem. Humana Press, 69–85.

Silva, S.S., Mussatto, S.I., Santos, J.C., Santos, D.T., Polizel, J., 2007. Cell immobilization and xylitol production using sugarcane bagasse as raw material. Appl. Biochem. Biotechnol. 141(2–3), 215–227.

Sindhu, R., Kuttiraja, M., Binod, P., Janu, K.U., Sukumaran, R.K., Pandey, A., 2011. Dilute acid pretreatment and enzymatic saccharification of sugarcane tops for bioethanol production. Bioresour. Technol. 102(23), 10915–10921.

Singh, S., Sarma, S., Agarwal, M., Goyal, A., Moholkar, V.S., 2015a. Ultrasound enhanced ethanol production from *Parthenium hysterophorus*: a mechanistic investigation. Bioresour. Technol. 188, 287–294

Kamal, S.M.M., Mohamad, N.L., Abdullah, A.G.L., Abdullah, N., 2011. Detoxification of sago trunk hydrolysate using activated charcoal for xylitol production. Proc. Food Sci. 1, 908–913.

Slininger, P.J., Bolen, P.L., Kurtzman, C.P., 1987. Pachysolen tannophilus: properties and process consideration for ethanol production from D–xylose. Enzyme Microb. Technol. 9, 5–15.

Soccol, C.R., de Souza Vandenberghe, L.P., Medeiros, A.B.P., Karp, S.G., Buckeridge, M., Ramos, L.P., Pitarelo, A.P., Ferreira–Leitão, V., Gottschalk, L.M.F., Ferrara, M.A., 2010. Bioethanol from lignocelluloses: status and perspectives in Brazil. Bioresour. Technol. 101(13), 4820–4825.

Soleimani, M., Tabil, L., 2014. Evaluation of biocomposite–based supports for immobilized–cell xylitol production compared with a free–cell system. Biochem. Eng. J. 82, 166–173.

Sreenivas Rao, R., Prakasham, R.S., Krishna Prasad, K., Rajesham, S., Sharma, P.N., Venkateswar Rao, L., 2004. Xylitol production by *Candida sp*: parameter optimization using Taguchi approach. Process Biochem. 39, 951–56.

Sreenivas–Rao, R., Pavana–Jyothi, N., Prakasham, R., Sarma, P., Venkateswar–Rao, L., 2006. Xylitol production from corn fiber and sugarcane bagasse hydrolysates by *Candida tropicalis*. Bioresour. Technol. 97,1974–78.

Sulaiman, A.Z., Ajit, A., Yunus, R.M., Chisti, Y., 2011. Ultrasound–assisted fermentation enhances bioethanol productivity. Biochem. Eng. 54, 141−150.

Sun, Y., Cheng, J., 2002. Hydrolysis of lignocellulosic materials for ethanol production: a review. Bioresour. Technol. 83(1), 1–11.

Sun, Y., Cheng, J.J., 2005. Dilute acid pretreatment of rye straw and bermudagrass for ethanol production. Bioresour. Technol. 96(14), 1599–1606.

Suryadi, H., Katsuragi, T., Yoshida, N., Suzuki, S., Tani, Y., 2000. Polyol production by culture of methanol–utilizing yeast. J. Biosci. Bioeng. 89, 236–40.

Swati, G., Haldar, S., Ganguly, A., Chatterjee, P., 2013. Investigations on the kinetics and thermodynamics of dilute acid hydrolysis of *Parthenium hysterophorus L.* substrate. Chem. Eng. J. 229, 111–117.

Tada, K., Horiuchi, J.I., Kanno, T., Kobayashi, M., 2004. Microbial xylitol production from corn cobs using *Candida magnoliae*. J. Biosci. Bioeng. 98(3), 228–230.

Tada, K., Kanno, T., Horiuchi, J., 2012. Enhanced production of bioxylitol from corn cobs by *Candida magnoliae*. Ind. Eng. Chem. Res. 51(30), 10008–14.

Taherzadeh, M.J., Karimi, K., 2008. Pretreatment of lignocellulosic wastes to improve ethanol and biogas production: a review. Int. J. Mol. Sci. 9, 1621–1651.

Tengerdy, R.P., Szakacs, G., 2003. Bioconversion of lignocellulose in solid substrate fermenta–tion. Biochem. Eng. J. 13(2–3), 169–179.

Tesfaw, A., Assefa, F., 2014. Current trends in bioethanol production by *Saccharomyces cerevisiae*: substrate, inhibitor reduction, growth variables, co culture, and immobilization. Int. Sch. Res. Notic. 1–11.

Teymouri, F., Laureano–Perez, L., Alizadeh, H., Dale, B.E., 2005. Optimization of the ammonia fiber explosion (AFEX) treatment parameters for enzymatic hydrolysis of corn stover. Bioresour. Technol. 96(18), 2014–2018.

Timung, R., Naik Deshavath, N., Goud, V.V., Dasu, V.V., 2016. Effect of subsequent dilute acid and enzymatic hydrolysis on reducing sugar production from sugarcane bagasse and spent citronella biomass. J. Energ.

Rafiqul, I.S.M., Sakinah, A.M., 2013. Processes for the production of xylitol: a review. Food Rev. Int. 29(2), 127–156.

van Dijken, J. P., Scheffers, W. A., 1986. Redox balances in the metabolism of sugars by yeasts. FEMS Microbiol. Rev. 32, 199–224.

van Rantwijk, F., Lau, R.M., Sheldon, R.A., 2003. Biocatalytic transformations in ionic liquids. Trends Biotechnol. 21(3), 131–138.

Vargas Betancur, G.J., Pereira Jr, N., 2010. Sugarcane bagasse as feedstock for second generation ethanol production: Part I: Diluted acid pretreatment optimization. Electron. J. Biotechnol. 13(3), 10–11.

Velmurugan, R., Incharoensakdi, A., 2016. Proper ultrasound treatment increases ethanol production from simultaneous saccharification and fermentation of sugarcane bagasse. RSC Adv. 6(94), 91409–91419.

Villarreal, M., Prata, A., Felipe, M., Silva, J.A.E., 2006. Detoxification procedures of eucalyptus hemicellulose hydrolysate for xylitol production by *Candida guilliermondii*. Enzyme Microb. Technol. 40(1), 17–24.

Wang, L., Wu, D., Tang, P., Fan, X., Yuan, Q., 2012. Xylitol production from corncob hydrolysate using polyurethane foam with immobilized *Candida tropicalis*. Carbohydr. Polym. 90(2), 1106–1113.

Wang, L., Liu, N., Guo, Z., Wu, D., Chen, W., Chang, Z., Yuan, Q., Hui, M., Wang, J., 2016. Nitric acid–treated carbon fibers with enhanced hydrophilicity for *Candida tropicalis* immobilization in xylitol fermentation. Mater. 9(3), 206.

Yat, S.C., Berger, A., Shonnard, D.R., 2008. Kinetic characterization for dilute sulfuric acid hydrolysis of timber varieties and switchgrass. Bioresour. Technol. 99(9), 3855–3863.

Yewale, T., Panchwagh, S., Rajagopalan, S., Dhamole, P.B., Jain, R., 2016. Enhanced xylitol production using immobilized *Candida tropicalis* with non–detoxified corn cob hemicellulosic hydrolysate. 3 Biotech. 6(1), 1–10.

Yoshitake, J., Obiwa, H., Shimamura, M., 1971. Production of polyalcohol by *Corynebacterium sp*. Production of pentitol from aldopentose. Agric. Biol. Chem. 35, 905–911.

Yoshitake, J., Ishizaki, H., Shimamura, M., Imai, T., 1973. Xylitol production by an *Enterobacfer species*. Agric. Biol. Chem. 37, 2261–2267.

Yoshitake, J., Shimamura, M., Ishizaki, H., Irie, Y., 1976. Xylitol production by *Enferobacter liquefaciens*. Agric. Biol. Chem. 40, 1493–1503.

Zhao, X., Cheng, K., Liu, D., 2009. Organosolv pretreatment of lignocellulosic biomass for enzymatic hydrolysis. Appl. Microbiol. Biotechnol. 82(5), 815–827.

Zhang, Y.H.P., Ding, S.Y., Mielenz, J.R., Cui, J.B., Elander, R.T., Laser, M., Lynd, L.R., 2007. Fractionating recalcitrant lignocellulose at modest reaction conditions. Biotechnol. Bioeng. 97(2), 214–223.

Zhang, J., Geng, A., Yao, C., Lu, Y., Li, Q., 2012. Xylitol production from D–xylose and horticultural waste hemicellulosic hydrolysate by a new isolate of *Candida athensensis* SB18. Bioresour. Technol. 105, 134–41.

Zhang, Q., Li, Y., Xia, L., Liu, Z., 2014. Enhanced xylitol production from statistically optimized fermentation of cotton stalk hydrolysate by immobilized *Candida tropicalis*. Chem. Biochem. Eng. Q. 28(1), 87–93.

Zhu, J., Yong, Q., Xu, Y., Yu, S., 2011. Detoxification of corn stover prehydrolyzate by trialkylamine extraction to improve the ethanol production with *Pichia stipitis* CBS 5776. Bioresour. Technol. 102(2), 1663–1668.

Zhu, Z., Sathitsuksanoh, N., Vinzant, T., Schell, D.J., McMillan, J.D., Zhang, Y.H.P., 2009. Comparative study of corn stover pretreated by dilute acid and cellulose solvent-based lignocellulose fractionation: Enzymatic hydrolysis, supramolecular structure, and substrate accessibility. Biotechnol. Bioeng. 103(4), 715–724.

Zimbardi, F., Viola, E., Nanna, F., Larocca, E., Cardinale, M., Barisano, D., 2007. Acid impregnation and steam explosion of corn stover in batch processes. Ind. Crop Prod. 26(2), 195–206.

# CHAPTER 3

# OPTIMIZATION OF PROCESS PARAMETERS FOR DILUTE ACID HYDROLYSIS OF SUGARCANE BAGASSE

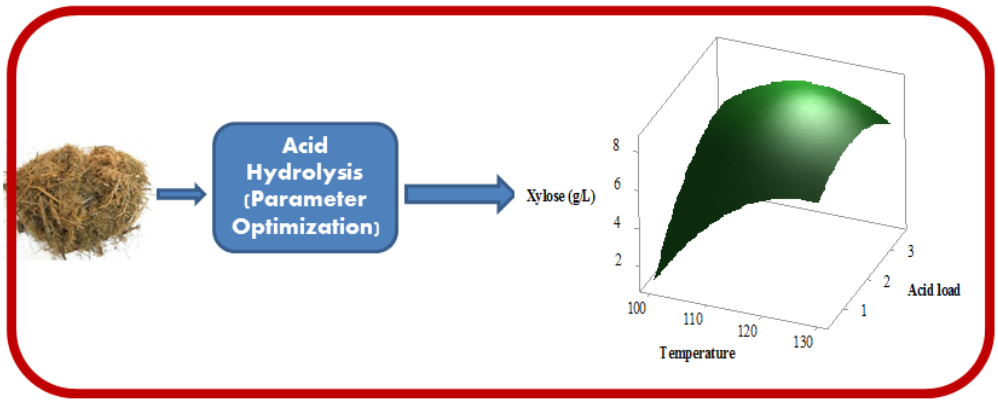

# CHAPTER 3

# OPTIMIZATION OF PROCESS PARAMETERS FOR DILUTE ACID HYDROLYSIS OF SUGARCANE BAGASSE

## 3.1 Introduction

Significant research has been devoted for production of chemicals and biofuels from lignocellulosic materials (Himmel et al., 2007). Lignocellulosic materials are an abundant and inexpensive source of sugars for the production of biofuels and value–added chemicals. Sugarcane bagasse is among the lignocelulosic materials for the synthesis of biofuels and value–added products such as xylitol (Laopaiboon et al., 2010).

Like other lignocellulosic materials the main components of sugarcane bagasse are cellulose, hemicellulose, and lignin. Moreover, it also consists of ash, extractives and others. Because of its heterogeneous nature, hemicellulose is of particular interest for researchers i.e. hemicellulose is depolymerized into its monomeric units, mainly xylose, and their subsequent conversion into biofuels and value–added products via microbial fermentation (Harmsen et al., 2010).

The conversion of lignocellulosic biomass to fermentable sugars is the key step in the production value–added products. Due to the crystallinity of cellulose, degree of polymerization, moisture content, available surface area and lignin content, it is required to alter the structure of cellulosic biomass for hydrolysis (Mosier et al., 2005). Pretreatment has been recognised as one of the most expensive processing steps in lignocellulosic biomass to fermentable sugars conversion. The goal of any pretreatment is to increase the surface area and porosity, modification of lignin structure,

removal of lignin, (partial) depolymerisation of hemicellulose, removal of hemicellulose, and reduce the crystallinity of cellulose. An effective pretreatment should avoid the need for reducing the size of biomass particle, preserve the pentose (hemicellulose) fractions, limit the formation of degradation products that inhibit the growth of fermentative microorganism, minimize energy demands and the pretreatment agent should have low cost and be capable of recycling inexpensively (Karp et al., 2013).

Hydrolyis of lignocellulosic biomass with concentrated acids such as $H_2SO_4$ and HCl can result in improvement of enzymatic hydrolysis of the lignocellulosic biomass to release fermentable sugars. Although they are powerful agents for cellulose hydrolysis, concentrated acids are toxic, corrosive, hazardous, and thus require reactors that are resistant to corrosion, which makes the pretreatment process very expensive. Furthermore, the concentrated acid must be recovered after hydrolysis to make the process economically feasible (Sun and Cheng, 2002; Converse et al., 1989).

Dilute acid hydrolysis has been widely used for pretreatment of lignocellulosic biomass. This is due high hydrolysis rate, specific towards hemicellulose, and more economical than enzymatic, concentrated acid and base pretreatment (Hosseini et al., 2010). Dilute sulphuric acid hydrolysis is a common technique for sugarcane bagasse (Lavarack et al., 2002). However, other reagents such as hydrochloric, nitric and phosphoric acids can also be used for hydrolysis.

The yield of fermentable sugars during acid hydrolysis is affected by various process parameters such as hydrolysis temperature, hydrolysis time, concentration of acid and solid to liquid ratio etc. The conventional method of optimization of the process parameters involves varying one factor at a time and keeping the others constant. This is often useful but does not explain the effect of interaction between the various factors under consideration. Optimization of process parameters using statistical methods with response surface methodology has overcome the limitation of the convetional method. The objective of statistical design of experiments is to

optimize a response (output variable), which is influenced by several independent variables (Khuri and Cornell, 1987).

In this chapter, we have statstically optimized the process parameters (viz. acid concentration or acid load, hydrolysis temperature, and hydrolysis time) of dilute acid hydrolysis of sugarcane bagasse. Prior to statstical optimization, the composition of sugarcane bagasse and effect of solid to liquid ratio on dilute acid hydrolysis of sugarcane bagasse has first been analyzed. Box Behnken design (BBD) has been used to design and optimize the process parameters of dilute sulphuric acid hydrolysis conditions and the interaction among these parameters on dilute acid hydrolysis of sugarcane bagasse to obtain maximum xylose yield with minimum inhibitory by–products for the subsequent biosynthesis of xylitol. Finally, monomeric sugars (viz.glucose, xylose and arabinose) and inhibitory by–products (acetic acid, furfural and 5–HMF) in the hemicellulosic hydrolysate have also been analyzed under the optimum conditions.

## 3.2 Materials and methods

### 3.2.1 Materials

Sugarcane bagasse was obtained from local area in Guwahati, Assam (India). The biomass was dried and ground into small pieces. It was then sieved using 25 BSS mesh screen to obtain fraction with size less than 0.6 mm. The size of biomass particles for hydrolysis has been chosen on the basis of previous literature. Lavarack et al. (2002) showed in their research on hydrolysis of sugarcane bagasse that particle size did not have significant influence on kinetics of hemicellulose hydrolysis. Jonglertjunya et al. (2014) reported that optimum particle size for acid hydrolysis of sugarcane bagasse was in the range of 0.212–1.80 mm. On the basis of these two previous studies, the upper limit of biomass particle size in present study was fixed as 600 µm (0.6 mm). The sieved biomass was stored in a zipped lock plastic bag at ambient temperature until use. All other analytical grade chemicals for compositional analysis, acid hydrolysis and analysis were obtained from Merck, Germany and Himedia, India.

### 3.2.2 Determination of extractives

The amount of extractives in sugarcane bagasse was estimated using Soxhlet extraction apparatus through extraction thimbles. Acetone 60 mL for 1 g of oven dried bagasse was used as the solvent for extraction and the temperature was held at 70℃ for a 4 h run period on the heating mantle. The sample was air dried for few minutes at room temperature. It was then dried at 105°C in an oven until a constant weight was obtained and then cooled in a desiccator. The weight percent (wt%) of the extractives content was evaluated as the difference in weight between the raw extractive–laden bagasse and extractive–free bagasse (Di Blasi et al., 1999; Adeeyo et al., 2015).

### 3.2.3 Hemicellulose analysis

1 g of extracted dried bagasse was transferred into a 250 mL Erlenmeyer flask. 150 mL of 0.5 M NaOH was added. The mixture was boiled for 3.5 h with distilled water so as to increase the heating effect and minimize lime scales that can come from tap water. It was filtered after cooling through vacuum filtration and washed until neutral pH. The residue was dried to a constant weight at 105°C in an oven. The difference between the sample weight before and after this treatment was the hemicellulose content (wt%) of oven dried bagasse (Ayeni et al., 2013a; Ayeni et al., 2013b).

### 3.2.4 Lignin analysis

0.3 g of dried extracted bagasse was weighed in glass test tubes and 3 mL of 72 wt% $H_2SO_4$ was added. The sample was kept at room temperature for 2 h with carefully shaking at 30 min intervals to allow for complete hydrolysis. After the initial hydrolysis, 84 mL of distilled water was added in order to get 4 wt% $H_2SO_4$ solutions. The second step of hydrolysis was made to occur in an autoclave for 1 h at 121°C. The mixture was then cooled at room temperature. Sugarcane bagasse hydrolysate was filtered through vacuum filtration. The acid insoluble lignin was determined by drying the residues at 105℃ and cooled in a desiccator. The acid soluble lignin fraction was determined by measuring the absorbance of the acid hydrolysed samples at

278 nm. The lignin content (wt%) was calculated as the summation of acid insoluble lignin and acid soluble lignin (Sluiter et al., 2008; Adeeyo et al., 2015).

### 3.2.5 Determination of cellulose

The cellulose content (wt%) was determined by difference, assuming that extractives, hemicellulose, lignin, and cellulose are the only components of the entire sugarcane bagasse.

### 3.2.6 Acid hydrolysis of sugarcane bagasse

Sugarcane bagasse was treated with dilute sulphuric acid to hydrolyse hemicellulose. The upper and lower limit values of the process parameters for dilute acid hydrolysis of sugarcane bagasse were fixed on the basis of previous literature. Thus, the bagasse samples were treated with 0.5–3.5% v/v $H_2SO_4$, temperature range of 100°–130°C and treatment time of 10–40 min. Prior to statstical optimization of these process parameters, solid to liquid ratio was optimized in preliminary experiments and fixed as 1:30 (w/v). Hydrolysis was carried out in an autoclave (Model: LAC–5040S, Daihan Labtech Co. Ltd., South Korea) at a pressure of 15 psi. The valve of autoclave was depressurized in impulsive mode after completion of the hydrolysis. The biomass sample was cooled in an ice bath after the pretreatment to stop the hydrolysis reaction.

### 3.2.7 Analytical methods

After dilute sulphuric acid hydrolysis, the reaction mixture was centrifuged at 6000 rpm for 10 min and then filtered in a vacuum filter (0.45 µm membrane filter). The monomeric sugar concentrations (viz. glucose, xylose, and arabinose) and acetic acid were determined by HPLC (Make: Perkin Elmer, Series 200) using Hiplex–H column (Make: Varian, 300 mm × 5 µm × 4.6 mm) coupled with Refractive Index detector, 0.005 M $H_2SO_4$ as mobile phase and flow rate of 0.6 mL/min at a column temperature of 60°C. Concentrations of the inhibitory by–products (furfural and 5–HMF) in the hydrolysate were determined by HPLC (Shimadzu, Model: UFLC SPD–20A) equipped with reverse phase C–18 column (5 µm × 4.6 mm × 250 mm) and UV detector at 280

nm. The mobile phase was a mixture of acetonitrile and water (80:20 v/v) with flow rate of 1 mL/min.

### 3.2.8 Experimental design

The process parameters (viz. temperature, concentration of $H_2SO_4$, and hydrolysis time) for dilute acid hydrolysis of sugarcane bagasse were optimized using response surface methodology with Box Behnken design (BBD). As explained earlier, the upper and lower limit values of the process parameters were fixed based on the previous literature. The coded and actual levels of the variables are given in Table 3.1.

**Table 3.1.** Coded and actual levels of the variables for Box–Behnken design

| Independent variables | Symbols | Coded and actual levels | | |
|---|---|---|---|---|
| | | –1 | 0 | +1 |
| Temperature (°C) | $X_1$ | 100 | 115 | 130 |
| Hydrolysis time (min) | $X_2$ | 10 | 25 | 40 |
| Acid load ($H_2SO_4$ concn. % v/v) | $X_3$ | 0.5 | 2 | 3.5 |

**Table 3.2.** Box–Behnken design with experimental and predicted responses of dependent variable (xylose concentration, g/L)

| Run no. | Temperature (°C), $X_1$ | Hydrolysis time (min), $X_2$ | Acid load (% v/v), $X_3$ | Xylose (g/L) | |
|---|---|---|---|---|---|
| | | | | Experimental | Predicted |
| 1 | –1 (100) | –1 (10) | 0 (2) | 2.19 ± 0.06 | 2.36 |
| 2 | +1 (130) | –1 (10) | 0 (2) | 7.21 ± 0.26 | 7.08 |
| 3 | –1 (100) | +1 (40) | 0 (2) | 5.63 ± 0.17 | 5.76 |
| 4 | +1 (130) | +1 (40) | 0 (2) | 7.64 ± 0.23 | 7.50 |
| 5 | –1 (100) | 0 (25) | –1 (0.5) | 1.15 ± 0.03 | 1.10 |
| 6 | +1 (130) | 0 (25) | –1 (0.5) | 6.65 ± 0.20 | 6.91 |
| 7 | –1 (100) | 0 (25) | +1 (3.5) | 5.97 ± 0.18 | 5.73 |
| 8 | +1 (130) | 0 (25) | +1 (3.5) | 6.32 ± 0.24 | 6.38 |
| 9 | 0 (115) | –1 (10) | –1 (0.5) | 3.29 ± 0.10 | 3.18 |

| | | | | | |
|---|---|---|---|---|---|
| 10 | 0 (115) | +1 (40) | –1 (0.5) | 7.01 ± 0.21 | 6.93 |
| 11 | 0 (115) | –1 (10) | +1 (3.5) | 6.99 ± 0.25 | 7.07 |
| 12 | 0 (115) | +1 (40) | +1 (3.5) | 7.02 ± 0.27 | 7.13 |
| 13 | 0 (115) | 0 (25) | 0 (2) | 7.93 ± 0.31 | 7.92 |
| 14 | 0 (115) | 0 (25) | 0 (2) | 8.27 ± 0.34 | 7.92 |
| 15 | 0 (115) | 0 (25) | 0 (2) | 7.56 ± 0.29 | 7.92 |

The complete BBD design constituting 15 individual runs (with 12 factorials and 3 replicates at the center points) is shown in Table 3.2. Each experimental run was performed in triplicate and average value of response variable (xylose concentration) was considered for analysis. The response variable (xylose concentration) for process parameters optimization was fitted to the $2^{nd}$–order polynomial regression equation as follows:

$$Y = \beta_o + \sum \beta_i X_i + \sum \beta_{ii} X_i^2 + \sum \beta_{ij} X_{ij} \quad (3.1)$$

where: $Y$ is the response; $\beta_o$ a constant; $\beta_i$ the linear coefficients; $\beta_{ii}$ the squared coefficients; and $\beta_{ij}$ the interaction coefficients.

MINITAB statistical software 17.1 (Trial Version) was used for the analysis and optimization of the experimental data. Analysis of variance (ANOVA) was performed in order to evaluate the statistical significance of the model.

## 3.3 Results and discussion

### 3.3.1 Compositional analysis of sugarcane bagasse

The compositional analysis of sugarcane bagasse is shown in Table 3.3 with comparison of results obtained in the present work to the literature values for the same biomass. The composition of sugarcane bagasse analysed in the present study was as follows: cellulose = 40.27 wt%, hemicellulose = 30.13 wt%, lignin = 27.14 wt% and extractives = 2.46 wt% on dry basis. Adeeyo et al. (2015) studied the compositional characterization of Nigerian sugarcane bagasse by

the same method as we used in the present study. The results of their research work were cellulose = 35.28 wt%, hemicellulose = 33.28 wt%, lignin = 25.20 wt%, extractives = 2.14 wt% and ash = 4.1 wt%. Timung et al. (2016) have studied the chemical composition of Indian sugarcane bagasse. The results of their study were as follows: cellulose = 40.15 wt%, hemicellulose = 22.78 wt%, lignin = 20.81 wt% using TGA method and extractives = 0.9 and 6.5 wt% with hexane and ethanol as a solvent for extraction, respectively.

The results of the present study were comparable to other results done by various researchers as shown in Table 3.3. The variation in the composition of sugarcane bagasse depends on various factors such as the plant genetics, growth conditions, age and processing conditions, geographical locations, methods (procedures) developed for analysis, the type of solvents used in the compositional analysis (Rafiqul and Sakinah, 2013; Adeeyo et al., 2015).

**Table 3.3.** Comparison of composition of sugarcane bagasse in the present study with literature values (wt%) on dry basis

| Cellulose (wt%) | Hemicellulose (wt%) | Lignin (wt%) | Extractives (wt%) | Ash (wt%) | References |
|---|---|---|---|---|---|
| 40.27 ± 1.3 | 30.13 ± 0.9 | 27.14 ± 0.6 | 2.46 ± 0.2 | – | Present study |
| 35.28 | 33.28 | 25.20 | 2.14 | 4.1 | Adeeyo et al. 2015 |
| 40.15 | 22.78 | 20.81 | 6.5 | – | Timung et al. 2016 |
| 39 | 26.2 | 24 | – | – | Aguilar et al. 2002 |
| 43 | 31 | 11 | 9 | 6 | Martin et al. 2007 |

### 3.3.2 Effect of solid to liquid ratio on dilute acid hydrolysis

Figures 3.1 and 3.2 show the effect of solid to liquid ratio on xylose yield for 2% v/v $H_2SO_4$ and 1% v/v $H_2SO_4$, respectively at 120°C hydrolysis of sugarcane bagasse. The experimental results

in Figs. 3.1 and 3.2 indicated that as the solid to liquid ratio varied from 1:10 to 1:30, the yield of xylose increased. This was expected as decreasing the solid to liquid ratio reduced the rate at which the xylose decomposed as the xylose produced is more dilute within the hydrolysate. Excess of liquid phase in hydrolysis mixture (solid to liquid ratio of 1:30) helps in maximum hydrolysis (maximum xylan dissolution) of hemicellulosic fraction. Large excess of liquid phase also reduces bulk concentration of monomeric sugars resulting from hydrolysis, which helps in minimizing their further degradation to inhibitory by–products such as furfural. Lavarack et al. (2002) have also confirmed that decreasing the solid to liquid ratio from 1:5 to 1:20 increased the xylose yield. Amenaghawon et al. (2014) have studied the statistical optimization of dilute sulphuric acid hydrolysis condition of cassava bagasse. They obtained a maximum sugar yield of 81.63% at an optimum solid to liquid ratio of 1:25 (g/mL).

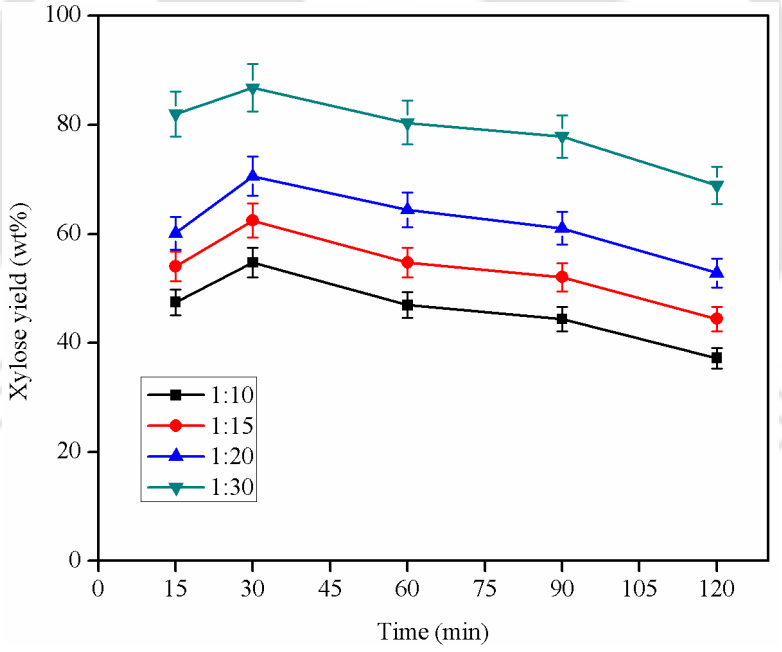


**Figure 3.1.** The effect of solid to liquid ratio on xylose yield (wt%) in dilute acid hydrolysis of sugarcane bagasse (120$^{o}$C and 2% v/v $H_2SO_4$)

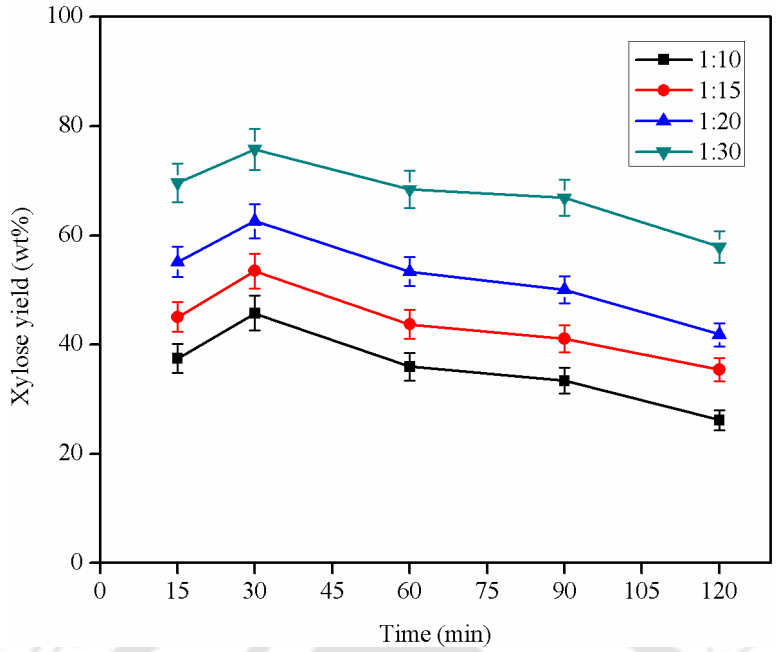


**Figure 3.2.** The effect of solid to liquid ratio on xylose yield (wt%) in dilute acid hydrolysis of sugarcane bagasse (120°C and 1% v/v $H_2SO_4$)

### 3.3.3 Optimization of process parameters for dilute acid hydrolysis of sugarcane bagasse

Complete Box Behnken design (BBD) with the experimental and predicted xylose concentration is shown in Table 3.2. The maximum xylose concentration (8.27 g/L) was obtained at the center points, i.e. 2% v/v $H_2SO_4$ concentration, temperature of 115°C and 25 min (experiment run no. 14). The corresponding minimum xylose concentration (1.15 g/L) was obtained at 0.5% v/v $H_2SO_4$ concentration, temperature of 100°C and 25 min (experiment run no. 5). This depicts that at lower temperature and acid concentration the xylose extraction was also lower. At higher temperature, lowering of the xylose concentration might be due to formation of by–products from the xylose, whereas the lower temperature was not sufficient enough to hydrolyse sugarcane bagasse.

The second order polynomial model equation for the fitted data using coded values of independent variables and concentration of xylose as a response variable is as follows:

$$Xylose(g/L) = 7.92 + 1.615X_1 + 0.956X_2 + 1.021X_3 - 1.646X_1X_1 - 0.599X_2X_2 - 1.244X_3X_3 - 0.745X_1X_2 - 1.290X_1X_3 - 0.922X_2X_3 \quad (3.2)$$

The *p*– and *t*–values of linear, quadratic and interaction coefficients for the second order polynomial model are given in Table 3.4. Analysis of variance (ANOVA) for the fitted quadratic model is shown in Table 3.5. The model summary for regression coefficients ($R^2$ = 99.2%, adjusted $R^2$ = 97.8% and predicted $R^2$ = 92.8%) depicts that the quadratic model fits to the experimental data. The *t*–test, *F*– and *p*–values indicate relative significance of independent variables of quadratic polynomial model coefficients. A large *t*–stat value and *p*–value ≤ 0.05 depicts significance of the coefficients and the corresponding independent variable. Relative *F*–values of linear, interaction and quadratic coefficients indicate the significance of the individual effect of the independent variables and the magnitude of interaction between them. From the ANOVA results shown in Table 3.5, the *F*–value for the model, linear, quadratic, and interaction coefficients are 70.39, 120.47, 50.19, and 40.50, respectively. *p*–values for all the linear, interaction and square coefficients are < 0.05, which depicts that all variables have significant effect on dilute sulphuric acid hydrolysis of sugarcane bagasse. The Lack of Fit with *F*–value and *p*–value of 0.67 and 0.65, respectively, indicates that Lack of Fit is not significant as compared to the pure error or the model was significant.

**Table 3.4.** Model coefficients, *t*– and *p*–values for second order regression model

| Term | Coefficient | *t*–value | *p*–value |
|---|---|---|---|
| Constant ( $\beta_o$ ) | 7.920 | 43.150 | 0.000 |
| *Linear coefficients* | | | |
| Temperature ( $X_1$ ) | 1.615 | 14.370 | 0.000 |
| Time ( $X_2$ ) | 0.956 | 8.510 | 0.000 |
| Acid load ( $X_3$ ) | 1.021 | 9.090 | 0.000 |
| *Quadratic coefficients* | | | |
| Temperature × Temperature ( $X_1X_1$ ) | –1.646 | –9.950 | 0.000 |
| Time × Time ( $X_2X_2$ ) | –0.599 | –3.620 | 0.015 |
| Acid load × Acid load ( $X_3X_3$ ) | –1.244 | –7.520 | 0.001 |
| *Interaction coefficients* | | | |
| Temperature × Time ( $X_1X_2$ ) | –0.745 | –4.690 | 0.005 |
| Temperature × Acid load ( $X_1X_3$ ) | –1.290 | –8.120 | 0.000 |
| Time × Acid load ( $X_2X_3$ ) | –0.922 | –5.800 | 0.002 |

**Table 3.5.** ANOVA for quadratic model

| Source | DF | SS | MS | *F*–value | *p*–value |
|---|---|---|---|---|---|
| Model | 9 | 64.022 | 7.113 | 70.390 | 0.000 |
| Linear | 3 | 36.525 | 12.175 | 120.470 | 0.000 |
| Quadratic | 3 | 15.217 | 5.072 | 50.190 | 0.000 |
| Interaction | 3 | 12.280 | 4.093 | 40.500 | 0.001 |
| Error | 5 | 0.505 | 0.101 | | |
| Lack–of–Fit | 3 | 0.253 | 0.084 | 0.670 | 0.645 |
| Pure error | 2 | 0.2522 | 0.1261 | | |
| Total | 14 | 64.527 | | | |

DF is the degree of freedom; SS is the sum of squares; MS is the mean square; significant p values, $p \leq 0.05$; $R^2 = 0.992$; predicted $R^2 = 0.928$; adjusted $R^2 = 0.978$.

**Table 3.6.** Analysis of the contour plots

| Parameter space for maximum xylose concentration | | | | |
|---|---|---|---|---|
| Contour plot | Range of parameters | | | |
| | Temperature,°C | Time, min | Acid load, % v/v | Xylose, g/L |
| Temperature vs time | 112 to 128 | 18 to 40 | 2* | 8 |
| Temperature vs Acid load | 113 to 127 | 25* | 1.4 to 3.1 | 8 |
| Time vs Acid load | 115* | –0.24 to 1 | 1.3 to 3.1 | 8 |

*– parameter values at the center points

The interactions among the various process variables involved in BBD in dilute acid hydrolysis of sugarcane bagasse were evaluated by plotting the interaction plots (Figs. 3.3A–C) and contour plots (Figs. 3.4A–C) for xylose yield. The interaction and contour plots were constructed showing the interaction among two factors by holding others at their centre values for the yield of xylose. Fig. 3.3A depicts the effect of temperature and hydrolysis time on xylose yield when $H_2SO_4$ concentration was set at 2% v/v as the center point. It was evident that the predicted xylose yield continuously increased with the increase of temperature up to 120°C for the hydrolysis times 25 and 40 min and 130°C for 10 min hydrolysis time. It was revealed from Fig. 3.3A that at 100°C, xylose yield = 2.25 g/L at 10 min, xylose yield = 4.75 g/L at 25 min and xylose yield = 5.85 g/L at 40 min. Thus, at lower temperatures, longer hydroysis time gives higher xylose yield. It was

also found that with higher temperature and lower hydrolysis time the xylose yield increased (i.e. for >120$^{o}$C, xylose yield for 25 min > xylose yield for 40 min). Fig. 3.3B shows the interaction effect of temperature and acid concentration or acid load. As depicted from the Fig. 3.3B, the xylose yield increased continuously with temperature range of the experiment i.e. 100–130$^{o}$C for acid concentrations 0.5, 2% v/v. The xylose yield increased from 1.15 g/L and 4.75 g/L at 100$^{o}$C to 6.95 g/L and 7.85 g/L at 130$^{o}$C for 0.5 and 2% v/v acid load, respectively. For 3.5% v/v acid load, the xylose yield increased up to center point temperature (xylose yield = 7.75 g/L at 115$^{o}$C) and then decreased continuously (xylose yield = 6.50 g/L at 130$^{o}$C). These results showed that at higher acid load, lower temperature increased the yield of xylose. However, at higher temperature, higher acid load lowers the yied of xylose. This implies that at lower acid concentration and temperature, it is hard to extract xylose from the lignocellulosic biomass. The interaction effect of time and acid load is shown in Fig. 3.3C. As shown from Fig. 3.3C, at acid concentrations of 0.5 and 2% v/v the xylose yield increased continuously with hydrolysis time. Higher acid load and shorter hydrolysis time gives an increased xylose yield. Conversely, lower acid load and shorter hydrolysis time resulted in lower xylose yield as evident form Fig. 3.3C.

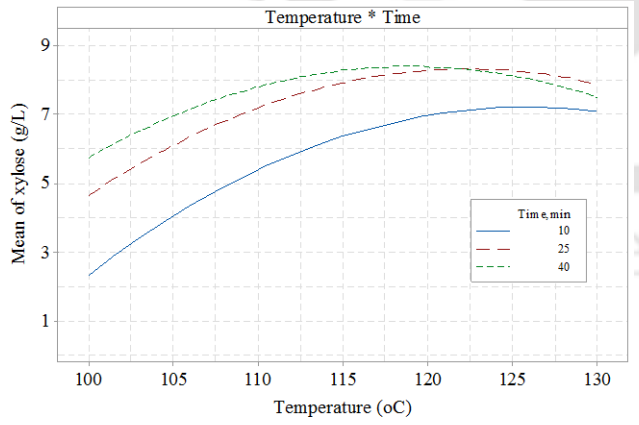


(A)

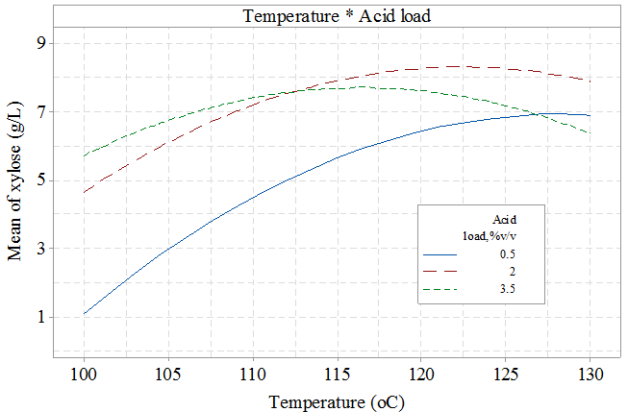


(B)

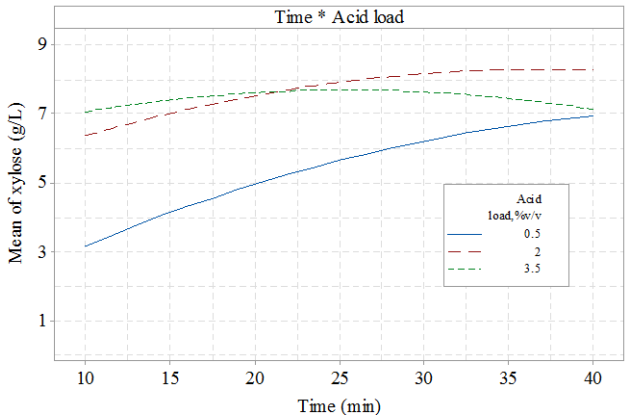


(C)

**Figure 3.3**. Interaction effects for xylose yield (g/L) between: (A) temperature and time, (B) temperature and acid load, (C) time and acid load

The contour plots (shown in Fig. 3.4); which are graphical representation of regression model equation 3.2; represent infinitive number of combinations of two test variables, with the third variable maintained at its zero (center point) level. The contours were plotted to observe the interaction of two independent variables. An elliptical contour plot is obtained by the interaction of temperature with acid load Fig. 3.4A indicating a strong interaction between the parameters. An elliptical nature contour plots are obtained in Fig. 3.4B (temperature vs time) and Fig. 3.4C (time vs acid load) depicting significant interaction between the variables. It was also confirmed by the *t*– and *p*–values of their interaction coefficients. The parameter space for maximum xylose concentration for the range of two variables fixing the third variable at its centre point is shown in Table 3.6. The range of the variables was represented in the actual values. The maximum xylose concentration of 8 g/L was obtained in all the ranges.

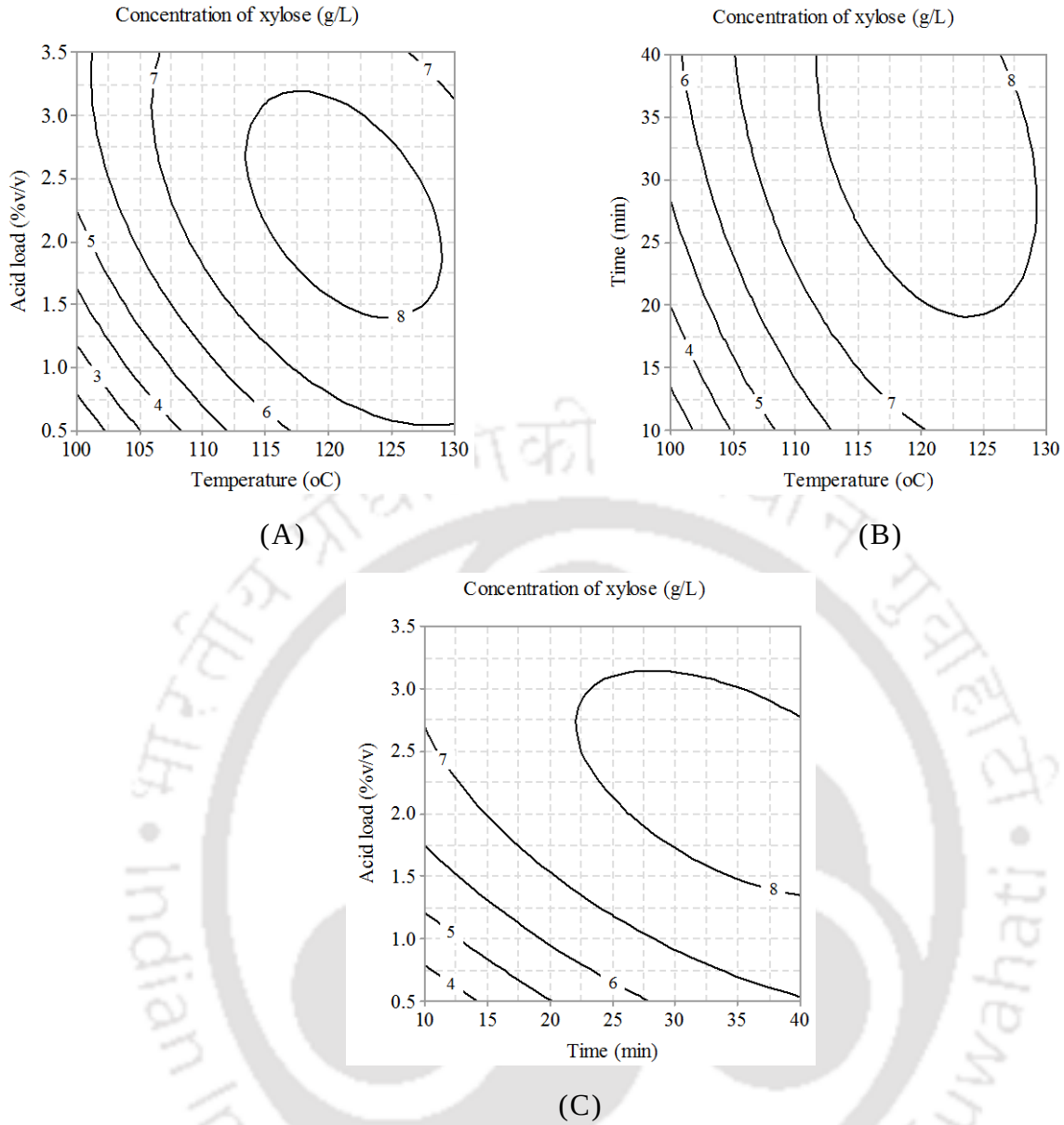


**Figure 3.4.** Contour plots: (A) interaction between temperature and acid load, (B) interaction between temperature and time, (C) interaction between time and acid load. The values of variables are shown in coded units.

Figure 3.5 depicts the desirability plot for the optimum values of the process parameters for dilute sulphuric acid hydrolysis of sugarcane bagasse. The optimum values of the process parameters under this model were concentration of $H_2SO_4$ = 2% v/v, temperature = 120℃ and hydrolysis time = 33 min. The maximum xylose concentration of 8.49 g/L with a corresponding yield of 84.5% w/w hemicellulose was obtained with the optimum values. Hong et al. (2016) have studied the optimal conditions of dilute acid hydrolysis of corn stover. The optimum process parameters

for maximum xylose concentration of 6.09 g/L was temperature = 120°C, $H_2SO_4$ concentration = 2.5% w/v and hydrolysis time = 90 min. Moutta et al. (2013) reported optimization of sugarcane leaves hydrolysis and obtained a maximum xylose concentration of 56.5 g/L under the optimum hydrolysis conditions of $H_2SO_4$ concentration = 2.9% w/v, temperature = 130°C, solid to liquid ratio = 1:4 and hydrolysis time = 30 min. However, along with maximum xylose concentration considerable inhibitory by–products were formed at these optimal conditions which are toxic for fermentative microorganisms. Laopaiboon et al. (2010) reported in their study that maximum xylose concentrations of 8.44 g/L was obtained with optimal process parameters of $H_2SO_4$ concentration = 5% v/v, temperature = 120°C and hydrolysis time = 60 min from sugarcane bagasse.

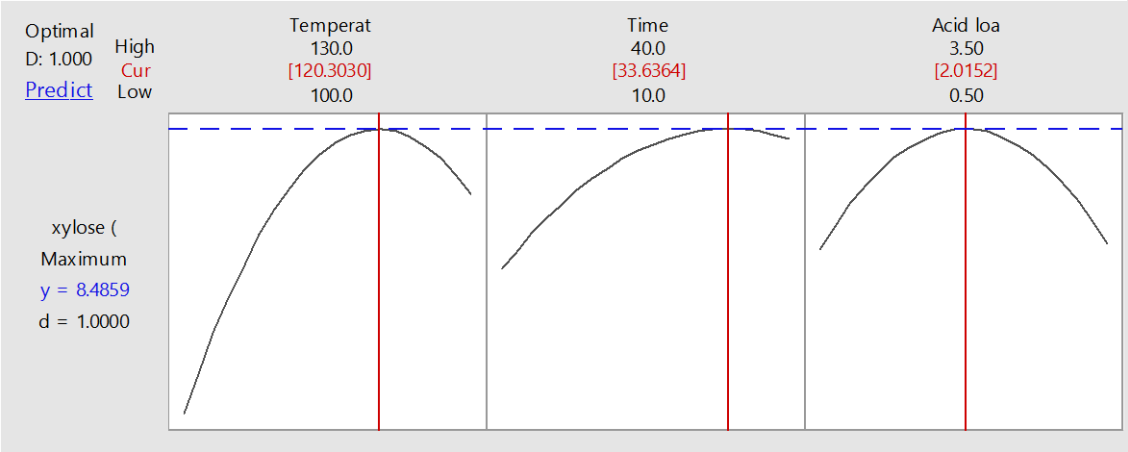


**Figure 3.5.** Desirability plot for optimum values of the process parameters for maximum xylose yield in dilute acid hydrolysis of sugarcane bagasse

### 3.3.4 Validation of experiments

Optimum process parameters for maximum xylose concentration predicted by the BBD experiments and RSM analysis have been corroborated by validation experiments of dilute sulphuric acid hydrolysis of sugarcane bagasse. The validation experiments were conducted in triplicate under optimized conditions of $H_2SO_4$ concentration = 2% v/v, temperature = 120°C, hydrolysis time = 33 min and solid to liquid ratio = 1:30 w/v to ascertain reproducibility of

results. The results of validation experiment under the optimum conditions agreed well with model predictions.

### 3.3.5 Analysis of hemicellulosic hydrolysate at the optimum conditions

Upon completion of dilute sulphuric acid hydrolysis of sugarcane bagasse under optimum conditions, the hydrolysate medium was analyzed for the presence of various sugar monomers and inhibitory by–products. The analysis results of hemicellulosic hydrolysate with sugar monomers and inhibitory by–products are depicted in Fig. 3.6. It was observed that the optimum conditions of dilute acid hydrolysis of sugarcane bagasse resulted in monomeric sugars in the hydrolysate consisting of xylose = 8.68 g/L, glucose = 2.43 g/L and arabinose = 1.23 g/L. Moreover, inhibitory by–products (viz. acetic acid = 1.02 g/L, furfural = 0.36 g/L and 5–HMF = 0.21 g/L) were generated in dilute sulphuric acid catalyzed hydrolysis of sugarcane bagasse at optimum conditions. pH adjustment with acid and base is sufficient to detoxify these inhibitory by–products formed with optimized hydrolysis condition for the subsequent fermentation of the hydrolysate to produce xylitol using *Candida tropicalis*.

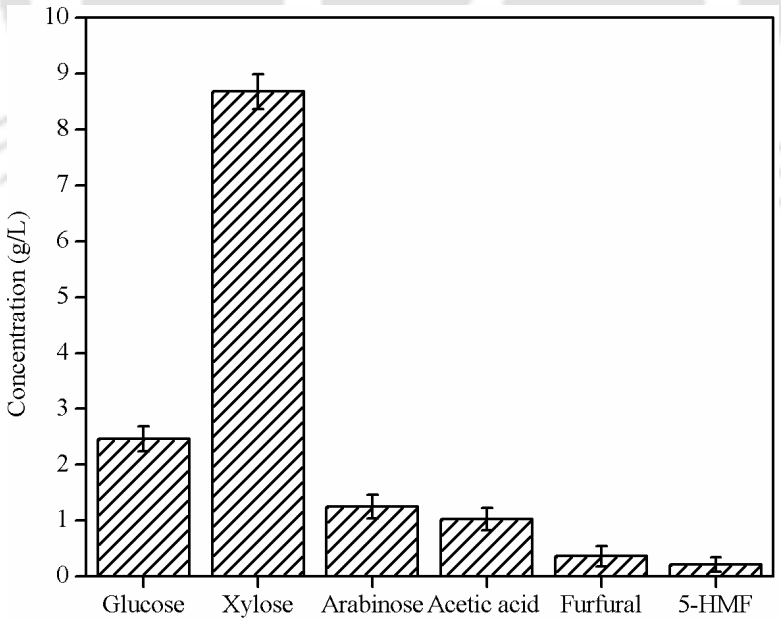


**Figure 3.6** Analysis of hemicellulosic hydrolysate at the optimum conditions

### 3.4 Conclusions

A hemicellulosic hydrolysate with xylose concentration of 8.49 g/L, corresponding to the yield of 84.5% w/w hemicellulosic fraction, was obtained under the optimized conditions for dilute sulphuric acid hydrolysis of sugarcane bagasse (viz. 120°C, 2% v/v $H_2SO_4$ concentration and hydrolysis time of 33 min). Generation of inhibitory by–products under the optimized dilute acid hydrolysis conditions was limited. Therefore, further detoxifications of the inhibitory by–products were not necessary except pH adjustment in the fermentation of the hydrolysate for the production of xylitol. The results showed that sugarcane bagasse is a potential lignocellulosic biomass for the production of biofuels and value–added chemicals.

**References**

Adeeyo, O.A., Oresegun, O.M., Oladimeji, T.E., 2015. Compositional analysis of lignocellulosic materials: Evaluation of an economically viable method suitable for woody and non–woody biomass. Am. J. Eng. Res. 4(4), 14–19.

Aguilar, R., Ramırez, J.A., Garrote, G., Vázquez, M., 2002. Kinetic study of the acid hydrolysis of sugar cane bagasse. J. Food Eng. 55(4), 309–318.

Amenaghawon, N.A., Ogbeide, S.E., Okieimen, C.O., 2014. Application of statistical experimental design for the optimisation of dilute sulphuric acid hydrolysis of cassava bagasse. Acta Polytech. Hung. 11(9), 239–250.

Ayeni, A.O., Banerjee, S., Omoleye, J.A., Hymore, F.K., Giri, B.S., Deshmukh, S.C., Pandey, R.A., Mudliar, S.N., 2013. Optimization of pretreatment conditions using full factorial design and enzymatic convertibility of shea tree sawdust. Biomass Bioenerg. 48, 130–138.

Ayeni, A.O., Hymore, F.K., Mudliar, S.N., Deshmukh, S.C., Satpute, D.B., Omoleye, J.A., Pandey, R.A., 2013. Hydrogen peroxide and lime based oxidative pretreatment of wood

waste to enhance enzymatic hydrolysis for a biorefinery: Process parameters optimization using response surface methodology. Fuel 106, 187–194.

Chandel, A.K., Kapoor, R.K., Singh, A., Kuhad, R.C., 2007. Detoxification of sugarcane bagasse hydrolysate improves ethanol production by Candida shehatae NCIM 3501. Bioresour. Technol. 98(10), 1947–1950.

Converse, A.O., Kwarteng, I.K., Grethlein, H.E., Ooshima, H., 1989. Kinetics of thermochemical pretreatment of lignocellulosic materials. Appl. Biochem. Biotechnol. 20(1), 63–78.

Di Blasi, C., Signorelli, G., Di Russo, C., Rea, G., 1999. Product distribution from pyrolysis of wood and agricultural residues. Ind. Eng. Chem. Res. 38(6), 2216–2224.

Harmsen, P.F.H., Huijgen, W., Bermudez, L., Bakker, R., 2010. Literature review of physical and chemical pretreatment processes for lignocellulosic biomass. Energ. Res. Centre Nether. 2010, 10–13.

Himmel, M.E., Ding, S.Y., Johnson, D.K., Adney, W.S., Nimlos, M.R., Brady, J.W., Foust, T.D., 2007. Biomass recalcitrance: engineering plants and enzymes for biofuels production. Sci. 315(5813), 804–807.

Hong, E., Kim, J., Rhie, S., Ha, S.J., Kim, J., Ryu, Y., 2016. Optimization of dilute sulfuric acid pretreatment of corn stover for enhanced xylose recovery and xylitol production. Biotechnol. Bioprocess Eng. 21(5), 612–619.

Hosseini, S.A., Lambert, R., Kucherenko, S., Shah, N., 2010. Multiscale modeling of hydrothermal pretreatment: from hemicellulose hydrolysis to biomass size optimization. Energ. Fuels 24(9), 4673–4680.

Jiang, L.Q., Fang, Z., Li, X.K., Luo, J., Fan, S.P., 2013. Combination of dilute acid and ionic liquid pretreatments of sugarcane bagasse for glucose by enzymatic hydrolysis. Process Biochem. 48(12), 1942–1946.

Jonglertjunya, W., Makkhanon, W., Siwanta, T., Prayoonyong, P., 2014. Dilute acid hydrolysis of sugarcane bagasse for butanol fermentation. Chiang Mai J. Sci. 41(1), 60–70.

Karp, S.G., Woiciechowski, A.L., Soccol, V.T., Soccol, C.R., 2013. Pretreatment strategies for delignification of sugarcane bagasse: a review. Braz. Arch. Biol. Technol. 56(4), 679–689.

Khuri, A.I., Cornell, J.A., 1987. Determining optimum conditions: Response surface design and analysis. New York, Marcel Dekker, 149–205.

Laopaiboon, P., Thani, A., Leelavatcharamas, V., Laopaiboon, L., 2010. Acid hydrolysis of sugarcane bagasse for lactic acid production. Bioresour. Technol. 101(3), 1036–1043.

Lavarack, B.P., Griffin, G.J., Rodman, D., 2002. The acid hydrolysis of sugarcane bagasse hemicellulose to produce xylose, arabinose, glucose and other products. Biomass Bioenerg. 23(5), 367–380.

Martín, C., Klinke, H.B., Thomsen, A.B., 2007. Wet oxidation as a pretreatment method for enhancing the enzymatic convertibility of sugarcane bagasse. Enzyme Microb. Technol. 40(3), 426–432.

Mosier, N., Wyman, C., Dale, B., Elander, R., Lee, Y.Y., Holtzapple, M., Ladisch, M., 2005. Features of promising technologies for pretreatment of lignocellulosic biomass. Bioresour. Technol. 96(6), 673–686.

Moutta, R.D.O., Ferreira–Leitão, V.S., Bon, E.P.D.S., 2014. Enzymatic hydrolysis of sugarcane bagasse and straw mixtures pretreated with diluted acid. Biocatal. Biotransform. 32(1), 93–100.

Moutta, R.O., Chandel, A.K., Rodrigues, R.C.L.B., Silva, M.B., Rocha, G.J.M., Silva, S.S., 2012. Statistical optimization of sugarcane leaves hydrolysis into simple sugars by dilute sulfuric acid catalyzed process. Sugar Tech. 14(1), 53–60.

Pattra, S., Sangyoka, S., Boonmee, M., Reungsang, A., 2008. Bio–hydrogen production from the fermentation of sugarcane bagasse hydrolysate by Clostridium butyricum. Int. J. Hydrogen Energ. 33(19), 5256–5265.

Rafiqul, I.S.M., Sakinah, A.M., 2013. Processes for the production of xylitol: a review. Food Rev. Int. 29(2), 127–156.

RG, C., Godoy, G.G., Goncalves, A.R., 2012. Study of sugarcane bagasse pretreatment with sulfuric acid as a step of cellulose obtaining. World Academy Sci. Eng. Technol. Int. J. Biol. Biomol. Agric. Food Biotechnol. Eng. 6(1), 6–10.

Saha, B.C., Iten, L.B., Cotta, M.A., Wu, Y.V., 2005. Dilute acid pretreatment, enzymatic saccharification, and fermentation of rice hulls to ethanol. Biotechnol. Prog. 21(3), 816–822.

Sindhu, R., Kuttiraja, M., Binod, P., Janu, K.U., Sukumaran, R.K., Pandey, A., 2011. Dilute acid pretreatment and enzymatic saccharification of sugarcane tops for bioethanol production. Bioresour. Technol. 102(23), 10915–10921.

Sluiter, A., Hames, B., Ruiz, R., Scarlata, C., Sluiter, J., Templeton, D., Crocker, D., 2008. Determination of structural carbohydrates and lignin in biomass. Lab. Anal. Proced. 1617.

Sun, Y., Cheng, J., 2002. Hydrolysis of lignocellulosic materials for ethanol production: a review. Bioresour. Technol. 83(1), 1–11.

Timung, R., Naik Deshavath, N., Goud, V.V., Dasu, V.V., 2016. Effect of subsequent dilute acid and enzymatic hydrolysis on reducing sugar production from sugarcane bagasse and spent citronella biomass. J. Energ.

Vargas Betancur, G.J., Pereira Jr, N., 2010. Sugarcane bagasse as feedstock for second generation ethanol production: Part I: Diluted acid pretreatment optimization. Electron. J. Biotechnol. 13(3), 10–11.

# CHAPTER 4

# KINETIC AND THERMODYNAMIC ANALYSIS OF DILUTE ACID HYDROLYSIS OF SUGARCANE BAGASSE

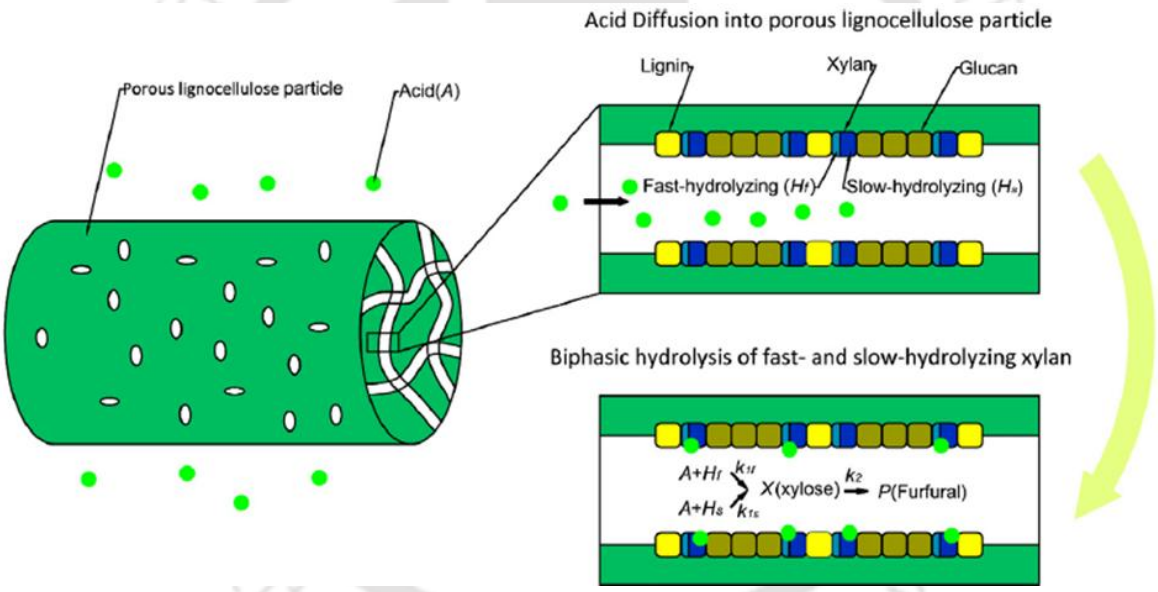


*(Reproduced from Chen et al., Bioresource Technology, vol. 177, pp. 8-16, 2015 with copyright permission of Elsevier)*

# CHAPTER 4

# KINETIC AND THERMODYNAMIC ANALYSIS OF DILUTE ACID HYDROLYSIS OF SUGARCANE BAGASSE

## 4.1 Introduction

With annual production of more than 340 million tons of sugarcane, India stands second in the world (after Brazil) in sugarcane production. Most of the sugarcane is utilized for sugar production. The bagasse left over after crushing of sugarcane is a potential low cost feedstock for fermentation–based biochemicals production due to its high cellulose and hemicellulose content (Harmsen et al., 2010). Production of biochemicals from lignocellulosic biomass essentially involves two steps: hydrolysis of hemicellulosic and cellulosic fractions of biomass followed by fermentation of the reducible sugars in the hydrolysate. The kinetics of hydrolysis of lignocellulosic biomass depends on physical factors such as porosity or surface area of biomass, the crystallinity of cellulosic fraction, in addition to hemicellulosic and lignin content of the biomass (Lavarack et al., 2002). The biomass pretreatment process is essentially aimed at removal of lignin and hemicellulose, in addition to reduction in cellulose crystallinity and rise in porosity of materials. Hemicellulose fraction in the biomass can be removed through process of dilute acid hydrolysis, catalysed by common acids such as sulphuric acid or hydrochloric acid (Hosseini et al., 2010; Jensen et al., 2008; Rodrıguez–Chong et al., 2004). Hemicellulose is a large polysaccharide with xylose (a pentose sugar) as the main building block. The process of dilute acid hydrolysis results in pentose sugars rich hydrolysate with xylose as the major

component. In addition to xylose, the hydrolysate from dilute acid hydrolysis may also contain some glucose and arabinose. From perspective of biosynthesis, xylose is seminal molecule and can be converted through fermentation route to numerous value–added products such as xylitol (Arrizon et al., 2012).

The chemical mechanism of dilute acid hydrolysis of polysaccharides in lignocellulosic biomass (viz. hemicellulose and cellulose) is quite complex (Aguilar et al., 2002; Lavarack et al., 2002; Lavarack et al., 2000; Lu et al., 2008). This reaction system is heterogeneous; as the substrate is in the solid phase while the catalyst in the liquid phase. The hydrolysis reaction is a multistep process, which includes 4 major steps (Aguilar et al., 2002) as follows: (1) diffusion of protons through the lignocellulosic biomass, (2) protonation and cleavage of ether bond between sugar monomers, (3) generation and solvation of carbocation intermediates with regeneration of protons and concurrent production of sugar monomers, oligomers and polymers, and (4) back diffusion of reaction products from biomass matrix in liquid phase. Empirical models have been used for analysis of complex reaction systems (Gámez et al., 2006; Rodrıguez–Chong et al., 2004). The first ever empirical model for dilute acid catalysed saccharification of wood (Douglas fir) was proposed by Saeman (1945) which comprised of two consecutive first order reactions, with kinetic constants of similar magnitude.

$$\text{Cellulose} \xrightarrow{k_1} \text{Glucose} \xrightarrow{k_2} \text{Decomposition products} \qquad (4.1)$$

This model could be generalized for polysaccharides in biomass (Lenihan et al., 2010; Orozco et al., 2013) as:

$$\underset{\text{(cellulose/hemicellulose)}}{\text{Polysaccharide}} \xrightarrow{k_1} \underset{\text{(glucose, xylose, arabinose etc.)}}{\text{Sugar monomers}} \xrightarrow{k_2} \underset{\text{(furfural, HMF etc.)}}{\text{Decomposition products}} \qquad (4.2)$$

Both steps of the above model are considered as pseudo–homogenous 1$^{st}$–order reactions (Maloney et al., 1985; Mehlberg and Tsao, 1979). In principle, the acid hydrolysis of biomass is a heterogeneous reaction. However, for modelling of this system, several simplified approaches have been proposed. The “pseudo homogeneous” words essentially refer to reaction near xylan–

water interface, in which the xylan dissolution is preceded to reaction. The most common approach of correlating experimental data, total xylan is considered to be composed of two fractions, each of which reacted as per homogeneous first order kinetic law. Fast–dissolving xylan reacts with greater kinetic constant, which is the "easy–to–hydrolyse–fraction" of hemicellulose, while slow dissolving xylan is the "difficult–to–hydrolyse–fraction". The first step represents the release of oligomers and monomers due to hydrolysis of cellulose or (glucan), xylan, arabinan etc., while the second step represents the decomposition of monomers into different products such as furfural, 5–hydroxymethyl furfural (5–HMF), formic acid etc. (Chen et al., 1996). It is also assumed that there are no reactions between the main fractions of lignocellulosic materials. The simultaneous differential equations for mass balance of polysaccharide, monomers and decomposition products can be solved to yield following time profile for monomeric sugars (Aguilar et al., 2002):

$$M = M_o e^{-k_2 t} + P_o \frac{k_1}{k_2 - k_1}\left(e^{-k_1 t} - e^{-k_2 t}\right) \tag{4.3}$$

where, *M* and *P* represent concentrations of monomeric and polymeric fractions. Saeman's model (1945) does not fit well for hydrolysis of hemicellulose, and hence a modified biphasic model has been suggested for analysis of dilute acid hydrolysis of hemicellulose (Lenihan et al., 2010; Orozco et al., 2013). This model has been described in greater detail in subsequent sections. Fitting of the experimental profiles of different products of dilute acid hydrolysis to the modified biphasic model yields kinetic constants, which give insight into the physical mechanism of the process and influence of various reaction parameters on xylose yield. These results also help in identifying optimum conditions for the hydrolysis.

In the present study, we have investigated the kinetic and thermodynamic features of xylose production through dilute acid hydrolysis of sugarcane bagasse. The dilute acid hydrolysis also results in by–products which act as inhibitors of microbial growth and fermentation. Principal by–products are: (1) acetic acid that results from hydrolysis of acetyl groups bonded to the

hemicellulosic monomers, and (2) furfural, which is generated as oxidative degradation products of pentose sugars like xylose. Some soluble phenolic products are also generated from acid catalysed oxidation of pentose sugars. In the present study, we have also analysed the kinetics of formation of three products, viz. glucose, arabinose and acetic acid, and it is obvious that the kinetics of furfural and 5–hydroxymethyl furfural (5–HMF) is included within xylose and glucose kinetic analysis. The experimental profiles of different products of dilute acid hydrolysis have been fitted to empirical kinetic models. As explained in subsequent sections, our analysis has identified optimum conditions for maximum xylose yield through hemicellulose hydrolysis, with concurrent minimum production of inhibitors.

## 4.2 Materials and methods

### 4.2.1 Materials

Sugarcane bagasse was obtained from local area in Guwahati, Assam (India). The biomass was dried and ground into small pieces. It was then sieved using 25 BSS mesh screen to obtain fraction with size less than 0.6 mm.

The composition of sugarcane bagasse was determined in previous chapter (chapter 3) as: cellulose = 40.27 wt%, hemicellulose = 30.13 wt%, lignin = 27.14 wt%, and extractives = 2.46 wt% on dry basis. All other analytical grade chemicals for acid hydrolysis and analysis were obtained from Merck, Germany and Himedia, India.

### 4.2.2 Acid hydrolysis of sugarcane bagasse

Sugarcane bagasse was treated with dilute sulphuric acid for hydrolysis of the hemicellulosic fraction. The bagasse samples were treated with 2% v/v $H_2SO_4$ at temperatures of 100°, 110°, 120°, 130°C and reaction time of 5, 10, 15, 30, 60, 90, 120 min at a solid to liquid ratio of 1:30 (w/v). Hydrolysis was carried out in an autoclave (Model: LAC–5040S, Daihan Labtech Co. Ltd., South Korea) at a pressure of 15 psi. The valve of autoclave was depressurized in impulsive mode after completion of the pretreatment. The biomass sample was cooled by immersing in an

ice bath after the pretreatment to stop the hydrolysis reaction.

### 4.2.3 Analytical methods

After dilute acid hydrolysis, the reaction mixture was centrifuged at 6000 rpm for 10 min and then filtered in a vacuum filter (0.45 µm membrane filter). The concentrations of reducing (or fermentable) sugars (viz. glucose, xylose, and arabinose), and acetic acid in the filtrate (or hydrolysate) were determined by HPLC (Make: Perkin Elmer, Series 200) using Hiplex–H column (Make: Varian, 300 mm × 5 µm × 4.6 mm) coupled with Refractive Index detector. The mobile phase was 0.005 M $H_2SO_4$ with flow rate of 0.6 mL/min at column temperature of 60°C. Concentrations of inhibitory compounds (furfural and 5–HMF) in hydrolysate were determined using HPLC (Shimadzu, Model: UFLC SPD–20A) equipped with reverse phase C–18 column (5 µm × 4.6 mm × 250 mm) and UV detector at 280 nm. The mobile phase in this analysis was a mixture of acetonitrile and water (80:20 v/v) at flow rate of 1 mL/min.

### 4.2.4 Kinetic and thermodynamic analysis

The actual chemical mechanism of hemicellulosic hydrolysis is quite complex. Therefore, lumped parameter models have been applied for kinetic analysis of hydrolysis. The original model proposed by Saeman (1945) for dilute acid hydrolysis of cellulose from fir has been modified for hydrolysis of hemicellulosic fraction in lignocellulosic biomass. The modified hydrolysis model is essentially a biphasic model which assumes that hydrolysis proceeds through two parallel pseudo–$1^{st}$ order reactions, in which one reaction has relatively much faster kinetics than the other (Lenihan et al., 2010; Orozco et al., 2013) The faster reaction corresponds to hydrolysis of "easy–to–hydrolyse" fraction of hemicellulose (represented as α), while the slower reaction represents hydrolysis of "difficult–to–hydrolyse" fraction of hemicellulose, represented as (1 – α). The "easiness" of hydrolysis of hemicellulose depends on many factors as follows: hemicellulose is essentially a heteroxylan and has mixed structure (crystalline +amorphous). The dissolution of xylan in the water (with acid) precedes the hydrolysis reaction. Fast reacting xylan

dissolves faster and undergoes quick hydrolysis. The higher the amorphous component in the hemicellulose structure, the faster the dissolution and higher the "ease" of hydrolysis. The optimal conditions of hydrolysis (which represent the "ease" of hydrolysis) are determined by both the sugar composition as well as the main types of glycosidic bonds that is, by the specific type of polysaccharide present in biomass. The biphasic kinetic model also assumes that overall hydrolysis reaction rates are independent of heat and mass transfer effects. There are two basic rationales underlying neglection of heat and mass transfer effects: (1) significantly small quantity of biomass in relatively large quantity of liquid, and (2) high temperature of the process that results in high heat transfer rates as well as fast diffusion of reactants across biomass matrix. Reaction scheme and kinetic expressions for the modified Saeman (1945) biphasic kinetic model are given below:

$$\left[\begin{array}{l}\text{Fast reacting xylan } (H_f) \xrightarrow{k_f} \\ \text{Slow reacting xylan } (H_s) \xrightarrow{k_s}\end{array}\right] \text{Xylose } (X) \xrightarrow{k_2} \text{Furfural } (F) \tag{4.4}$$

$$\frac{dC_{Hf}}{dt} = -k_f C_{Hf} \tag{4.5}$$

$$\frac{dC_{Hs}}{dt} = -k_s C_{Hs} \tag{4.6}$$

$$\frac{dC_X}{dt} = k_f C_{Hf} + k_s C_{Hs} - k_2 C_X \tag{4.7}$$

$$\frac{dC_F}{dt} = k_2 C_X \tag{4.8}$$

Solution of eqs. 4.5–4.8 yields time profile of xylose concentration ($C_X$) as:

$$C_X = \frac{\alpha k_f C_{Ho}}{k_2 - k_f}\left(e^{-k_f t} - e^{-k_2 t}\right) + \frac{k_s (1-\alpha) C_{Ho}}{k_2 - k_s}\left(e^{-k_s t} - e^{-k_2 t}\right) \tag{4.9}$$

where: $C_{Ho}$ is the total hemicellulosic fraction (sum of fast, $C_{Hf}$, and slow, $C_{Hs}$, reacting xylans) given as $C_{Ho} = C_{Hfo} + C_{Hso}$; α is the fraction of easy–to–hydrolyse xylan and is defined as $\alpha = C_{Hfo}/C_{Ho}$. $C_X$ and $C_F$ are concentrations of xylose and furfural respectively, the subscript 'o'

denotes the initial concentration. The initial condition for solution of eq. 4.9 is $C_{Xo} = 0$.

Kinetic constants of biphasic model, viz. $k_s$, $k_f$ and, $k_2$ for formation and degradation of xylose are assumed to obey Arrhenius law, $k = A\exp(-E/RT)$ where $k$ is the reaction rate constant, $E$ is the activation energy (kJ/mol) for reaction, $R$ is the universal gas constant ($8.3143\times10^{-3}$ kJ/mol·K), T is the temperature (K) and $A$ is the pre–exponential factor ($min^{-1}$). The kinetic constants or $k_i$ values have been obtained by fitting the kinetic expression to the experimental data using MATLAB Version: R2015a (8.5.0.197613). The kinetic expression was provided as custom equation to the curve fitting module, which fitted the time profiles to kinetic model with non–linear least–square fitting algorithm. Activation energy and pre–exponential factors for different reactions were determined from the slope and intercept of the Arrhenius plot, respectively.

Thermodynamic parameters of hemicellulose hydrolysis were also determined as follows:

Enthalpy change ($\Delta H$) in hydrolysis is related to activation energy (E) as:

$$\Delta H = E - RT \tag{4.10}$$

where $T$ is the hydrolysis temperature (K).

The entropies of hydrolysis ($\Delta S$) are obtained from Eyring equation using the value of reaction rate constants ($k$) and enthalpies change ($\Delta H$) as:

$$\frac{\Delta S}{R} = \ln\left(\frac{h}{k_B}\right) + \ln\left(\frac{k}{T}\right) + \frac{\Delta H}{RT} \tag{4.11}$$

where, $h$ is the Planck's constant ($6.626\times10^{-34}$ J·s) and $k_B$ is the Boltzmann constant ($1.381\times10^{-23}$ J/K).

The Gibbs free energy ($\Delta G$) for hydrolysis is determined as:

$$\Delta G = \Delta H - T\Delta S \tag{4.12}$$

## 4.3 Results and discussion

### 4.3.1 Sugarcane bagasse hemicellulose hydrolysis

As noted earlier, dilute sulphuric acid hydrolysis of sugarcane bagasse was carried out at

temperatures of 100°, 110°, 120° and 130°C for the yield of monomeric sugars (glucose, xylose, and arabinose), and inhibitory by–products (acetic acid, furfural and 5–HMF). There are two main products of hydrolysis process: pentose sugars (xylose and arabinose) and hexose sugar (glucose). The pentose sugars are further decomposed mainly to furfural, while glucose is decomposed mainly to 5–HMF. Acetic acid is an independent product originating from acetyl groups present in xylan heteropolymer (or the hemicellulose). Fig. 4.1 (A, B, C, D, E, and F) shows the effect of hydrolysis temperature and time on the yield of xylose, glucose, arabinose, and inhibitory by–products (acetic acid, furfural and 5–HMF), respectively. Time profiles of xylose yield in hydrolysis at different temperatures are shown in Fig. 4.1A. Xylose yield increases proportionately with time in the initial stages of hydrolysis for all temperatures. However, for temperatures higher than 100$^{o}$C, the xylose concentration reduces after reaching a maximum. This result is attributed to oxidative degradation of xylose to furfural. For the highest hydrolysis temperature of 130°C, the maximum xylose concentration (9.2 g/L) occurs at 15 min of treatment, with subsequent fall. The final values of xylose concentrations in the solution at completion of 120 min of hydrolysis with corresponding temperatures are as follows: 9.3 g/L (100°C), 8.7 g/L (110°C), 6.9 g/L (120°C) and 6.2 g/L (130°C). Aguilar et al. (2002) have reported peak value of 23.4 g/L for xylose concentration during dilute $H_2SO_4$ (2 wt%) hydrolysis of sugarcane baggase. However, the solid–to–liquid ratio used by Aguilar et al. (2002) was much higher, viz. 1:10. Due to higher concentration of xylose, the subsequent oxidation to furfural was also higher (~ 20% of initial concentration). For the lowest hydrolysis temperature of 100°C, however, very little oxidation of xylose to furfural occurs, and a continuous rise in xylose concentration is seen during 120 min of treatment. The maximum xylose yields at different temperatures (with corresponding treatment periods) with respect to initial hemicellulose present in biomass were as follows: 82 wt% at 100°C (120 min), 84.2 wt% at 110°C (90 min), 86.5 wt% at 120°C (30 min), 80.8 wt% at 130°C (15 min).

Time profiles of glucose concentrations in hydrolysis at different temperatures are shown in Fig.

4.1B. Glucose is essentially a product of hydrolysis of hemicellulose heteropolymers (Liu et al., 2012) and amorphous fractions of cellulose (Singh et al., 2014). Unlike xylose profiles, the concentration of glucose in the solution continuously increases. However, small concentrations of 5–HMF detected in the solution point towards oxidation of glucose. The maximum glucose yield of 15 and 25 wt% was reached at temperatures of 100° and 130°C, respectively in 120 min of hydrolysis.

Fig. 4.1C shows the arabinose profiles at different temperatures during hydrolysis. It is evident from results shown in Fig. 4.1C that with rise in hydrolysis temperature from 100°–130°C, the arabinose yield increased from 10–12% w/w of hemicellulose in first 60 min of treatment. For hydrolysis periods > 60 min, the arabinose yield reduced for temperatures of 120° and 130°C. This effect is attributed to oxidative degradation of arabinose to furfural at relatively higher temperatures and longer hydrolysis time.

Acetic acid is essentially a product of hydrolysis of acetyl groups present in hemicellulose heteropolymers. Fig. 4.1D shows the trends in acetic acid production at different temperatures of hydrolysis. Profiles of acetic acid concentration show sharp rise in initial stages of hydrolysis followed by almost levelling off. The final concentrations of acetic acid obtained (at the end of 120 min hydrolysis) at different reaction temperatures are as follows: 1.09 g/L (100°C), 1.13 g/L (110°C), 1.19 g/L (120°C) and 1.24 g/L (130°C). It is evident from these results that higher temperatures favour the yield of acetic acid with a maximum yield of 8.9% w/w hemicellulose at 130°C in 120 min.

In dilute sulphuric acid hydrolysis of sugarcane bagasse, the inhibitory by–products furfural and 5–HMF are generated due to oxidative degradation of pentose and hexose sugars, respectively. Fig. 4.1E and F show the trends of furfural and 5–HMF formation during hydrolysis at different temperatures. It is evident from Figs. 4.1E and F that yields of these degradation products are proportionate to temperature and period of treatment. Maximum yields of 15 wt% furfural and 4.5 wt% 5–HMF were reached at a temperature of 130°C in 120 min.

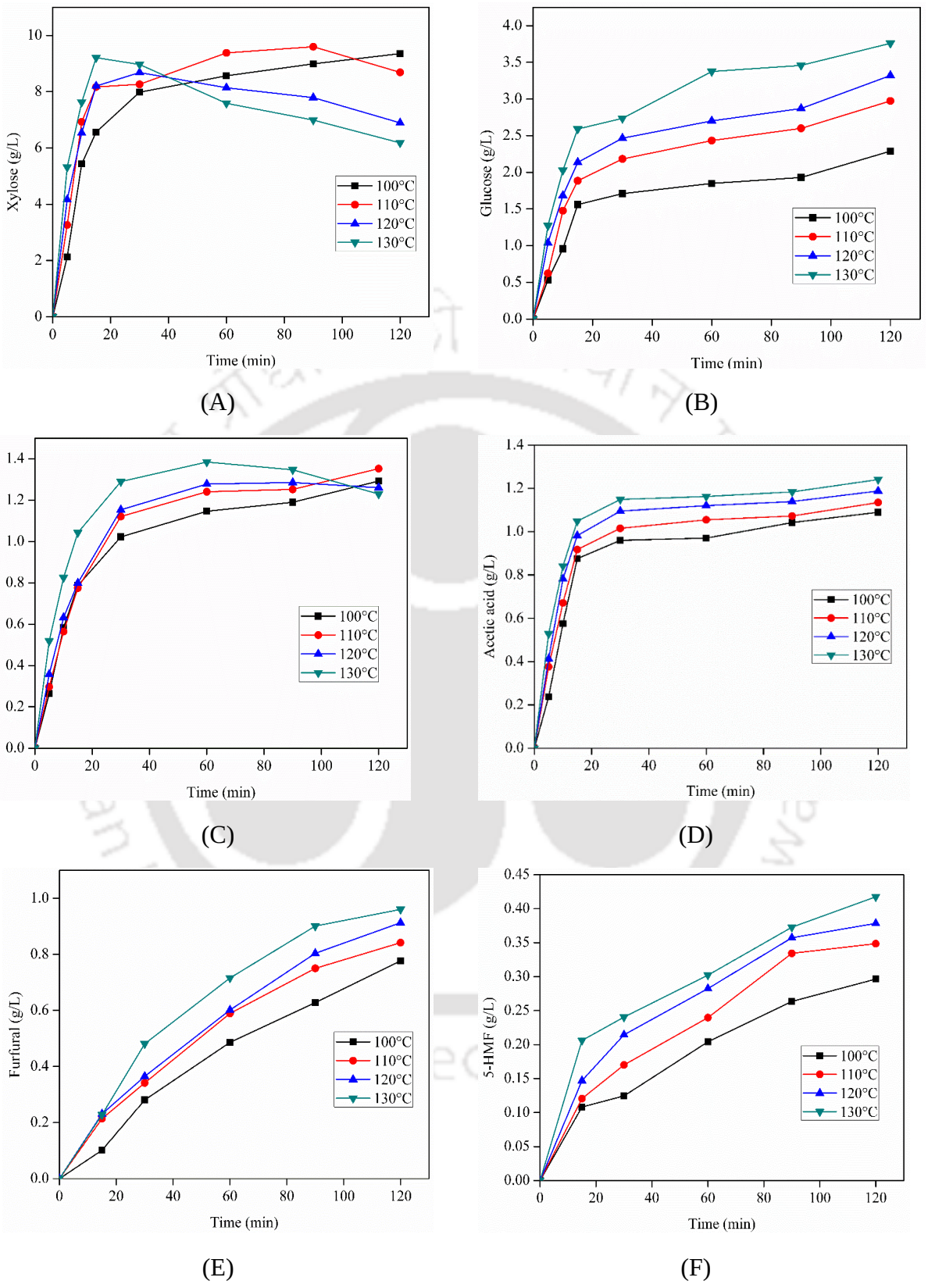


**Figure 4.1.** Time profiles of different products during acid hydrolysis of the sugarcane baggase. (A) xylose, (B) glucose, (C) arabinose, (D) acetic acid, (E) furfural, and (F) 5–HMF.

### 4.3.2 Kinetic analysis of glucose during dilute acid hydrolysis

The modified Saeman's model was used for kinetic analysis of glucose formation and degradation. This model hypothesises that total glucan in biomass comprises of two fractions, viz. (1) easy–to–hydrolyse or susceptible fraction, and (2) hard–to–hydrolyse or non–susceptible fraction. $\beta$ (g of susceptible glucan/g of total glucan) represents the susceptible glucan fraction. The time profiles of glucose can be determined by modifying eq.4.3. The oxidation product for glucose is 5–HMF. By modifying eq.4.3, the time variation of glucose during hydrolysis is written as:

$$G = G_o e^{-k_2 t} + \beta G_{no} \frac{k_1}{k_2 - k_1}\left(e^{-k_1 t} - e^{-k_2 t}\right) \qquad (4.13)$$

where: $G$ is instantaneous glucose concentration (g/L), $G_o$ is the initial glucose concentration (g/L, $G_o = 0$), $G_{no}$ is the initial glucan (g/L), $k_1$ is kinetic constant for glucose formation ($min^{-1}$), $k_2$ is kinetic constant of glucose degradation to HMF ($min^{-1}$). Kinetic parameters obtained after fitting of experimental profiles of glucose to the above model are depicted in Table 4.1. As seen from Table 4.1, $k_2$ values for all hydrolysis temperatures are two to three orders of magnitude smaller than $k_1$ values. This essentially indicates that glucose formation during hydrolysis is much faster than decomposition. Lower values of $k_2$ are possibly a consequence of higher activation energy of glucose decomposition to 5–HMF. The final concentrations of 5–HMF reached in the reaction mixture at different temperatures after 120 min of hydrolysis are as follows: 0.29 g/L at 100°C, 0.35 g/L at 110°C, 0.38 g/L at 120°C and 0.42 g/L at 130°C. The parameter $\beta$ was a strong function of hydrolysis temperature. Only 15% of the glucan was susceptible to hydrolysis at 100°C, which increased to 26% at 130°C. A possible explanation to this result can be given as follows: at lower hydrolysis temperature, glucose mainly forms from the hemicellulose heteropolymer and amorphous fractions of cellulose. However, at relatively higher temperature, a fraction of crystalline cellulose may also undergo hydrolysis that increases the glucose yield.

**Table 4.1.** Rate constants for glucose formation and degradation

| T (°C) | $k_1$ ($min^{-1}$) | $k_2$ ($min^{-1}$) | $\beta$ | $R^2$ |
|---|---|---|---|---|
| 100 | $7.16\times10^{-3}$ | 0 | 0.15 | 0.96 |
| 110 | $1.01\times10^{-2}$ | $2.67\times10^{-5}$ | 0.16 | 0.99 |
| 120 | $8.17\times10^{-3}$ | $5.53\times10^{-5}$ | 0.22 | 0.97 |
| 130 | $8.37\times10^{-3}$ | $7.75\times10^{-5}$ | 0.26 | 0.97 |

### 4.3.3 Kinetic analysis of arabinose during dilute acid hydrolysis

The kinetic analysis of arabinose formation and degradation can be done in analogous manner as glucose and the kinetic expression for the same can be written as follows:

$$A_r = A_{ro}e^{-k_2t} + \gamma A_{rno}\frac{k_1}{k_2 - k_1}\left(e^{-k_1t} - e^{-k_2t}\right) \qquad (4.14)$$

where: $A_r$ is instantaneous arabinose concentration (g/L), $A_{ro}$ is initial arabinose concentration (g/L, $A_{ro}$ = 0), $A_{rno}$ is the potential arabinan (g/L), $\gamma$ is g of susceptible arabinan/g of total arabinan, $k_1$ and $k_2$ are the rate constants for arabinose formation and decomposition ($min^{-1}$).

As shown in Table 4.2, the potential arabinan ($A_{rno}$) shows marginal variation from 3.38 g/L to 3.50 g/L, as the hydrolysis temperature increased from 100° to 130°C. The kinetic constants for arabinose degradation at all hydrolysis temperatures are two orders of magnitude smaller than the kinetic constants of arabinose formation. In fact, no degradation of arabinose occurs at 100° and 110°C, as evident from zero value of $k_2$ for these temperatures.

**Table 4.2.** Rate constants for arabinose formation and degradation

| T (°C) | $k_1$ ($min^{-1}$) | $k_2$ ($min^{-1}$) | $\gamma$ | $A_{rno}$ (g/L) | $R^2$ |
|---|---|---|---|---|---|
| 100 | $5.86\times10^{-2}$ | 0 | 0.41 | 3.38 | 0.99 |
| 110 | $6.09\times10^{-2}$ | 0 | 0.43 | 3.41 | 0.99 |
| 120 | $6.20\times10^{-2}$ | $8.51\times10^{-4}$ | 0.45 | 3.45 | 0.99 |
| 130 | $8.17\times10^{-2}$ | $16.30\times10^{-4}$ | 0.47 | 3.50 | 0.99 |

### 4.3.4 Kinetic analysis of acetic acid during dilute acid hydrolysis

Acetic acid results from hydrolysis of acetyl groups in hemicellulosic heteropolymers. A simple reaction scheme for acetic acid formation is given (Lavarack et al., 2002) as follows:

$$\text{Acetyl groups} \xrightarrow{k_1} \text{Acetic acid} \qquad (4.15)$$

Assuming 1st order kinetics for the reaction, the time profile of acetic acid formation can be determined as:

$$C_A = C_{Ao}\left(1 - e^{-k_1 t}\right) \qquad (4.16)$$

where: $C_A$ is instantaneous acetyl groups concentration (g/L), $C_{Ao}$ is concentration of acetyl groups (g/L), and $k_1$ is kinetic constant of acetic acid formation ($min^{-1}$). The kinetic parameters obtained after fitting of eq. 4.16 to experimental profiles of acetic acid at different hydrolysis temperatures are listed in Table 4.3. Although the kinetic constant $k_1$ shows proportionate increase with temperature, initial concentration of acetyl groups ($C_{Ao}$) shows marginal variation from 1.05 to 1.20 g/L, as the temperature increases from 100°C to 130°C. As a result, the final concentrations of acetic acid resulting from 120 min hydrolysis are almost similar at all temperatures: 1.09 g/L at 100°C, 1.13 g/L at 110°C, 1.19 g/L at 120°C and 1.24 g/L at 130°C.

**Table 4.3.** Rate constant for acetic acid formation

| T (°C) | $k_1$ ($min^{-1}$) | $C_{Ao}$ (g/L) | $R^2$ |
|---|---|---|---|
| 100 | $8.45\times10^{-2}$ | 1.05 | 0.97 |
| 110 | $9.99\times10^{-2}$ | 1.09 | 0.99 |
| 120 | $10.77\times10^{-2}$ | 1.16 | 0.99 |
| 130 | $12.38\times10^{-2}$ | 1.20 | 0.99 |

### 4.3.5 Kinetic and thermodynamic analysis of xylose during dilute acid hydrolysis

Table 4.4 shows the rate constants of xylose formation from easy–to–hydrolyse and hard–to–hydrolyse fractions of hemicellulose ($k_f$ and $k_s$) and further degradation of xylose to furfural ($k_2$). The easy–to–hydrolyse fraction of xylose at different hydrolysis temperatures was also

determined by fitting the kinetic expression to experimental data, and is listed in Table 4.4. As shown in Table 4.4, the rate constants $k_f$, $k_s$, and $k_2$ values increased with hydrolysis temperatures. However, $k_f$ values were at least one order of magnitude higher than $k_s$ values, which in turn were at least one order of magnitude higher than $k_2$ values. This essentially means that in the hydrolysis temperature range under consideration, xylose formation is much faster than degradation. In addition, the easy–to–hydrolyse fractions of xylose, i.e. $\alpha$ values, also showed increased with temperature of hydrolysis. $\alpha$ values varied in the range of 0.66–0.92 for temperature range of 100°–130°C. This result shows that the easy–to–hydrolyse fraction accounts for the largest portion of hemicellulose under all experimental conditions. The range of $\alpha$ values obtained in our work is similar to those reported in previous literature. For example, for dilute acid hydrolysis (2 wt% $H_2SO_4$) of sugarcane bagasse Chen et al. (2015) have reported values of α in the range of 0.55–0.83.

**Table 4.4.** Rate constants for xylose formation and degradation

| T (°C) | $k_f$ ($min^{-1}$) | $k_s$ ($min^{-1}$) | $k_2$ ($min^{-1}$) | $\alpha$ | $R^2$ |
|---|---|---|---|---|---|
| 100 | $7.03\times10^{-2}$ | $0.76\times10^{-2}$ | $0.48\times10^{-3}$ | 0.66 | 0.99 |
| 110 | $12.40\times10^{-2}$ | $1.10\times10^{-2}$ | $0.75\times10^{-3}$ | 0.82 | 0.98 |
| 120 | $16.0\times10^{-2}$ | $2.10\times10^{-2}$ | $2.6\times10^{-3}$ | 0.87 | 0.99 |
| 130 | $32.30\times10^{-2}$ | $3.10\times10^{-2}$ | $2.9\times10^{-3}$ | 0.92 | 0.97 |

Arrhenius plots (ln $k$ versus $1/T$) for determination of activation energy and pre–exponential factors of xylose formation and degradation are shown in Fig. 4.2, and the values of the Arrhenius parameters are listed in Table 4.5. The activation energies ($E$) of hydrolysis of hard–to–hydrolyse (61.14 kJ/mol) and easy–to–hydrolyse fractions (60.33 kJ/mol) of xylose are quite close. However, the pre–exponential factor ($A$) for easy–to–hydrolyse fraction ($1.95\times10^7$ $min^{-1}$) of xylose was one order of magnitude higher than that for hard–to–hydrolyse fraction ($2.63\times10^6$ $min^{-1}$). The activation energy and pre–exponential factor for xylose degradation were 83.40

kJ/mol and $2.21\times10^{8}$ $min^{-1}$, respectively. Significantly larger activation energy for xylose degradation (as compared to xylose formation) is indicative of difficulty of xylose degradation in the temperature range of hydrolysis used in the experiments.

The trends observed in kinetic constants ($k_f$, $k_s$ and $k_2$) and Arrhenius parameters with hydrolysis temperature in our study concur with previous literature, albeit with quantitative differences. Liu et al. (2012) have reported following kinetic constants for hemicellulose hydrolysis of sweet sorghum bagasse at 120°C: $k_f$ = 0.0311 $min^{-1}$, $k_s$ = 0.0026 $min^{-1}$ and $k_2$ = 0.0069 $min^{-1}$. Lavarack et al. (2002) have reported following activation energies for acid hydrolysis of sugarcane bagasse (4 wt% $H_2SO_4$): xylose formation = 73.5–88.1 kJ/mol and xylose degradation = 111.2 kJ/mol.

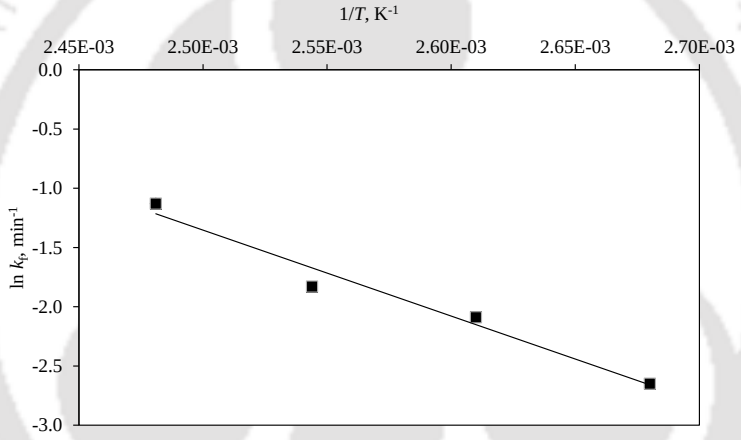


(A)

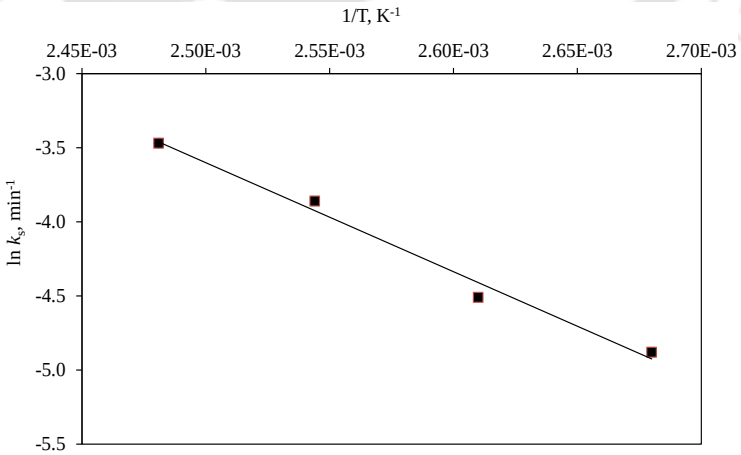


(B)

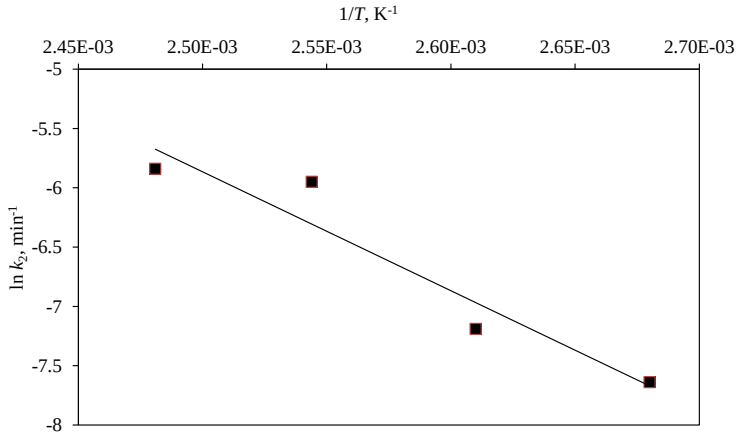


(C)

**Figure 4.2.** Arrhenius plots of different reactions during acid hydrolysis of sugarcane bagasse. (A) ln $k_f$ vs. 1/T, (B) ln $k_s$ vs. 1/T, (C) ln $k_2$ vs. 1/T

**Table 4.5.** Arrhenius parameters for xylose formation and degradation

| Reaction | Pre–exponential factor ($A$, $min^{-1}$) | Activation energy ($E$, kJ/mol) | $R^2$ |
|---|---|---|---|
| Fast hydrolysis | $1.95\times10^{7}$ | 60.33 | 0.97 |
| Slow hydrolysis | $2.63\times10^{6}$ | 61.14 | 0.98 |
| Xylose degradation | $2.21\times10^{8}$ | 83.40 | 0.92 |

The thermodynamic parameters for xylose formation and degradation are listed in Table 4.6 (A, B, and C). It could be inferred from Table 4.6A that values of enthalpy change for xylose formation (both easy–to–hydrolyse and hard–to–hydrolyse fractions) was positive indicating endothermic nature of the hydrolysis reaction.

Interestingly, the enthalpy change values show only slight reduction with temperature, which indicates relative insensitivity of this parameter to the reaction temperature in the temperature range (100°–130°C) used in the experiments. This result is attributed to no phase change occurring during hydrolysis reaction. The enthalpy change values for xylose degradation are significantly larger than xylose formation, which indicates relatively higher energy requirement for xylose degradation, as compared to its formation.

The entropy change in xylose formation and decomposition was determined using Eyring equation and is tabulated in Table 4.6B. The entropy change values for both slow and fast hydrolysis of xylose are negative, which corroborates stability of the products formed out of hydrolysis. Secondly, similar to enthalpy change, the entropy change values for both easy–to–hydrolyse and hard–to–hydrolyse fractions of hemicellulose are almost similar for all hydrolysis temperatures. This result is attributed to no phase and volume change during the reaction. As per basic principles of thermodynamics, any product from a process having negative entropy is designated as "stable", as negative entropy indicates increasing order in the system. Therefore, we have designated xylose as "stable product" from the basic perspective of thermodynamics and not specific related to chemical structure. It may be noted that xylose degradation also has negative entropy change, which means that it also leads to the stable product of furfural. However, the xylose formation has more negative entropy than degradation and on comparative basis; xylose is a relatively more stable product than furfural.

The Gibbs free energy change occurring in any process indicates spontaneity of the process. The Gibbs free energy changes of the dilute sulphuric acid hydrolysis of sugarcane bagasse are tabulated in Table 4.6C. Positive values of Gibbs free energy for hemicellulose hydrolysis indicate that the reaction is non–spontaneous (processes that occur with addition of external energy) and shows the endothermic nature of the reaction. The $\Delta G$ values for degradation of xylose are higher than $\Delta G$ values for hemicellulose hydrolysis, which indicates that (on relative basis) degradation of xylose is thermodynamically less favored process as compared to xylose formation. This result is in concurrence with order–of–magnitude smaller kinetic constants for xylose degradation, as compared to hemicellulose hydrolysis.

Similar results as in present study have been reported by Swati et al. (2013) for thermodynamic analysis of acid hydrolysis of *Parthenium hysterophorus*. The trends in thermodynamic parameters of $\Delta H$, $\Delta S$ and $\Delta G$ for dilute acid hydrolysis of hemicellulose fraction in *Parthenium hysterophorus* are same as present study. Swati et al. (2013) have reported that the concentration

of acid and biomass soaking time also influence the kinetic and thermodynamic parameters of dilute acid hydrolysis, in addition to temperature. Swati et al. (2013) have concluded that higher hydrolysis temperature, higher acid concentration and larger soaking time favor the formation of stable depolymerized products.

**Table 4.6.** Thermodynamic parameters for xylose formation and degradation

| Reaction (A) | Activation energy (kJ/mol) | $\Delta H_{100}$ (kJ/mol) | $\Delta H_{110}$ (kJ/mol) | $\Delta H_{120}$ (kJ/mol) | $\Delta H_{130}$ (kJ/mol) |
|---|---|---|---|---|---|
| Fast hydrolysis | 60.33 | 57.23 | 57.15 | 57.06 | 56.98 |
| Slow hydrolysis | 61.14 | 58.04 | 57.96 | 57.87 | 57.79 |
| Xylose degradation | 83.40 | 80.30 | 80.22 | 80.13 | 80.05 |

| Reaction (B) | $-\Delta S_{100}$ (kJ/mol·K) | $-\Delta S_{110}$ (kJ/mol·K) | $-\Delta S_{120}$ (kJ/mol·K) | $-\Delta S_{130}$ (kJ/mol·K) |
|---|---|---|---|---|
| Fast hydrolysis | 1.05 | 1.05 | 1.05 | 1.05 |
| Slow hydrolysis | 1.07 | 1.06 | 1.06 | 1.06 |
| Xylose degradation | 1.03 | 1.03 | 1.02 | 1.03 |

| Reaction (C) | $\Delta G_{100}$ (kJ/mol) | $\Delta G_{110}$ (kJ/mol) | $\Delta G_{120}$ (kJ/mol) | $\Delta G_{130}$ (kJ/mol) |
|---|---|---|---|---|
| Fast hydrolysis | 447.39 | 457.76 | 468.53 | 478.11 |
| Slow hydrolysis | 457.52 | 465.47 | 475.24 | 486.18 |
| Xylose degradation | 462.99 | 473.94 | 482.17 | 493.93 |

## 4.4 Conclusions

Kinetic and thermodynamic analysis in this study helps in identifying optimum conditions for sugarcane bagasse hydrolysis in temperature range of 100 –130 C at dilute acid concentration of

2% v/v and solid–liquid ratio of 1:30 w/v. Principal factors influencing xylose yield are temperature and time of hydrolysis. Smaller temperature of 100 C requires longer treatment period, while higher temperature of 130 C results in xylose degradation to inhibitory products. On the basis of xylose yield and production of inhibitors through xylose oxidation, optimum conditions for hydrolysis are determined as: temperature = 120 C, hydrolysis period = 30 min, xylose yield = 0.84 g/g hemicellulose.

**References**

Aguilar, R., Ramırez, J., Garrote, G., Vázquez, M., 2002. Kinetic study of the acid hydrolysis of sugar cane bagasse. J. Food Eng. 55(4), 309–318.

Arrizon, J., Mateos, J., Sandoval, G., Aguilar, B., Solis, J., Aguilar, M., 2012. Bioethanol and xylitol production from different lignocellulosic hydrolysates by sequential fermentation. J. Food Process Eng. 35(3), 437–454.

Chen, L., Zhang, H., Li, J., Lu, M., Guo, X., Han, L., 2015. A novel diffusion–biphasic hydrolysis coupled kinetic model for dilute sulfuric acid pretreatment of corn stover. Bioresour. Technol. 177, 8–16.

Chen, R., Lee, Y.Y., Torget, R., 1996. Kinetic and modeling investigationon on two–stage reverse–flow reactoras applied to dilute–acid pretreatment of agricultural residues. 17th Symp. Biotechnol. Fuels Chem. Springer. 133–146.

Gámez, S., González–Cabriales, J.J., Ramírez, J.A., Garrote, G., Vázquez, M., 2006. Study of the hydrolysis of sugar cane bagasse using phosphoric acid. J. Food Eng. 74(1), 78–88.

Harmsen, P., Huijgen, W., Bermudez, L., Bakker, R., 2010. Literature review of physical and chemical pretreatment processes for lignocellulosic biomass. Energy Res. Centre Nether. 10–13.

Hosseini, S.A., Lambert, R., Kucherenko, S., Shah, N., 2010. Multiscale modeling of hydrothermal pretreatment: from hemicellulose hydrolysis to biomass size optimization. Energ. Fuels. 24(9), 4673–4680.

Jensen, J., Morinelly, J., Aglan, A., Mix, A., Shonnard, D.R., 2008. Kinetic characterization of biomass dilute sulfuric acid hydrolysis: Mixtures of hardwoods, softwood, and switchgrass. AIChE J. 54(6), 1637–1645.

Jin, Q., Zhang, H., Yan, L., Qu, L., Huang, H., 2011. Kinetic characterization for hemicellulose hydrolysis of corn stover in a dilute acid cycle spray flow–through reactor at moderate conditions. Biomass Bioenerg. 35(10), 4158–4164.

Lavarack, B., Griffin, G., Rodman, D., 2002. The acid hydrolysis of sugarcane bagasse hemicellulose to produce xylose, arabinose, glucose and other products. Biomass Bioenerg. 23(5), 367–380.

Lavarack, B., Griffin, G., Rodman, D., 2000. Measured kinetics of the acid–catalysed hydrolysis of sugar cane bagasse to produce xylose. Catal. Today 63(2), 257–265.

Lenihan, P., Orozco, A., O'neill, E., Ahmad, M., Rooney, D., Walker, G., 2010. Dilute acid hydrolysis of lignocellulosic biomass. Chem. Eng. J. 156(2), 395–403.

Liu, X., Lu, M., Ai, N., Yu, F., Ji, J., 2012. Kinetic model analysis of dilute sulfuric acid–catalyzed hemicellulose hydrolysis in sweet sorghum bagasse for xylose production. Ind. Crop Prod. 38, 81–86.

Lu, X., Zhang, Y., Liang, Y., Yang, J., Zhang, S., Suzuki, E., 2008. Kinetic studies of hemicellulose hydrolysis of corn stover at atmospheric pressure. Korean J. Chem. Eng. 25(2), 302–307.

Maloney, M.T., Chapman, T.W., Baker, A.J., 1985. Dilute acid hydrolysis of paper birch: Kinetics studies of xylan and acetyl-group hydrolysis. Biotechnol. Bioeng. 27(3), 355–361.

Mehlberg, R., Tsao, G., 1979. Low liquid hemicellulose hydrolysis of hydrochloric acid. 178th ACS National Meeting, Washington, DC.

Orozco, A.M., Ala'a, H., Rooney, D., Walker, G.M., Ahmad, M.N., 2013. Hydrolysis characteristics and kinetics of waste hay biomass as a potential energy crop for fermentable sugars production using autoclave parr reactor system. Ind. Crop. Prod. 44, 1–10.

Rodrıguez–Chong, A., Ramírez, J.A., Garrote, G., Vázquez, M., 2004. Hydrolysis of sugar cane bagasse using nitric acid: a kinetic assessment. J. Food Eng. 61(2), 143–152.

Saeman, J.F., 1945. Kinetics of wood saccharification–hydrolysis of cellulose and decomposition of sugars in dilute acid at high temperature. Ind. Eng. Chem. 37(1), 43–52.

Singh, S., Khanna, S., Moholkar, V.S., Goyal, A., 2014. Screening and optimization of pretreatments for *Parthenium hysterophorus* as feedstock for alcoholic biofuels. Appl. Energ. 129(Supplement C), 195–206.

Swati, G., Haldar, S., Ganguly, A., Chatterjee, P., 2013. Investigations on the kinetics and thermodynamics of dilute acid hydrolysis of *Parthenium hysterophorus* L. substrate. Chem. Eng. J. 229, 111–117.

Yat, S.C., Berger, A., Shonnard, D.R., 2008. Kinetic characterization for dilute sulfuric acid hydrolysis of timber varieties and switchgrass. Bioresour. Technol. 99(9), 3855–3863.

# CHAPTER 5

# OPTIMIZATION OF MEDIUM COMPONENTS AND PROCESS PARAMETERS FOR XYLITOL BIO–PRODUCTION FROM SUGARCANE BAGASSE

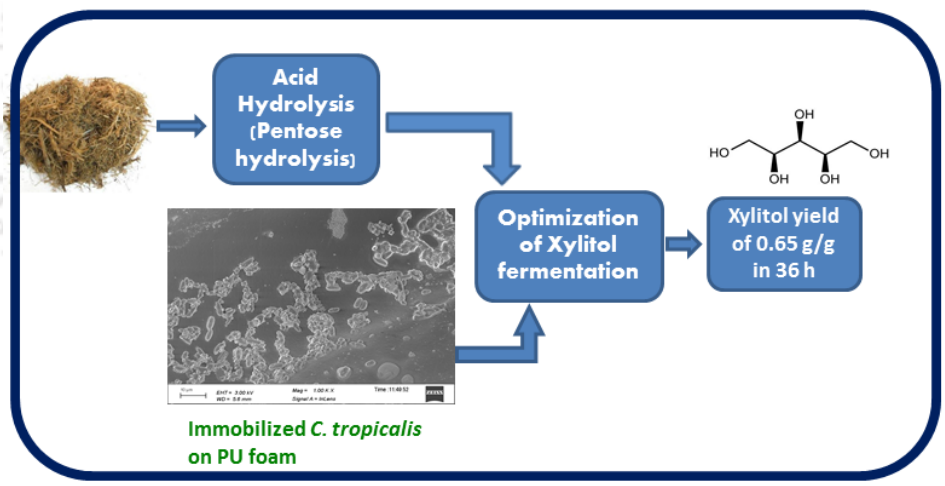

# CHAPTER 5

# OPTIMIZATION OF MEDIUM COMPONENTS AND PROCESS PARAMETERS FOR XYLITOL BIO–PRODUCTION FROM SUGARCANE BAGASSE

## 5.1 Introduction

Sugarcane bagasse, the residue after sugarcane extraction, is an important source of lignocellulosic biomass for the synthesis of biofuels and value–added chemicals such as xylitol. Sugarcane bagasse consists of cellulose, hemicellulose, lignin, and others like extractives, ash etc. (Harmsen et al., 2010). Preliminary step in bio–production of xylitol is dilute acid hydrolysis of the hemicellulosic fraction in biomass that results in pentose–rich hydrolysate. This hydrolysate can be fermented for xylitol synthesis (Ramesh et al., 2012; Tizazu and Moholkar, 2018). Xylitol is widely applicable in food, pharmaceutical, odonotogical industries (Ur–Rehman et al., 2015). Xylitol can be produced chemically by catalytic hydrogenation of D–xylose from hemicellulosic hydrolysate using nickel catalyst, or can be produced through biochemical route (as a natural metabolic intermediate) by some xylose utilizing microorganisms (Granström et al., 2001). Microbial xylitol production is more favourable for industrial applications due to mild fermentative conditions like atmospheric pressure and ambient temperature (Rao et al., 2006). Many yeast cells, including *C. tropicalis, D. hansenii, D. nepalensis, C. guilliermondii,* and *C. subtropicalis* species can effectively convert xylose into xylitol (Kumdam et al., 2012; Zhang et al., 2014).

Major bottleneck in production of xylitol with high yields is presence of inhibitors in the

hydrolysate. Previous authors have reported enhancement in yield and productivity of xylitol bio–production using various measures like: (1) decolorization, and detoxification of the hemicellulosic hydrolysate, (2) immobilization of the yeast cells using different immobilization support, (3) optimization of fermentative conditions (Zhang et al., 2014). Use of immobilized cells on different supports has also been attempted (for example, Prakash et al., 2011; Sarrouh et al., 2013; Soleimani et al., 2014; Yewale et al., 2016; Wang et al., 2016). Most commonly adopted technique for immobilization of microbial cells is entrapment in Ca-alginate beads. Other supports such as porous glass or polyurethane foam (PU) have also been used. Polyurethane (PU) foam as immobilization support has merit of high specific surface area for cell attachment and high void volume that makes it suitable for aerobic cultures. However, low diffusivity of the substrate and other nutrients through the porous matrix (or in other words high mass transfer resistance) is a limitation of PU foam (Wang et al., 2012; Pérez–Bibbins et al., 2016).

Principal factors influencing bio–production of xylitol are: (1) process parameters such as temperature, pH, agitation rate etc., and (2) medium composition (Ramesh et al., 2012). Several previous authors have addressed enhancement of xylitol production through optimization of the medium components and process parameters. Many previous authors have adopted one–variable–at–a–time (OVAT) approach for optimization of xylitol fermentation. The major limitation of this approach is that it does not reveal the relative significance of the optimization variables (either medium components or process parameters), and it also does not highlight the relative interaction among the variables.

Present study addresses the enhancement of xylitol fermentation using immobilized cells of *C. tropicalis* on PU foam with a dual approach. In the first step, we have optimized the fermentation medium using statistical experimental design (Plackett–Burman design followed by Central composite design). In the second step, the process parameters (viz. temperature, initial pH, shaking speed and substrate (xylose) concentration) have been optimized with Central composite design. The second step of optimization has been carried out using optimized medium in the first

step.

## 5.2 Materials and methods

### 5.2.1 Dilute acid hydrolysis for pentose–rich hydrolyzate

Sieved biomass of sugarcane bagasse (size < 0.6 mm) was obtained as per procedure described in our previous paper (Tizazu and Moholkar, 2018). Structural composition of sugarcane bagasse was determined as: cellulose = 40.27 wt%, hemicellulose = 30.13 wt%, lignin = 27.14 wt%, and extractives = 2.46 wt% on dry basis. Hemicellulosic fraction in sugarcane bagasse was hydrolyzed in an autoclave (Model: LAC–5040S, Daihan Labtech Co. Ltd., South Korea, pressure = 15 psi, temperature = 120°C, treatment time = 30 min) with dilute sulphuric acid (2% v/v $H_2SO_4$) and solid:liquid ratio = 1:30 (w/v) (Tizazu and Moholkar, 2018). Following completion of dilute acid hydrolysis, the reaction mixture was neutralized (pH 7) with CaO and filtered. The composition of the hydrolysate was determined using HPLC as: xylose = 8.68 g/L, glucose = 2.43 g/L, arabinose = 1.23 g/L, furfural = 0.37 g/L, 5–HMF = 0.21 g/L, and acetic acid = 1.05 g/L. Xylose concentration in hydrolysate was adjusted to the desired value according to the statistical experimental design by concentrating the solution using a rotavapor (Make: BUCHI, Model: Rotavapor R–210). The concentrated hydrolysate was used for fermentation.

### 5.2.2 Growth and maintenance of *C. tropicalis* culture

*C. tropicalis* MTCC 184 was purchased from Microbial Type Culture Collection (MTCC), Chandigarh (India). The microbial cells (lyophilized) were revived in yeast extract, peptone and dextrose (YPD) medium and kept in a rotary shaker (Make: Lab Companion; Model: SI–300R) at 30°C, 150 rpm for 24 h. The revived cells were grown on agar slant and kept at 4°C. The cultures were sub–cultured every 30 days. YPD medium composition in 1 L of distilled water was as follows: yeast extract = 3 g, peptone = 10 g, dextrose = 20 g. The medium pH was adjusted to 6.0 ± 0.2 using 1 N HCl. By adding 15 g/L of agar in YPD medium, the agar plates and slants were prepared.

### 5.2.3 Inoculum preparation and fermentation medium composition

Cells from the agar slant were aseptically inoculated in 100 mL of inoculum medium (taken in 250 mL flask) and were incubated at 30°C, 150 rpm for 24 h in a rotary shaker. The composition of inoculum medium (autoclaved at 15 psi, 121°C, for 20 min, initial pH = 6.0) was as follows: xylose 10 g/L, peptone 10 g/L, yeast extract 3 g/L, and dextrose 20 g/L. The fermentation was performed by varying composition of the medium and process parameters according to the statistical experimental design. Three polyurethane (PU) foam cubes with immobilized *C. tropicalis* were added to the fermentation broth for optimization experiment. Samples from the fermentation broth were periodically withdrawn for monitoring progress of fermentation.

### 5.2.4 Immobilization and cross–linking of *C. tropicalis* on PU foam

Polyurethane (PU) foam was procured from local market in Guwahati, Assam (India). Structural properties of polyurethane (PU) foam used as immobilization support were as follows: density = 320 kg/m$^3$, specific surface area = 1.52 × 10$^5$ m$^2$/m$^3$, average porosity = 95%, and pore diameter = 0.03 mm. The cells of *C. tropicalis* were immobilized on to the PU foam support by natural adsorption using the protocol reported by Bhasarkar et al. (2015). Polyurethane (PU) foam was cut into pieces of approx. cubical size (1 cm$^3$). Pieces of the polyurethane (PU) foam were added to the medium (after washing and autoclaving) during log phase of the culture, i.e. at 10 h (as per pre–determined growth profile). The mixture of microbial cells and immobilization support was incubated at 150 rpm, 30°C for 48 h. After incubation, PU foam pieces containing immobilized cells were removed from the broth. It was then mixed with phosphate buffer mixture (with 50 mM, and pH of 6.0) with agitation for 10 min. Pieces of the PU foam were then washed 2× with phosphate buffer. It was then dried for 24 h at ambient temperature. The dried immobilized PU foams were incubated with 0.1% gluteraldehyde mixture solution for cross–linking of cells for 1 h, followed by washing with phosphate buffer and drying. To confirm immobilization of *C. tropicalis* cells on PU foam, Lowry assay was performed as described by Dikshit and Moholkar

(2016). Presence of proteins in the solution was confirmed by positive Lowry assay tests, which were released from *C. tropicalis* cells immobilized on the surface of the PU foam. Moreover, FE–SEM micrographs (shown in Figs. 5.1A and B) confirm immobilization of the cells of *C. tropicalis* on PU foam.

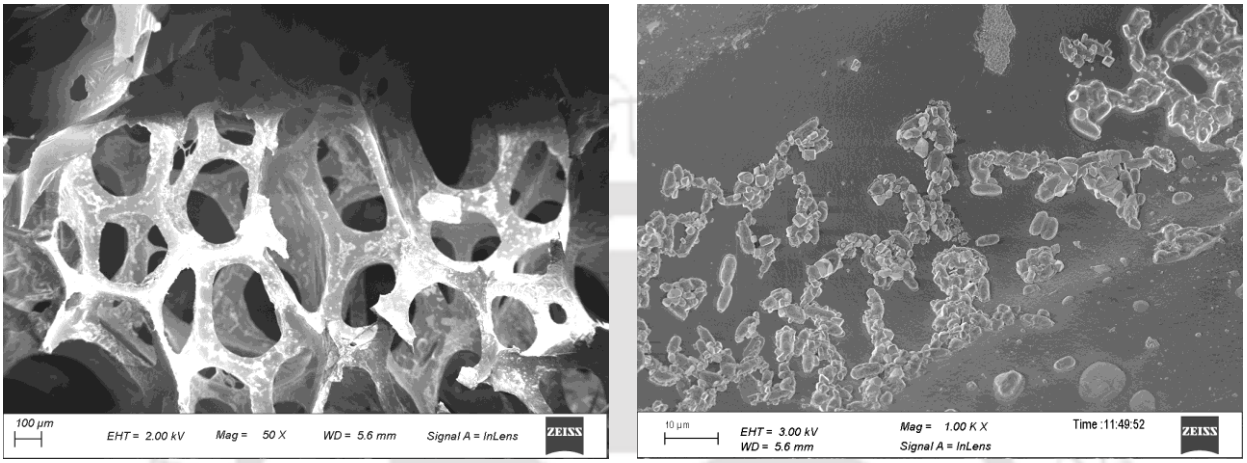


(A) (B)

**Figure 5.1.** (A) FE–SEM micrographs of native PU foam; (B) FE–SEM (Gold coating) micrographs of immobilized cells of *C. tropicalis* on PU foam

### 5.2.5 Ascertaining of equal number of cells in free and immobilized cultures

In order to confirm that the distribution of cells over PU foam support in consecutive experiments was nearly uniform, the procedure described by Dikshit and Moholkar (2016) was followed. The cells of *C. tropicalis* were grown at 30°C, 150 rpm and initial pH = 6.0 in two flasks (labelled as "control" and "test") each containing 100 mL of growth medium with composition: yeast extract 3 g/L, peptone 10 g/L, dextrose 20 g/L and xylose 10 g/L. The initial pH of the growth medium was adjusted to 6.0 ± 0.2 using 1 N HCl. Absorbance at 600 nm using UV–Vis spectro-photometer was recorded in order to determine the optical density in the medium in both flasks. At the onset of exponential phase the absorbance in both flasks was recorded and determined as 0.245 ± 0.004 (corresponding to cell density = 0.103 ± 0.002 g/L). At the onset of exponential

phase, 8 PU foam pieces with immobilized cells of *C. tropicalis* were added to the "test" flask. The cells in the "test" flask undertook immobilization on PU foam support for 24 h incubation. Following 24 h of fermentation and immobilization, by measuring absorbance and comparing with the "control" flask the non–immobilized cells present in broth of the "test" flask were determined. The densities of cells in the "test" flask and "control" flask were 0.384 g/L and 0.497 g/L, respectively. The amount of cells immobilized over the surface of 8 PU foam cubes mixed to "test" flask was the difference in these cell densities (0.113 g/L). Each PU foam piece was alone used for fermentation experiment in order to confirm constant distribution of 0.113 g of total immobilized cells over 8 polyurethane foam pieces. In each flask, the substrate (xylose) concentration of 20 g/L is kept for fermentation. At the end of 36 h fermentation, the final xylitol concentration was found to be 5.551 ± 0.021 g/L. This result confirms that distribution of cells over PU foam support was nearly uniform, and that the numbers of cells mixed to reaction mixture in each experiment were practically constant.

### 5.2.6 Analytical methods

Optical density (OD) of *C. tropicalis* cells in fermentation medium was determined with a UV–Vis spectrophotometer (Model: LAMBDA 35, Make: Perkin Elmer) by measuring absorbance at 600 nm. Aliquots withdrawn from the fermentation broth were centrifuged at 6000 rpm for 10 min, followed by filtration with 0.45 µm membrane syringe filter. The concentrations of glucose, xylose, and xylitol in the aliquots were determined by HPLC (Make: Perkin Elmer, Series 200) using Hiplex–H column (Make: Varian, 300 mm × 5 µm × 4.6 mm) coupled with Refractive Index detector. The eluent was 0.005 M $H_2SO_4$ as mobile phase with flow rate of 0.6 mL/min at column temperature of 60°C.

### 5.2.7 Experimental design for optimization of medium components and process parameters

Optimization of fermentation medium was performed using two–step procedure, viz. Plackett–

Burman design (PBD) followed by central composite design (CCD). Process parameters optimization has also been carried out by central composite design.

### 5.2.7.1 Plackett–Burman design (PBD)

Based on literature review on biosynthesis of xylitol with *C. tropicalis* immobilized on various supports (Yahashi et al., 1996; El–Batal and Khalaf, 2004; Wang et al., 2012; Ping et al., 2013; Zhang et al., 2014), seven potential medium components (along with their upper/lower limits) were selected for screening, viz. peptone, yeast extract, $K_2HPO_4$, $(NH_4)_2SO_4$, $KH_2PO_4$, $MgSO_4{\cdot}7H_2O$, and $CaCl_2{\cdot}2H_2O$ (refer to Table 5.1A for further details). MINITAB (Release 17.1, PA, USA, Trial Version) was used for devising the Plackett–Burman experimental design. Results of Plackett–Burman design were analyzed with 1$^{st}$–order polynomial equation:

$$Y = \beta_o + \sum_{i=1}^{n} \beta_i X_i \qquad (5.1)$$

Notation: $Y$ = response variable (xylitol), $\beta_o$ = intercepts, $\beta_i$ = linear coefficients and $X_i$ = optimization variables. Each experimental run was performed in triplicate and the average value of each experimental run was used for analysis. The significant variables from Plackett–Burman design outcome were further evaluated by using central composite design (CCD) for optimization of the significant variables.

**Table 5.1(A).** Plackett–Burman experimental design: Coded and actual values of variables

| Independent variables | Coded symbols | Levels | |
|---|---|---|---|
| | | Low (–1) | High (+1) |
| Yeast extract (g/L) | $X_1$ | 4 | 8 |
| Peptone (g/L) | $X_2$ | 8 | 12 |
| $K_2HPO_4$ (g/L) | $X_3$ | 0.1 | 1 |
| $KH_2PO_4$ (g/L) | $X_4$ | 0.1 | 1 |
| $(NH_4)_2SO_4$ (g/L) | $X_5$ | 1 | 5 |
| $MgSO_4{\cdot}7H_2O$ (g/L) | $X_6$ | 0.1 | 0.9 |
| $CaCl_2{\cdot}2H_2O$ (g/L) | $X_7$ | 0.1 | 0.5 |

**Table 5.1(B).** Plackett–Burman design for screening of medium components (Response variable: xylitol concentration, g/L)

| Run order | $X_1$ | $X_2$ | $X_3$ | $X_4$ | $X_5$ | $X_6$ | $X_7$ | Xylitol (g/L) | |
|---|---|---|---|---|---|---|---|---|---|
| | | | | | | | | Experimental | Predicted |
| 1 | +1 | –1 | +1 | –1 | –1 | –1 | +1 | 9.58 ± 0.143 | 9.72 |
| 2 | –1 | –1 | –1 | +1 | +1 | +1 | –1 | 5.65 ± 0.085 | 5.79 |
| 3 | +1 | +1 | +1 | –1 | +1 | +1 | –1 | 5.02 ± 0.075 | 5.29 |
| 4 | –1 | –1 | –1 | –1 | –1 | –1 | –1 | 10.14 ± 0.152 | 10.45 |
| 5 | +1 | +1 | –1 | +1 | +1 | –1 | +1 | 5.42 ± 0.081 | 5.84 |
| 6 | –1 | +1 | +1 | +1 | –1 | +1 | +1 | 7.45 ± 0.112 | 7.51 |
| 7 | +1 | +1 | –1 | +1 | –1 | –1 | –1 | 7.38 ± 0.110 | 6.96 |
| 8 | –1 | –1 | +1 | +1 | +1 | –1 | +1 | 8.79 ± 0.132 | 8.61 |
| 9 | –1 | +1 | –1 | –1 | –1 | +1 | +1 | 8.29 ± 0.124 | 8.23 |
| 10 | +1 | –1 | +1 | +1 | –1 | +1 | –1 | 6.22 ± 0.093 | 6.19 |
| 11 | –1 | +1 | +1 | –1 | +1 | –1 | –1 | 9.10 ± 0.137 | 8.83 |
| 12 | +1 | –1 | –1 | –1 | +1 | +1 | +1 | 6.17 ± 0.093 | 5.79 |

### 5.2.7.2 Medium components optimization using central composite design (CCD)

Four significant variables were identified from the Plackett–Burman design, viz. yeast extract, $(NH_4)_2SO_4$, $MgSO_4 \cdot 7H_2O$ and $KH_2PO_4$. The lower and upper limits of these variables were also chosen from the earlier Plackett–Burman design. The coded levels of these variables are shown in Table 5.3A. The complete CCD design constituting 31 individual runs (with 16 factorials, 8 star points and 7 replicates at the center points) is shown in Table 5.3B. Each experimental run was performed in triplicate and average value of response variable (xylitol concentration) was considered for analysis. The response variable (xylitol concentration) for medium components and process parameters optimization were fitted to the 2nd–order polynomial regression equation as follows:

$$Y = \beta_o + \sum_{i=1}^{4} \beta_i X_i + \sum_{i=1}^{4} \beta_{ii} X_i^2 + \sum_{i,j=1}^{4} \beta_{ij} X_i X_j \qquad (5.2)$$

Notation: $Y$ = response variable (xylitol concentration, g/L), $\beta_o$ = intercept term, $\beta_i$ = linear coefficients, $\beta_{ii}$ = quadratic coefficients, $\beta_{ij}$ = interaction coefficients, $X_i$ and $X_j$ = independent variables.

#### 5.2.7.3 Process parameters optimization using central composite design (CCD)

Four process parameters (viz. temperature, initial pH, shaking speed and substrate (xylose) concentration) were selected for optimization based on previous literature (El−Batal and Khalaf, 2004; Wang et al., 2012; Ping et al., 2013; Zhang et al., 2014). Upper and lower limits of these parameters in the CCD (depicted in Table 5.5A) were also chosen on the basis of reported literature. Complete CCD experimental design for optimization of process parameters is given in Table 5.5B. Each experimental run in the central composite design was performed in triplicate, and the average response (xylitol concentration) was taken for further analysis. The response variable (xylitol concentration) was fitted to $2^{nd}$ order polynomial model given in eq. 5.2.

### 5.2.8 Verification (validation) experiments

Following optimization of the medium composition and process parameters, a verification fermentation experiment was performed at optimum conditions to assess and compare experimental and model–predicted values of xylitol concentrations.

## 5.3 Results and discussion

### 5.3.1 Optimum number of PU foam cubes and its reusability

For determination of this parameter, the final xylitol concentration attained in 24 and 36 h was monitored with varying number of PU foam cubes (2 to 6) added to fermentation mixture. Fig. 5.2A depicts trends in final xylitol concentration with amount of PU foam cubes with immobilized cells of *C. tropicalis* added to fermentation mixture. It could be seen that the highest xylitol concentration for both 24 and 36 h fermentation was attained for 3 PU foam cubes added to medium. Reduction in xylitol yield for higher numbers of PU foam cubes is attributed to reduction in convection intensity in the medium due to hindrance offered by the cubes. This essentially results in increase in diffusional resistance (or mass transfer resistance) for transport of xylose/nutrients/xylitol in the void volume of PU foam, and also across cell membranes.

Dissolved oxygen concentration in the liquid medium entrapped in the pores of PU foam is also likely to be lesser than bulk medium. For immobilized PU foam cubes lower than 3, there was lower density of yeast cell in the fermentation medium resulting in lower xylitol production. Therefore, optimum numbers of immobilized PU foam cubes for xylitol fermentation using *C. tropicalis* was fixed as 3.

For the assessment of reusability of the biocatalyst, the PU foam cubes with immobilized cells from the first fermentation experiment were used in four consecutive experiments. Fig. 5.2B depicts the results of the reusability study. The xylitol concentration attained in the first fermentation was 9.81 g/L, which gradually reduced to 4.35 g/L at the end of fifth fermentation cycle which is 56% reduction. The reduction in xylitol concentration is attributed to reduction in the microbial cell density on PU foam due to detachment of the cells from the surface during long periods of cultivation.

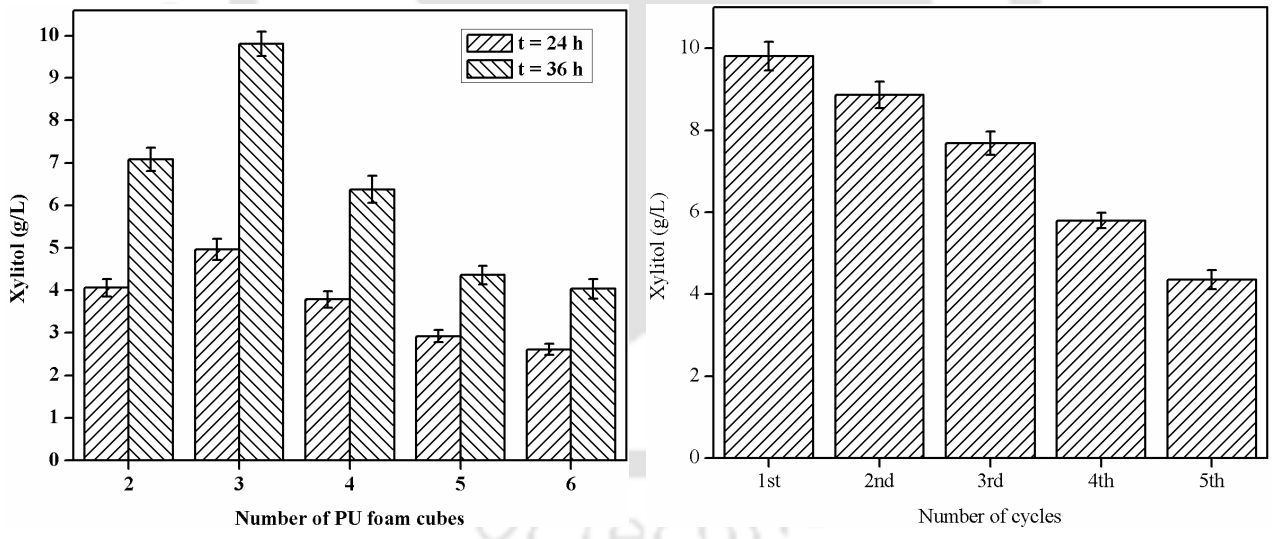


(A) (B)

**Figure 5.2.** (A) Optimization of amount of immobilized PU foam support (B) Reuseability of PU foam for the production of xylitol from sugarcane bagasse

### 5.3.2 Plackett–Burman (PBD) experimental design

The results of initial screening of medium components using Plackett–Burman design, with response variable xylitol concentration attained at the end of fermentation, is given in Table 5.2.

In the Plackett–Burman experimental design, final xylitol concentration attained in fermentation mixture varied from 5.02 g/L (run no. 3) to 10.14 g/L (run no. 4). Tables 5.2A and B show the analysis of Plackett–Burman design. Coefficients of 1$^{st}$–order model of Plackett–Burman design corresponding with their *t*– and *p*–values are shown in Table 5.2A, and the ANOVA for the 1$^{st}$–order regression equation is depicted in Table 5.2B. It is inferred from Table 5.2A that the *t*–values of yeast extract (6.13), $(NH_4)_2SO_4$ (5.68), $KH_2PO_4$ (4.71) and $MgSO_4{\cdot}7H_2O$ (7.40) are higher than the *t*–value limits (2.776) for Plackett–Burman design analysis, which shows their significant effect on xylitol production. Low *p*–values ($p \leq 0.05$) of the model coefficients (as depicted in Table 5.2B), and the pareto plot shown in Fig. 5.3 also confirms significance of the above medium components, as their *t*–values are above the threshold value of 2.776. The determination coefficient of the 1$^{st}$–order model with $R^2$ = 0.972 and adjusted $R^2$ = 0.923 confirms that 1$^{st}$ order regression equation fits very well to the experimental results.

**Table 5.2.** Results of Plackett–Burman design for screening of medium components
(A) Model coefficients, *t*– and *p*–values for the Plackett–Burman design

| Model term | Coefficient | *t*–value | *p*–value |
|---|---|---|---|
| Constant | 7.434 | 56.82 | 0.000 |
| $X_1$ | 0.803 | 6.13 | 0.004 |
| $X_2$ | 0.324 | 2.48 | 0.068 |
| $X_3$ | 0.259 | 1.98 | 0.119 |
| $X_4$ | 0.616 | 4.71 | 0.009 |
| $X_5$ | 0.742 | 5.68 | 0.005 |
| $X_6$ | 0.967 | 7.40 | 0.002 |
| $X_7$ | –0.183 | –1.39 | 0.235 |

(B) ANOVA for the Plackett–Burman design model

| Factor | SS | DF | MS | *F*–value | *p*–value |
|---|---|---|---|---|---|
| $X_1$ | 7.728 | 1 | 7.728 | 37.63 | 0.004 |
| $X_2$ | 1.261 | 1 | 1.261 | 6.14 | 0.068 |
| $X_3$ | 0.806 | 1 | 0.806 | 3.92 | 0.119 |

| | | | | | |
|---|---|---|---|---|---|
| $X_4$ | 4.551 | 1 | 4.551 | 22.16 | 0.009 |
| $X_5$ | 6.616 | 1 | 6.616 | 32.21 | 0.005 |
| $X_6$ | 11.233 | 1 | 11.233 | 54.69 | 0.002 |
| $X_7$ | 0.399 | 1 | 0.399 | 1.95 | 0.235 |
| Residual error | 0.822 | 4 | 0.205 | – | – |
| Total | 33.416 | 11 | – | – | – |

DF – degrees of freedom, SS – sum of squares, MS – mean square

$R^2$ = 0.975, adjusted $R^2$ = 0.932, predicted $R^2$ = 0.779; significant $p$ values, $p \leq 0.05$

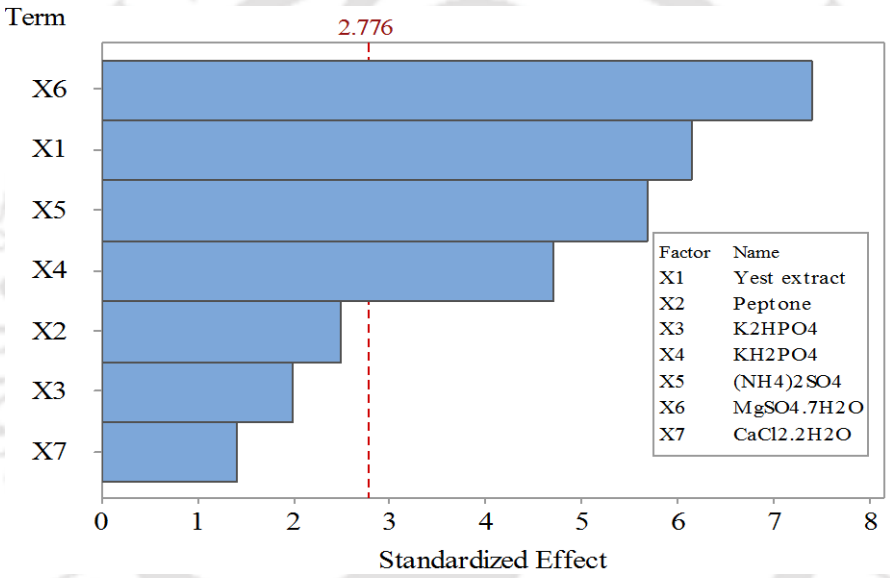


**Figure 5.3**. Pareto plot for Plackett–Burman analysis

### 5.3.3 Optimization of medium components using central composite design

Yeast extract, $KH_2PO_4$, $MgSO_4 \cdot 7H_2O$, and $(NH_4)_2SO_4$ have been identified as the significant medium components for the biosynthesis of xylitol using immobilized *C. tropicalis* on PU foam by the Plackett–Burman design. Among the 31 experimental sets of central composite design shown in Table 5.3B, maximum and minimum xylitol concentrations attained in fermentation mixture were 11.64 g/L (run no. 27) and 4.37 g/L (run no. 1). The 2$^{nd}$ order model equation fitted to the experimental data of CCD design (with variables in coded values) is as follows:

$$Xylitol\ (g/L) = 11.441 - 0.363X_1 + 0.681X_2 + 0.279X_3 + 0.539X_4 - 1.411X_1^2 - 0.816X_2^2 - 1.277X_3^2 - 1.145X_4^2 - 0.273X_1X_2 - 0.346X_1X_3 - 0.438X_1X_4 - 0.067X_2X_3 - 0.277X_2X_4 + 0.158X_3X_4 \quad (5.3)$$

**Table 5.3(A).** Central composite design for optimization of medium components: Coded and actual values of variables

| Independent variables | Coded symbols | Levels | | |
|---|---|---|---|---|
| | | Low (–α) | 0 | High (+α) |
| Yeast extract (g/L) | $X_1$ | 4 | 6 | 8 |
| $MgSO_4 \cdot 7H_2O$ (g/L) | $X_2$ | 0.10 | 0.50 | 0.90 |
| $KH_2PO_4$ (g/L) | $X_3$ | 0.15 | 0.55 | 0.95 |
| $(NH_4)_2SO_4$ (g/L) | $X_4$ | 1 | 3 | 5 |

**Table 5.3(B)** Central composite design for optimization of medium components (Response variable: Xylitol concentration, g/L)

| Run no. | Yeast extract ($X_1$) | $MgSO_4 \cdot 7H_2O$ ($X_2$) | $KH_2PO_4$ ($X_3$) | $(NH_4)_2SO_4$ ($X_4$) | Xylitol concentration (g/L) | |
|---|---|---|---|---|---|---|
| | | | | | Experimental | Predicted |
| 1 | –1 (5) | –1 (0.3) | –1 (0.35) | –1 (2) | 4.37 ± 0.065 | 4.41 |
| 2 | +1 (7) | –1 (0.3) | –1 (0.35) | –1 (2) | 5.48 ± 0.082 | 5.80 |
| 3 | –1 (5) | +1 (0.7) | –1 (0.35) | –1 (2) | 7.21 ± 0.108 | 7.01 |
| 4 | +1 (7) | +1 (0.7) | –1 (0.35) | –1 (2) | 7.53 ± 0.113 | 7.31 |
| 5 | –1 (5) | –1 (0.3) | +1 (0.75) | –1 (2) | 5.91 ± 0.089 | 5.48 |
| 6 | +1 (7) | –1 (0.3) | +1 (0.75) | –1 (2) | 5.87 ± 0.088 | 5.49 |
| 7 | –1 (5) | +1 (0.7) | +1 (0.75) | –1 (2) | 7.13 ± 0.107 | 7.81 |
| 8 | +1 (7) | +1 (0.7) | +1 (0.75) | –1 (2) | 6.86 ± 0.103 | 6.72 |
| 9 | –1 (5) | –1 (0.3) | –1 (0.35) | +1 (4) | 6.57 ± 0.098 | 6.61 |
| 10 | +1 (7) | –1 (0.3) | –1 (0.35) | +1 (4) | 6.64 ± 0.099 | 6.24 |
| 11 | –1 (5) | +1 (0.7) | –1 (0.35) | +1 (4) | 7.43 ± 0.111 | 8.09 |
| 12 | +1 (7) | +1 (0.7) | –1 (0.35) | +1 (4) | 6.31 ± 0.095 | 6.64 |
| 13 | –1 (5) | –1 (0.3) | +1 (0.75) | +1 (4) | 7.80 ± 0.117 | 8.30 |
| 14 | +1 (7) | –1 (0.3) | +1 (0.75) | +1 (4) | 6.46 ± 0.096 | 6.56 |
| 15 | –1 (5) | +1 (0.7) | +1 (0.75) | +1 (4) | 9.95 ± 0.149 | 9.53 |
| 16 | +1 (7) | +1 (0.7) | +1 (0.75) | +1 (4) | 6.45 ±0.097 | 6.69 |
| 17 | –α (4) | 0 (0.5) | 0 (0.55) | 0 (3) | 6.87 ± 0.103 | 6.52 |
| 18 | +α (8) | 0 (0.5) | 0 (0.55) | 0 (3) | 4.90 ± 0.073 | 5.07 |
| 19 | 0 (6) | –α (0.1) | 0 (0.55) | 0 (3) | 6.62 ± 0.096 | 6.81 |
| 20 | 0 (6) | +α (0.9) | 0 (0.55) | 0 (3) | 9.91 ± 0.148 | 9.54 |
| 21 | 0 (6) | 0 (0.5) | –α (0.15) | 0 (3) | 5.97 ± 0.089 | 5.77 |
| 22 | 0 (6) | 0 (0.5) | +α (0.95) | 0 (3) | 6.81 ± 0.102 | 6.89 |
| 23 | 0 (6) | 0 (0.5) | 0 (0.55) | –α (1) | 5.53 ±0.083 | 5.78 |
| 24 | 0 (6) | 0 (0.5) | 0 (0.55) | +α (5) | 8.37 ± 0.125 | 7.94 |
| 25 | 0 (6) | 0 (0.5) | 0 (0.55) | 0 (3) | 11.50 ± 0.163 | 11.58 |
| 26 | 0 (6) | 0 (0.5) | 0 (0.55) | 0 (3) | 11.53 ± 0.152 | 11.58 |
| 27 | 0 (6) | 0 (0.5) | 0 (0.55) | 0 (3) | 11.64 ± 0.145 | 11.58 |
| 28 | 0 (6) | 0 (0.5) | 0 (0.55) | 0 (3) | 11.59 ± 0.164 | 11.58 |

| | | | | | | |
|---|---|---|---|---|---|---|
| 29 | 0 (6) | 0 (0.5) | 0 (0.55) | 0 (3) | 11.60 ± 0.176 | 11.58 |
| 30 | 0 (6) | 0 (0.5) | 0 (0.55) | 0 (3) | 11.62 ± 0.168 | 11.58 |
| 31 | 0 (6) | 0 (0.5) | 0 (0.55) | 0 (3) | 11.57 ± 0.159 | 11.58 |

Values of the determination coefficients ($R^2$ = 0.979 and adjusted $R^2$ = 0.961) show that 2nd order regression equation fits very well to the experimental results. ANOVA for the fitted 2nd order regression equation is depicted in Table 5.4B.

The 2nd order model fitted to the experimental data is represented by the coded values of optimization parameters (medium components). The significance of the coefficients of these variables is indicated by their large *t*–stat and *F*– values and *p*–values ≤ 0.05. The *F*–values of interaction, linear, and square coefficients depict the significance of the individual effect of the optimization parameter (medium components) and the extent of interaction between the parameters. As shown in the ANOVA results shown in Table 5.4B, *F*–value of the model = 53.34, and *F*–value of linear coefficient = 27.97. The *p*–values of all the coefficients (linear, quadratic and interaction) except the interaction coefficients of $X_2X_3$ and $X_3X_4$ are ≤ 0.05, which depicts their significance. The Lack of Fit with *F*–value = 3.55 and *p*–value = 0.067 implies that Lack of Fit was insignificant or the model was significant.

**Table 5.4.** Results of central composite design for medium optimization
(A) Model coefficients, *t*– and *p*–values for the quadratic model

| Model term | Coefficient | *t*–value | *p*–value |
|---|---|---|---|
| Constant ($\beta_o$) | 11.441 | 66.57 | 0.000 |
| *Linear coefficients* | | | |
| Yeast extract ($X_1$) | –0.363 | –3.91 | 0.001 |
| $MgSO_4 \cdot 7H_2O$ ($X_2$) | 0.681 | 7.34 | 0.000 |
| $KH_2PO_4$ ($X_3$) | 0.279 | 3.02 | 0.008 |
| $(NH_4)_2SO_4$ ($X_4$) | 0.539 | 5.80 | 0.000 |
| *Quadratic coefficients* | | | |
| Yeast extract × Yeast extract ($X_1^2$) | –1.411 | –16.60 | 0.000 |
| $MgSO_4 \cdot 7H_2O$ × $MgSO_4 \cdot 7H_2O$ ($X_2^2$) | –0.816 | –9.60 | 0.000 |
| $KH_2PO_4$ × $KH_2PO_4$ ($X_3^2$) | –1.277 | –15.02 | 0.000 |
| $(NH_4)_2SO_4$ × $(NH_4)_2SO_4$ ($X_4^2$) | –1.145 | –13.46 | 0.000 |
| *Interaction coefficients* | | | |

| | | | |
|---|---|---|---|
| Yeast extract × $MgSO_4 \cdot 7H_2O$ ($X_1X_2$) | –0.273 | –2.40 | 0.029 |
| Yeast extract × $KH_2PO_4$ ($X_1X_3$) | –0.346 | –3.04 | 0.008 |
| Yeast extract × $(NH_4)_2SO_4$ ($X_1X_4$) | –0.438 | –3.85 | 0.001 |
| $MgSO_4 \cdot 7H_2O$ × $KH_2PO_4$ ($X_2X_3$) | –0.067 | –0.59 | 0.565 |
| $MgSO_4 \cdot 7H_2O$ × $(NH_4)_2SO_4$ ($X_2X_4$) | –0.277 | –2.44 | 0.027 |
| $KH_2PO_4$ × $(NH_4)_2SO_4$ ($X_3X_4$) | 0.158 | 1.39 | 0.183 |

(B) ANOVA for quadratic model

| Source | DF | SS | MS | *F*–value | *p*–value |
|---|---|---|---|---|---|
| Model | 14 | 154.401 | 11.029 | 53.34 | 0.000 |
| Linear | 4 | 23.130 | 5.783 | 27.97 | 0.000 |
| Quadratic | 4 | 123.397 | 30.849 | 149.21 | 0.000 |
| Interaction | 6 | 7.874 | 1.312 | 6.35 | 0.001 |
| Residual error | 16 | 3.308 | 0.207 | – | – |
| Lack–of–Fit | 10 | 2.829 | 0.283 | 3.55 | 0.067 |
| Pure error | 6 | 0.479 | 0.080 | – | – |
| Total | 30 | 157.709 | – | – | – |

DF – degrees of freedom, SS – sum of squares, MS – mean square. $R^2$ = 0.979, adjusted $R^2$ = 0.961, predicted $R^2$ = 0.893

(C) Analysis of contour plots

| Contour plot | Concentration range of variables for max. xylitol yield | | | | Xylitol (g/L) |
|---|---|---|---|---|---|
| | Yeast extract (g/L) | $MgSO_4 \cdot 7H_2O$ (g/L) | $KH_2PO_4$ (g/L) | $(NH_4)_2SO_4$ (g/L) | |
| Yeast extract vs. $MgSO_4 \cdot 7H_2O$ | 4.75–6.97 | 0.3–0.87 | 0.55* | 3* | 10 |
| Yeast extract vs. $KH_2PO_4$ | 4.82–6.96 | 0.5* | 0.35–0.81 | 3* | 10 |
| Yeast extract vs. $(NH_4)_2SO_4$ | 4.75–6.84 | 0.5* | 0.55* | 2.13–4.52 | 10 |
| $MgSO_4 \cdot 7H_2O$ vs. $(NH_4)_2SO_4$ | 6* | 0.29–0.87 | 0.55* | 1.94–4.45 | 10 |

Global optimum values of medium components:

| Yeast extract = | $MgSO_4 \cdot 7H_2O$ = | $KH_2PO_4$ = | $(NH_4)_2SO_4$ = |
|---|---|---|---|
| 5.78 g/L | 0.57 g/L | 0.58 g/L | 3.22 g/L |

Maximum xylitol concentration = 11.83 g/L

* Centre point values for the other two parameters

The interactions among different medium components involved in CCD were evaluated by plotting the interaction curves for maximum xylitol production. The interaction plots were

constructed showing the interaction among two factors by holding others at their center values for the prediction of xylitol yield as shown in Figs. 5.4A–D

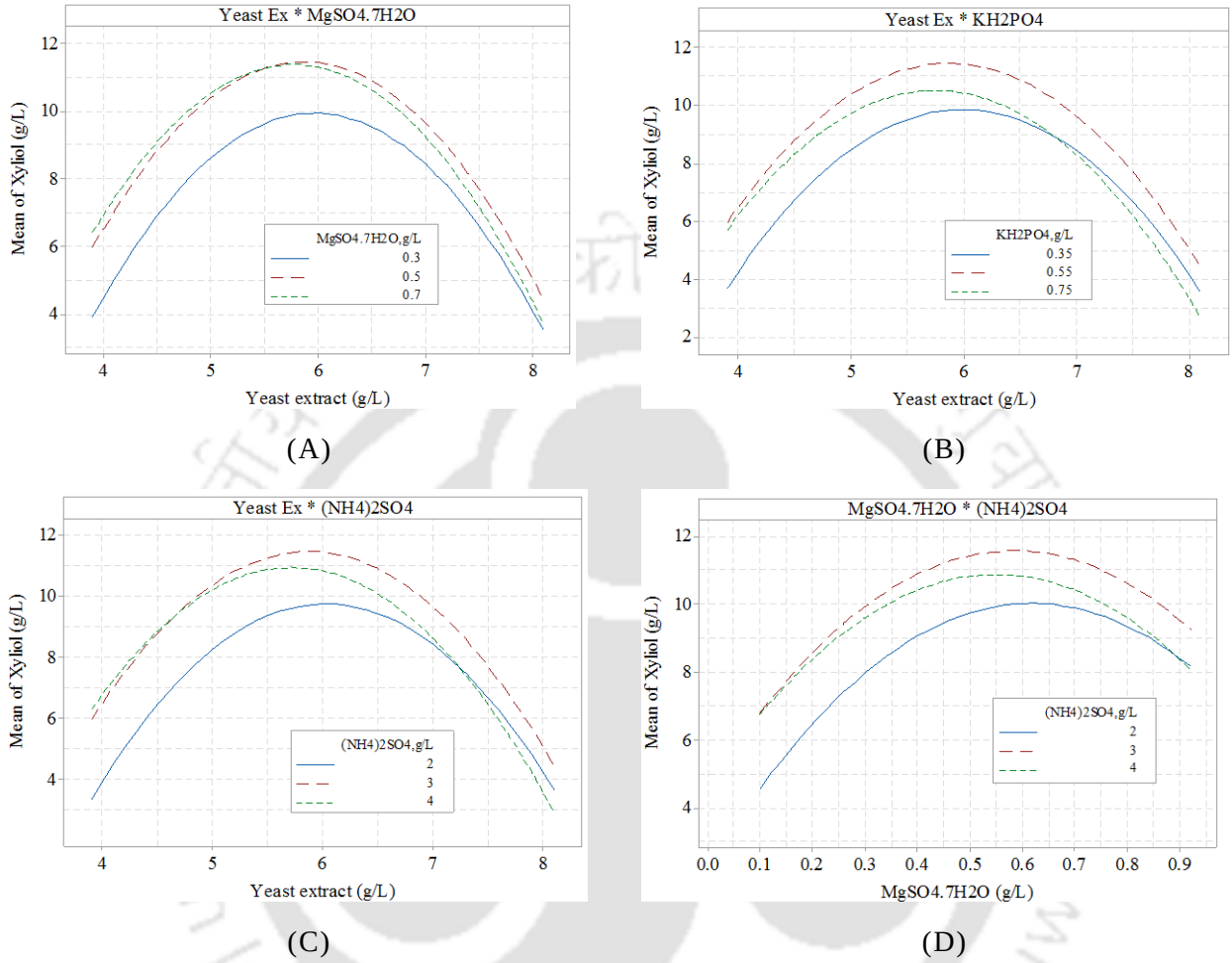


**Figure 5.4.** Interaction effects for xylitol yield (g/L) between: (A) yeast extract and $MgSO_4 \cdot 7H_2O$, (B) yeast extract and $KH_2PO_4$, (C) yeast extract and $(NH_4)_2SO_4$, (D) $MgSO_4.7H_2O$ and $(NH_4)_2SO_4$

Figs. 5.5A–D depicts the contour plots indicating the effect of two parameters on the xylitol production, while the other two parameters maintained at their center (zero) points. The contour plots in Figs. 5.5A–D have elliptical shape depicting the significant interactions between the variables in the xylitol fermentation using immobilized *C. tropicalis* on PU foam. The contour plots help us identify range of parameters for which the highest yield of xylitol is obtained. The range of parameters (corresponding to maximum xylitol yield) for any two parameters with

values of the other two parameters maintained at their center point is shown in Table 5.4C. All four optimization parameters (medium components) corresponding to maximum xylitol yield (global optimum) are also described in Table 5.4C. For all four combinations of two optimization parameters, maximum xylitol yield of 10 g/L was obtained.

The maximum xylitol concentration corresponding to the optimization of the four medium components using *C. tropicalis* immobilized on PU foam is 11.83 g/L (corresponding to yield of 0.63 g/g of xylose). The optimum values of the medium components for maximum xylitol yield as predicted by the quadratic model are: yeast extract = 5.78 g/L, $(NH_4)_2SO_4$ = 3.22 g/L, $MgSO_4 \cdot 7H_2O$ = 0.57 g/L and $KH_2PO_4$ = 0.58 g/L (shown in the optimization plot in Fig. 5.6). Ling et al. (2011) optimized the production of xylitol from biomass source (corncob hemicellulose hydrolysate) using *C. tropicalis* HDY–02 by screening the significant variables with PBD followed by CCD experimental design for optimization of the significant medium components. The researchers obtained optimum medium components of $(NH_4)_2SO_4$ = 5.0 g/L, $KH_2PO_4$ = 1.30 g/L, yeast extract = 4.60 g/L and $MgSO_4 \cdot 7H_2O$ = 0.60 g/L. Under these optimum medium components the xylitol yield of 0.73 g/g of xylose was achieved in continuous fed–batch experiments.

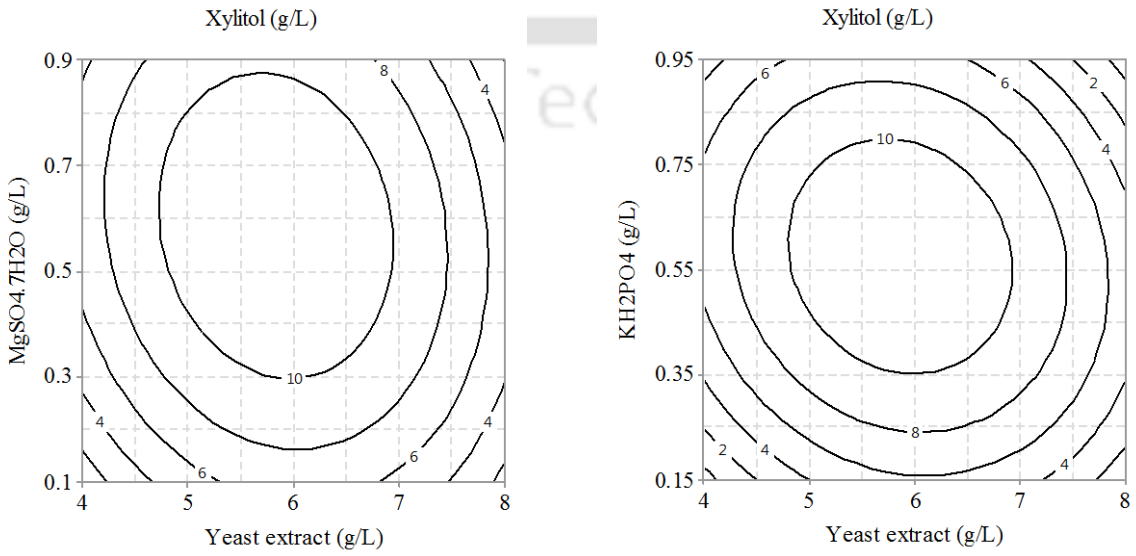

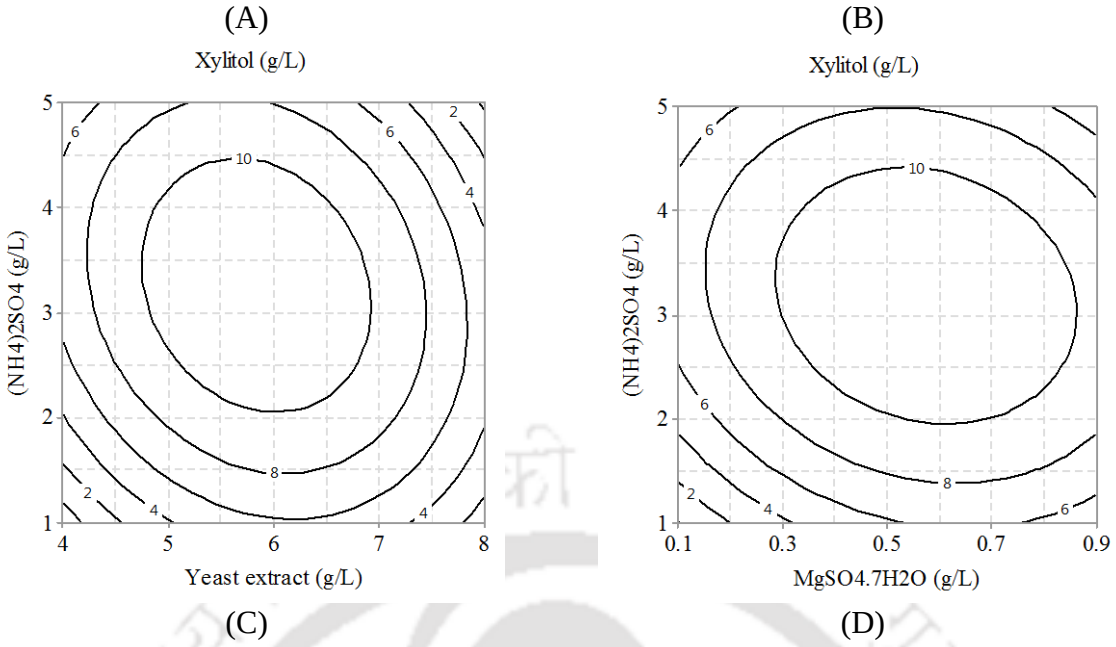


**Figure 5.5.** Contour plots for optimized medium components (A) yeast extract and $MgSO_4 \cdot 7H_2O$ (B) yeast extract and $KH_2PO_4$ (C) yeast extract and $(NH_4)_2SO_4$ (D) $MgSO_4 \cdot 7H_2O$ and $(NH_4)_2SO_4$

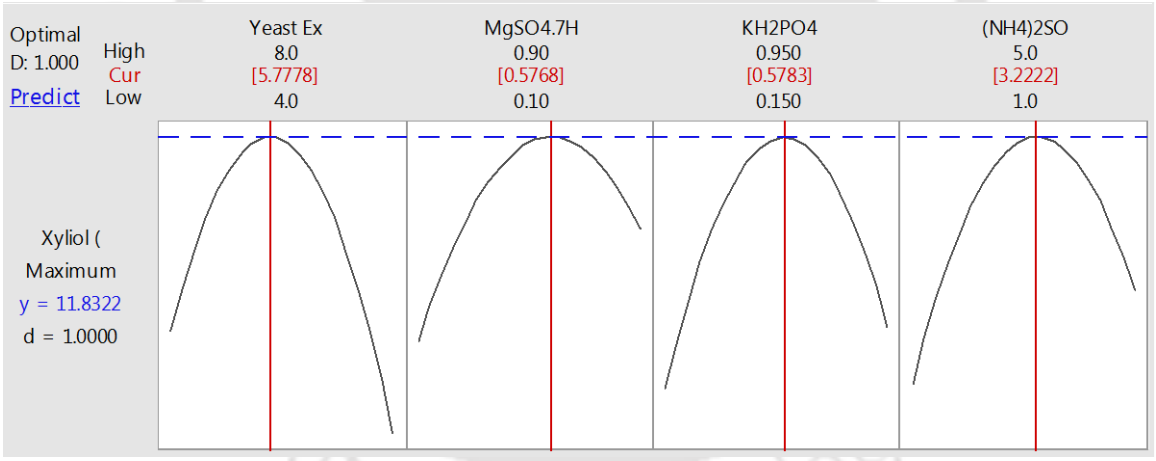


**Figure 5.6.** Desirability plot for optimum values for the medium components for xylitol production using *C. tropicalis* immobilized on PU foam.

### 5.3.4 Optimization of process parameters using central composite design

The complete CCD comprising 31 sets of experiments along with response variable (xylitol concentration) for each set is given in Table 5.5B. The maximum and minimum xylitol concentrations obtained in the 31 experimental sets of the CCD design were 11.67 g/L (run no. 20) and 4.43 g/L (run no. 1), respectively.

The quadratic model equation for the fitted data (with variables in coded values) is as follows:

$$\begin{aligned} Xylitol(g/L) = {} & 11.484 - 0.366X_1 + 0.746X_2 + 0.239X_3 + 0.462X_4 - 1.405X_1^2 \\ & - 0.933X_2^2 - 1.397X_3^2 - 1.132X_4^2 - 0.429X_1X_2 - 0.338X_1X_3 \\ & - 0.298X_1X_4 + 0.084X_2X_3 - 0.287X_2X_4 + 0.326X_3X_4 \end{aligned} \quad (5.4)$$

**Table 5.5(A)**. Central composite design for process parameters optimization: Coded and actual values of the variables

| Independent variables | Coded symbols | Levels | | |
|---|---|---|---|---|
| | | Low (–α) | 0 | High (+α) |
| Temperature ($^oC$) | $X_1$ | 24 | 30 | 36 |
| Initial pH | $X_2$ | 5 | 6 | 7 |
| Shaking speed (rpm) | $X_3$ | 130 | 150 | 170 |
| Substrate (xylose, g/L) | $X_4$ | 10 | 20 | 30 |

**Table 5.5(B).** Central composite design for optimization of process parameters (Response variable: Xylitol concentration, g/L)

| Run no. | Temperature ($X_1$) | Initial pH ($X_2$) | Shaking speed ($X_3$) | Xylose conc. ($X_4$) | Xylitol concentration (g/L) | |
|---|---|---|---|---|---|---|
| | | | | | Experimental | Predicted |
| 1 | –1 (27) | –1 (5.5) | –1 (140) | –1 (15) | 4.43 ± 0.071 | 4.59 |
| 2 | +1 (33) | –1 (5.5) | –1 (140) | –1 (15) | 5.87 ± 0.094 | 5.99 |
| 3 | –1 (27) | +1 (6.5) | –1 (140) | –1 (15) | 7.63 ± 0.122 | 7.35 |
| 4 | +1 (33) | +1 (6.5) | –1 (140) | –1 (15) | 7.35 ± 0.118 | 7.03 |
| 5 | –1 (27) | –1 (5.5) | +1 (160) | –1 (15) | 5.14 ± 0.082 | 4.93 |
| 6 | +1 (33) | –1 (5.5) | +1 (160) | –1 (15) | 5.18 ± 0.083 | 4.98 |
| 7 | –1 (27) | +1 (6.5) | +1 (160) | –1 (15) | 7.48 ± 0.119 | 8.02 |
| 8 | +1 (33) | +1 (6.5) | +1 (160) | –1 (15) | 6.36 ± 0.102 | 6.35 |
| 9 | –1 (27) | –1 (5.5) | –1 (140) | +1 (25) | 6.15 ± 0.098 | 6.04 |
| 10 | +1 (33) | –1 (5.5) | –1 (140) | +1 (25) | 6.57 ± 0.105 | 6.24 |
| 11 | –1 (27) | +1 (6.5) | –1 (140) | +1 (25) | 7.23 ± 0.116 | 7.64 |
| 12 | +1 (33) | +1 (6.5) | –1 (140) | +1 (25) | 6.04 ± 0.097 | 6.13 |
| 13 | –1 (27) | –1 (5.5) | +1 (160) | +1 (25) | 7.15 ± 0.114 | 7.68 |
| 14 | +1 (33) | –1 (5.5) | +1 (160) | +1 (25) | 6.37 ± 0.104 | 6.53 |
| 15 | –1 (27) | +1 (6.5) | +1 (160) | +1 (25) | 9.86 ± 0.158 | 9.62 |
| 16 | +1 (33) | +1 (6.5) | +1 (160) | +1 (25) | 6.71 ± 0.107 | 6.76 |
| 17 | 0 (30) | 0 (6) | 0 (150) | 0 (20) | 11.64 ± 0.186 | 11.63 |
| 18 | 0 (30) | 0 (6) | 0 (150) | 0 (20) | 11.59 ± 0.185 | 11.63 |
| 19 | 0 (30) | 0 (6) | 0 (150) | 0 (20) | 11.56 ± 0.184 | 11.63 |
| 20 | 0 (30) | 0 (6) | 0 (150) | 0 (20) | 11.67 ± 0.187 | 11.63 |
| 21 | –α (24) | 0 (6) | 0 (150) | 0 (20) | 6.95 ± 0.111 | 6.60 |
| 22 | +α (36) | 0 (6) | 0 (150) | 0 (20) | 4.87 ± 0.078 | 5.13 |
| 23 | 0 (30) | –α (5) | 0 (150) | 0 (20) | 6.27 ± 0.100 | 6.26 |

| | | | | | | |
|---|---|---|---|---|---|---|
| 24 | 0 (30) | +α (7) | 0 (150) | 0 (20) | 9.32 ± 0.149 | 9.24 |
| 25 | 0 (30) | 0 (6) | –α (130) | 0 (20) | 5.25 ± 0.084 | 5.42 |
| 26 | 0 (30) | 0 (6) | +α (170) | 0 (20) | 6.63 ± 0.106 | 6.37 |
| 27 | 0 (30) | 0 (6) | 0 (150) | –α (10) | 5.89 ± 0.094 | 6.03 |
| 28 | 0 (30) | 0 (6) | 0 (150) | +α (30) | 8.11 ± 0.129 | 7.88 |
| 29 | 0 (30) | 0 (6) | 0 (150) | 0 (20) | 11.65 ± 0.186 | 11.63 |
| 30 | 0 (30) | 0 (6) | 0 (150) | 0 (20) | 11.43 ± 0.173 | 11.63 |
| 31 | 0 (30) | 0 (6) | 0 (150) | 0 (20) | 11.37 ± 0.162 | 11.63 |

Individual linear and quadratic coefficients of all four process parameters have significant effect on xylitol production, as indicated by their large *t*–values and *p*–values ≤ 0.05 (Table 5.6A). Most of the interaction coefficients are also found to be significant. Only exception is the interaction coefficient between initial pH and shaking speed ( $X_2X_3$ ), which has *t*–value = 0.96 and *p*–value = 0.353 indicating insignificant effect on xylitol production. Table 5.6B depicts the ANOVA results of interaction, linear and quadratic coefficients. Large *F*–values and *p*–values ≤ 0.05 for the coefficients indicate their significant effect of the parameters on xylitol fermentation. Values of determination coefficients, $R^2$ = 0.988 and adjusted $R^2$ =0.978, show that the 2nd order regression equation fits very well to experimental data. The Lack of Fit has *F*–value = 2.93 and *p*–value = 0.101, which implies its insignificance. This is a corroboration of significance of quadratic model.

**Table 5.6**. Results of central composite design for process parameters optimization
(A) Model coefficients, *t*– and *p*–values for the quadratic model

| Model term | Coefficient | *t*–value | *p*–value |
|---|---|---|---|
| Constant ( $\beta_o$ ) | 11.484 | 86.78 | 0.000 |
| *Linear coefficients* | | | |
| Temperature ( $X_1$ ) | –0.366 | –5.12 | 0.000 |
| Initial pH ( $X_2$ ) | 0.746 | 10.44 | 0.000 |
| Shaking speed ( $X_3$ ) | 0.239 | 3.35 | 0.002 |
| Xylose conc. ( $X_4$ ) | 0.462 | 6.46 | 0.000 |
| *Quadratic coefficients* | | | |
| Temperature × Temperature ( $X_1^2$ ) | –1.405 | –21.45 | 0.000 |
| Initial pH × Initial pH ( $X_2^2$ ) | –0.933 | –14.25 | 0.000 |
| Shaking speed × Shaking speed ( $X_3^2$ ) | –1.397 | –21.34 | 0.000 |

| | | | |
|---|---|---|---|
| Xylose conc. × Xylose conc. ( $X_4^2$ ) | –1.132 | –17.29 | 0.000 |
| *Interaction coefficients* | | | |
| Temperature × Initial pH ( $X_1X_2$ ) | –0.429 | –4.90 | 0.000 |
| Temperature × Shaking speed ( $X_1X_3$ ) | –0.338 | –3.86 | 0.001 |
| Temperature × Xylose conc. ( $X_1X_4$ ) | –0.299 | –3.41 | 0.004 |
| Initial pH × Shaking speed ( $X_2X_3$ ) | 0.084 | 0.96 | 0.353 |
| Initial pH × Xylose conc. ( $X_2X_4$ ) | –0.287 | –3.28 | 0.005 |
| Shaking speed × Xylose conc. ( $X_3X_4$ ) | 0.326 | 3.73 | 0.002 |

(B) ANOVA for quadratic model

| Source | DF | SS | MS | *F*–value | *p*–value |
|---|---|---|---|---|---|
| Model | 14 | 165.732 | 11.838 | 96.56 | 0.000 |
| Linear | 4 | 23.051 | 5.763 | 47.00 | 0.000 |
| Quadratic | 4 | 133.352 | 33.338 | 271.92 | 0.000 |
| Interaction | 6 | 9.329 | 1.555 | 12.68 | 0.000 |
| Residual error | 16 | 1.962 | 0.123 | – | – |
| Lack–of–Fit | 10 | 1.628 | 0.163 | 2.93 | 0.101 |
| Pure error | 6 | 0.334 | 0.056 | – | – |
| Total | 30 | 167.694 | – | – | – |

DF – degrees of freedom, SS – sum of squares, MS – mean square. $R^2$ = 0.988, adjusted $R^2$ = 0.978, predicted $R^2$ = 0.941

(C) Analysis of contour plots

| Contour plot | Range of process variables for maximum xylitol yield | | | | Xylitol (g/L) |
|---|---|---|---|---|---|
| | Temperature ($^o$C) | Initial pH | Shaking speed (rpm) | Substrate (xylose) (g/L) | |
| Temperature vs Initial pH | 26.1–32.9 | 5.5–6.8 | 150* | 20* | 10 |
| Temperature vs Shaking speed | 26.3–32.8 | 6* | 140–161 | 20* | 10 |
| Temperature vs Substrate (xylose) | 26.2–32.9 | 6* | 150* | 15–27.4 | 10 |
| Initial pH vs Substrate (xylose) | 30* | 5.5–6.7 | 150* | 14.5–26.5 | 10 |
| Shaking speed vs Substrate (xylose) | 30* | 6* | 140–162 | 15–27 | 10 |

**Global optimum values of process parameters:**

Temperature = 29.3$^o$C  Initial pH = 6.2  Shaking speed = 151 rpm  Substrate (xylose) concentration = 20.9 g/L

Maximum xylitol concentration = 11.89 g/L

* Centre point values for the other two parameters

The interaction among different process parameters involved in central composite design (CCD) were assessed by plotting the interaction curves for maximum xylitol production. The interaction plots were constructed showing the interaction among two factors by holding others at their center values for the prediction of xylitol yield as shown in Figs. 5.7A–E. The interaction among fermentation temperature and initial pH for xylitol yield at center levels of xylose concentration (20 g/L) and shaking speed (150 rpm) is shown in Fig 5.7A. It was revealed that increasing the temperature from 25$^{o}$ to 30$^{o}$C increased the yield of xylitol for pH values 5.5, 6 and 6.5 with lower xylitol yield at pH 5.5 and higher xylitol yield at pH 6.5 for 25$^{o}$C. Maximum xylitol yield of 11.52 g/L was attained for the intial pH of 6 and 6.5 at 30$^{o}$C as depicted from Fig.5.7A. Lower xylitol yield was obtained at low pH (5.5) for all the temperature ranges. These observations could be explained in terms of the limited ionization of functional groups of the enzyme xylose reductase (XR) at low pH condition. The interaction effects of temperature and shaking speed (Fig. 5.7B), temperature and xylose concentration (Fig. 5.7C), and shaking speed and xylose concentration (Fig. 5.7E) show similar trends in which the xylitol yield attained a maximum value and then dropped continuously within the intervals of the process parameters considered. Fig. 5.7D depicts the interaction effect of pH and xylose concentration. As revealed from Fig. 5.7D, maximum xylitol yield (xylitol = 10.15 g/L at xylose concentration 15 g/L, xylitol = 10.85 g/L at xylose concentration 25 g/L, and xylitol = 11.75 g/L at xylose concentration 20 g/L) was obtained at pH range of 6 to 6.5. Xylitol yield at 20 g/L xylose concentration is higher than that of 25 g/L xylose concentration in the pH range 5.5 to 7. Moreover, the xylitol yield of 15 g/L xylose concentration is higher than that of 25 g/L xylose concentration in the pH range 6.7 to 7, as shown in Fig. 5.7D. These results indicate that there is substrate inhibition during fermentation process for higher xylose concentrations. Moreover, the concentration of inhibitory by–products increased as xylose concentration increased in the hydrolysate which resulted in lowering of the xylitol yield. Higher and lower shaking speed also decreased the xylitol yield as shown in Fig

5.7B. This could be due to mass transfer limitations in fermentation mixture at lower shaking speed and detachment of microbial cells from immobilization support at higher shaking speed.

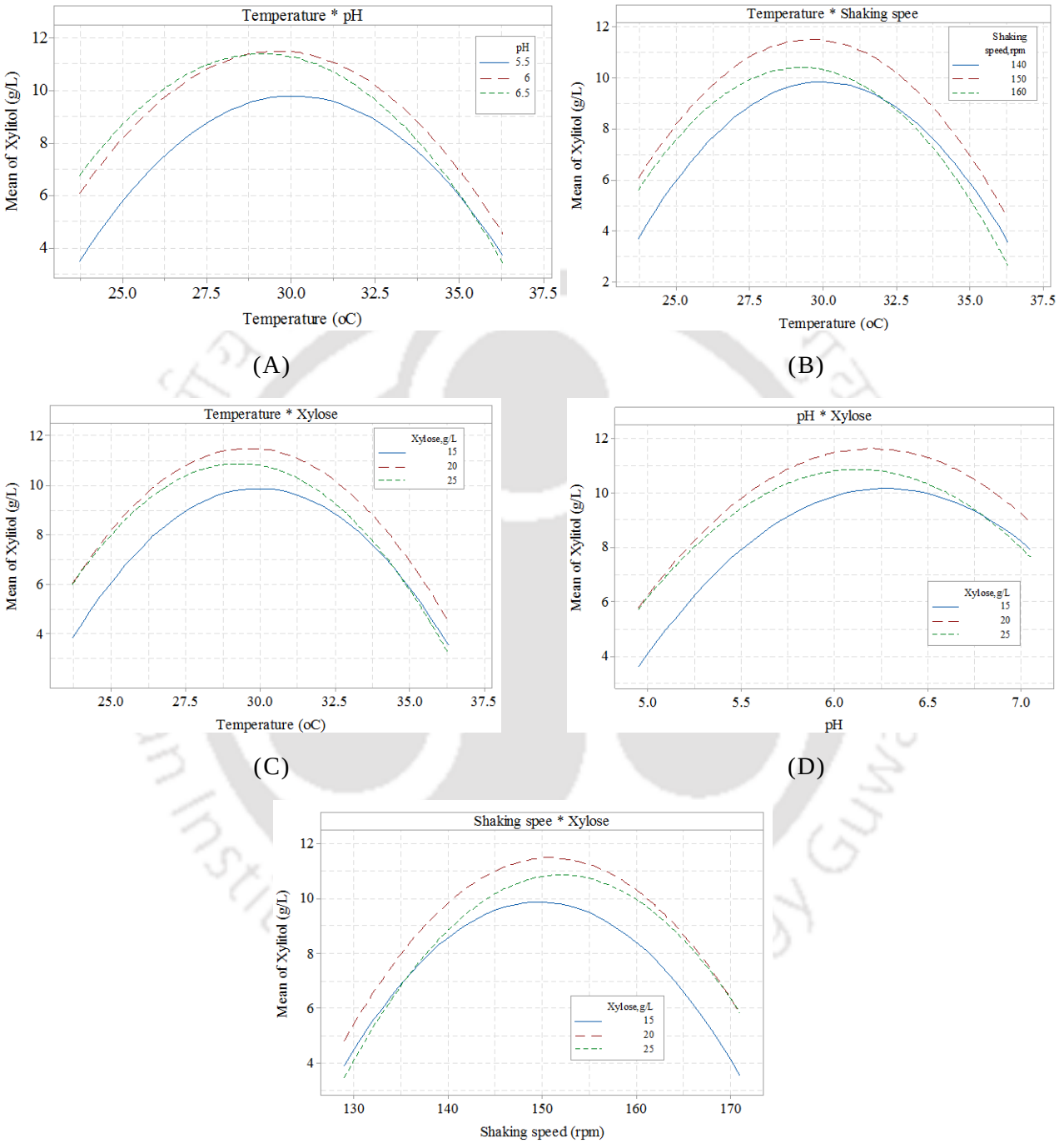


**Figure 5.7.** Interaction effects for xylitol yield (g/L) between: (A) temperature and pH, (B) temperature and shaking speed, (C) temperature and xylose concentration, (D) pH and xylose concentration, (E) shaking speed and xylose concentration

Figs. 5.8A–E depicts the contour plots indicating the effect of two parameters on the xylitol production, while the other two variables maintained at their centre–point (or zero) level. The contour plots in Figs. 5.8A–E have elliptical shape depicting significant interaction between the variables in xylitol production using immobilized *C. tropicalis* on PU foam. The interactions of these variables are also proven by the *F*– and *p*–values of their interaction coefficients as indicated in Table 5.6B. The range of process variables for maximum xylitol concentration maintaining the other two process variables at their centre–points is shown in Table 5.6C. All four optimization process parameters (corresponding to maximum xylitol yield or global optimum) are also presented in Table 5.6C. For all four combinations of two optimization parameters, a maximum xylitol yield of 10 g/L was achieved.

The maximum xylitol concentration corresponding to the optimization of the variables (process parameters) using *C. tropicalis* immobilized on PU foam is 11.89 g/L (corresponding to yield of 0.65 g/g of xylose). The optimum values of the process parameters for maximum xylitol yield as predicted by the $2^{nd}$ order model are: temperature = 29.3$^{o}$C, initial pH = 6.2, shaking speed = 151 rpm and substrate (xylose) concentration = 20.9 g/L (shown in Fig. 5.9). Ramesh et al. (2012) have studied fermentation medium and process parameters optimization for xylitol production from corncob hydrolysate using *C. guillermondii* (NCIM 3124). The optimal values of process variables reported by Ramesh et al. (2012) for xylitol yield of 0.71 g/g are: temperature = 29.9$^{o}$C, xylose concentration = 16.5 g/L, pH = 7.3, agitation speed = 160 rpm.

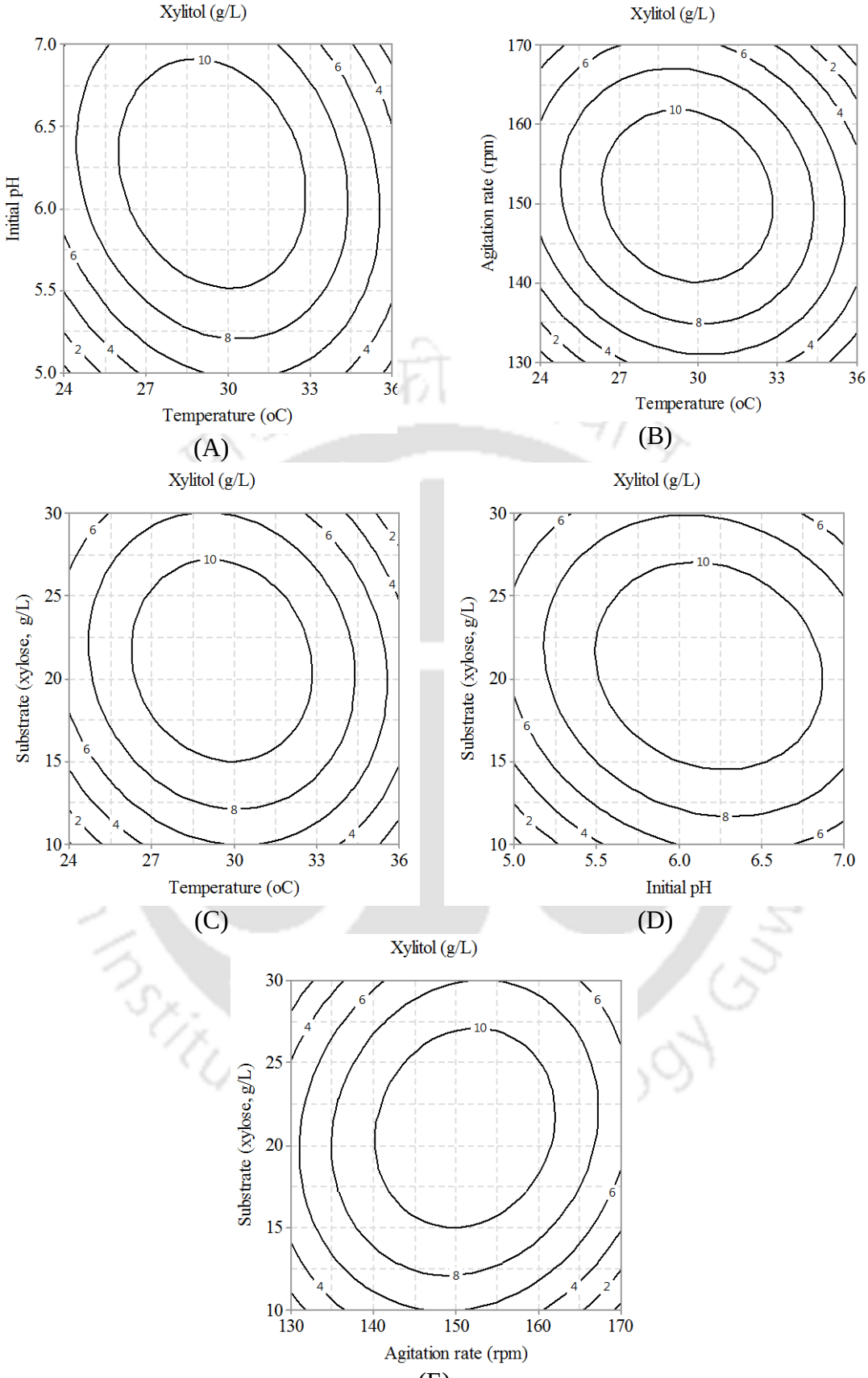


**Figure 5.8.** Contour plots for optimized process parameters (A) temperature and initial pH (B) temperature and agitation rate (C) temperature and substrate (xylose) (D) initial pH and substrate (xylose) (E) agitation rate and substrate (xylose)

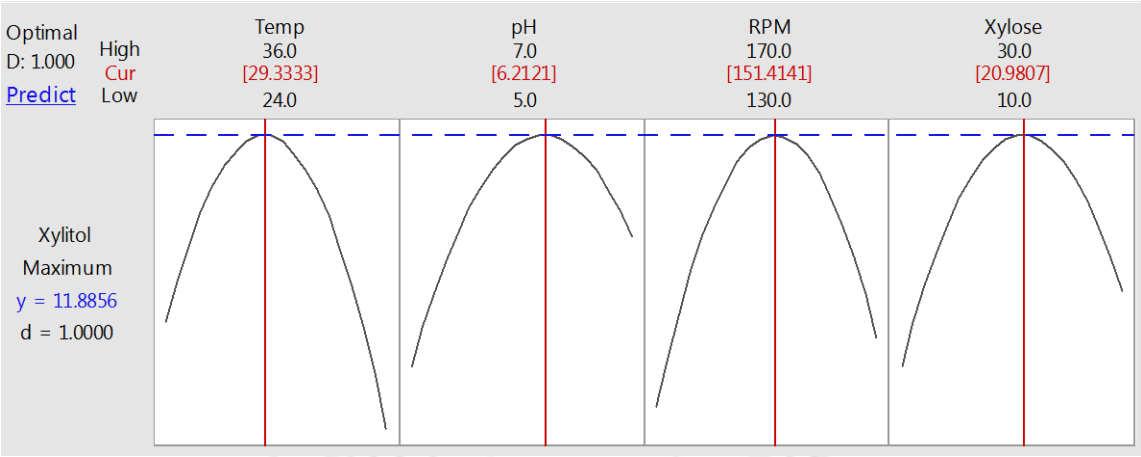


**Figure 5.9.** Desirability plot for optimum values of the process parameters for xylitol production from sugarcane bagasse using immobilized *C. tropiclis* on PU foam support.

### 5.3.5 Verification experiments for xylitol production using optimized parameters

Fermentation experiments (in triplicate) with optimum medium composition and process parameter values were conducted for the validation of statistical analysis predicted by the CCD for xylitol production. The maximum xylitol concentration of 11.92 g/L with immobilized *C. tropicalis* MTCC 184 corresponding to the xylitol yield of 0.65 g/g xylose or 71% of the theoretical yield of xylitol was achieved. The validation experiment with immobilized *C. tropicalis* closely agreed with the prediction of CCD analysis (11.89 g/L).

### 5.3.6 Analysis of optimum values of medium components and process parameters

Medium components optimization for xylitol bio–production have revealed yeast extract, $(NH_4)_2SO_4$, $MgSO_4 \cdot 7H_2O$ and $KH_2PO_4$ as the significant medium components. In the following section, we have tried to identify physiological rational for the same. In xylitol production, xylose reductase (XR) is the key enzyme, which catalyzes initial reaction in the xylose metabolism pathway, the NAD(P)H dependent reduction of xylose to xylitol. Xylose reductase is classified into the aldose reductase (ALR) family, a member of the aldo–keto reductase (AKR) superfamily (Jez and Penning, 2001). Su et al. (2010) have reported a study on the influence of various metal ions on the activity of free and immobilized xylose reductase from *C. tropicalis*. The study of Su

et al. (2010) revealed that the metal–ion free xylose reductase obtained on dialysis against EDTA (5 mM) had insignificant activity which was refurbished by the addition of $Mg^{2+}$ ions (2 mM). This enzyme was stabilized by $Ca^{2+}$ and $Mg^{2+}$, while the metal ions (viz. $Co^{2+}$, $Cu^{2+}$ and $Fe^{3+}$) had an inhibitory effect. $KH_2PO_4$ provides growth enhancing nutrients of potassium and phosphate in the fermentation medium, and also maintains pH at desired value (Dikshit and Moholkar, 2016). Yeast extract, which is a complex mixture of proteins, and vitamins and amino acids, provide growth factors that have specific role in catalytic and structural reactions essential for growth of yeast cells. $(NH_4)_2SO_4$ essentially acts as a source of utilizable nitrogen for cell growth, in addition to providing utilizable sulphur (Yalcin and Ozbas, 2008).

The optimum values of process parameters also give an insight into the physical mechanism of the xylitol fermentation. The optimum value of shaking speed (150 rpm) indicates influence of diffusional resistance for the substrate into the pores of the immobilization matrix. Mass transfer limitations affect substrate access of the cells present in the pores of PU foam, and thus retard the fermentation rate. Back diffusion of the product (xylitol) from the pores to the bulk is also hindered due to mass transfer. This essentially implies that intensification of agitation (or convection) in fermentation mixture is a possible means of augmenting xylose metabolism and the xylitol yield. Relatively low value of optimum substrate concentration (20 g/L xylose) is essentially indicative of substrate inhibition of the enzymes in metabolic pathway. This feature needs further careful study. Use of fed–batch mode for fermentation, which maintains average substrate concentrations in fermentation mixture at relatively low values, is a possible solution for avoiding the substrate inhibition and augmenting the xylitol yields.

## 5.4 Conclusions

Statistical optimization of xylitol production from immobilized *C. tropicalis* MTCC 184 on PU foam has revealed yeast extract, $MgSO_4 \cdot 7H_2O$, $KH_2PO_4$ and $(NH_4)_2SO_4$ as significant medium components and initial pH, agitation rate, initial substrate concentration and temperature as

significant process parameters. The medium components provide essential growth factors and utilizable potassium, nitrogen, sulphur sources, in addition to augmenting and stabilizing activity of xylose reductase. Diffusional resistance for substrate in immobilization matrix and influence of substrate inhibition is evident from optimum values of process parameters. At optimum conditions, xylitol yield of 0.65 g/g xylose is achieved, which is comparable with previous literature.

Excessive amount of immobilized PU foam has a mass transfer and circulation limitation resulting in deficient substrate and dissolved oxygen supply to the cells inside the support. Lower amount of it also has lower cells population in the fermentation medium which lowers the xylitol production. Therefore, optimum amount of immobilized PU foam was essential for the production of xylitol with *Candida tropicalis*.

Yeast extract, a complex mixture of proteins, vitamins and amino acids, essential for growth of yeast; $MgSO_4 \cdot 7H_2O$ provide Mg and sulphur sources; $(NH_4)_2SO_4$ provide inorganic nitrogen and sulphur sources; and $KH_2PO_4$ helps to maintain the pH of the fermentation medium are essential components of the production of xylitol.

**References**

Agarwal, M., Dikshit, P.K., Bhasarkar, J.B., Borah, A.J. and Moholkar, V.S., 2016. Physical insight into ultrasound–assisted biodesulfurization using free and immobilized cells of *Rhodococcus rhodochrous* MTCC 3552. Chem. Eng. J. 295, 254–267.

Bisswanger, H., 2002. Multiple equilibria. Enzyme kinetics: principles and methods, 5–50.

Bhasarkar, J.B., Dikshit, P.K. and Moholkar, V.S., 2015. Ultrasound assisted biodesulfurization of liquid fuel using free and immobilized cells of *Rhodococcus rhodochrous* MTCC 3552: a mechanistic investigation. Bioresour. Technol. 187, 369–378.

Chakma, S. and Moholkar, V.S., 2011. Mechanistic features of ultrasonic desorption of aromatic pollutants. Chem. Eng. J. 175, 356–367.

Chakma, S. and Moholkar, V.S., 2015. Investigation in mechanistic issues of sonocatalysis and sonophotocatalysis using pure and doped photocatalysts. Ultrason. Sonochem. 22, 287–299.

Choudhury, H.A., Malani, R.S. and Moholkar, V.S., 2013. Acid catalyzed biodiesel synthesis from Jatropha oil: mechanistic aspects of ultrasonic intensification. Chem. Eng. J. 231, 262–272.

Chu, J., Li, B., Zhang, S. and Li, Y., 2000. On–line ultrasound stimulates the secretion and production of gentamicin by *Micromonospora echinospora*. Process Biochem. 35(6), 569–572.

Dai, C., Xiong, F., He, R., Zhang, W. and Ma, H., 2017. Effects of low–intensity ultrasound on the growth, cell membrane permeability and ethanol tolerance of *Saccharomyces cerevisiae*. Ultrason. Sonochem. 36, 191–197.

Dikshit, P.K. and Moholkar, V.S., 2016. Optimization of 1, 3–dihydroxyacetone production from crude glycerol by immobilized *Gluconobacter oxydans* MTCC 904. Bioresour. Technol. 216, 1058–1065.

Dikshit, P.K., Kharmawlong, G.J. and Moholkar, V.S., 2018. Investigations in sonication–induced intensification of crude glycerol fermentation to dihydroxyacetone by free and immobilized *Gluconobacter oxydans*. Bioresour. Technol. 256, 302–311.

El–Batal, A.I. and Khalaf, S.A., 2004. Xylitol production from corn cobs hemicellulosic hydrolysate by *Candida tropicalis* immobilized cells in hydrogel copolymer carrier. Int. J. Agric. Biol. 6, 1066–1073.

Goswami, P.P., Choudhury, H.A., Chakma, S. and Moholkar, V.S., 2013. Sonochemical synthesis and characterization of manganese ferrite nanoparticles. Ind. Eng. Chem. Res. 52(50), 17848–17855.

Granström, T., Ojamo, H. and Leisola, M., 2001. Chemostat study of xylitol production by

*Candida guilliermondii*. Appl. Microb. Biotechnol. 55(1), 36–42.

Harmsen, P.F.H., Huijgen, W., Bermudez, L. and Bakker, R., 2010. Literature review of physical and chemical pretreatment processes for lignocellulosic biomass. Wageningen UR Food Biobas. Res. 1184.

Jez, J.M. and Penning, T.M., 2001. The aldo–keto reductase (AKR) superfamily: an update. Chem. Biol. Interact. 130, 499–525.

Khanna, S., Jaiswal, S., Goyal, A. and Moholkar, V.S., 2012. Ultrasound enhanced bioconversion of glycerol by *Clostridium pasteurianum*: a mechanistic investigation. Chem. Eng. J. 200, 416–425.

Khanna, S., Goyal, A. and Moholkar, V.S., 2013. Mechanistic investigation of ultrasonic enhancement of glycerol bioconversion by immobilized *Clostridium pasteurianum* on silica support. Biotechnol. Bioeng. 110(6), 1637–1645.

Kilian, S.G. and Van Uden, N., 1988. Transport of xylose and glucose in the xylose–fermenting yeast *Pichia stipitis*. Appl. Microbiol. Biotechnol. 27(5–6), 545–548.

Kumdam, H.B., Murthy, S.N. and Gummadi, S.N., 2012. A statistical approach to optimize xylitol production by *Debaryomyces nepalensis* NCYC 3413 in vitro. Food Nutri. Sci. 3(08), 1027.

Ling, H., Cheng, K., Ge, J. and Ping, W., 2011. Statistical optimization of xylitol production from corncob hemicellulose hydrolysate by *Candida tropicalis* HDY–02. New Biotechnol. 28(6), 673–678.

Moholkar, V.S., Sable, S.P. and Pandit, A.B., 2000. Mapping the cavitation intensity in an ultrasonic bath using the acoustic emission. AIChE J. 46(4), 684–694.

Painting, K. and Kirsop, B., 1990. A quick method for estimating the percentage of viable cells in a yeast population, using methylene blue staining. World J. Microbiol. Biotechnol. 6(3), 346–347.

Pérez–Bibbins, B., Torrado–Agrasar, A., Salgado, J.M., Mussatto, S.I. and Domínguez, J.M.,

2016. Xylitol production in immobilized cultures: a recent review. Crit. Rev. Biotechnol. 36(4), 691–704.

Ping, Y., Ling, H.Z., Song, G. and Ge, J.P., 2013. Xylitol production from non–detoxified corncob hemicellulose acid hydrolysate by *Candida tropicalis*. Biochem. Eng. J. 75, 86–91.

Prakash, G., Varma, A.J., Prabhune, A., Shouche, Y. and Rao, M., 2011. Microbial production of xylitol from D–xylose and sugarcane bagasse hemicellulose using newly isolated thermotolerant yeast *Debaryomyces hansenii*. Bioresour. Technol. 102(3), 3304–3308.

Ramesh, S., Muthuvelayudham, R. and Viruthagiri, T., 2012. Application of factorial design to the study of xylitol production from corncob hemicellulose hydrolysate by *Candida guilliermondii*. J. Biochem. Technol. 4(1), 518–523.

Rao, R.S., Jyothi, C.P., Prakasham, R.S., Sarma, P.N. and Rao, L.V., 2006. Xylitol production from corn fiber and sugarcane bagasse hydrolysates by *Candida tropicalis*. Bioresour. Technol. 97(15), 1974–1978.

Sarrouh, B. and Da Silva, S.S., 2013. Repeated batch cell–immobilized system for the biotechnological production of xylitol as a renewable green sweetener. Appl. Biochem. Biotechnol. 169(7), 2101–2110.

Singh, S., Sarma, S., Agarwal, M., Goyal, A., Moholkar, V.S., 2015a. Ultrasound enhanced ethanol production from *Parthenium hysterophorus*: a mechanistic investigation. Bioresour. Technol. 188, 287–294.

Singh, S., Agarwal, M., Sarma, S., Goyal, A., Moholkar, V.S., 2015b. Mechanistic insight into ultrasound induced enhancement of simultaneous saccharification and fermentation of *Parthenium hysterophorus* for ethanol production. Ultrason. Sonochem. 26, 249–256.

Singh, S., Agarwal, M., Bhatt, A., Goyal, A. and Moholkar, V.S., 2015c. Ultrasound enhanced enzymatic hydrolysis of *Parthenium hysterophorus*: A mechanistic investigation. Bioresour. Technol. 192, 636–645.

Stephanopoulos, G., Aristidou, A.A. and Nielsen, J., 1998. Metabolic engineering: principles and methodologies. Academic press.

Su, Y., Li, W., Zhu, W., Yu, R., Fei, B., Wen, T., Cao, Y. and Qiao, D., 2010. Characterization of xylose reductase from *Candida tropicalis* immobilized on chitosan bead. African J. Biotechnol. 9(31), 4954–4965.

Soleimani, M. and Tabil, L., 2014. Evaluation of biocomposite–based supports for immobilized–cell xylitol production compared with a free–cell system. Biochem. Eng. J. 82, 166–173.

Suresh, K., Ranjan, A., Singh, S. and Moholkar, V.S., 2014. Mechanistic investigations in sono–hybrid techniques for rice straw pretreatment. Ultrason. Sonochem. 21(1), 200–207.

Tizazu, B.Z. and Moholkar, V.S., 2018. Kinetic and thermodynamic analysis of dilute acid hydrolysis of sugarcane bagasse. Bioresour. Technol. 250, 197–203.

Tochampa, W., Sirisansaneeyakul, S., Vanichsriratana, W., Srinophakun, P., Bakker, H.H. and Chisti, Y., 2005. A model of xylitol production by the yeast *Candida mogii*. Bioprocess Biosyst. Eng. 28(3), 175–183.

Ur–Rehman, S., Mushtaq, Z., Zahoor, T., Jamil, A. and Murtaza, M.A., 2015. Xylitol: a review on bioproduction, application, health benefits, and related safety issues. Crit. Rev. Food Sci. Nutri. 55(11), 1514–1528.

Wang, L., Wu, D., Tang, P., Fan, X. and Yuan, Q., 2012. Xylitol production from corncob hydrolysate using polyurethane foam with immobilized *Candida tropicalis*. Carbohydr. Polym. 90(2), 1106–1113.

Wang, L., Liu, N., Guo, Z., Wu, D., Chen, W., Chang, Z., Yuan, Q., Hui, M. and Wang, J., 2016. Nitric acid–treated carbon fibers with enhanced hydrophilicity for *Candida tropicalis* immobilization in xylitol fermentation. Mater. 9(3), 206.

Yahashi, Y., Hatsu, M., Horitsu, H., Kawai, K., Suzuki, T. and Takamizawa, K., 1996. D–glucose feeding for improvement of xylitol productivity from D–xylose using *Candida tropicalis* immobilized on a non–woven fabric. Biotechnol. Lett. 18(12), 1395–1400.

Yalçın, S.K. and Özbaş, Z.Y., 2008. Effects of ammonium sulphate concentration on growth and glycerol production kinetics of two endogenic wine yeast strains. Indian J. Biotechnol. 7, 89–93.

Yewale, T., Panchwagh, S., Rajagopalan, S., Dhamole, P.B. and Jain, R., 2016. Enhanced xylitol production using immobilized *Candida tropicalis* with non–detoxified corn cob hemicellulosic hydrolysate. 3 Biotech. 6(1), 75.

Zhang, Q., Li, Y., Xia, L. and Liu, Z., 2014. Enhanced xylitol production from statistically optimized fermentation of cotton stalk hydrolysate by immobilized *Candida tropicalis*. Chem. Biochem. Eng. Q. 28(1), 87–93.

# CHAPTER 6

# INVESTIGATIONS IN ULTRASOUND–ASSISTED INTENSIFICATION OF XYLITOL BIO–PRODUCTION FROM SUGARCANE BAGASSE

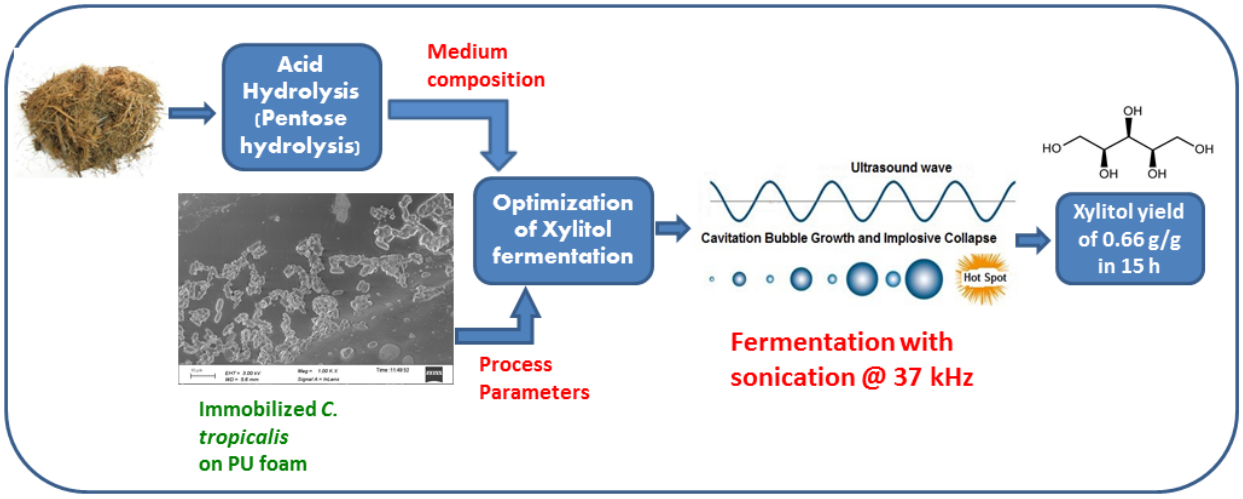

# CHAPTER 6

# INVESTIGATIONS IN ULTRASOUND–ASSISTED INTENSIFICATION OF XYLITOL BIO–PRODUCTION FROM SUGARCANE BAGASSE

## 6.1 Introduction

The major limitation of biological/biochemical processes for large scale application is slow kinetics. Moreover, microbial fermentation processes have strong mass transfer limitations. Previous authors have adopted different strategies for enhancement of both kinetics and yield of fermentation based processes such as: (1) optimization of medium components and process paramenters, (2) immobilization of the microbial cells in various supports, and (3) ultrasound irradiation at low frequency of the fermentation mixture etc.

Sonication is a relatively new technique for enhancement of physical, chemical and biological processes by introduction of energy into the system at extremely small spatial and temporal scales. The beneficial effects of sonication which are responsible for intensification of the processes are essentially manifested through phenomenon of cavitation, which comprises of nucleation, growth and transient implosive collapse of gas or vapor bubbles. Application of sonication (or ultrasound irradiation) has been attempted for past few years for enhancement of kinetics and yield of biological/biochemical processes – especially the fermentation–based processes (Dikshit et al., 2018; Khanna et al., 2012; Khanna et al. 2013; Lunelli et al., 2014; Singh et al., 2014; Singh et al., 2015a,b,c). Ultrasound, and its secondary effect of cavitation, induces energy into the fermentation mixtures on extremely short temporal and spatial scale. The

physical and chemical effects of ultrasound and cavitation lead to intensification of the fermentation processes through different mechanisms (Subhedar and Gogate, 2014; Subhedar et al., 2015; Sulaiman et al., 2011, 2013). The principal physical mechanism of intensification is generation of strong micro–convection in the medium which overcomes the mass transfer limitations, while the principal chemical mechanism is generation of highly reactive radicals that accelerate various chemical reactions in the medium. The micro–convection generated by ultrasound and cavitation also induces conformational changes in the secondary structure of extracellular and intracellular enzymes, which results in unfolding of the enzyme proteins and augmentation of the enzyme activity. A sizeable literature has been published in the area of ultrasound–assisted processes for production of biochemical and biofuels (Gogate and Kabadi, 2009; Bundhoo and Mohee, 2018).

In this chapter, we have reported our studies in ultrasound–assisted xylitol production through fermentation of dilute acid (or pentose–rich) hydrolysate of sugarcane bagasse. Sugar cane is a major crop grown in India (> 300 million tons per year (Aradhye and Slette, 2016)) and very large amounts of bagasse are available from sugar factories. Being a lignocellulosic biomass, bagasse is a potential feedstock for fermentative bioprocesses. The hemicellulosic and cellulosic fraction of bagasse can be hydrolysed to fermentable sugars by dilute acid and enzymatic hydrolysis, respectively. The pentose–rich hydrolysate (comprising of xylose as the major component) can be fermented with suitable microbial cultures, e.g. *C. tropicalis*, to yield xylitol, which is a low calorie five–carbon sugar substitute for diabetic patients. With dual approach of coupling experimental results to a kinetic model, we have also attempted to gain physical insight into the enhancement of xylitol fermentation induced by sonication. Fitting of experimental profiles of xylitol fermentation to the kinetic model (which comprises of five ordinary differential equations) using Genetic Algorithm gives mechanistic accounts of the links between physical/chemical effects of ultrasound and cavitation and the biochemistry of xylitol fermentation.

## 6.2 Materials and methods

### 6.2.1 Dilute acid hydrolysis of sugarcane bagasse for hydrolysate

Sugarcane bagasse, obtained from local market in Guwahati, India, used in the present study had following composition: cellulose = 40.3 wt%, hemicellulose = 30.1 wt%, lignin = 27.1 wt%, and extractives = 2.5 wt% on dry basis. Sieved biomass (after washing and drying, fraction size < 0.6 mm) was used for dilute acid hydrolysis of hemicellulosic fraction in an autoclave (Model: LAC–5040S, Daihan Labtech Co. Ltd., South Korea) under following conditions: time = 30 min, 15 psi pressure, 2% v/v $H_2SO_4$, 120°C, solid:liquid ratio = 1:30 (w/v). pH of the reaction mixture was adjusted to neutral with CaO after hydrolysis, followed by separation of solid residue by filtration. The pentose–rich hydrolysate had following composition as determined by HPLC: glucose = 2.43 g/L, xylose = 8.68 g/L, arabinose = 1.23 g/L, furfural = 0.37 g/L, 5–HMF = 0.21 g/L and acetic acid = 1.05 g/L. Prior to fermentation, the hydrolysate was concentrated using a rotavapor (Make: BUCHI, Model: Rotavapor R–210) to adjust the xylose concentration to 20.7 g/L.

### 6.2.2 Growth and maintenance of *Candida tropicalis* culture

*C. tropicalis* MTCC 184 was procured from Microbial Type Culture Collection (MTCC), Chandigarh (India). The microbial cells (lyophilized) were recuperated in yeast extract, peptone and dextrose (YPD) medium and kept in a rotary shaker (Make: Lab Companion; Model: SI–300R) at 30°C, 150 rpm for 24 h. The recuperated cells of *C. tropicalis* were grown on agar slant and kept at 4°C. The cultures were sub–cultured every 30 days. YPD medium composition in 1 L of distilled water was as follows: yeast extract = 3 g, peptone = 10 g, dextrose = 20 g. The medium pH was adjusted to 6.0 ± 0.2 using 1 N HCl. By adding 15 g/L of agar in YPD medium, the agar plates and slants were prepared.

### 6.2.3 Inoculum preparation and fermentation medium composition

Cells from the agar slant were aseptically inoculated in 100 mL of inoculum medium (taken in 250 mL flask) and were incubated at 30°C, 150 rpm for 24 h in a rotary shaker. The composition of inoculum medium (autoclaved at 15 psi, 121°C, for 20 min, initial pH = 6.0) was as follows: xylose 10 g/L, peptone 10 g/L, yeast extract 3 g/L, and dextrose 20 g/L. The fermentation was performed in previously optimized (Chapter 5) composition of the medium and process parameters. Experiments of xylitol fermentation were carried out by shaking the fermentation mixture (50 mL of fermentation mixture in 150 mL Erlenmeyer flask) at rate of 150 rpm in an orbital incubator–shaker (Make: Lab Companion; Model: SI–300R). Samples from the fermentation broth were periodically withdrawn for monitoring progress of fermentation. Each independent experiment was carried out in triplicate and average values were obtained for analysis of substrate and product profiles in each experiment. The amount of aliquots of fermentation mixture taken for each sampling was 200 µL.

For fermentations using immobilized cells, three polyurethane (PU) foam cubes (optimized in previous chapter) with immobilized *C. tropicalis* were added to the fermentation broth.

### 6.2.4 Experimental set up for sonication

Ultrasound–assisted xylitol fermentation using *C. tropicalis* was carried out at optimum medium composition and optimum process parameters, determined in the statistical design of experiments in previous chapter. Sonication of the fermentation mixture for production of xylitol was carried out in an ultrasound bath (Elmasonic, Germany, Model: P–30H, Capacity: 2.8 L, Max Power: 80 W, Frequency: 37 kHz). A schematic diagram of experimental setup for ultrasonic irradiation of xylitol production is shown in Fig. 6.1.

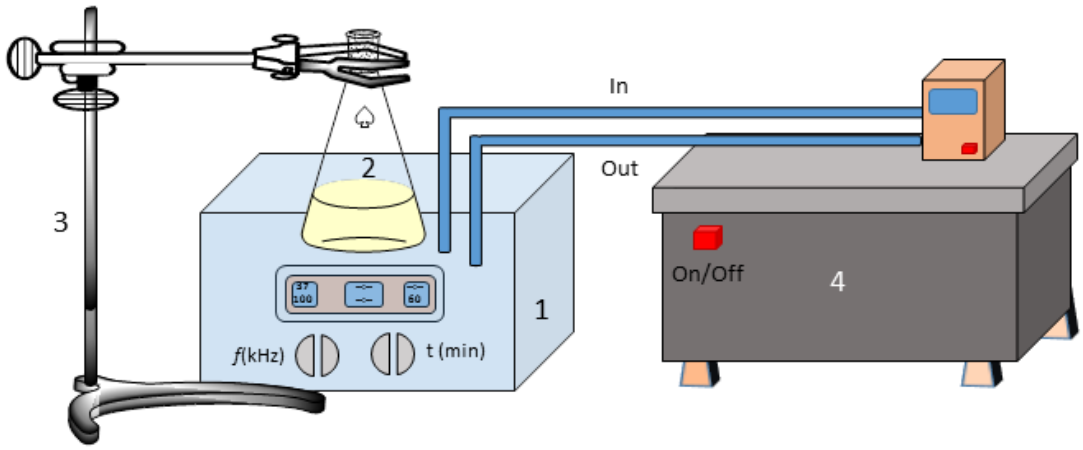


**Figure 6.1.** Schematic diagram of the experimental setup for sonication

*Notations:* (1) ultrasound bath; (2) fermentation flask; (3) flask stand system; (4) temperature controlled water circulation bath.

The pressure amplitude of ultrasound waves in the bath was determined as 150 kPa by calorimetric technique (Chakma and Moholkar, 2011). The actual acoustic power dissipation in the bath was determined calorimetrically as 18.58 W, which corresponded to acoustic intensity of 1.48 W/cm$^2$. Position of the fermentation flask was adjusted in the central region of ultrasound bath filled with water. The location of the flask was carefully kept same in all experiments to avoid artifacts due to spatial variation of acoustic intensity in the bath (Moholkar et al., 2000). The temperature of the fermentation mixture was maintained at 30±2$^o$C by replacing water in the sonication bath at regular periods. Control experiments of xylitol fermentation were carried out by shaking the fermentation mixture at rate of 150 rpm in an orbital incubator–shaker (Make: Lab Companion; Model: SI–300R). In test experiments, the fermentation mixture was subjected to a pre–optimized intermittent sonication at 10% duty cycle (i.e. 9 min of shaking at 150 rpm and 1 min of sonication for every 10 min of fermentation). Fermentations in both control and test experiments were carried out till 90% of initial xylose consumption. Aliquots of fermentation mixture were withdrawn for monitoring time profiles of biomass, glucose, xylose and xylitol. Each independent experiment was carried out in triplicate and six samples of fermentation

mixture (or aliquots of fermentation mixture) were obtained for analysis of substrate and product profiles in each experiment. The amount of aliquots of fermentation mixture taken for each sampling was 200 µL. The sampling frequency in control and test experiments (6 h in control and 3 h in test fermentations) was based on preliminary experiments in which we assessed the relative change of substrate and product concentrations in the successive samples drawn from fermentation mixture.

### 6.2.5 Morphological changes in *C. tropicalis* cells during sonication

Morphology of the *C. tropicalis* MTCC 184 cells may change during prolonged sonication. To assess this effect, flow cytometer analysis (BD Calibur™ Flow Cytometer, BD Biosciences, USA) of the aliquots of fermentation mixture at the end of fermentation were carried out in both control and test experiments. Relative changes in the FSC (Forward Scatter) and SSC (Side Scatter) of the cells depict the morphological changes. Forward–scattered light (FSC) is proportional to cell–surface area or size, and side–scattered light (SSC) is proportional to cell granularity or internal complexity.

### 6.2.6 Determination of viability of *C. tropicalis* cells

Viability of *C. tropicalis* MTCC 184 cells before and after ultrasound irradiation was assessed using methylene–blue staining (Painting and Kirsop, 1990). Samples of fermentation broth and methylene–blue solution (0.1% w/v) were mixed in the ratio of 1:1 and incubated for 5 min. *C. tropicalis* cells were counted on hemocytometer at 40× magnifications. The viability of cells was determined as follows:

$$\text{Viability (\%)} = \frac{\text{Number of live (unstained) cells}}{\text{Number of live (unstained) cells + Number of dead (stained) cells}} \times 100$$

### 6.2.7 Analytical methods

Optical density of *C. tropicalis* cells in fermentation mixture was assessed using a UV–Vis spectrophotometer (Make: Perkin Elmer, Model: LAMBDA 35) by measuring absorbance at 600

nm. Aliquots taken from the fermentation broth were centrifuged (6000 rpm for 10 min) followed by filtration with 0.45 µm membrane syringe filter. The concentrations of glucose, xylose and xylitol in the fermentation samples were assessed by HPLC (Make: Perkin Elmer, Series 200) using Hiplex–H column (Make: Varian, 300 mm × 5 µm × 4.6 mm) coupled with Refractive Index detector. The mobile phase was 0.005 M $H_2SO_4$ with flow rate of 0.6 mL/min at column temperature of 60°C.

### 6.2.8 Kinetic model for xylitol fermentation

Prior to description of the kinetic model, we would like to ponder over the rationale of correlating experimental results with the model. Our motivation for fitting of experimental data to a kinetic model was only to obtain a physical insight into the ultrasound assisted fermentation process, i.e. identification of the basic mechanism through which the fermentation process is intensified with sonication. Every theoretical model has certain limitations, and all assumptions made in the model may not be obeyed during experiments. This would obviously give quantitative deviations of simulated data from the experimental profiles. Moreover, the numerical methods used for fitting of the experimental data to model also has certain limitations due to which deviations may occur from theoretical predictions. Despite its limitations and constraints, most of the trends in the experimental profiles are captured by the model–predicted profiles. In the context of present study, where we attempt to identify and understand the links between physical/chemical effects of sonication and the intrinsic physiology of fermentation by analysing relative variations in the model parameters for control and test experiments, a qualitative match between experimental and model–predicted profiles is sufficient.

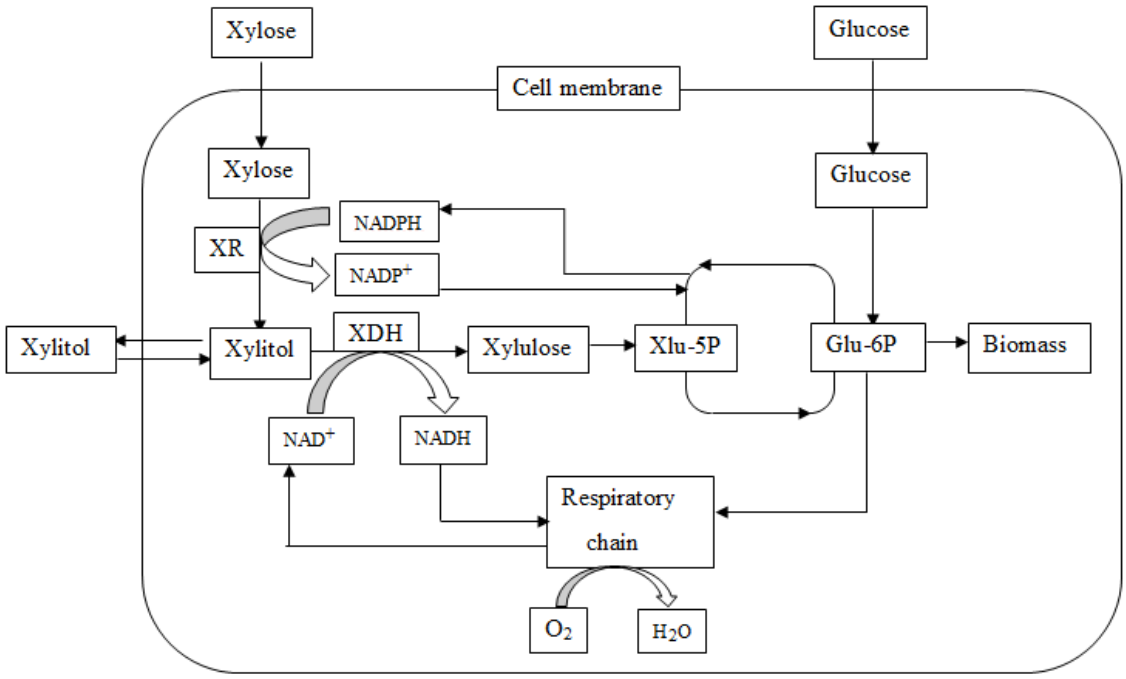


**Figure. 6.2.** Model representation of hydrolysate (viz. glucose and xylose) metabolism in *Candida tropicalis* (*Adopted from Tochampa et al., 2005*)

Tochampa et al. (2005) have reported a mathematical model for xylitol production by fermentation of glucose/xylose mixture using *C. mogii*, which has been adopted for present study. Main assumptions of this model are: (1) Initial pH of the fermentation mixture stays constant during fermentation, and has no significant effect on enzyme activity and cell growth; (2) All nutrients in the fermentation medium are in excess but for the carbon sources (glucose and xylose) in hydrolysate; (3) Major products of metabolism are biomass, xylitol and $CO_2$; (4) Under optimal growth conditions, the growth rate far exceeds the death rate (which implies that death rate of cells is not considered in model).

The equations of the fermentation model have been devised as follows: First step of xylose metabolism is its conversion to xylitol in yeast cells. The specific growth rate ( $\mu$ ) was modeled on the basis of contributions of glucose in the hydrolysate and xylitol inside the cell. Biomass growth rate in hydrolysate fermentation was modeled using Monod type kinetic equation as follows:

$$\frac{dX}{dt}=\left[\mu_g^{\max}\frac{C_g}{K_{s,g}+C_g}+\mu_{xit}^{\max}\frac{C_{xit}^{in}}{K_{s,xit}+C_{xit}^{in}}\cdot\frac{K_r}{K_r+C_g}\right]X \tag{6.1}$$

where: $X$ is the biomass concentration (g/L); $\mu_g^{\max}$ and $\mu_{xit}^{\max}$ are the maximum specific growth rates with sole substrate of glucose and xylitol ($h^{-1}$), respectively; $C_g$ and $C_{xit}^{in}$ are the concentrations of glucose in the medium and xylitol inside the cells (g/L), respectively; $K_{s,g}$ and $K_{s,xit}$ are the Monod saturation constants for glucose and xylitol (g/L), respectively; and $K_r$ is the repression constant by glucose (g/L).

Kilian et al. (1998) reported that in co–substrate fermentation, e.g. glucose/xylose mixture as substrate, the uptake of one sugar is affected by the presence of other sugars. This is because transport of the two substrates is facilitated by same diffusion system. Therefore, the specific uptake rates of glucose and xylose in fermentation are modeled by considering that carrier enzyme was competitively inhibited by the two substrates (Bisswanger, 2002). Considering this, the specific uptake rates of glucose and xylose in the hydrolysate fermentation are related to the biomass concentration as described in eqs. 6.2 and 6.3:

$$\frac{dC_g}{dt}=-\left[q_g^{\max}C_g\Big/\left\{C_g+K_{s,g}\left(1+C_{xy}/K_{i,xy}\right)\right\}\right]X \tag{6.2}$$

$$\frac{dC_{xy}}{dt}=-\left[q_{xy}^{\max}C_{xy}\Big/\left\{C_{xy}+K_{s,xy}\left(1+C_g/K_{i,g}\right)\right\}\right]X \tag{6.3}$$

where: $q_g^{\max}$ and $q_{xy}^{\max}$ are the maximum specific uptake rates of glucose and xylose ($h^{-1}$), respectively; $K_{i,xy}$ and $K_{i,g}$ are constants for inhibition of glucose uptake by xylose and inhibition of xylose uptake by glucose (g/L), respectively; $K_{s,g}$ is the Monod saturation constant for glucose (g/L); $C_{xy}$ and $C_g$ are concentrations of xylose and glucose in the medium (g/L), respectively.

The specific rate of formation of intracellular xylitol and the specific rate of uptake of xylose are correlated assuming that each mole of xylose taken up by the cell is quantitatively transformed to

xylitol. Rate of utilization of intracellular xylitol for biomass growth is correlated to the specific growth rate under assumption that xylitol utilization within the yeast cell preferentially results in generation of biomass. Thus, compared to biomass growth, maintenance term was insignificant. Stephanopoulos et al. (1998) reported that the rate of molecular diffusion can be determined from modified Fick's law. As per this law, the mass flux of xylitol across the membrane is directly proportional to: (1) the permeability coefficient of the membrane ($P_{xit}$); (2) the difference between intracellular and extracellular concentrations of xylitol ($C_{xit}^{in} - C_{xit}^{ex}$); and (3) the specific surface area of the cell ($a_{cell}$). Therefore, from mass balance, the time variations of intracellular ($C_{xit}^{in}$) and extracellular ($C_{xit}^{ex}$) xylitol concentrations are given by eqs. 6.4 and 6.5 as follows:

$$\frac{dC_{xit}^{in}}{dt} = \rho_X \left[ \frac{M_{w,xit}}{M_{w,xy}} q_{xy}^{\max} \frac{C_{xy}}{C_{xy} + K_{s,xy}\left(1 + C_g / K_{i,g}\right)} - \frac{\mu_{xit}}{Y_{X/xit}} - 3.6\times10^6 P_{xit} a_{cell} \left(C_{xit}^{in} - C_{xit}^{ex}\right) \right] \quad (6.4)$$

$$\frac{dC_{xit}^{ex}}{dt} = \left[ 3.6\times10^6 P_{xit} a_{cell} \left(C_{xit}^{in} - C_{xit}^{ex}\right) \right] X \quad (6.5)$$

where: where: $M_{w,xit}$ and $M_{w,xy}$ are the molecular weights of xylitol and xylose (g/mol), respectively; $\mu_{xit}$ is the specific growth rate on xylitol ($h^{-1}$); $Y_{X/xit}$ is the biomass yield on xylitol (g/g); $P_{xit}$ is permeability coefficient of the membrane (m/s), $\rho_X$ and $a_{cell}$ are mass density of the yeast cell (g/L) and the specific surface area of the cell ($m^2$/g), respectively.

The set of five ordinary differential equations (ODEs) listed above for variables $X$, $C_g$, $C_{xy}$, $C_{xit}^{in}$ and $C_{xit}^{ex}$ contain 11 kinetic parameters, viz. $\mu_g^{\max}$, $\mu_{xit}^{\max}$, $K_{s,g}$, $K_{s,xy}$, $K_{s,xit}$, $K_r$, $K_{i,xy}$, $K_{i,g}$, $q_g^{\max}$, $q_{xy}^{\max}$ and $P_{xit}$. These kinetic parameters are representatives of the physiology of xylitol fermentation. Fitting of the experimental profiles of $X$, $C_g$, $C_{xy}$, and $C_{xit}^{ex}$ to the above model equations using Genetic Algorithm Optimization Toolbox (GAOT) in MATLAB Version: R2015a (8.5.0.197613) yields the values of the kinetic parameters in the model. The experimental profiles in control and test experiments were fitted to the kinetic model by independently solving

the ordinary differential equations of the model for each parameter (using Runge–Kutta adaptive step size method as initial value problem) over entire fermentation period assuming continuous sampling. The numerical solution of the differential equation for each parameter was compared with corresponding experimental value only when the cumulative time periods in simulations corresponded with discrete experimental sampling periods (e.g. 3, 6, 9 h for test, and 6, 12, 18 h for control experiments), and the values of the kinetic parameters in the model were adjusted using Genetic Algorithm till the total RMS error between simulated and experimental values of the parameter was minimized. Therefore, the values of the kinetic parameters obtained from the modelling are representative of the physical factors influencing fermentation.

## 6.3 Results and discussion

### 6.3.1 Experimental results of ultrasound–assisted fermentation using *Candida tropicalis*

The time profiles of biomass, glucose, xylose, and xylitol concentrations in control (mechanical shaking) and test (mechanical shaking and intermittent sonication at 10% duty cycle) fermentations are depicted in Figs. 6.3A and B, respectively. It can be inferred from Fig. 6.3A that xylitol accumulation in the fermentation mixture was seen only after ~6 h after start of fermentation in control experiment. A plausible reason for this effect is glucose content of the hydrolysate. *C. tropicalis* cells preferentially consume glucose. In addition, xylose reductase (an enzyme associated with xylitol metabolism) is also inhibited by glucose. As a consequence, xylose utilization by *C. tropicalis* cells is delayed resulting in lag of xylitol formation. Xylose consumption by *C. tropicalis* cells is commensed after glucose concentration in the fermentation mixture is reduced to negligible level. Comparing the profiles in Figs. 6.3A and B, we can perceive that the lag period for xylose consumption (or xylitol formation) is much smaller (just 3 h) for the test experiments, as compared to control experiments. Reduction of the lag period of xylose consumption (or acceleration of xylitol formation) is attributed to faster glucose consumption in presence of sonication. Maximum xylitol concentration in the fermentation

mixture in both control and test experiments is seen when the xylose concentration reduces to low values (< 3 g/L).

Continuation of fermentation further results in consumption of xylitol by *C. tropicalis* cells for reproduction of the cells and cell maintenance. This implies that fermentation be stopped after drop of xylose concentration in the fermentation mixture below a prescribed level – typically < 10% of the initial value.

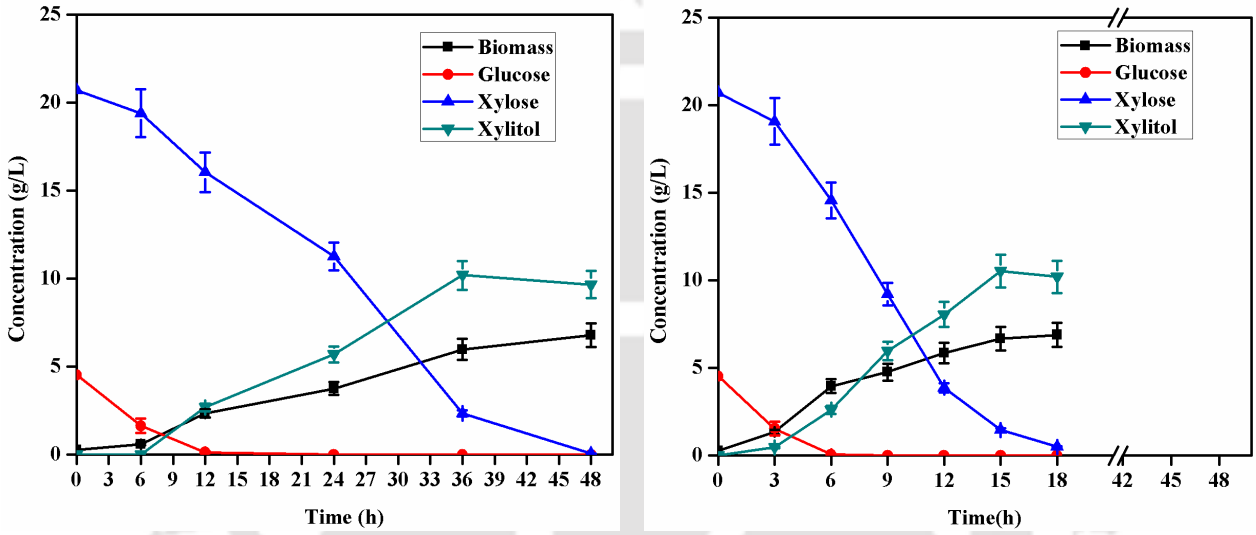


**Figure 6.3.** Time profiles of biomass, glucose, xylose and xylitol concentrations in hydrolysate fermentation by *C. tropicalis* in (A) control experiments (B) test experiments

The results of maximum xylitol fermentation in control and test experiments are summarized in Table 6.1. Sonication of fermentation mixture resulted in marginal rise in final xylitol yield. As seen from Table 6.1, final xylitol yield of 0.559 g/g and 0.611 g/g of xylose was obtained in control and test experiments, respectively, which essentially corresponded to 62% and 68% of the theoretical yield. Final biomass yield of 0.252 g/g in control experiments also increased marginally to 0.295 g/g (corresponding to 17% rise) in test experiments. Although final yields of xylitol and biomass increased marginally with sonication, the kinetics of fermentation showed sharp rise with sonication. The uptake rate of xylose increased from 0.506 g/L h in control

experiment to 1.149 g/L h in test experiment, and the volumetric productivity of xylitol also augmented from 0.283 g/L h in control experiment to 0.702 g/L h in test experiment (Table 6.1). Thus, sonication of fermentation mixture resulted in 2× rise in rate of xylose consumption, and 2.5× rises in rate of xylitol production. Another distinct effect of sonication on xylitol fermentation was in terms of enhanced kinetics. As evident from the profiles depicted in Figs. 6.3A and B (and also Table 6.1), time required for consumption of >90% of initial xylose reduced from 36 h in control experiments to just 15 h in test experiments.

Comparative analysis with literature on xylitol synthesis from lignocellulosic biomass (specifically, the xylitol yield and productivity) is given as follows: Hernández et al. (2016) studied supplementation of maltose, sucrose, cellobiose or glycerol with the sugarcane straw hemicellulosic hydrolyzate and their effect as co–substrates on xylitol production by *C. guilliermondii* FTI 20037. Sucrose (10 g/L) and glycerol (0.7 g/L) supplementation increased the xylose uptake rate by 8.9% and 6.9% (viz. 1.11 and 1.09 g/L h), respectively. For only sucrose as the additive, final xylitol concentration of 36.11 g/L (12.88% increment) and xylitol productivity of 0.75 g/L h (8.69% increment) was obtained. Guamán–Burneo et al. (2015) have studied xylitol production from sugarcane bagasse hemicellulose hydrolysates as a substrate using *Candida tropicalis* and *Cyberlindnera galapagoensis* f.a., sp. nov. yeasts. The xylitol yield and productivity of 0.67 g/L and 0.38 g/L h and 0.64 g/L and 0.33 g/L h with *Candida tropicalis* and *galapagoensis* f.a., sp. nov., respectively was obtained. Kumar et al. (2015) studied fermentation of xylose–rich and glucose–rich hydrolysate of sugarcane bagasse using the thermo–tolerant yeast *Kluyveromyces sp.* IIPE453. The yeast could grow on xylose–rich hydrolysate at 50°C with the biomass yield and maximum specific growth rate of 0.58 g/g and 0.13 $h^{-1}$, respectively. Xylitol yield of 0.61 g/g total reducing sugars was obtained in 112 h (corresponding to xylitol productivity of 0.13 g/L h), with sugar consumption rate of 0.23 g/L h. *Kluyveromyces sp.* IIPE453 with pure xylose as substrate resulted in xylitol and biomass yield of 0.65 g/g and 0.43 g/g, respectively (Kumar et al., 2009). de Mancilha and Karim (2003) reported the xylitol

production from corn stover hydrolysate using *C. mogii*. The xylitol and biomass yields of 0.41 and 0.24 g/g, respectively, were obtained. Carvalho et al. (2004) have reported the xylitol production from sugarcane bagasse hemicellulose hydrolysate using *C. guilliermondii* in a stirred tank reactor. xylitol yield of 0.81 g/g was obtained in 120 h of fermentation with productivity of 0.40 g/L h. Sampaio et al. (2008) have reported xylitol production using D–xylose as substrate under microaerobic conditions with xylitol yield and productivity of 0.76 g/g and 1.0 g/L h, respectively.

**Table 6.1.** Fermentation parameters evaluated at maximum xylitol production in hydrolysate fermentation using *C. tropicalis* under control experiments and test experiments

| Kinetic parameters | Control experiments | Test experiments |
|---|---|---|
| Fermentation time (h) to reach maximum xylitol concentration | 36 | 15 |
| Residual xylose at max. xylitol concentration (g/L) | 2.344 ± 0.46 | 1.458 ± 0.39 |
| Maximum biomass concentration (g/L) | 5.979 ± 0.59 | 6.679 ± 0.67 |
| Maximum xylitol concentration (g/L) | 10.196 ± 0.82 | 10.529 ± 0.94 |
| Biomass yield, $Y_{X/(g+xy)}$ (g/g) | 0.252 | 0.295 |
| Xylitol yield, $Y_{xit/xy}$ (g/g) | 0.559 | 0.611 |
| Specific growth rate, $\mu$ (1/h) | 0.038 | 0.043 |
| Specific uptake rate of xylose, $q_{xy}$ (g/g h) | 0.085 | 0.172 |
| Specific formation rate of xylitol, $q_{xit}$ (g/g h) | 0.047 | 0.105 |
| Volumetric uptake rate of xylose, $Q_{xy}$ (g/L h) | 0.506 | 1.149 |
| Volumetric productivity of xylitol, $Q_{xit}$ (g/L h) | 0.283 | 0.702 |

### 6.3.2 Kinetic analysis of xylitol fermentation using *Candida tropicalis* cells

Simulated time profiles of the four parameters, viz. glucose, xylose, biomass and xylitol, in control and test experiments are shown in Figs. 6.4 and 6.5, respectively.

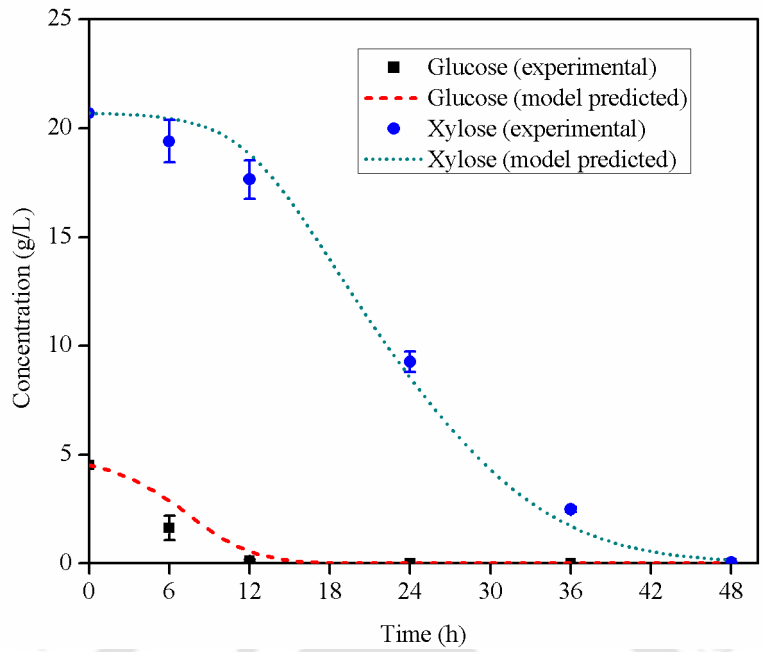


(A)

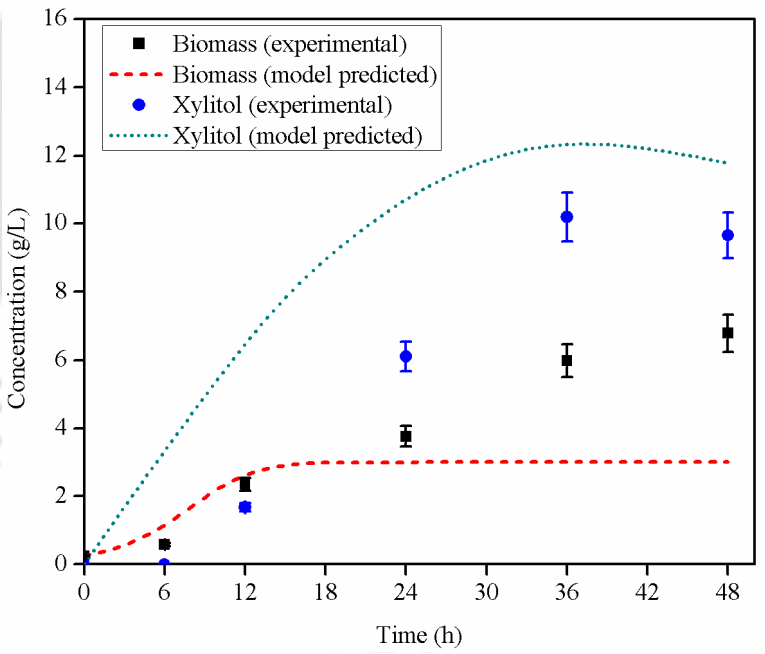


(B)

**Figure 6.4.** Experimental and simulated time profiles of (A) glucose and xylose (B) biomass and xylitol concentrations in hydrolysate fermentation by *C. tropicalis* under control experiments

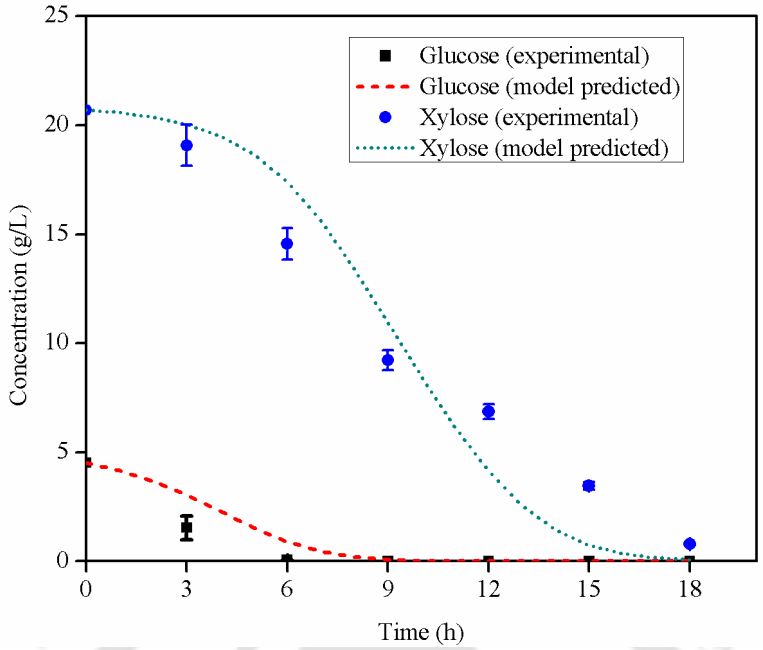


(A)

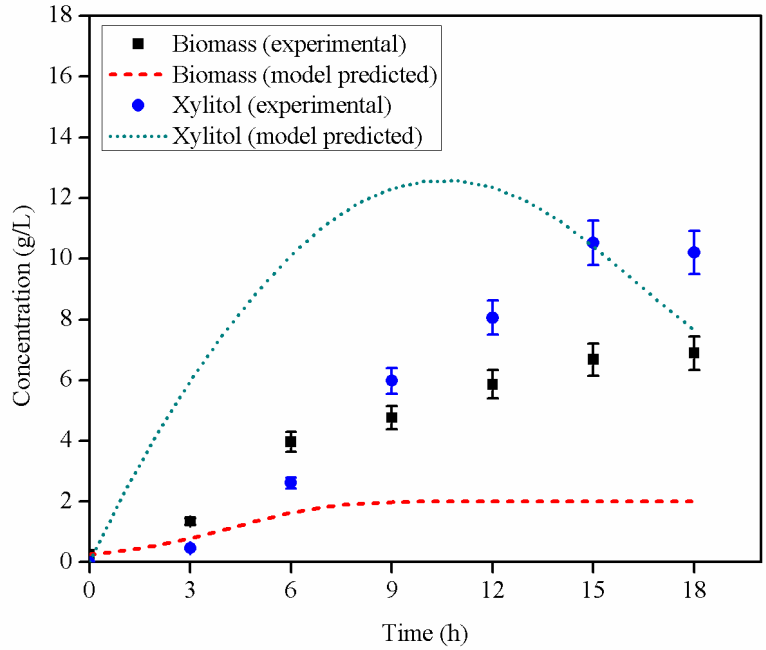


(B)

**Figure 6.5.** Experimental and simulated time profiles of (A), glucose and xylose (B) biomass and xylitol concentrations in hydrolysate fermentation by *C. tropicalis* under test experiments

The values of kinetic parameters for xylitol fermentation in control and test experiments are shown in Table 6.2. Typical trends in different kinetic parameters in control and test experiments can be identified as follows:

(1) Greater values of maximum specific growth rate on glucose ( $\mu_g^{max}$ ) and on xylitol ( $\mu_{xit}^{max}$ ) were obtained in test experiments, as compared to control experiments. Moreover, the Monod saturation constants for xylose ( $K_{s,xy}$ ), glucose ( $K_{s,g}$ ) and xylitol ( $K_{s,xit}$ ) also reduced in the test experiments. Reduction in Monod saturation constants, or the substrate concentration required to achieve half of maximum specific growth rate of cell mass, is essentially a consequence of enhanced enzyme–substrate affinity. This might be attributed to morphological changes in the secondary structure of intracellular enzymes involved in xylitol metabolism, which results in unfolding of enzyme structure and exposure of inner hydrophobic groups comprising substrate binding sites.

(2) Permeability of the membranes of *C. tropicalis* cells also undergoes distinct change due to strong micro–turbulence generated by sonication, as evident from permeability coefficient, $P_{xit}$. As seen from Table 6.2, permeability coefficient in test experiments shows 20× rise than control experiments. Higher membrane permeability augments the diffusion of substrates, nutrients and metabolite products across the cell membrane. This is manifested in terms of rise in $\mu_g^{max}$, $\mu_{xit}^{max}$ and the biomass yield $Y_{X/(g+xy)}$ in test experiments. Higher membrane permeability assists faster metabolism (or faster substrate utilization) due to faster transport of substrates across the cell membrane. Moreover, lesser bulk concentration of substrates is required to achieve maximum specific growth rates.

(3) Larger values of $q_{xy}^{max}$ and $q_g^{max}$ (i.e. maximum specific uptake rate of xylose and glucose, respectively) also represent enhanced transport of substrates in test experiments under influence of sonication.

(4) Sonication of the fermentation mixture also results in reduction of substrate inhibition of enzymes in xylose metabolism, as depicted by higher values of inhibition constants for glucose uptake ($K_{i,xy}$) and xylose uptake ($K_{i,g}$). Concurrent rise in enzyme–substrate affinity and reduction of enzyme inhibition has synergistic effect on xylitol metabolism, which is manifested in terms of enhanced kinetics.

(5) The value of the repression constant by glucose, $K_r$ remains unaltered in both control and test experiments. This is an intrinsic physiological property of the cell, which is not influenced by physical and chemical effects of ultrasound and cavitation.

**Table 6.2**. Model kinetic parameters fitted for xylitol production using *C. tropicalis* under control experiments and test experiments

| Model fitted kinetic parameters | Control experiments | Test experiments |
|---|---|---|
| Maximum specific growth rate on glucose, $\mu_g^{max}$ (1/h) | 0.584 | 0.769 |
| Maximum specific growth rate on xylitol, $\mu_{xit}^{max}$ (1/h) | 0.276 | 0.393 |
| Maximum specific uptake rate of xylose, $q_{xy}^{max}$ (g/g h) | 0.502 | 1.998 |
| Maximum specific uptake rate of glucose, $q_g^{max}$ (g/g h) | 2.457 | 3.997 |
| Monod saturation constant for xylose, $K_{s,xy}$ (g/L) | 7.003 | 5.002 |
| Monod saturation constant for glucose, $K_{s,g}$ (g/L) | 5.004 | 4.005 |
| Monod saturation constant for xylitol, $K_{s,xit}$ (g/L) | 14.295 | 12.876 |
| Inhibition constant of glucose uptake by xylose, $K_{i,xy}$ (g/L) | 9.014 | 11.999 |
| Inhibition constant of xylose uptake by glucose, $K_{i,g}$ (g/L) | 0.201 | 0.299 |
| Repression constant by glucose, $K_r$ (g/L) | 0.178 | 0.141 |
| Permeability coefficient of the membrane, $P_{xit}$ (m/s) | $1.67 \times 10^{-10}$ | $3.40 \times 10^{-9}$ |

### 6.3.3 Analysis on change in morphology and viability of *C tropicalis* cells

The results of flow cytometry analysis of *C. troplicalis* cells in control and test fermentations are depicted in Figs. 6.6A & C and 6.6B & D, respectively. It could be inferred from Figs. 6.6A and B, >96% of the acquisition dot points fall in lower left (LL) quadrant. This implies that exposure to sonication does not alter the SSC and FSC of microbial cells. The internal complexity and morphology of the cells remain unchanged after exposure to ultrasound. Moreover, methylene blue–staining and cell counting (as depicted in Figs. 6.7A and B) confirm that negligible cell death occurred during exposure to sonication, which resulted in > 80% cell viability in both control and test fermentations.

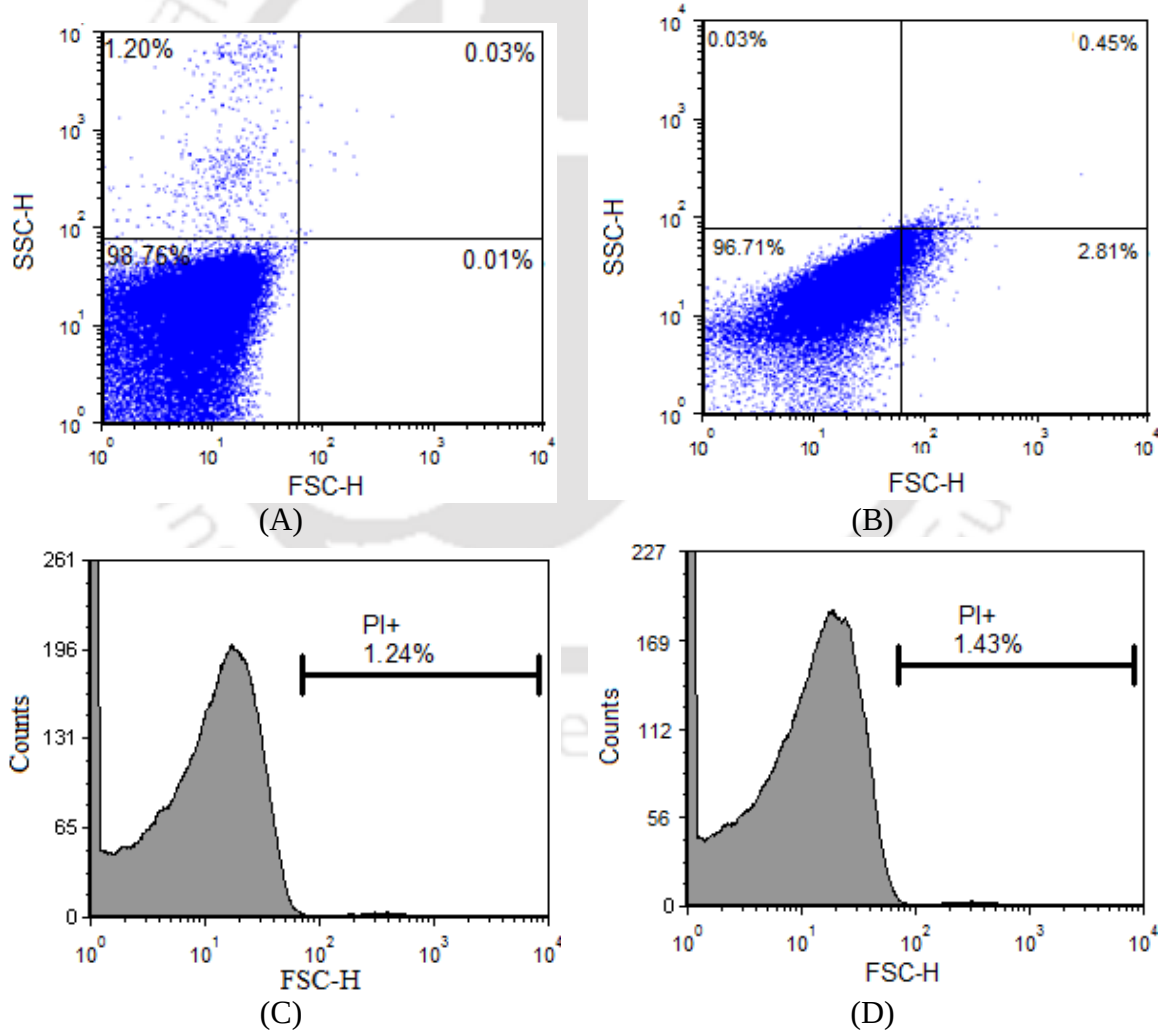

**Figure 6.6.** Flow cytometry analysis for morphological changes in *C. tropicalis* MTCC 184: (A) and (B) Acquisition dot plots (FSC vs SSC) in control and test experiments, respectively; (C) and (D) Histogram plots (counts vs FSC) in control and test experiments, respectively

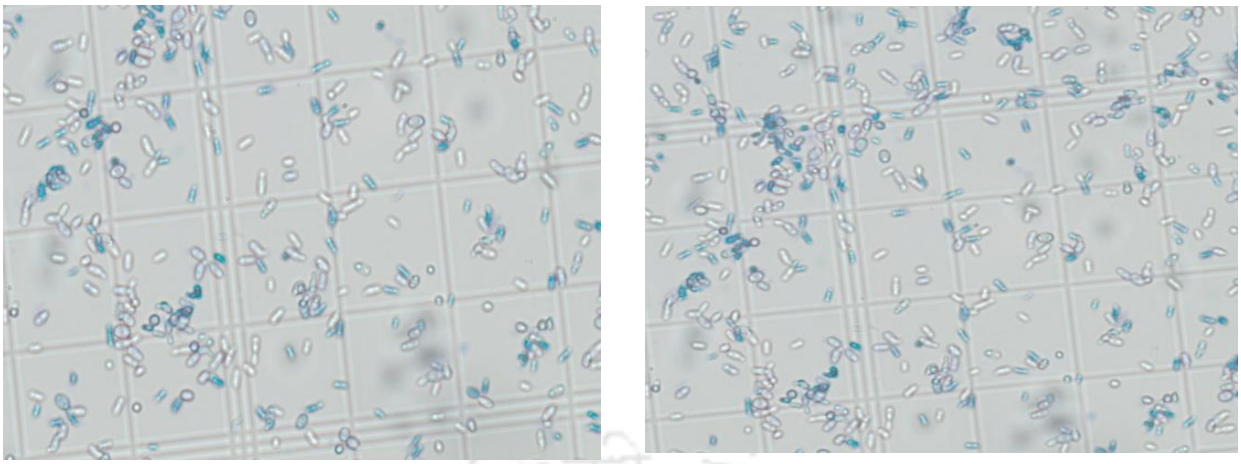

(A) (B)

**Figure 6.7.** Methylene blue stained micrographs of *C. tropicalis* cells at the end of fermentation in: (A) control experiments and (B) test experiments

### 6.3.4 Experimental results of ultrasound–assisted fermentation using immobilized *C. tropicalis* cells

The time profiles of biomass, glucose, xylose, and xylitol concentrations in control (mechanical agitation) and test (mechanical agitation and intermittent sonication at 10% duty cycle) fermentations are depicted in Figs. 6.8A and B, respectively. As shown in Fig. 6.8A, for control experiment, there was a lag to xylitol accumulation. This is attributed to presence of glucose in the hydrolysate, which is preferentially consumed by *C. tropicalis* cells. Moreover, glucose is also a known inhibitor of xylose reductase, an enzyme associated with xylitol metabolism. As a consequence, the rate of xylose utilization by *C. tropicalis* cells is retarded.

Xylose metabolism (or xylose consumption) is triggered after completion of glucose consumption. As compared to the control experiment, the xylose consumption (or xylitol production) commences sooner (3 h since start of experiment) in the test experiment, as seen in Fig. 6.8B. This is essentially a result of accelerated glucose consumption in presence of sonication. Another interesting feature of xylitol fermentation in control and test conditions (as revealed from Figs. 6.8A and B) is that xylitol concentration in fermentation mixture peaks at the moment of complete xylose consumption. If the fermentation is allowed to proceed further, the *C.*

*tropicalis* cells consume accumulated xylitol for reproduction of the cells and cell maintenance. This necessitates that fermentation be terminated after xylose concentration in the fermentation mixture is reduced below a prescribed level – typically < 10% of the initial value.

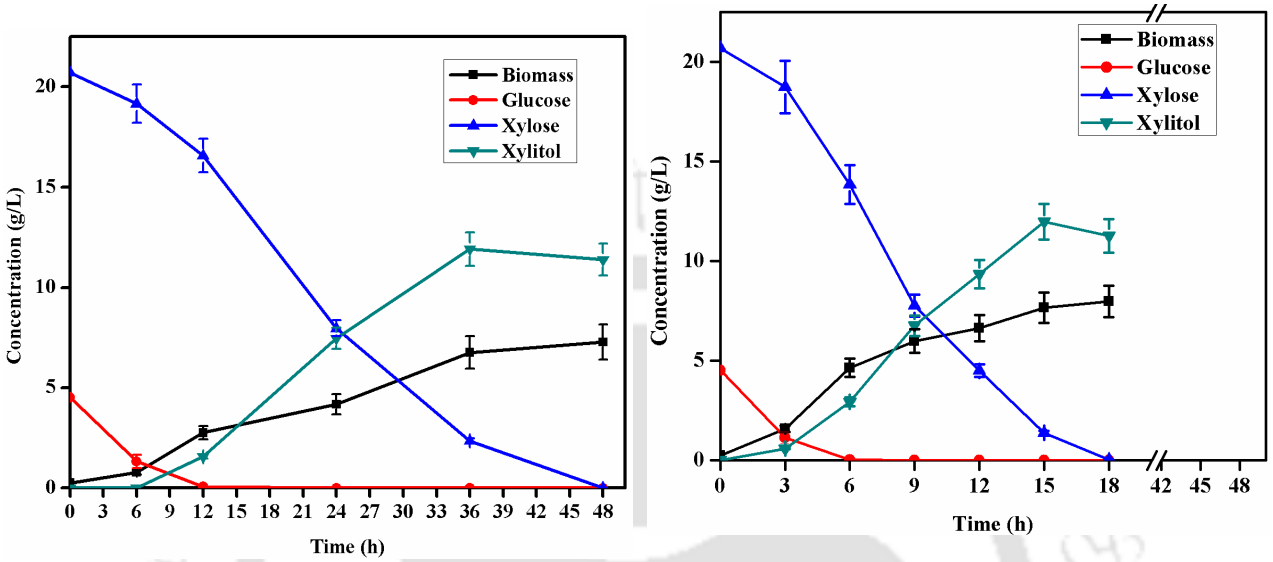


(A) (B)

**Figure 6.8.** Time profiles of biomass, glucose, xylose and xylitol concentrations in hydrolysate fermentation by immobilized *C. tropicalis* under (A) control experiments and (B) test experiments

Final results of xylitol fermentation in control and test experiments are given in Table 6.3. As shown in Table 6.3, the xylitol yield of 0.649 g/g and 0.664 g/g of xylose was obtained in control and test experiments, respectively, which essentially corresponded to 71% and 73% of the theoretical yield. The biomass yield of 0.284 g/g in control experiments also increased marginally to 0.329 g/g (corresponding to 16% rise) in test experiments. However, a marked rise of 2.4× was seen in xylose consumption and xylitol production in the test experiment. As seen from Figs. 6.8A and B (and also Table 6.3), the time required for consumption of >90% of initial xylose reduced from 36 h in control experiments to just 15 h under sonication in test experiments.

**Table 6.3.** Fermentation parameters evaluated at maximum xylitol production in control and test experiments using immobilized *C. tropicalis* cells

| Parameters | Control experiments | Test experiments |
|---|---|---|
| Maximum xylitol concentration (g/L) | 11.817 ± 0.834 | 11.967 ± 0.897 |
| Residual xylose at max. xylitol concentration (g/L) | 2.348 ± 0.117 | 1.378 ± 0.096 |
| Biomass yield, $Y_{X/(g+xy)}$ (g/g) | 0.284 | 0.329 |
| Xylitol yield, $Y_{xit/xy}$ (g/g) | 0.649 | 0.664 |
| Specific growth rate, $\mu$ (1/h) | 0.040 | 0.048 |
| Specific uptake rate of xylose, $q_{xy}$ (g/g h) | 0.075 | 0.157 |
| Specific formation rate of xylitol, $q_{xit}$ (g/g h) | 0.049 | 0.104 |
| Volumetric uptake rate of xylose, $Q_{xy}$ (g/L h) | 0.510 | 1.201 |
| Volumetric productivity of xylitol, $Q_{xit}$ (g/L h) | 0.331 | 0.798 |
| Fermentation time (h) to reach maximum xylitol concentration | 36 | 15 |

### 6.3.5 Kinetic analysis of xylitol fermentation using immobilized *C. tropicalis* cells

Simulated time profiles of the four parameters, viz. glucose, xylose, biomass and xylitol, in control and test experiments are shown in Figs. 6.9 and 6.10, respectively.

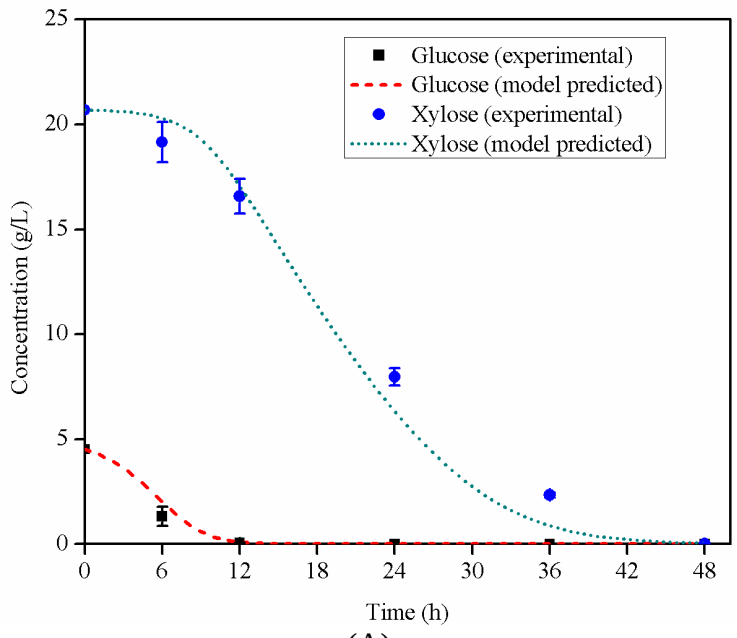


(A)

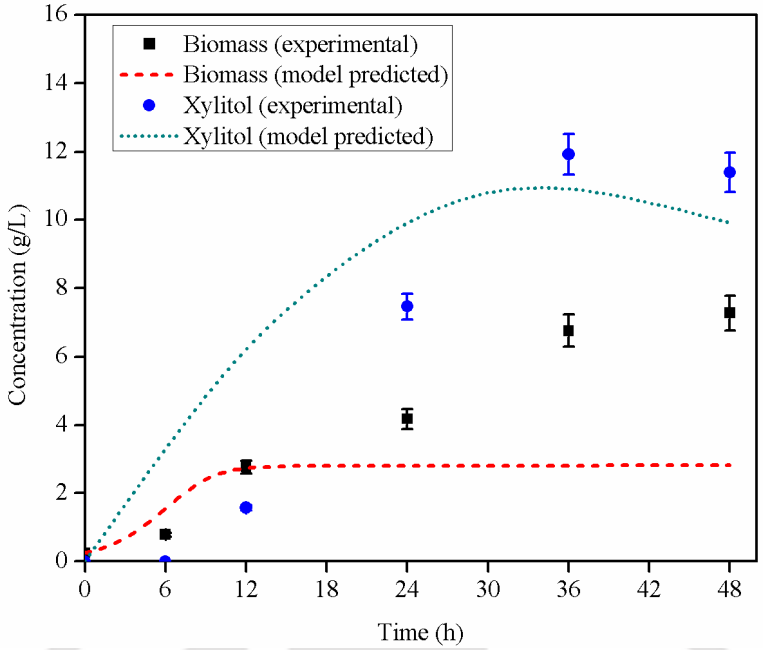


(B)

**Figure 6.9.** Experimental and simulated time profiles of (A) glucose and xylose (B) biomass and xylitol concentrations in hydrolysate fermentation using immobilized *C. tropicalis* in control experiments

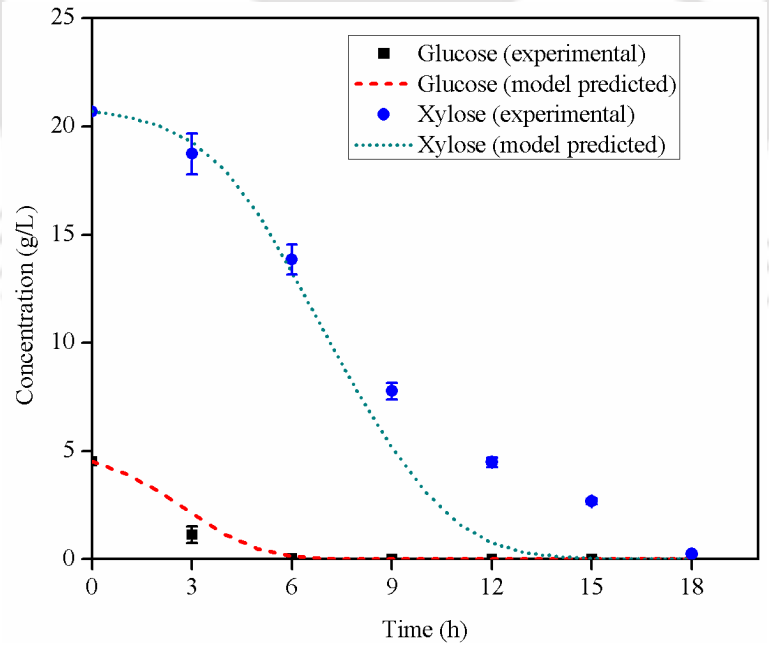


(A)

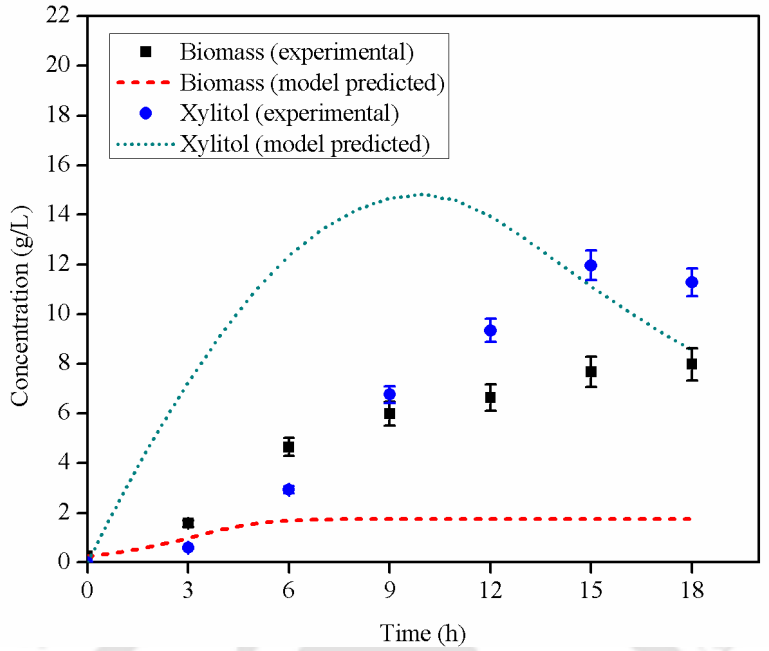


(B)

**Figure 6.10.** Experimental and simulated time profiles of: (A) glucose and xylose, (B) biomass and xylitol concentrations in hydrolysate fermentation using immobilized *C. tropicalis* in test experiments

The values of kinetic parameters for xylitol fermentation in control and test experiments are shown in Table 6.4. As compared to the control experiments, the maximum specific growth rate on glucose ( $\mu_g^{max}$ ) and on xylitol ( $\mu_{xit}^{max}$ ) increased; whereas the Monod saturation constants for xylose ( $K_{s,xy}$ ), glucose ( $K_{s,g}$ ) and xylitol ( $K_{s,xit}$ ) decreased in the test experiments. The reduction in Monod saturation constants (which is the substrate concentration required to achieve half of maximum specific growth rate of cell mass) essentially represents enhanced enzyme–substrate affinity. This could be attributed to morphological changes in the secondary structure of intracellular enzymes involved in xylitol metabolism. Strong micro–turbulence generated by sonication also induces change in membrane permeability (represented by permeability coefficient, $P_{xit}$ ). As seen from Table 6.4, the value of $P_{xit}$ in test experiments shows 10–fold rise as compared to control experiments. Rise in membrane permeability results in efficient diffusion of substrates, nutrients and metabolite products across the cell membrane. Rise in $\mu_g^{max}$ , $\mu_{xit}^{max}$ and

the biomass yield $Y_{X/(g+xy)}$, which represent faster metabolism (or faster substrate utilization) are attributed to faster transport of substrates across the cell membrane due to which lesser bulk concentration of substrates is required to achieve maximum specific growth rates. Enhanced transport of substrates due to sonication in test experiments is also represented by rise in maximum specific uptake rate of xylose ($q_{xy}^{max}$) and glucose ($q_{g}^{max}$). Sonication of the fermentation mixture also results in reduction of the inhibition effects of the substrates. Increase in the values of inhibition constants for glucose uptake ($K_{i,xy}$) and xylose uptake ($K_{i,g}$) are representative of the reduced inhibition effects. Simultaneous rise in enzyme–substrate affinity and reduced inhibition effect have synergistic effect on xylitol metabolism that results in faster kinetics. The repression constant by glucose, $K_r$ remains practically constant in both control and test experiments. This is an intrinsic physiological property of the cell, which remains unaffected by the physical and chemical effects induced by sonication.

**Table 6.4.** Model kinetic parameters for xylitol fermentation in control and test experiments

| Model fitted kinetic parameters | Control experiments | Test experiments |
|---|---|---|
| Maximum specific growth rate on glucose, $\mu_g^{max}$ (1/h) | 0.698 | 0.856 |
| Maximum specific growth rate on xylitol, $\mu_{xit}^{max}$ (1/h) | 0.304 | 0.432 |
| Maximum specific uptake rate of xylose, $q_{xy}^{max}$ (g/g h) | 0.497 | 2.334 |
| Maximum specific uptake rate of glucose, $q_g^{max}$ (g/g h) | 2.972 | 4.999 |
| Monod saturation constant for xylose, $K_{s,xy}$ (g/L) | 5.705 | 4.014 |
| Monod saturation constant for glucose, $K_{s,g}$ (g/L) | 4.516 | 3.016 |
| Monod saturation constant for xylitol, $K_{s,xit}$ (g/L) | 13.667 | 11.178 |
| Inhibition constant of glucose uptake by xylose, $K_{i,xy}$ (g/L) | 9.887 | 11.997 |
| Inhibition constant of xylose uptake by glucose, $K_{i,g}$ (g/L) | 0.189 | 0.398 |
| Repression constant by glucose, $K_r$ (g/L) | 0.117 | 0.128 |
| Permeability coefficient of the membrane, $P_{xit}$ (m/s) | $2.37 \times 10^{-10}$ | $2.56 \times 10^{-9}$ |

***Comparison with previous literature:*** Previous authors who applied sonication for enhancement of different fermentation systems have reported similar effect of sonication on physiology of the fermentation, as observed in present study. Dikshit et al. (2018) have studied sonication enhanced dihydroxyacetone (DHA) synthesis from crude glycerol using both free and immobilized cells of *G. oxydans.* Results of their study revealed that sonication of the reaction mixture at 37 kHz, and 20% duty cycle induced conformational changes in the secondary structure of intracellular proteins, which augmented the activity of intracellular enzyme. This assisted in faster metabolism of crude glycerol and enhanced productivity of DHA. Enhancement of activity of intracellular enzymes due to conformational changes in secondary structure leading to enhancement in activity is also reported by Agarwal et al. (2016) for biodesulfurization process using *R. rhodochrous* and dibenzothiophene as substrate. Singh et al. (2015a,b) studied ultrasound–assisted ethanol synthesis from fermentation of *P. hysterophorus* using *S. cerevisiae.* Sonication was revealed to enhance cellular transport of substrates, nutrients and products. Moreover, sonication also augmented enzyme–substrate affinity and reduced inhibition effects of substrate and products. The death rate of the cells showed marked reduction during sonication due to dilution of the toxic substances. Singh et al. (2015b) have reported significant enhancement of both enzymatic hydrolysis of delignified biomass as well as fermentation of the hydrolysate with application of sonication. Enhancement in enzyme–substrate affinity with concurrent reduction in substrate/product inhibition is also reported by Khanna et al. (2012) and Sarma et al. (2017) for fermentation of crude glycerol using *C. pasteurianum*. These effects were manifested in terms of ~ 2× enhancement in kinetics of crude glycerol fermentation. Dai et al. (2017) investigated the effect of ultrasound on growth, morphological change, membrane permeability and alcohol tolerance of *S. cerevisiae* in the optimum growth phase in ethanol fermentation. They also observed that sonication enhanced membrane permeability of *S. cerevisiae,* resulting in faster intracellular and extracellular material exchange. Chu et al. (2000) have reported improved gentamicin productivity by *M. echinospora* with sonication at 25 kHz. The structure of the cell

wall of the bacterial species was modified during sonication with enhanced permeability resulting in enhanced release of gentamicin from cell in the broth.

### 6.3.6 Analysis on change in morphology and viability of *C tropicalis* cells

The results of flow cytometry analysis of in control (mechanical shaking) and test (ultrasound–treated) fermentations are depicted in Figs. 6.11A & B and 6.11C & D, respectively. As revealed in Figs. 6.11A and C, >98% of the acquisition dot points fall in lower left (LL) quadrant. This essentially confirms that SSC and FSC of the *C. tropicalis* cells remain practically unaltered after sonication. Thus, the internal complexity and morphology of the cells remain unchanged after exposure to ultrasound, or in other words, no noticeable adverse impact of sonication is seen on the yeast cells. Moreover, methylene–blue staining and cell counting (as shown Fig. 6.12) confirmed that negligible cell death appeared due to ultrasound treatment and the cell viability was >80% in both control and test samples. This result is yet another confirmation that sonication did not have any adverse impact on morphology of yeast cells.

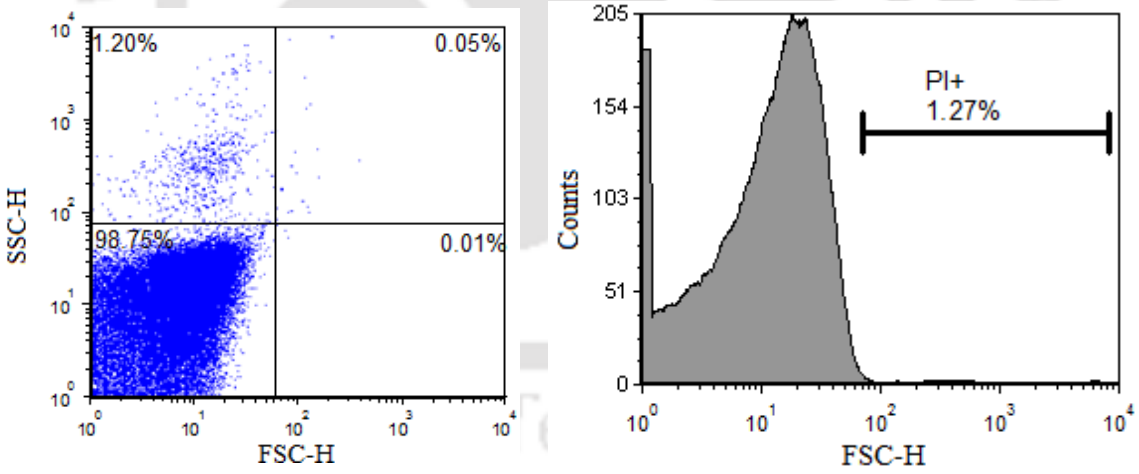


(A) (B)

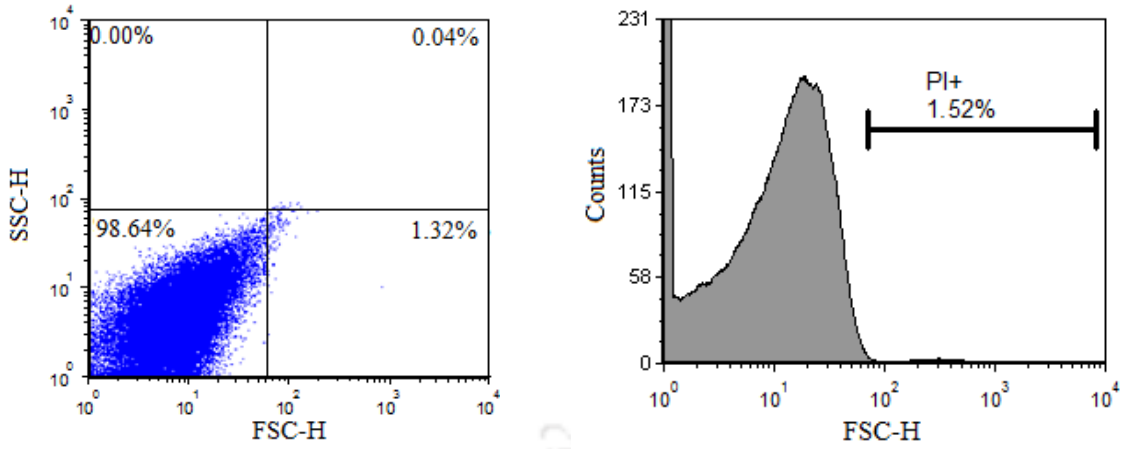


(C) (D)

**Figure 6.11**. Flow cytometry analysis for morphological changes in immobilized *C. tropicalis* cells: (A) and (C) Acquisition dot plots (FSC vs SSC) in control and test experiments, respectively; (B) and (D) Histogram plots (counts vs FSC) in control and test experiments, respectively

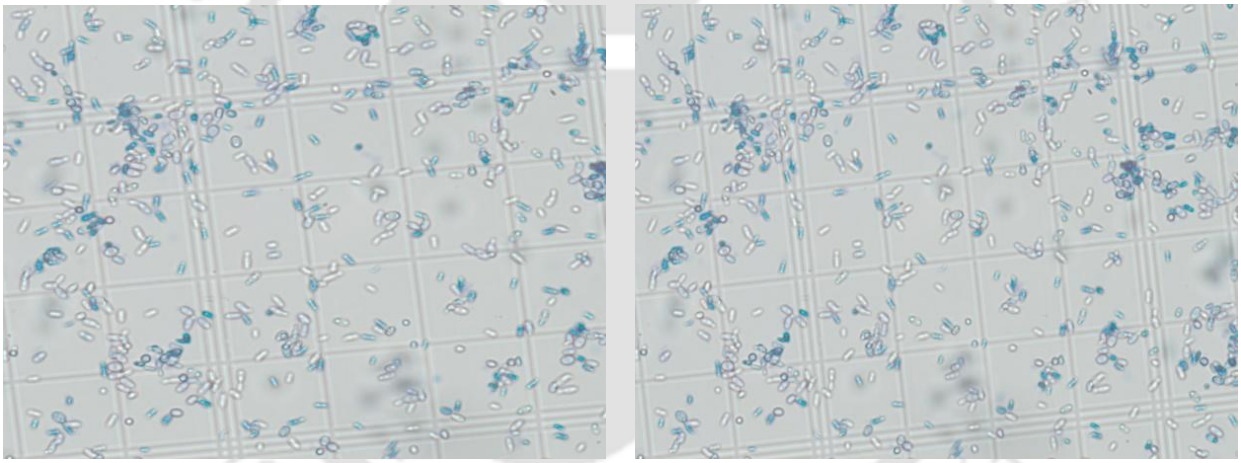

(A) (B)

**Figure 6.12.** Micrographs of methylene–blue stained *C. tropicalis* cells at the end of fermentation: (A) control experiments and (B) test experiments

## 6.4 Conclusions

The present study has investigated enhancement effect of sonication on xylitol fermentation and has also attempted to gain mechanistic insight into the process. Although sonication of fermentation mixture resulted in marginal (17–20%) rise in final xylitol and biomass yields, the kinetics of the fermentation showed drastic enhacement. 2.5× enhancement in xylitol productivity

and 2× rise in specific uptake rate of xylose was achieved under ultrasound assisted fermentation. Comparative assessment of the parameters of kinetic model for fermentation under test and control condition revealed that sonication promoted the uptake and utilization of substrates for cell growth and increased enzyme–substrate affinity. The inhibition effect of substrate was also reduced with sonication. 10–20× enhancement in permeability of cell membrane caused faster diffusion of substrates, nutrients and metabolite products across the cell membrane which resulted in faster xylose metabolism and enhanced kinetics of fermentation.

**References**

Agarwal, M., Dikshit, P.K., Bhasarkar, J.B., Borah, A.J., Moholkar, V.S., 2016. Physical insight into ultrasound–assisted biodesulfurization using free and immobilized cells of *Rhodococcus rhodochrous* MTCC 3552. Chem. Eng. J. 295, 254–267.

Aradhye, A., Slette, J., 2016. Sugar Annual, Global Agricultural Information Network (GAIN Report No. IN6057, 26 April 2016), USDA Foreign Agricultural Service, India.

Arrizon, J., Mateos, J.C., Sandoval, G., Aguilar, B., Solis, J., Aguilar, M.G., 2012. Bioethanol and xylitol production from different lignocellulosic hydrolysates by sequential fermentation. J. Food Process Eng. 35(3), 437–454.

Berłowska, J., Pielech–Przybylska, K., Balcerek, M., Dziekońska–Kubczak, U., Patelski, P., Dziugan, P., Kręgiel, D., 2016. Simultaneous saccharification and fermentation of sugar beet pulp for efficient bioethanol production. BioMed. Res. Int.

Beszédes, S., László, Z., Horváth, Z.H., Szabó, G., Hodúr, C., 2011. Comparison of the effects of microwave irradiation with different intensities on the biodegradability of sludge from the dairy– and meat–industry. Bioresour.Technol. 102, 814–821.

Bharadwaja, S.T.P., Singh, S., Moholkar, V.S., 2015. Design and optimization of a sono–hybrid process for bioethanol production from *Parthenium hysterophorus*. J. Taiwan Inst. Chem. Eng. 51, 71–78.

Bisswanger, H., 2002. Multiple equilibria. Enzyme kinetics: principles and methods, 5–50.

Bochu, W., Lanchun, S., Jing, Z., Yuanyuan, Y., Yanhong, Y., 2003. The influence of $Ca^{2+}$ on the proliferation of *Saccharomyces cerevisiae* and low ultrasonic on the concentration of $Ca^{2+}$ in the *Saccharomyces cerevisiae* cells. Colloids Surf. B. 32(1), 35–42.

Bundhoo, Z.M., Mohee, R., 2018. Ultrasound–assisted biological conversion of biomass and waste materials to biofuels: A review. Ultrason. Sonochem. 40, 298–313.

Camargo, D., Sene, L., Variz, D.I.L.S., de Almeida Felipe, M.D.G., 2015. Xylitol bioproduction in hemicellulosic hydrolysate obtained from sorghum forage biomass. Appl. Biochem. Biotechnol. 175(8), 3628–3642.

Carvalho, W., Santos, J.C., Canilha, L., e Silva, J.B.A., Felipe, M.G., Mancilha, I.M., Silva, S.S., 2004. A study on xylitol production from sugarcane bagasse hemicellulosic hydrolysate by Ca–alginate entrapped cells in a stirred tank reactor. Process Biochem. 39(12), 2135–2141.

Chakma, S., Moholkar, V.S., 2011. Mechanistic features of ultrasonic desorption of aromatic pollutants. Chem. Eng. J. 175, 356–367.

Chu, J., Li, B., Zhang, S., Li, Y., 2000. On–line ultrasound stimulates the secretion and production of gentamicin by *Micromonospora echinospora*. Process Biochem. 35(6), 569–572.

Dai, C., Xiong, F., He, R., Zhang, W., Ma, H., 2017. Effects of low–intensity ultrasound on the growth, cell membrane permeability and ethanol tolerance of *Saccharomyces cerevisiae*. Ultrason. Sonochem. 36, 191–197.

Da Silva, S.S., Afschar, A.S., 1994. Microbial production of xylitol from D–xylose using *Candida tropicalis*. Bioprocess Eng. 11(4), 129–134.

de Mancilha, I.M., Karim, M.N., 2003. Evaluation of ion exchange resins for removal of inhibitory compounds from corn stover hydrolyzate for xylitol fermentation. Biotechnol. Prog. 19(6), 1837–1841.

Dikshit, P.K., Kharmawlong, G.J., Moholkar, V.S., 2018. Investigations in sonication–induced intensification of crude glycerol fermentation to dihydroxyacetone by free and immobilized *Gluconobacter oxydans*. Bioresour. Technol. 256, 302–311.

Hernández–Pérez, A.F., Costa, I.A.L., Silva, D.D.V., Dussan, K.J., Villela, T.R., Canettieri, E.V., Carvalho Jr, J.A., Neto, T.S., Felipe, M.G.A., 2016. Biochemical conversion of sugarcane straw hemicellulosic hydrolyzate supplemented with co–substrates for xylitol production. Bioresour. Technol. 200, 1085–1088.

Gogate, P.R., Kabadi, A.M., 2009. A review of applications of cavitation in biochemical engineering/biotechnology. Biochem. Eng. J. 44(1), 60–72.

Guamán–Burneo, M.C., Dussán, K.J., Cadete, R.M., Cheab, M.A., Portero, P., Carvajal–Barriga, E.J., da Silva, S.S., Rosa, C.A., 2015. Xylitol production by yeasts isolated from rotting wood in the Galápagos Islands, Ecuador, and description of *Cyberlindnera galapagoensis* fa, sp. nov. Antonie Van Leeuwenhoek, 108(4), 919–931.

Khanna, S., Jaiswal, S., Goyal, A., Moholkar, V.S., 2012. Ultrasound enhanced bioconversion of glycerol by *Clostridium pasteurianum*: a mechanistic investigation. Chem. Eng. J. 200–202, 416–425.

Khanna, S., Jaiswal, S., Goyal, A., Moholkar, V.S., 2013. Mechanistic investigation of ultrasonic enhancement of glycerol bioconversion by immobilized *Clostridium pasteurianum* on silica support. Biotechnol. Bioeng. 110, 1637–1645.

Kilian, S.G., Van Uden, N., 1988. Transport of xylose and glucose in the xylose–fermenting yeast *Pichia stipitis*. Appl. Microbiol. Biotechnol. 27(5–6), 545–548.

Kumar, S., Dheeran, P., Singh, S.P., Mishra, I.M., Adhikari, D.K., 2015. Bioprocessing of bagasse hydrolysate for ethanol and xylitol production using thermotolerant yeast. Bioprocess Biosyst. Eng. 38(1), 39–47.

Kumar, S., Singh, S.P., Mishra, I.M., Adhikari, D.K., 2009. Ethanol and xylitol production from glucose and xylose at high temperature by *Kluyveromyces sp*. IIPE453. J. Ind. Microbial. Biotechnol. 36(12), 1483.

Lunelli, F.C., Sfalcin, P., Souza, M., Zimmermann, E., Pra, V.D., Foletto, E.L., Jahn, S.L., Kuhn, R.C., Mazutti, M.A., 2014. Ultrasound–assisted enzymatic hydrolysis of sugarcane bagasse for the production of fermentable sugars. Biosyst. Eng. 124, 24–28.

Moholkar, V.S., Sable, S.P., Pandit, A.B., 2000. Mapping the cavitation intensity in an ultrasonic bath using the acoustic emission. AIChE J. 46(4), 684–694.

Nikolić, S., Mojović, L., Rakin, M., Pejin, D., Pejin, J., 2010. Ultrasound–assisted production of bioethanol by simultaneous saccharification and fermentation of corn meal. Food Chem. 122(1), 216–222.

Painting, K., Kirsop, B., 1990. A quick method for estimating the percentage of viable cells in a yeast population, using methylene blue staining. World J. Microbiol. Biotechnol. 6(3), 346–347.

Sampaio, F.C., Chaves–Alves, V.M., Converti, A., Passos, F.M.L., Coelho, J.L.C., 2008. Influence of cultivation conditions on xylose–to–xylitol bioconversion by a new isolate of *Debaryomyces hansenii*. Bioresour. Technol. 99(3), 502–508.

Sarma, S., Anand, A., Dubey, V.K., Moholkar, V.S., 2017. Metabolic flux network analysis of hydrogen production from crude glycerol by *Clostridium pasteurianum*. Bioresour. Technol. 242, 169–177.

Singh, S., Bharadwaja, S.T.P., Yadav, P.K., Moholkar, V.S., Goyal, A., 2014. Mechanistic investigation in ultrasound–assisted (alkaline) delignification of *Parthenium hysterophorus* biomass. Ind. Eng. Chem. Res. 53, 14241–14252.

Singh, S., Sarma, S., Agarwal, M., Goyal, A., Moholkar, V.S., 2015a. Ultrasound enhanced ethanol production from *Parthenium hysterophorus*: a mechanistic investigation. Bioresour. Technol. 188, 287–294.

Singh, S., Agarwal, M., Sarma, S., Goyal, A., Moholkar, V.S., 2015b. Mechanistic insight into ultrasound induced enhancement of simultaneous saccharification and fermentation of *Parthenium hysterophorus* for ethanol production. Ultrason. Sonochem. 26, 249–256.

Singh, S., Agarwal, M., Bhatt, A., Goyal, A., Moholkar, V.S., 2015c. Ultrasound enhanced enzymatic hydrolysis of *Parthenium hysterophorus*: A mechanistic investigation. Bioresour. Technol. 192, 636–645.

Subhedar, P.B., Gogate, P.R., 2014. Enhancing the activity of cellulase enzyme using ultrasonic irradiations. J. Mol. Catal. B. Enzym. 101, 108–114.

Subhedar, P.B., Babu, N.R., Gogate, P.R., 2015. Intensification of enzymatic hydrolysis of waste newspaper using ultrasound for fermentable sugar production. Ultrason. Sonochem. 22, 326–332.

Sulaiman, A.Z., Ajit, A., Yunus, R.M., Chisti, Y., 2011. Ultrasound–assisted fermentation enhances bioethanol productivity. Biochem. Eng. J. 54(3), 141–150.

Sulaiman, A.Z., Ajit, A., Chisti, Y., 2013. Ultrasound mediated enzymatic hydrolysis of cellulose and carboxymethyl cellulose. Biotechnol. Prog. 29, 1448–1457.

Suresh, K., Ranjan, A., Singh, S., Moholkar, V.S., 2014. Mechanistic investigations in sono–hybrid techniques for rice straw pretreatment. Ultrason. Sonochem. 21, 200–207.

Suslick, K.S., 1990. Sonochem. Sci. 247, 1439–1445.

Sutkar, V.S., Gogate, P.R., 2009. Design aspects of sonochemical reactors: techniques for understanding cavitational activity distribution and effect of operating parameters. Chem. Eng. J. 155(1–2), 26–36.

Tizazu, B.Z., Moholkar, V.S., 2018. Kinetic and thermodynamic analysis of dilute acid hydrolysis of sugarcane bagasse. Bioresour. Technol. 250, 197–203.

Tochampa, W., Sirisansaneeyakul, S., Vanichsriratana, W., Srinophakun, P., Bakker, H.H., Chisti, Y., 2005. A model of xylitol production by the yeast *Candida mogii*. Bioprocess Biosyst. Eng. 28(3), 175–183.

Ur–Rehman, S., Mushtaq, Z., Zahoor, T., Jamil, A., Murtaza, M.A., 2015. Xylitol: a review on bioproduction, application, health benefits, and related safety issues. Crit. Rev. Food Sci. Nutr. 55(11), 1514–1528.

Velmurugan, R., Incharoensakdi, A., 2016. Proper ultrasound treatment increases ethanol production from simultaneous saccharification and fermentation of sugarcane bagasse. RSC Adv. 6(94), 91409–91419.

# CHAPTER 7

# OVERVIEW AND SUGGESTIONS FOR FUTURE WORK

# CHAPTER 7

# OVERVIEW AND SUGGESTIONS FOR FUTURE WORK

## 7.1 Overview of the Thesis Work

The present thesis work has addressed the issue of optimization, modelling and intesnsification of the bioprocess for conversion of sugarcane bagasse into a value–added product, xylitol. The main aim of the work has been tackled in a step–by–step approach for optimization and modelling of dilute acid hydrolysis of sugarcane bagasse to obtain fermentable pentose rich (xylose) hydrolysate as a substrate for subsequent fermentation. Optimization of the medium components and process parameters for xylitol production from the hydrolysate using immobilized *Candida tropicalis* on PU foam, modelling, and intensification of the fermentation of pentose rich (xylose) hydrolysate for xylitol production have been done. The microorganism used in the study was a native isolate *Candida tropicalis*. Fermentation of sugarcane bagasse hemicellulosic hydrolysate for the production of xylitol was carried out in batch mode. Following to medium components and process parameters optimization, intensification the fermentation process for the conversion of sugarcane bagasse hemicellulose hydrolysate into xylitol has been carried out using ultrasound irradiation of the fermentation mixture.

In this final Chapter, we present an overview of the main results of the preceding chapters. These results, when viewed and analysed at a glance, give an idea of potential of the bioprocess of sugarcane bagasse to xylitol.

In Chapter 3, statistical optimization of process parameters for dilute acid hydrolysis of sugarcane bagasse for maximum xylose yield is reported. Prior to statistical optimization, the chemical compostion of sugarcane bagasse and the effect of solid to liquid ratio on xylose yield were analysed. The process parameters considered for optimization were hydrolysis temperature, acid concentration (or acid load) and hydrolysis time. Optimum levels of these parameters were determined by Box Behnken design (BBD) method of optimization. The optimum values of the process parameters for dilute acid hydrolysis of sugarcane bagasse were: Temperature = 120$^{o}$C, acid concentration = 2% v/v, and hydrolysis time = 33 min. At optimum conditions, a maximum xylose concentration of 8.68 g/L corresponding to 85% hemicellulose fraction of sugarcane bagasse was obtained. The composition of other monomeric sugars (glucose = 2.46 g/L, arabinose = 1.25 g/L) and inhibitory products (acetic acid = 1.02 g/L, furfural = 0.37 g/L, and 5–HMF = 0.22 g/L) in the hydrolysate has also been analyzed under optimal conditions of dilute sulfuric acid hydrolysis of sugarcane bagasse.

In Chapter 4, we have addressed the kinetic and thermodynamic features of dilute acid (2% v/v $H_2SO_4$, 1:30 w/v) hydrolysis of sugarcane bagasse. Time profiles of xylose formation in range of 100°–130°C and treatment period of 0–120 min have been analysed with modified biphasic Saeman model. Generation of glucose, arabinose and inhibitory products (furfural, 5–HMF and acetic acid) have also been analysed. Easy–to–hydrolyse fraction of hemicellulose increased with temperature. Activation energies for hydrolysis and xylose degradation were 60.3 and 83.4 kJ/mol, respectively. Thermodynamic analysis revealed $\Delta H$ = 57.06 kJ/mol and $\Delta S$ = –1.05 kJ/mol for hydrolysis. Moreover, xylose formation is thermodynamically more favoured ($\Delta G$ = 468.53 kJ/mol) than degradation ($\Delta G$ = 482.17 kJ/mol).

In Chapter 5, we have presented optimization of medium components and process parameters xylitol production from sugarcane bagasse using *C. tropicalis* MTCC 184 immobilized on PU foam. Plackett–Burman design revealed that out of seven medium components, 4 medium components, viz. yeast extract, $MgSO_4 \cdot 7H_2O$, $KH_2PO_4$ and $(NH_4)_2SO_4$; as significant

components. These medium components were further optimized using central composite design (CCD) method to find their optimum values. Optimization of process parameters, viz. temperature, initial pH, shaking speed and substrate (xylose) concentration, has been done at the optimized values of medium components. Optimum values of these parameters for maximum xylitol yield = 0.65 g/g of xylose are: yeast extract = 5.78 g/L, $(NH_4)_2SO_4$ = 3.22 g/L, $KH_2PO_4$ = 0.58 g/L, $MgSO_4 \cdot 7H_2O$ = 0.57 g/L and temperature = 29.3$^oC$, initial pH = 6.2, shaking speed = 151 rpm and initial xylose concentration = 20.9 g/L. Medium components provide essential growth factors and utilizable potassium, phosphate, nitrogen, sulphur sources. Activity of xylose reductase in metabolic pathway is stabilized and augmented by $Mg^{2+}$.

In Chapter 6, we have addressed ultrasound–assisted xylitol production through fermentation of dilute acid (pentose–rich) hydrolysate of sugarcane bagasse using free and immobilized cells of *Candida tropicalis*. Sonication of fermentation mixture at optimum conditions (optimized in Chapter 5) was carried out in ultrasound bath (37 kHz and 10% duty cycle). Time profiles of substrate and product in control (mechanical shaking) and test (mechanical shaking + sonication) fermentations were fitted to kinetic model using Genetic Algorithm (GA) optimization. Maximum xylitol yield of 0.56 g/g and 0.61 g/g of xylose was achieved in control and test fermentations, respectively, in free cells of *C. tropicalis*. Moreover, the xylitol yield of 0.65 g/g and 0.66 g/g of xylose was obtained in control and test experiments, respectively in immobilized cells of *C. tropicalis*, which essentially corresponded to 71% and 73% of the theoretical yield.

Although sonication of fermentation mixture resulted in marginal (17–20%) rise in final xylitol and biomass yields, the kinetics of the fermentation showed drastic enhacement. 2.5× enhancement in xylitol productivity and 2× rise in specific uptake rate of xylose was achieved under ultrasound assisted fermentation. Comparative assessment of the parameters of kinetic model for fermentation under test and control condition revealed that sonication promoted the uptake and utilization of substrates for cell growth and increased enzyme–substrate affinity. The inhibition effect of substrate was also reduced with sonication. 10–20× enhancement in

permeability of cell membrane caused faster diffusion of substrates, nutrients and metabolite products across the cell membrane, which resulted in faster xylose metabolism and enhanced kinetics of fermentation. Flow cytometry analysis of in control (mechanical shaking) and test (ultrasound–treated) fermentations was crried out. The results of flow cytometry essentially confirmed that SSC and FSC of the *C. tropicalis* cells remain practically unaltered after sonication. Thus, the internal complexity and morphology of the cells remain unchanged after exposure to ultrasound, or in other words, no noticeable adverse impact of sonication is seen on the yeast cells.

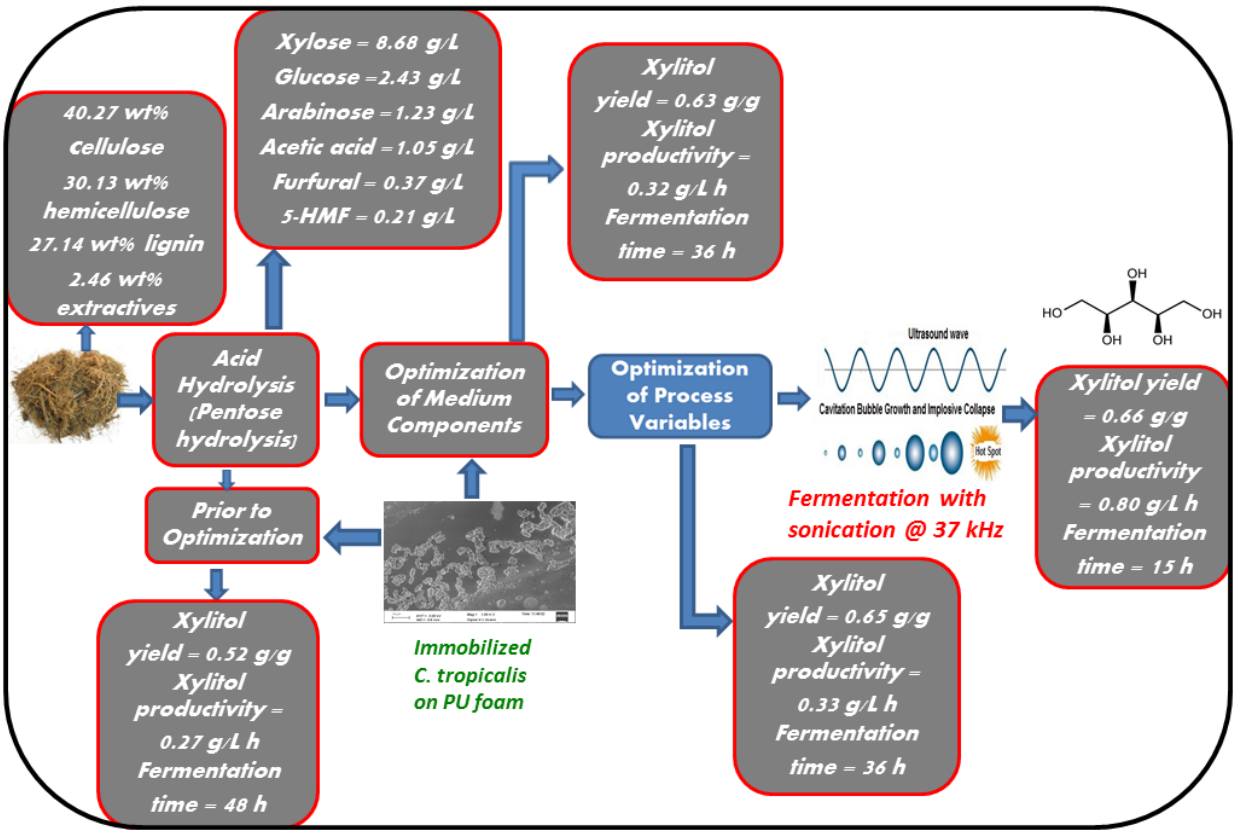


**Figure 7.1.** Schematic representation of the major results of the thesis work

## 7.2 Suggestions for Future Work

The present thesis work has presented optimization, modelling and intensification of the biochemical process for converting sugarcane bagasse into a value–added product, xylitol using

immobilized cells of *Candida tropicali* on PU foam on laboratory scale. The results of this thesis work can give more guidlines for development of a large-scale process. Some suggestions to work further in this area can be given as follows:

1. All the experiments in this thesis were conducted in laboratory scale. These studies can be conducted in large–scale process by using bioreactors.
2. Extraction of enzyme xylose reductase (XR) from *C. tropicalis* cells, purification and immobilization can be done for further experiments without immobilizing the whole cells.
3. The microorganism used in the present thesis is a commericial native strain. This strain can be replaced with a genetically modified strain for better yield and productivity.
4. The ultrasound enhanced processes need further optimization with higher frequencies. The ultrasound frequency for present study was kept constant (37 kHz), experiments with different frequencies will be able to ascertain individual contribution of ultrasound to the process.

भारतीय प्रौद्योगिकी संस्थान गुवाहाटी
Indian Institute of Technology Guwahati

# RESEARCH OUTPUTS

## Publications in International Journals

1. Tizazu, B.Z., Moholkar, V.S., 2018. Kinetic and thermodynamic analysis of dilute acid hydrolysis of sugarcane bagasse. Bioresour. Technol. 250, 197–203.
2. Tizazu, B.Z., Roy, K., Moholkar, V.S., 2018. Mechanistic Investigations in Ultrasound–Assisted Xylitol Fermentation. Ultrason. Sonochem. 48, 321–328.
3. Tizazu, B.Z., Roy, K., Moholkar, V.S., 2018. Ultrasonic Enhancement of Xylitol Production from Sugarcane Bagasse using Immobilized *Candida tropicalis* MTCC 184. Bioresour. Technol. 268, 247–258.
4. Tizazu, B.Z., Moholkar, V.S. Ultrasound–Assisted Bio–xylitol Synthesis: Review and Analysis (*Under preparation*).

## Conference Presentations

1. Optimization of Dilute Sulphuric Acid Hydrolysis of Sugarcane bagasse for Enhanced Xylose Recovery using RSM. 2$^{nd}$ International conference on ensurning sustainable development throught research in science and technology 2017, June, 8$^{th}$–10$^{th}$, Adama Science and Technology Universtiy, Ethiopia. (Oral presentations)
2. Kinetic Model Analysis of Dilute Acid Hydrolysis of Sugarcane bagasse for Xylose Production. 2$^{nd}$ National conference on emerging technologies (NCETCPDIC–2017), July, 18$^{th}$–20$^{th}$, 024, 224–230 Defence University, Ethiopia. (Oral presentations)

3. Effect of Glucose Addition on Xylose Fermentation for Xylitol Production by *Candida tropicalis* MTCC 184, in Research Conclave 2018 organized by Indian Institute of Technology Guwahati, Guwahati, Assam, India March, 2018. (Oral presentations)
4. Medium Optimization for Bioproduction of Xylitol from Sugarcane Bagasse Hemicellulosic Hydrolysate using Immobilized *Candida Tropicalis* MTCC 184 on PU Foam, in Reflux 2018 organized by Department of Chemical Engineering Indian Institute of Technology Guwahati, Guwahati, Assam, India March, 2018. (Oral presentations)
5. Kinetic Model Analysis of Dilute Acid Hydrolysis of Sugarcane bagasse for Xylose Production. 3rd Annual research conference on Science, Technology and Innovation for transforming economies, 2017, June, 8th–9th, Addis Ababa Science and Technology University, Ethiopia. (Poster presentation)

**APPENDIX:** Growth profile curve ($A_1$) and standard calibration plots ($A_2$ and $A_3$)

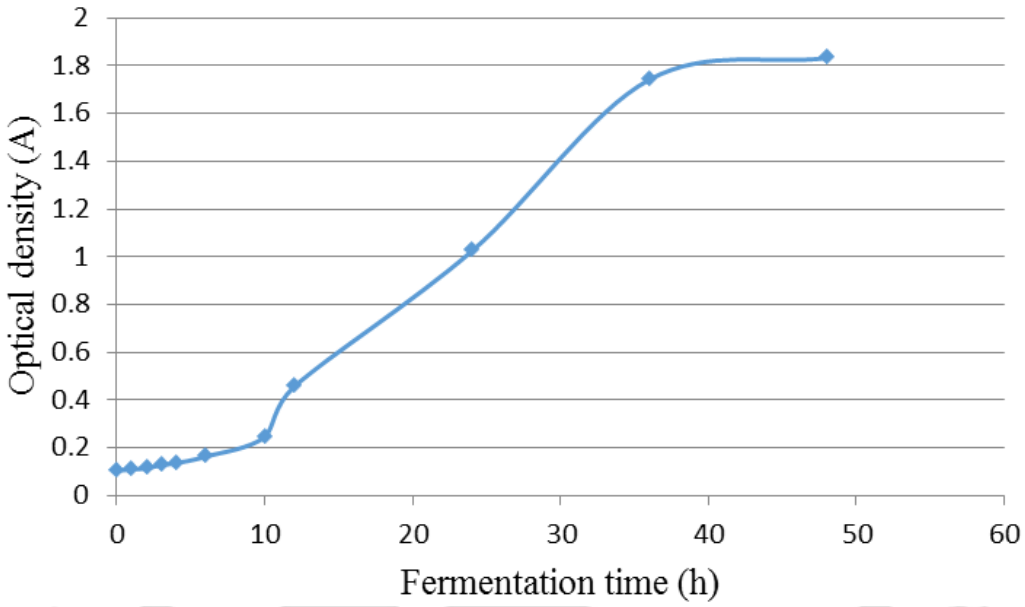


Figure $A_1$. Growth profile curve *C. tropicalis*

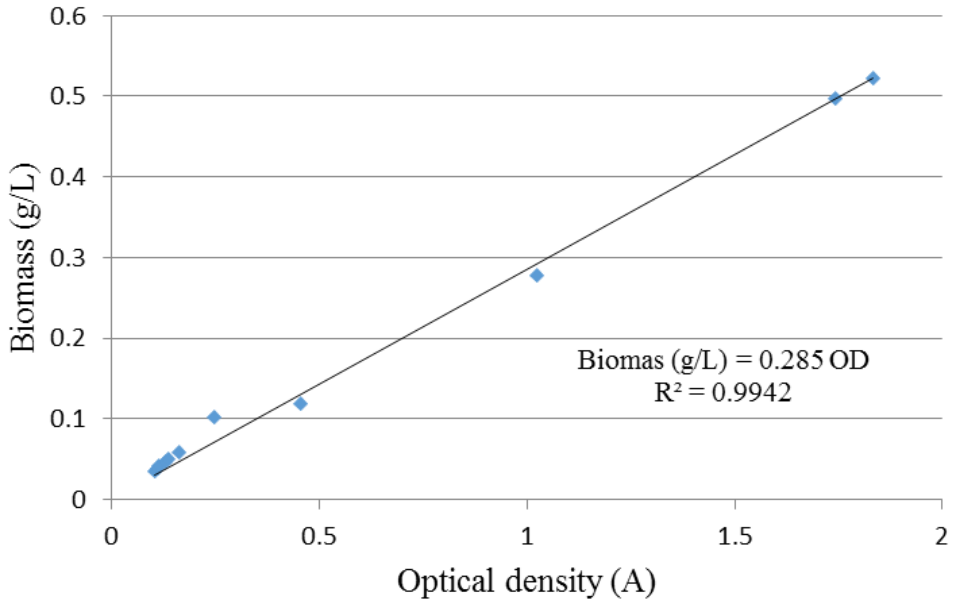


Figure $A_2$. Standard calibration plot of biomass

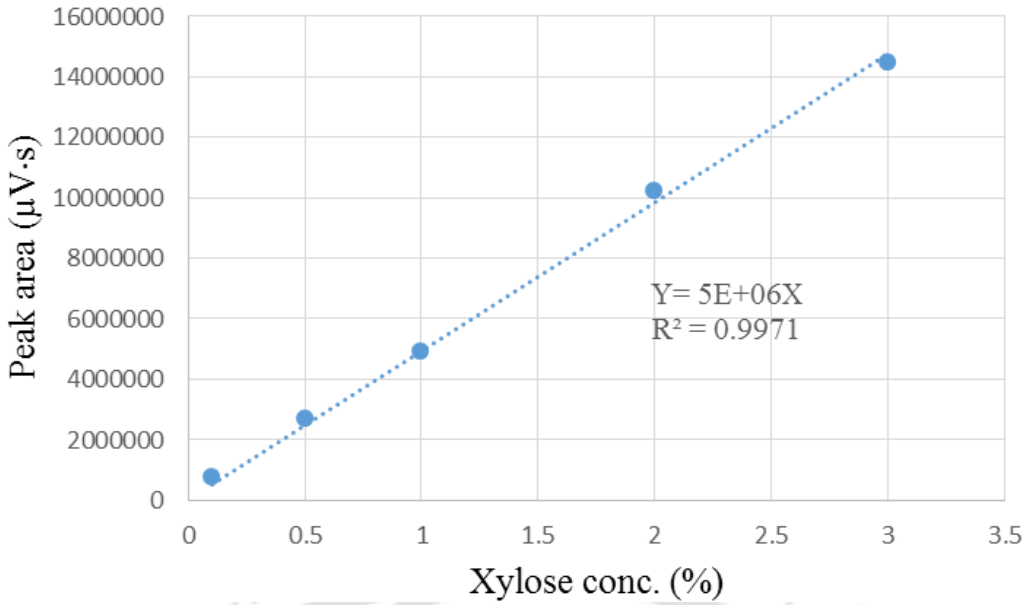
16000000
14000000
12000000
10000000
8000000
6000000
4000000
2000000
0
Peak area (µV·s)
Y= 5E+06X
R² = 0.9971
0
0.5
1
1.5
2
2.5
3
3.5
Xylose conc. (%)

(A)

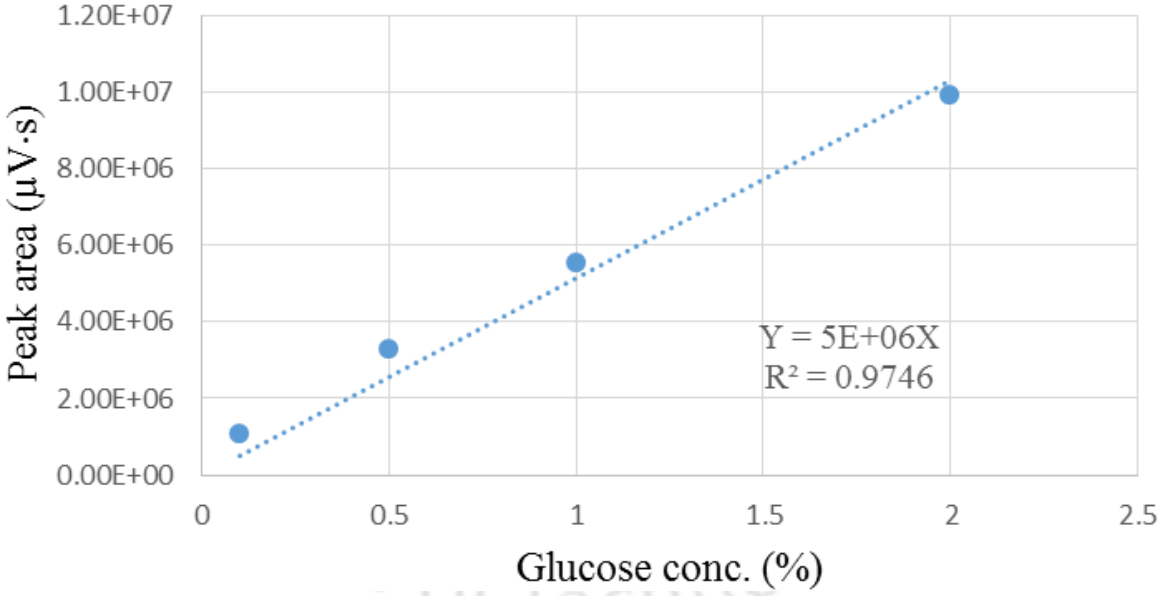
1.20E+07
1.00E+07
8.00E+06
6.00E+06
4.00E+06
2.00E+06
0.00E+00
Peak area (µV·s)
Y = 5E+06X
R² = 0.9746
0
0.5
1
1.5
2
2.5
Glucose conc. (%)

(B)

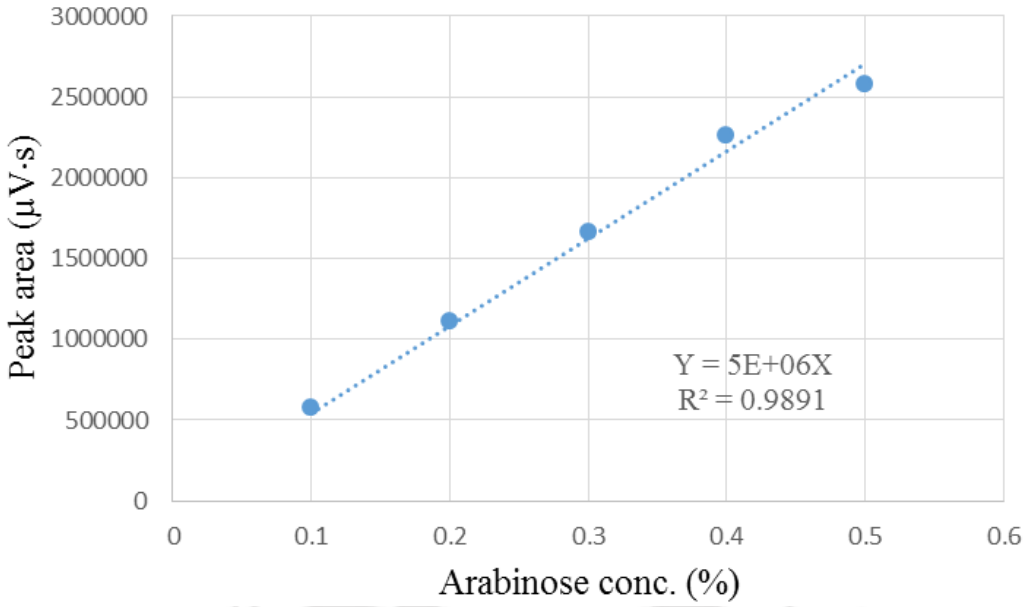
3000000
2500000
2000000
1500000
1000000
500000
0
Peak area (µV·s)
Y = 5E+06X
R² = 0.9891
0
0.1
0.2
0.3
0.4
0.5
0.6
Arabinose conc. (%)

(C)

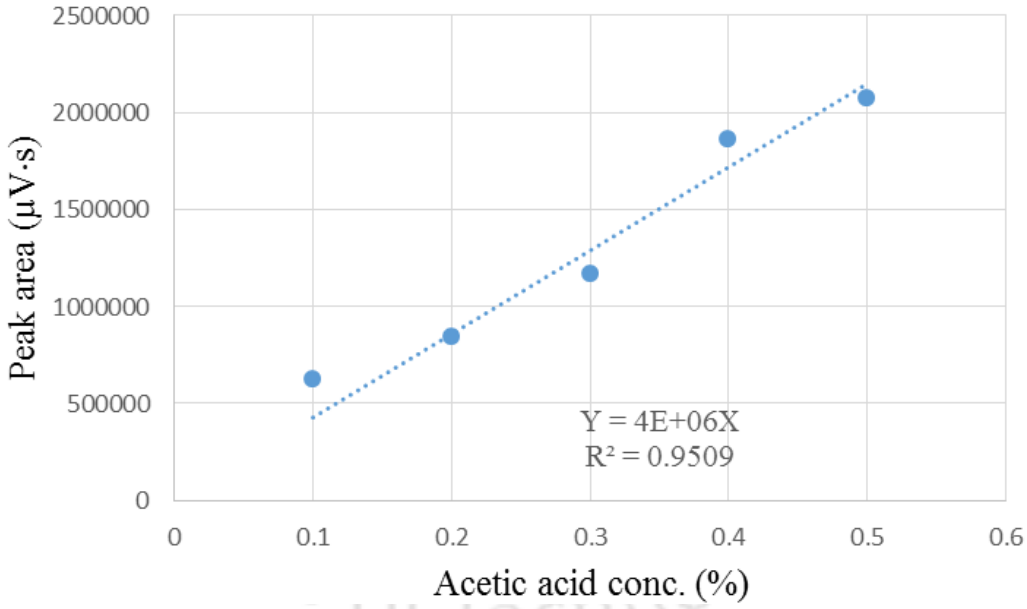
2500000
2000000
1500000
1000000
500000
0
Peak area (µV·s)
Y = 4E+06X
R² = 0.9509
0
0.1
0.2
0.3
0.4
0.5
0.6
Acetic acid conc. (%)

(D)

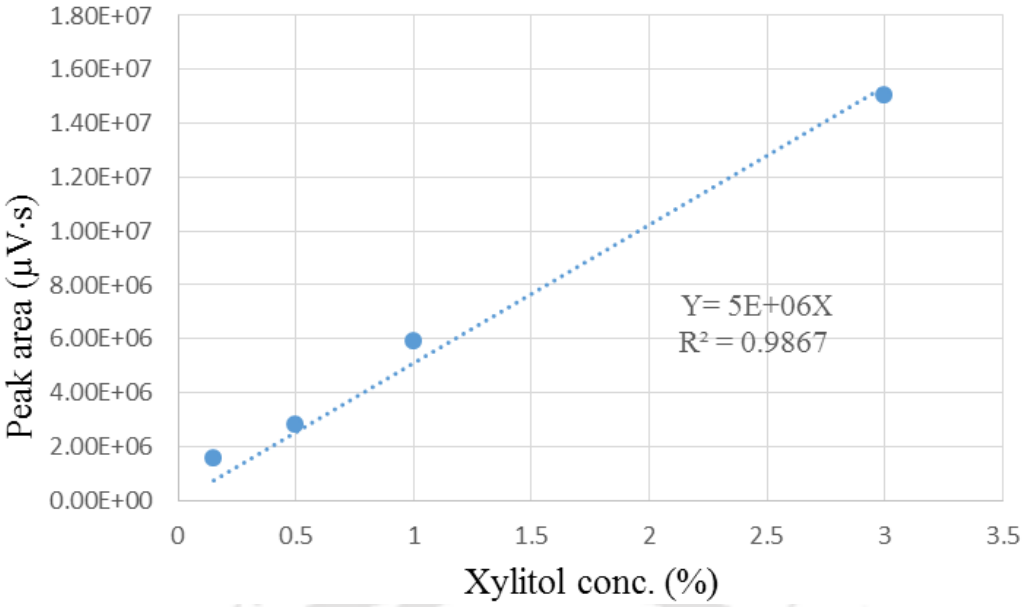


(E)

Figure $A_3$. Standard calibration plots of (A) Xylose, (B) Glucose, (C) Arabinose (D) Acetic acid and (E) Xylitol. *Note*: (% = g/100 mL)